13 Compression and uplift of the external massifs in the Helvetic zone

13.1 Structure and evolution of the external basement massifs (Aar, Aiguilles-Rouges/Mt. Blanc)

O. A. Pfiffner, S. Sahli & M. Stäuble

Contents

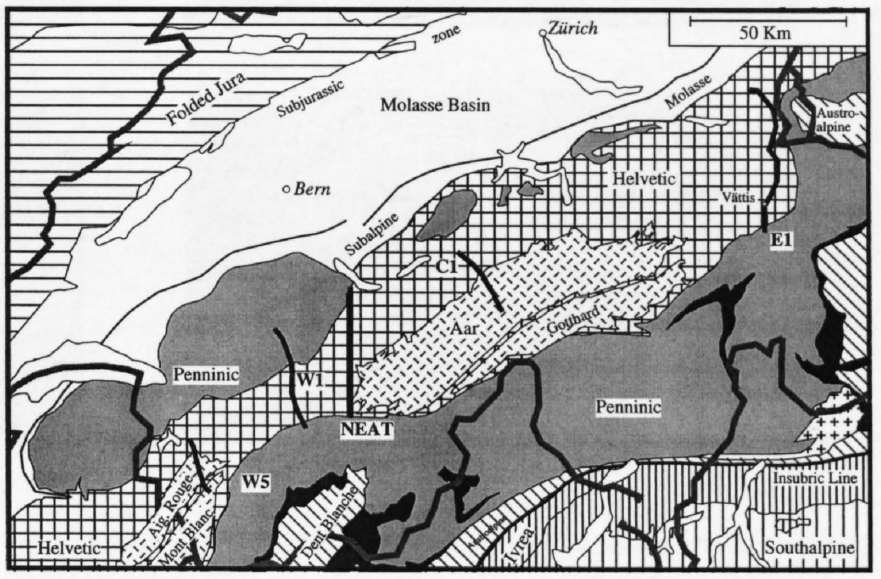

Figure 13.1-1
Simplified tectonic map covering the external basement massifs and showing traces of seismic lines E1, C1, W1, W5 and trace of cross section along km 618 (NEAT-Lötschberg, Kandertal).

13.1.1 Geologic framework

The northern and western, external part of the Central and Western Alps contain several elongate shaped basement uplifts referred to as massifs. The pre-Triassic crystalline basement exposed in these massifs is the southern and eastern continuation of the European foreland exposed in the Bohemian massif, the Black Forest and Vosges, as well as the Massif Central. The top of this European basement dips gently beneath the Alpine nappes to depths around 7 km below sea level (see Chapter 8 for the Central Alps, Guellec et al. 1990 for the Western Alps). Within the basement uplift the top basement contact is located at up to 4 or 5 km above sea level. The resulting vertical heave of over 10 km is a crustal scale feature. The aim of this chapter is to shed light on the structure and evolution of these basement uplifts.

In map view the basement uplifts form elongate domes. Their crest lines are arranged in an en échelon, right-stepping pattern. NRP 20 crossed the Aiguilles-Rouges (with adjoining Mt Blanc) and Aar (with adjoining Gotthard) massifs at four locations (see Figure 13.1-1). Line C1 crosses the culmination of the Aar massif where it is highest. Line W5 is located on the eastern, plunging side of the Aiguilles-Rouges culmination. Line W1 traverses the Rawil depression between the Aiguilles-Rouges/Mont Blanc and Aar massif. Line E1, finally, crosses a subdome of the Aar massif exposed in the tectonic window of Vättis.

The crystalline basement of the massifs contains three groups of rocks (see von Raumer et al. 1993 for a review):

(1) Polymetamorphic gneisses, schists and metasediments of pre-Variscan age.
(2) Carboniferous and Permo-Carboniferous sediments and volcanics. The older sediments were folded in the Variscan orogeny and metamorphosed by Late-Variscan intrusives. The younger sediments and volcanics accumulated in post-Variscan graben structures.

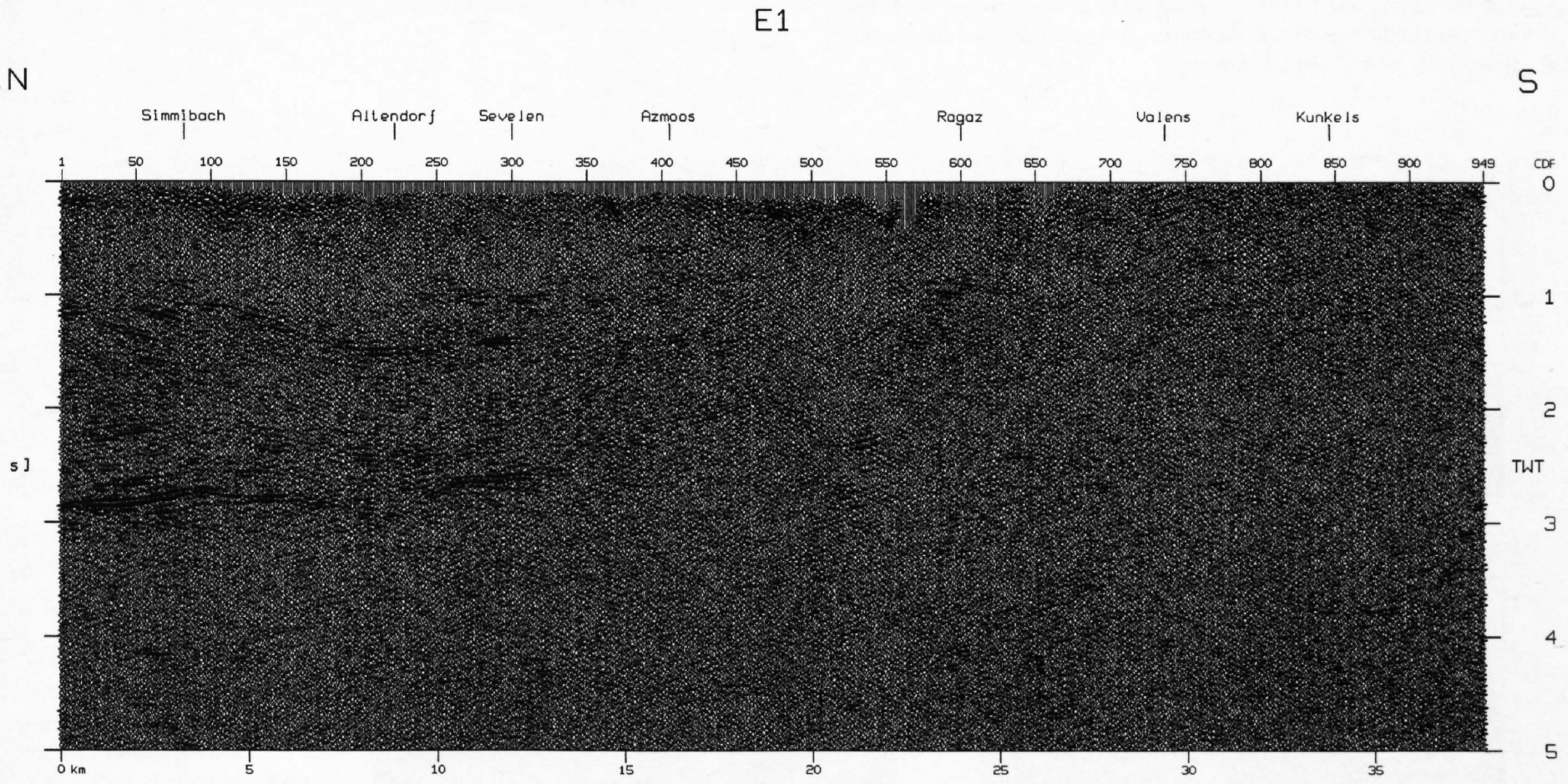

Figure 13.1-2
Detail of seismic section E1 covering the Aar massif. Unmigrated Vibroseis stack.

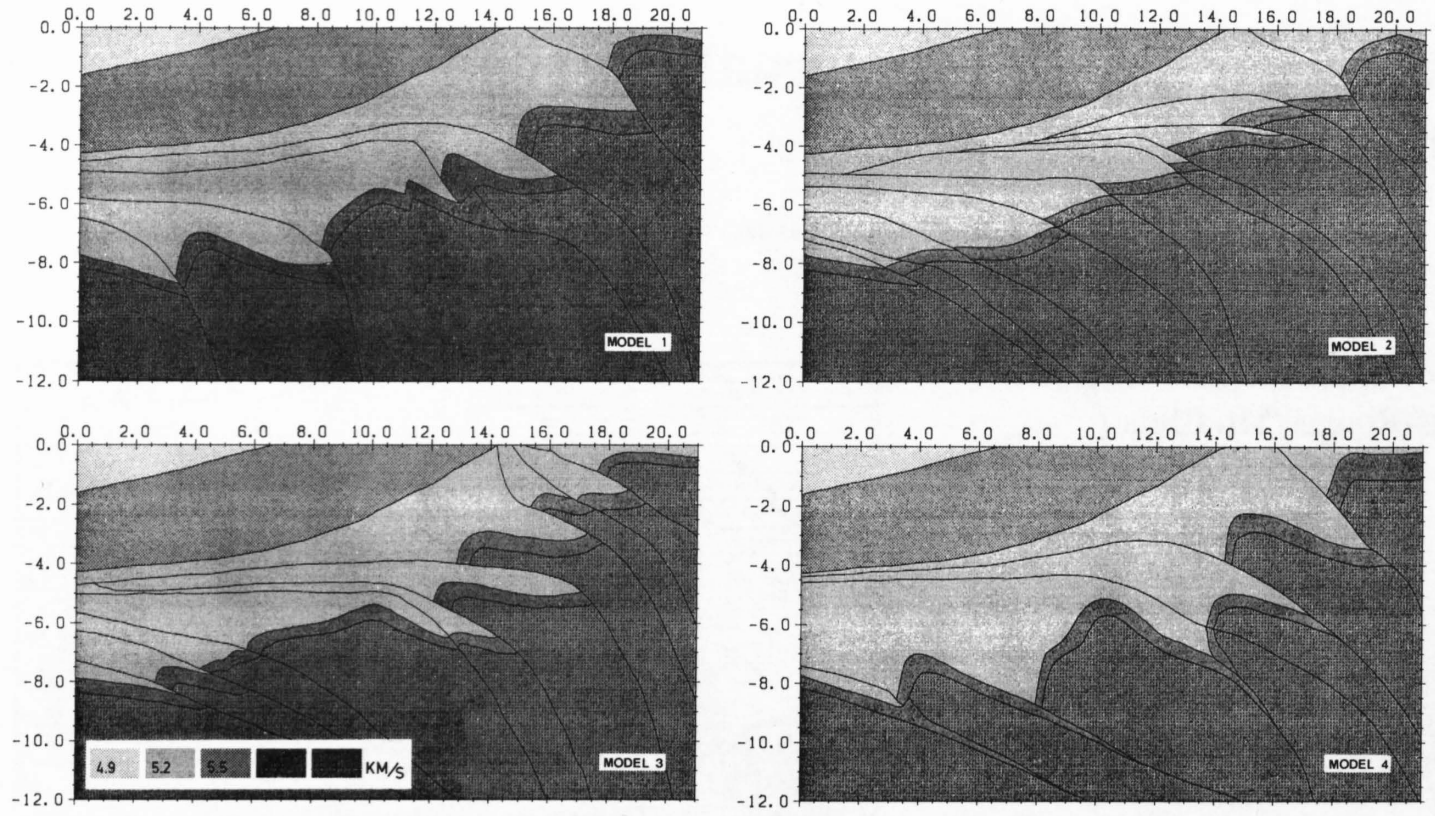

Figure 13.1-3
Four possible structural models of the northern flank of the Aar massif used in 2D seismic modeling.

(3) Late-Variscan and post-Variscan granitoids and associated volcanics. The granitoids occur in part as large intrusive bodies forming the structural backbone of the massifs.

The Alpine overprint was to some extent controlled by the Variscan structures (see e. g. Pfiffner et al. 1990 a): Granite bodies are upthrusted as basement wedges along steeply dipping intrusive contacts reactivated as thrust faults (e. g. Frisal thrust). In other instances Variscan volcanics form the core of large scale Alpine anticlines (e. g. Windgällen fold). The northern flank of the massifs deformed at anchimetamorphic conditions and under relatively lower temperatures (see Groshong et al. 1984, Frey et al. 1980, Breitschmid 1982, Burkhard 1988) as compared to the southern, more internal part. As a consequence the internal and external parts of the massifs show quite contrasting deformation styles. To the north discrete shear surfaces produce fold-and-thrust structures lacking penetrative grain-scale deformation (e. g. Kammer 1989). A typical example is the recumbent fold with the basement protrusion from the Jungfrau region shown in Figure 13.1-14, which will be discussed in more detail below (Line C1). A structural style with pervasive grain-scale Alpine deformation leading to axial planar foliations is found in the south (e. g. Steck 1984, Pfiffner et al. 1990 a).

The crystalline basement is generally overlain by Mesozoic-Cenozoic sediments. Triassic dolomites and Late Jurassic-Cretaceous limestones are the mechanically strong layers. These sediments were partly detached from their basement and were affected by folding and imbricate thrusting (cf. e. g. Pfiffner 1978 in the eastern, Heim 1878, Krebs 1925, Funk et al. 1983, Kammer 1989 in the central and Collet & Parejas 1931 in the western Aar massif; Gourlay 1986 in the Aiguilles-Rouges massif). A more detailed discussion of these structures will be given below.

13.1.2 Structure and geometry in profile and map view

In the following the seismic reflection data covering the basement uplifts and their geologic interpretation will be discussed proceeding from eastern to western Switzerland.

13.1.2.1 Transect through the eastern Aar massif Vättis subdome (Line E1)

Line E1 shown in Figure 13.1-2 transects the eastern Aar massif across a second order culmination. At Vättis the crystalline basement is exposed in a tectonic window, the top basement being at about 1000 m above sea level. To the north, reflections at 2.5–3 sTWT are stemming from the Mesozoic: they can be traced from line E5 (see Chapter 8) to line E4 which intersects E1 at the latter's N(W) termination. These reflections loose their strong amplitude towards the south and are thus difficult to trace. Several faint reflections can be seen at successively shallower depth, and plunging to the south. In any case no strong reflections at about 2.5 sTWT indicating a southward continuing slab of Mesozoic overridden by crystalline basement (Aar massif) can be detected.

In order to get insight into the effect of complex Alpine structure on the seismic response, 2D and 3D seismic modeling was carried out (Stäuble & Pfiffner 1991, Stäuble et al., 1993).

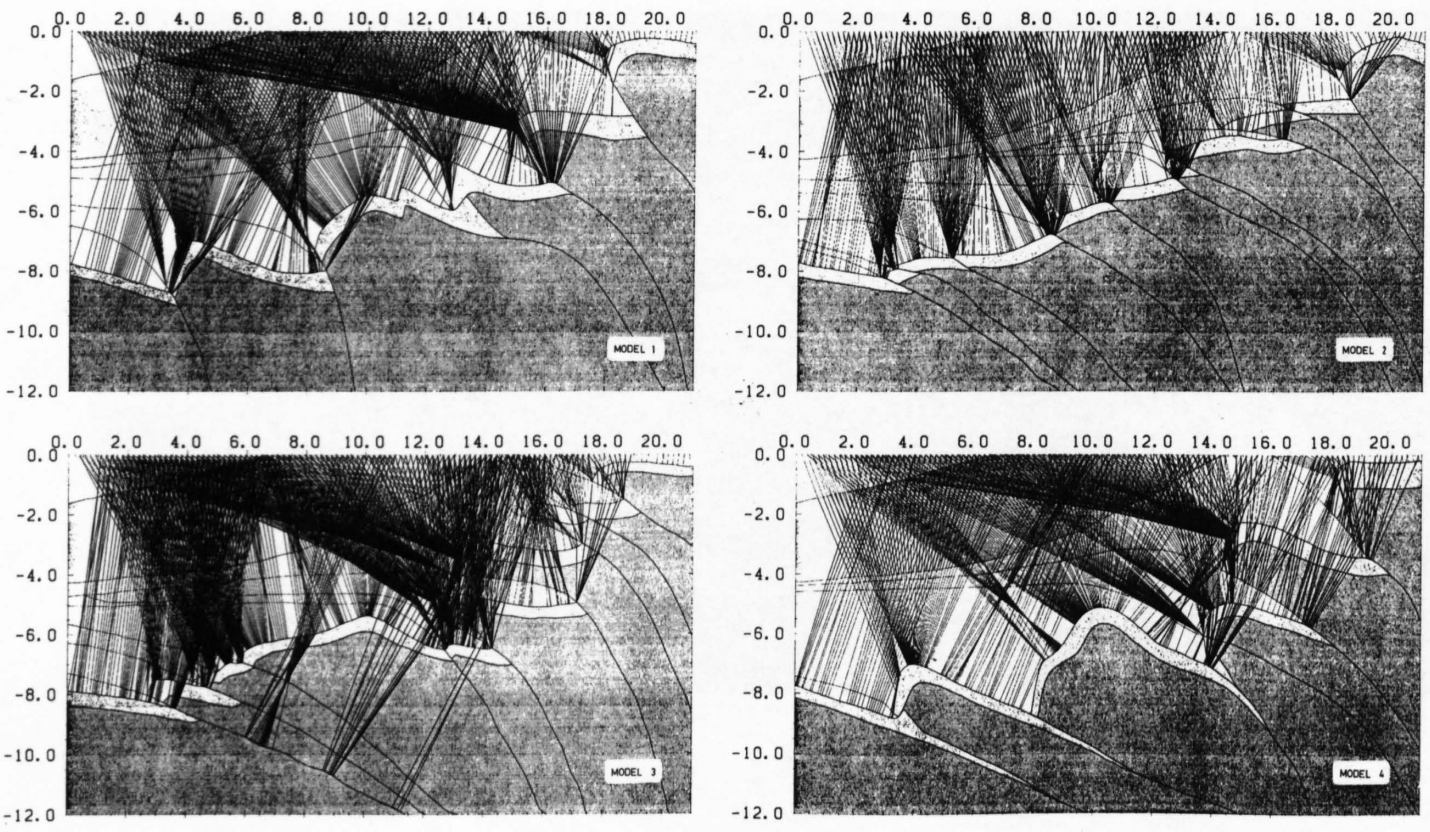

Figure 13.1-4
Ray plot of normal incidence ray tracing to the top of the Mesozoic for the four models. Normal-incidence ray tracing imitates a Vibroseis data set. Note focussing and defocussing of seismic rays due to complex reflector geometry.

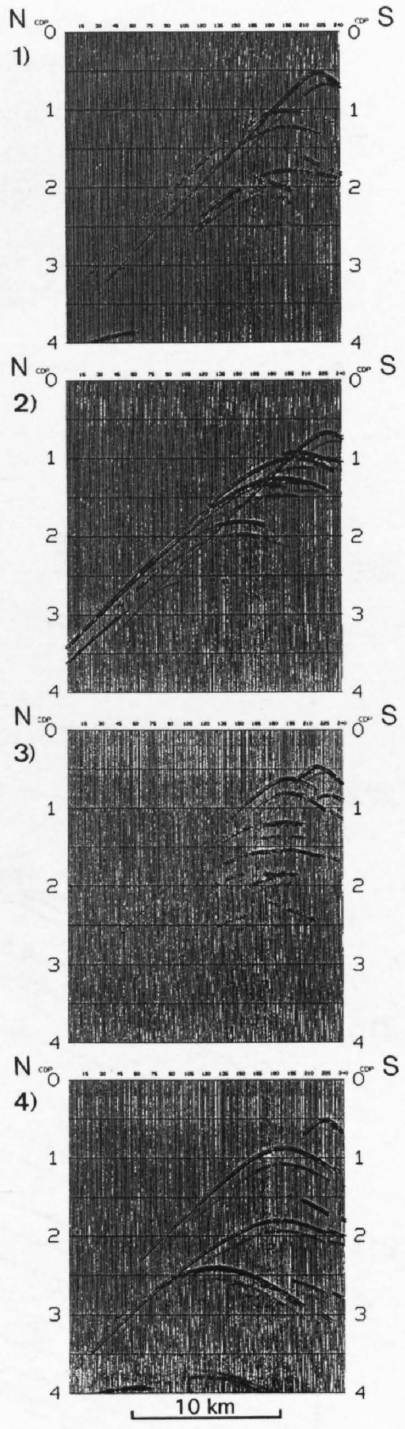

Figure 13.1-5
Synthetic seismograms of normal incidence ray tracing of the four models. (2D modeling, 80 m CDP spacing). Note short horizontal reflections and long diffractions caused by complex reflector geometry.

2D modeling:

Based on seismic data and their interpretation, as well as geological field observations (Pfiffner et al. 1990a and b) four different geologic models of the northern flank of the Aar massif basement uplift can be envisaged and were subsequently tested. The models are presented in Figure 13.1-3. They were intended to represent very different geometries considering ray path and reflections. The surfaces used for the models are, from the top to the bottom: The Säntis Thrust, the Glarus Thrust, the transition from Tertiary Molasse and Flysch sediments to Mesozoic carbonates, and the basement-cover contact. The velocities used for the individual layers were derived from different sources such as borehole data, physical property measurements (Sellami et al. 1990), refraction seismic recordings (Ye & Ansorge 1990) and inversions of tau-p transformed receiver gathers.

The model size is 21 by 12 km and closely follows the path used for the NRP 20 profile. As this study concentrates on the basement-cover relationship, the top layers of the model, i. e. the Säntis and the Lower Glarus Nappes are identical in all four models. These layers are needed as they contribute significantly to the ray path and travel time but are not visible as individual reflections in the seismic section.

The northernmost 2–3 km of the models are also very similar as this part of the model is not well constrained by seismic or geologic data. The difference in the individual models lies in the structure of the basement-cover contact on the northern flank of the Aar massif.

Model 1: The structural style is characterized by steep, basement cored ramp-anticlines, with little displacement at the high-angle ramps. These structures compare to the ones observed in the Tödi area (Pfiffner et al. 1990a, figure 2c). The shape of the anticline is also based on results of a 3-D ray tracing study of the structure immediately to the north of this area (see Stäuble et al. 1993 and below).

Model 2: In this model shortening is thought to have occured along thrusts dipping at around 45° and with only minor folding only in the south. In this model shortening is reduced to a minimum.

Model 3: This model is similar to model 1 as it also displays ramp anticlines, but differs in that the thrusts dip at shallower angle at the basement-cover contact. As a consequence ramp-anticlines are of small dimensions and the general structure is dominated by a vertical stack of relatively flat lying lithological elements (particularly evident in the southern part).

Model 4: The characterstics of this model are basement thrusts which form a steep ramp in the vicinity of the basement-cover contact. This thrust geometry produces ramp anticlines with steep northern limbs. This model is characterized by thin layers of Mesozoic rocks pinched between the basement blocks, as well as by large-scale anticlines with overturned limbs. Structures of this type are comparable to the ones observed in the lower part of the Reuss valley and in the central part of the Aar massif (Heim 1878; Kammer 1989; Pfiffner et al. 1990a).

The 2D modeling techniques used implied both, normal-incidence and offset ray tracing of individual shots. Ray path analysis of both techniques (see Figures 13.1-4 and 13.1-6) shows that focussing and defocussing plays an important role. In the synthethic seismograms shown in Figures 13.1-5 and 13.1-7 only a few subhorizontal reflections are observed due to the complex structural situations. In the case of tilted and folded reflectors focussing and defocussing tends to produce short discontinuous reflections and long diffractions.

The comparison of the synthetic seismograms with the observed data does not yield a simple answer as to which model is best. Several limiting factors related to the method and to the models must be taken into account. When comparing normal-incidence ray tracing with observed, stacked data the assumption is made that common mid point (CMP) equals common depth point (CDP). This is only true in a geological situation with flat layers. An additional shortcoming is the assumption of the two-dimensionality in both, geologic models and synthetic seismograms: the geology shows laterally varying structure and therefore the observed sesimic section contains information (reflections, diffractions etc.) coming from the side (see below) which cannot be directly compared to a synthetic seismogram from 2-D ray tracing.

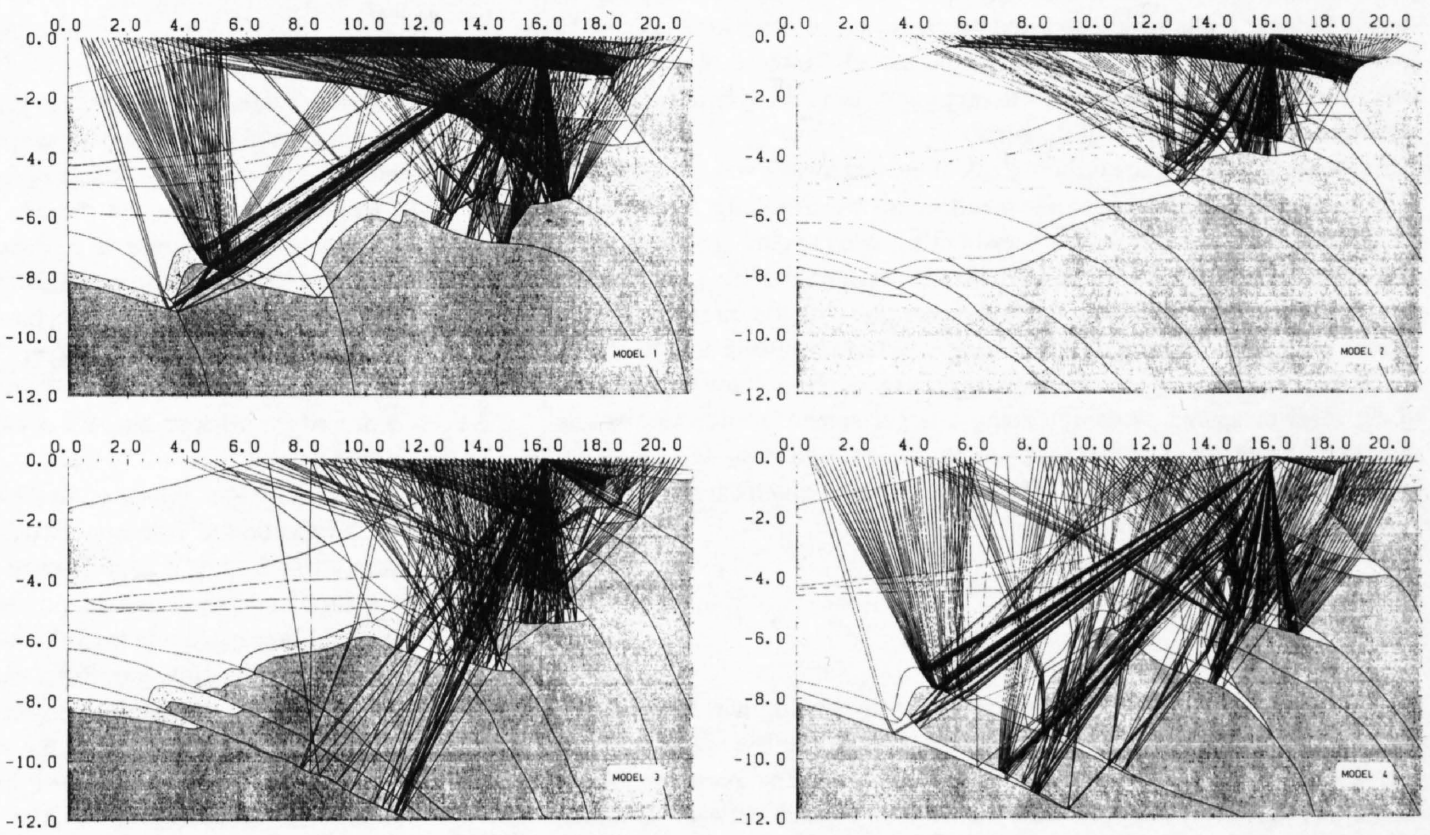

Figure 13.1-6
Ray plot of the offset ray tracing of the four models. Note focussing and defocussing of seismic rays.

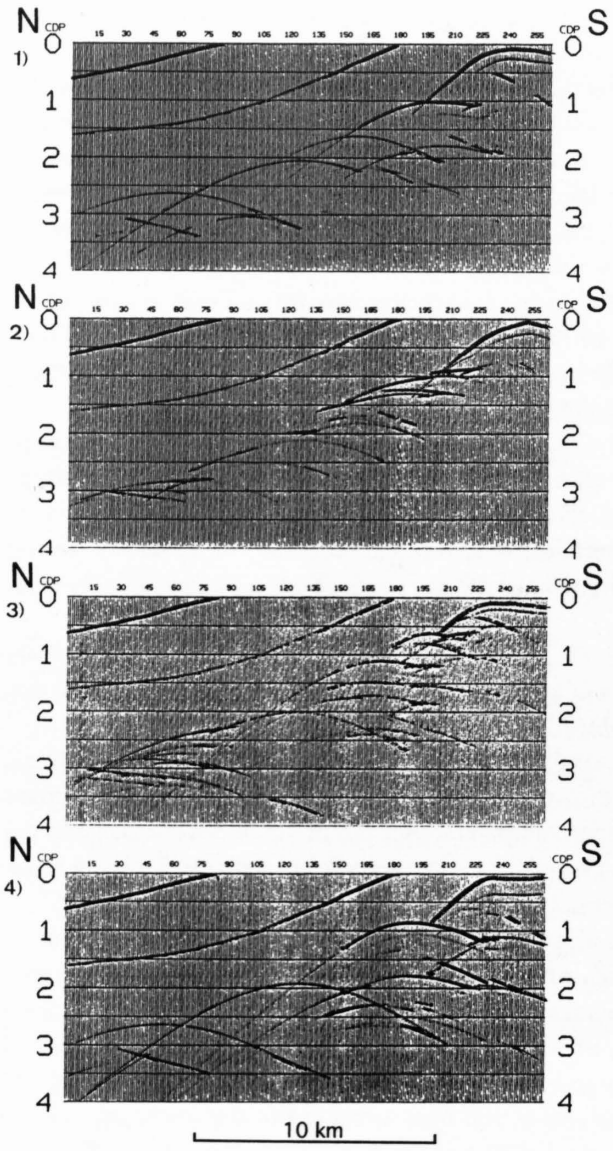

Figure 13.1-7
Synthetic seismograms of offset ray tracing (2D modeling, 80 m CDP spacing). Offset ray tracing imitates seismic data gathered from single dynamite shots. Note steeply N-dipping reflections originating from ramp anticlines in the N part of the models.

Comparison of the synthetic seismograms of the normal-incidence and the offset ray tracing shows that all the model answers contain events that are comparable with some events in either the Vibroseis or the explosion data set, but not in both.

Important in this evaluation are not only the matching reflections (these will be present in most cases), but also those strong reflections, that have no equivalent in the observed data and thus can indicate which part of the model has to be wrong. In this sense model 3 and 4 can be excluded, in that both synthetic seismograms show strong, south dipping reflections (b in both synthetic sections) below 3 sTWT originating from the thrust faults in both models. A thrust fault putting basement onto a layer of sedimentary rocks reaching far into the basement would be an ideal reflector and certainly would, if present, show up in the observed section.

The analysis of 2-D ray tracing suggest that the structural style of model 1 yields overall the best matching events. This model proposes thrusting on steeply dipping faults with associated basement-cored ramp-anticlines and a fold with an overturned limb. Results from model 2 indicate that a component of low-angle faulting with north dipping basement-cover interfaces are present in the southern part of the section.

The seismic section of the northern flank of the Aar massif was considered to be of poor quality, as long continuous reflections were missing. As shown by modeling, the lack of this feature may not be related to data quality or to the lack of layers with large impedance contrasts. Rather, it could be a function of the complex subsurface structure in conjunction with the spread geometry. Defocussing and scattering on larger scale structures results in areas that cannot be sampled at all by the seismic experiment, as the rays are reflected out of the receiver spread. Although using a larger spread would improve the sampling of such previously missed structures, it would at the same time degrade the stack because of NMO and residual statics which cannot be calculated correctly for very large offsets.

3D modeling:

Forward modeling with 3D normal-incidence ray tracing was used to produce synthetic seismograms. The base for this modeling is a 3D model consisting of 16 layers with varying seismic velocities. The geometry of the model was iteratively changed until a satisfactory match between synthetic

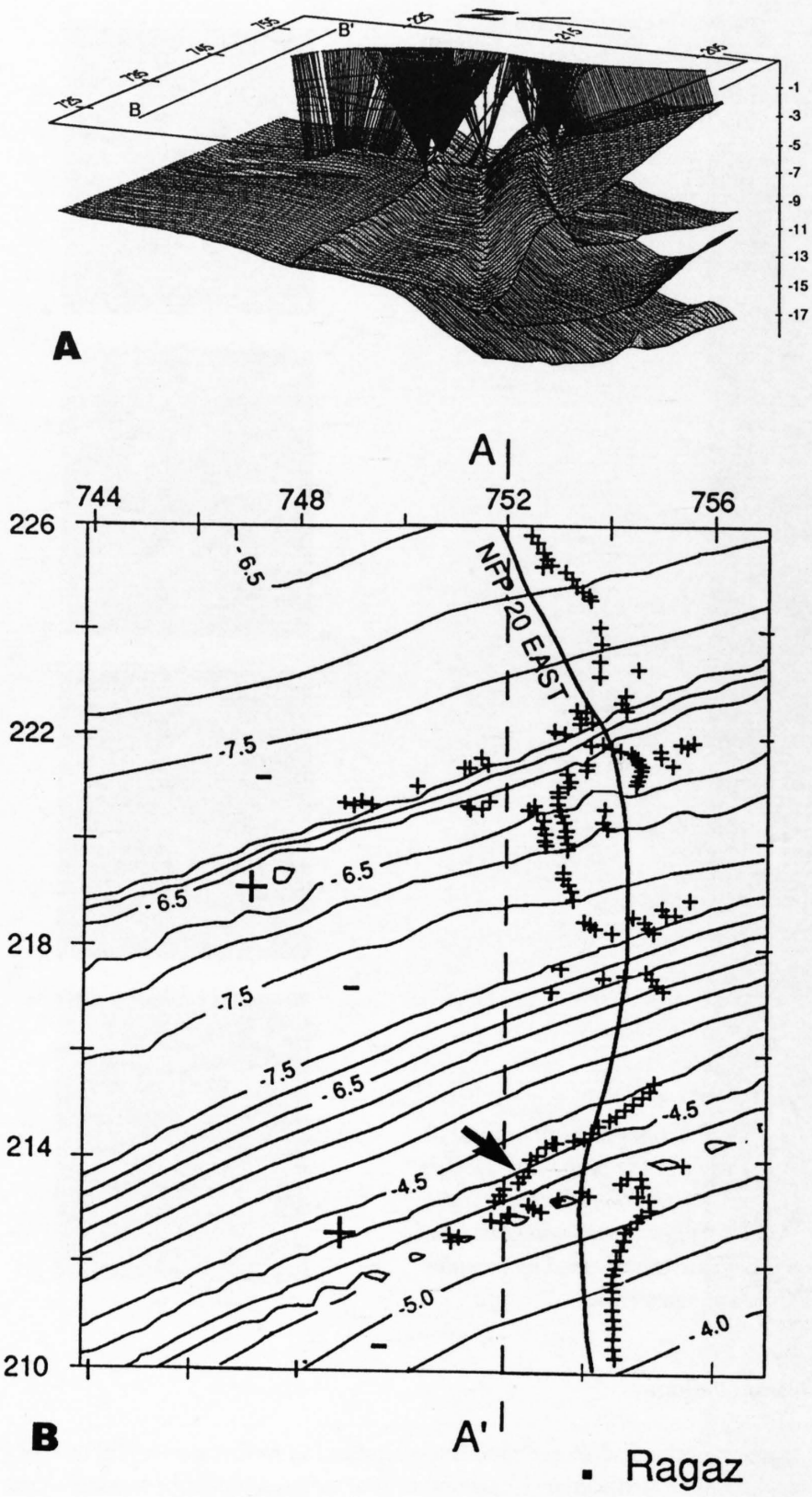

Figure 13.1-8
3D model of the northern flank of the Aar massif. Numbers on the horizontal axes are km of the Swiss National grid net. Numbers on vertical axis and on structure contours are depth below sea level in km.
A: Display of the "top Mesozoic" reflector with ray paths. B: Contour map of the same horizon with ray end-points (+). Map in B covers only the western part of the model shown in A. Structural highs and lows are indicated by large + and – symbols. Arrow points to structural high (anticline) discussed in text.

and observed data was obtained. In Figure 13.1-8 the top basement reflector of the "final model" is shown in perspective view, as well as in map view.

A comparison between the observed section and the synthetic section (Figure 13.1-9) shows that although there is a close overall correspondence, at a smaller scale several minor discrepancies exist where position and shape of the synthetic reflections do not match perfectly with the observed data. Several limiting factors must be taken into account to evaluate these mismatchs:

(1) The model only contains 16 layers, which is obviously a simplification of the real situation. In view of the particular geologic structure and the resolution of the seismic data, we consider this to be a sufficient approximation, however.

(2) The velocity functions used in the model are approximations. Thus, e. g. for a reflection at 1 second Two-Way-Time (1s TWT), modeled with a velocity of 5 km/s, a large error of +/–10% in the velocity amounts to a variation in depth of the order of +/–250 m.

(3) With this uncertainty in the velocity, the dip of the contoured surfaces are approximations only, too. But a change in dip would also result in sampling the layer at different positions. For instance for a reflector outcropping 7 km laterally from the seismic section, a change in depth by 100 m would result in a change in cross dip of 0.75 degrees and an up-dip shift of the sampling point of 30 m.

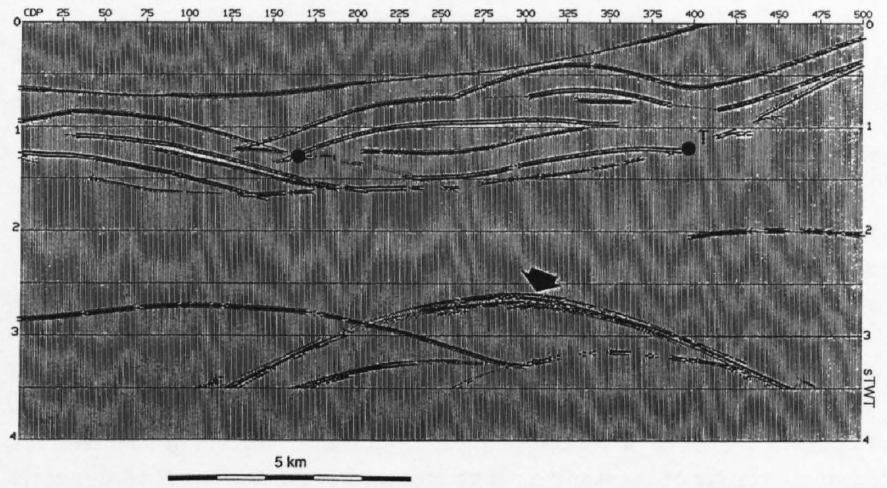

Figure 13.1-9
Synthetic seismogram from 3D normal-incidence ray tracing. Arrow marks anticline discussed in text.

(4) When processing seismic data the 1D assumption that a CMP is equal to a CDP is made. However, in a 3D situation this assumption is not always fulfilled and as a consequence, energy originating from a broad area is summed into a single CDP. This results in a considerable smearing (or loss in resolution) of the reflection. Incidentally this "smearing" works in favour of the modeling technique, as small structural differences cannot always be modeled in detail. In Figure 13.1-8 the rays fan out of the 2D plane, showing that the CMP-CDP assumption is not fulfilled. Moreover, normal-incidence ray tracing considers only rays with coincident shot and receiver points and therefore does not necessarily sample exactly the same areas as the field experiment.

Ray-path analysis shows a strong 3D effect resulting in out-of-plane reflections and diffractions. The arcuate reflection between 2.5 and 3.5 s TWT indicated by an arrow in Figure 13.1-9 appears as a single strong event. Detailed analysis of the rays contributing to this reflection (Figure 13.1-8b, arrow) however shows that it is a composite of several out-of-plane reflections. In addition recording of seismic data is often oblique to the geologic structures. Consequently, conventional migration techniques repositioning reflections in a 2D plane, result in a wrong position for reflections like the ones discussed above and thus in an erroneous interpretation. Furthermore, out-of-plane diffractions with a small curvature could be mistakenly treated as reflections. The 3-D ray-tracing modeling technique used here yields good control of reflector geometry, and avoids many of the problems inherent to 2D migration.

The geologic section corresponding to the 3D final model with the best matching synthetic seismogram is shown in Figure 13.1-10. The basement-cover contact on the northern flank of the Aar Massif is at a depth of about –7.5 km beneath the central part of the study area. It then rises southwards in a series of steps due to thrusting and folding to reach the surface at Vättis. In the model the northernmost of these steps appears as a ramp anticline (marked with an arrow in Figures 13.1-8, 13.1-9, 13.1-10). This structure was unexpected from a first view of the seismic field data or from geological observations.

A basal thrust putting basement onto a layer of autochthonous Mesozoic cover rocks has been proposed for this transect (Pfiffner, 1985) as well as for a transect through the Western Alps (Butler, 1986; Guellec et al., 1990–2nd hypothesis). If present, such a slab of Mesozoic carbonates should have been recorded. If, on the other hand, as suggested by Guellec et al (1990–1st hypothesis) for the Western Alps, a low-angle thrust fault putting basement onto basement is postulated, this contact would likely be associated with a mylonite zone. The absence of reflections in the E1 profile can be explained in several ways:

1. There is no such thrust fault.
2. The thrust fault is associated with a very thin mylonite zone (beyond the resolution of the seismic experiment) and therefore possibly being of little importance (i. e. having a small displacement only).
3. The thrust fault and the associated mylonite zone dip steeply (and are therefore not imaged seismically) and the displacement is relatively small.

In the geologic interpretation (Figure 13.1-10) the last possibility is retained. This structural style is in fact observed at the surface some 50 km farther west (Pfiffner et al. 1990a).

Kinematic sequence

The fold-and-thrust structures in the transect of E1 evolved in a sequence of several deformation phases which are discussed in more detail in Milnes & Pfiffner 1977, 1980; Pfiffner 1978, 1982, 1985 and 1986. The associated fold or thrust structures are labelled in the cross section in Figure 13.1-11 accordingly. In summary the following kinematic sequence can be recognized:

1. Pizol phase: An early phase of detachment and thrusting of Mesozoic-Cenozoic sediments which were originally deposited more than 50 km S of the Aar massif. These exotic units were emplaced onto the youngest, Eocene-Oligocene sediments of the autochthonous Aar massif cover without leaving any traces of deformation.

2. Cavistrau phase: This phase is a predecessor of the main, Calanda phase and produced structures only locally. These structures imply early large-scale recumbent folds whose inverted limbs were refolded by the subsequent phase.

3. Calanda phase: This main phase of deformation resulted in a pervasive cleavage parallel to the axial surfaces of associated folds and parallel to the surfaces of active thrust faults. It is interesting to note that, apart from refraction effects, the general orientations of the Calanda phase axial surfaces and cleavage remain constant across the Aar massif's culmination. The basal thrust of the Helvetic nappes, the Glarus thrust, was already active as a

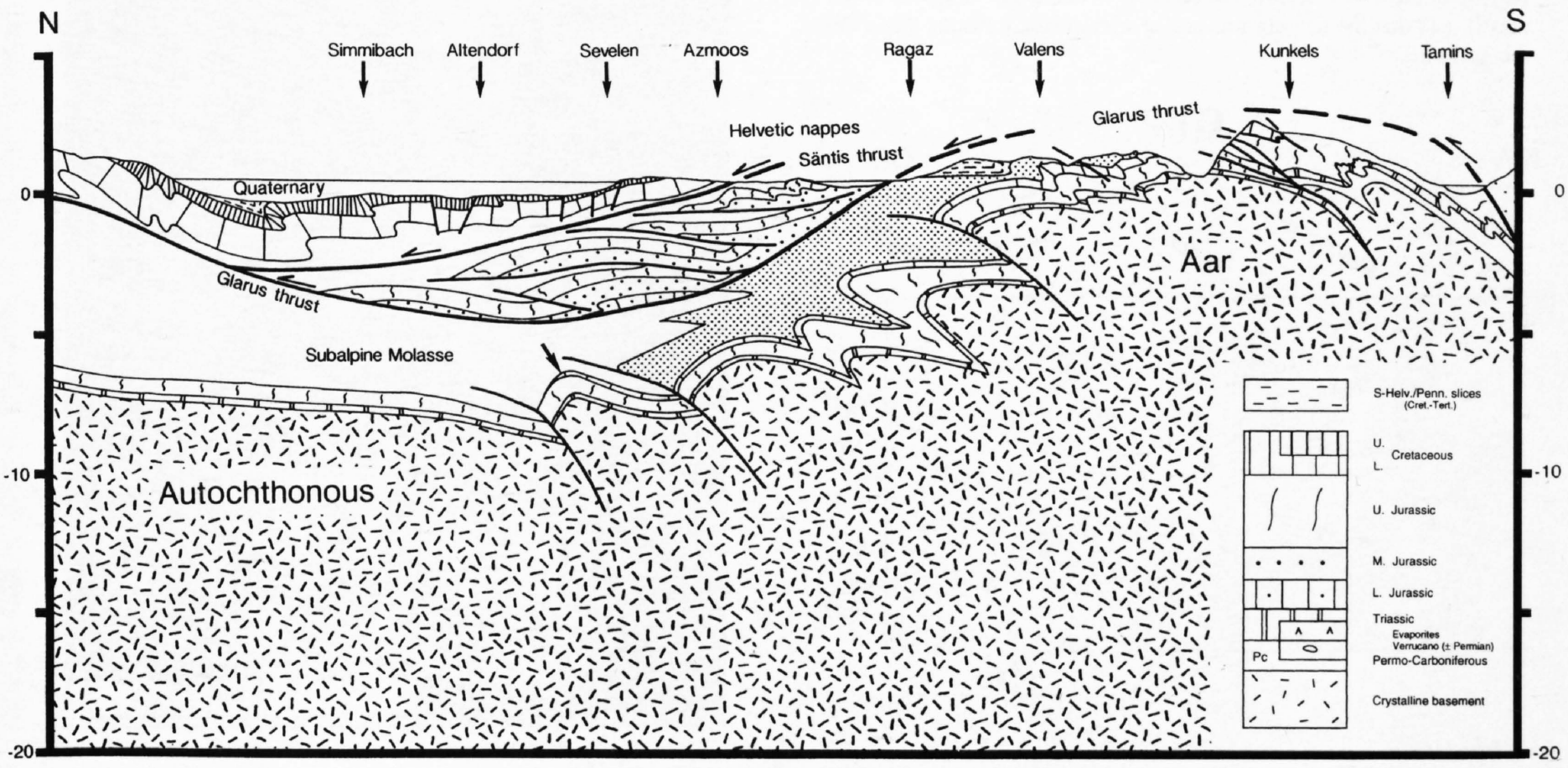

Figure 13.1-10
Geologic profile across the Aar massif along line E1. Arrow marks anticline discussed in text.

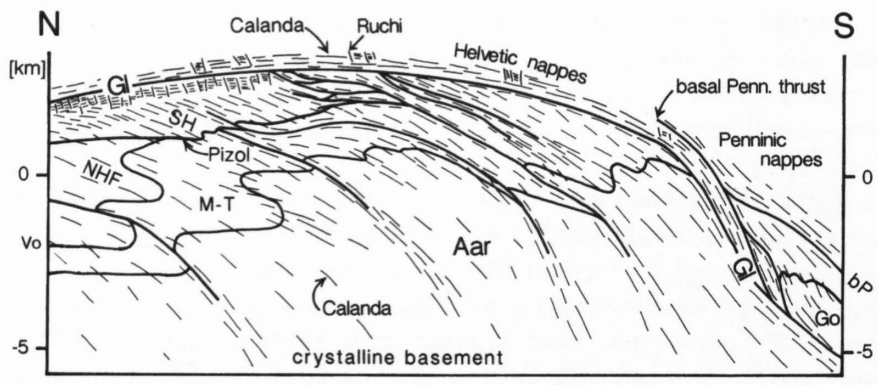

Figure 13.1-11
Schematic profile across eastern Aar massif showing traces of cleavages and their relation to folds and thrust faults. Calanda phase cleavage cuts across early thrust faults (base of Vorstegstock and South Helvetic/Penninic slices) but is parallel to major fold axial surfaces and thrust faults (including Glarus thrust). Steeply dipping Ruchi phase cleavage is of patchy appearance and is mainly concentrated along Glarus thrust.

bP:	*basal Penninic thrust*	*SH:*	*South-Helvetic and Penninic strip sheets*
Gl:	*Glarus thrust*		
Vo:	*Vorstegstock thrust*	*NHF:*	*North-Helvetic Flysch*
Go:	*Gotthard massif*	*M-T:*	*Mesozoic-Tertiary cover*

stretching fault (i. e. a thrust fault with differential ductile stretching in the hanging wall and footwall parallel to the transport direction).

4. Ruchi phase: This late phase of deformation produced a crenulation cleavage of patchy appearance and is related to late northward transport of the Helvetic nappes along the Glarus thrust resulting in an inverse metamorphic zonation.

These deformation phases are defined as local kinematic sequences in the Infrahelvetic complex. Although some of them can also be recognized in the overlying Helvetic nappes they are not meant to be "chronostructural" units. In fact they are likely to be diachronous (Groshong et al. 1984).

In a general way the thrust diplacements of Infrahelvetic units overlying the Aar massif's culmination vary according to structural position. The lowermost units, involving also basement rocks, are less displaced than the upper, more allochthonous units. It seems that the mechanically stronger basement formed a somewhat rigid, slowly deforming core with a soft shell consisting of flakes of detached cover sediments.

Seen at large-scale in cross-sectional view there is a discordancy between the Calanda phase cleavage in the hanging wall and footwall of the Glarus thrust (Figure 13.1-11). Two points are of particular relevance in the context of the basement uplift's evolution:

1) The constant orientation of the Calanda phase structures in the Infrahelvetic complex across the Aar massif's culmination.
2) The smooth shape of the Glarus thrust, which is unaffected by the (Calanda phase) thrust faults in its footwall. These features suggest that the bulging of the massif occurred in response to internal deformation of the massif, and that the bulging was coeval with ductile thrusting along the Glarus thrust.

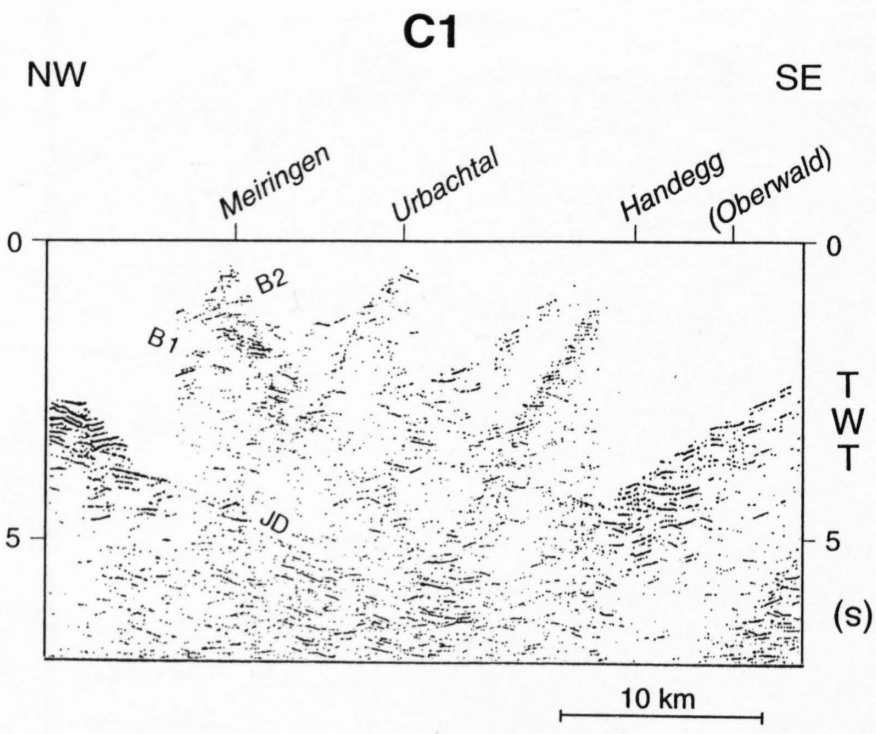

Figure 13.1-12
Detail of seismic section C1 covering northern flank of Aar massif. B1: Mesozoic cover of foreland, B2: Mesozoic cover of Aar massif, JD: Jura detachment (?)

13.1.2.2 Transect through the central Aar massif (Line C1)

Line C1 traverses the Aar massif in the central part of the culmination (Haslital, see Figure 13.1-1). The seismic data (cf. Figure 13.1-12) are of poor quality. However the conspicuous reflections B1 at 2.2–2.5 sTWT beneath shot point Meiringen most probably correspond to the autochthonous Mesozoic of the foreland. This follows from a comparison with the industry lines in the Brünig area (Bodmer & Gunzenhauser 1992). Reflection group B1 extends from shot point Meiringen with a relatively steep dip about halfway to shot point Urbachtal. An additional group of northdipping reflections (B2 in Figure 13.1-12) can be followed upward and southward and line up with the Mesozoic cover of the Aar massif as observed at the surface N of shotpoint Urbachtal. The geometry of this northern flank of the Aar massif is much better imaged on the industry seismic line in the Klein Melchtal (see Figure 13.1-13a). This industry line was recorded about 10 km to the east of line C1.Two distinct reflection bands can be distinguished on the migrated stack shown in Figure 13.1-13a: one is dipping north from the SSE-end of the section (at 1 s TWT), the other, subhorizontal one extending at 2.5 s TWT from the NNW-end of the seismic section. The discussion of the reflections is based on the line drawing shown in Figure 13.1-13a, which covers a longer section than Figure 13.1-13b. The subhorizontal reflection group B1 in Figure 13.1-13b stems from the autochthonous Mesozoic strata of the foreland. The strong double-cyclic band at the base (at 2.5s TWT may well originate form the top of the Triassic carbonates (Muschelkalk), while the uppermost reflection (at 2.25 sTWT) can be correlated to the top of the Mesozoic carbonates (see also Chapter 8). The north-dipping reflection band, located at 0.75–1 sTWT at the SSE end of the line, originates from the Mesozoic cover of the Aar massif. The lower double cyclic band is taken to stem from the top of the Triassic Röti dolomite, the upper weaker reflection from the top of the lower Cretaceous or upper Jurassic limestones. To the SSE the extrapolation of reflection group B2 lines up smoothly with the Aar massif's Mesozoic cover as observed at the surface in the Gental area.

The geologic profile of Figure 13.1-14 takes all these data into account. It follows from these that a layer of autochthonous Mesozoic sediments of the

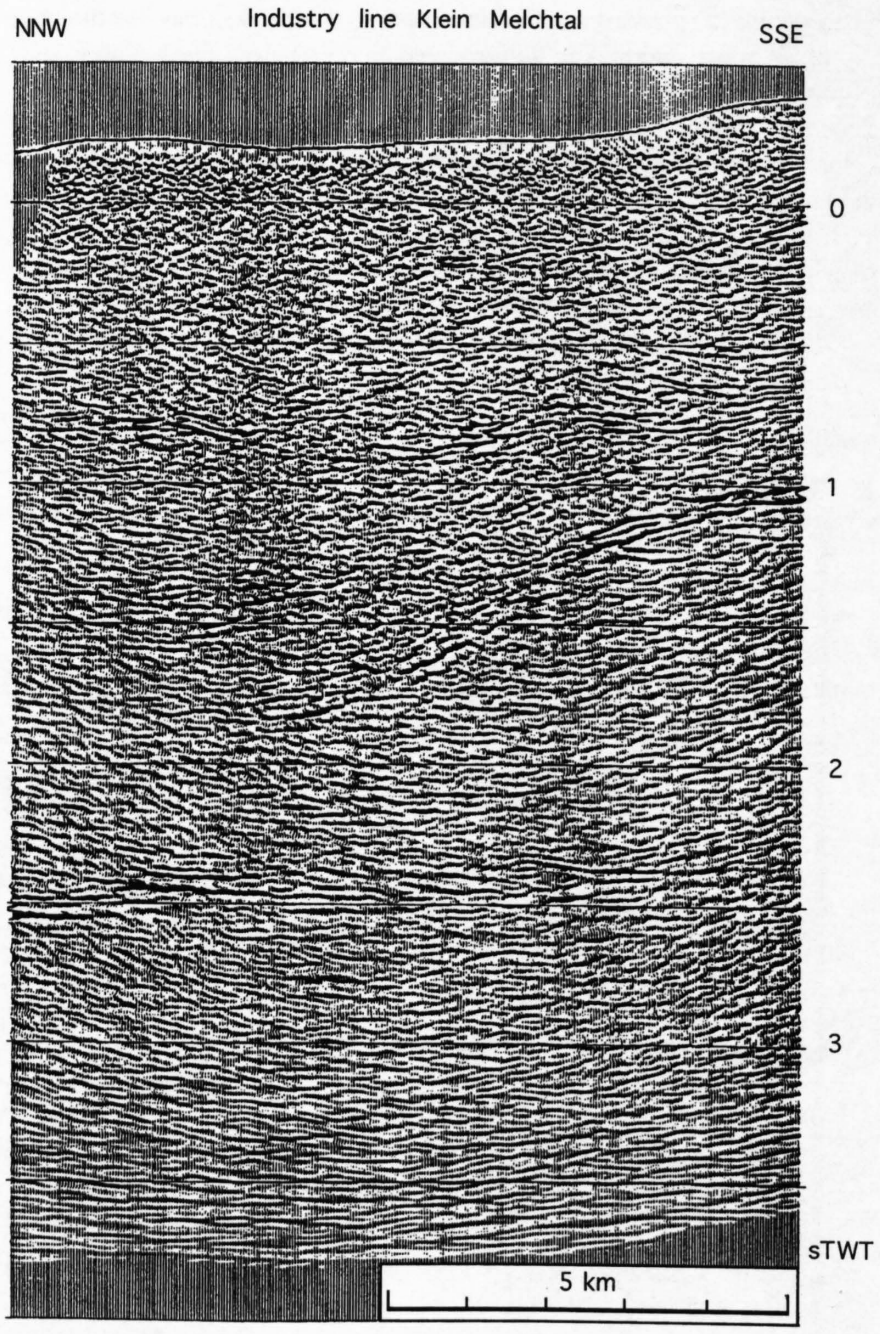

Figure 13.1-13a
Migrated stack of the segment of the Industry line Klein Melchtal covering the transition from the northern flank of the Aar massif to the foreland.

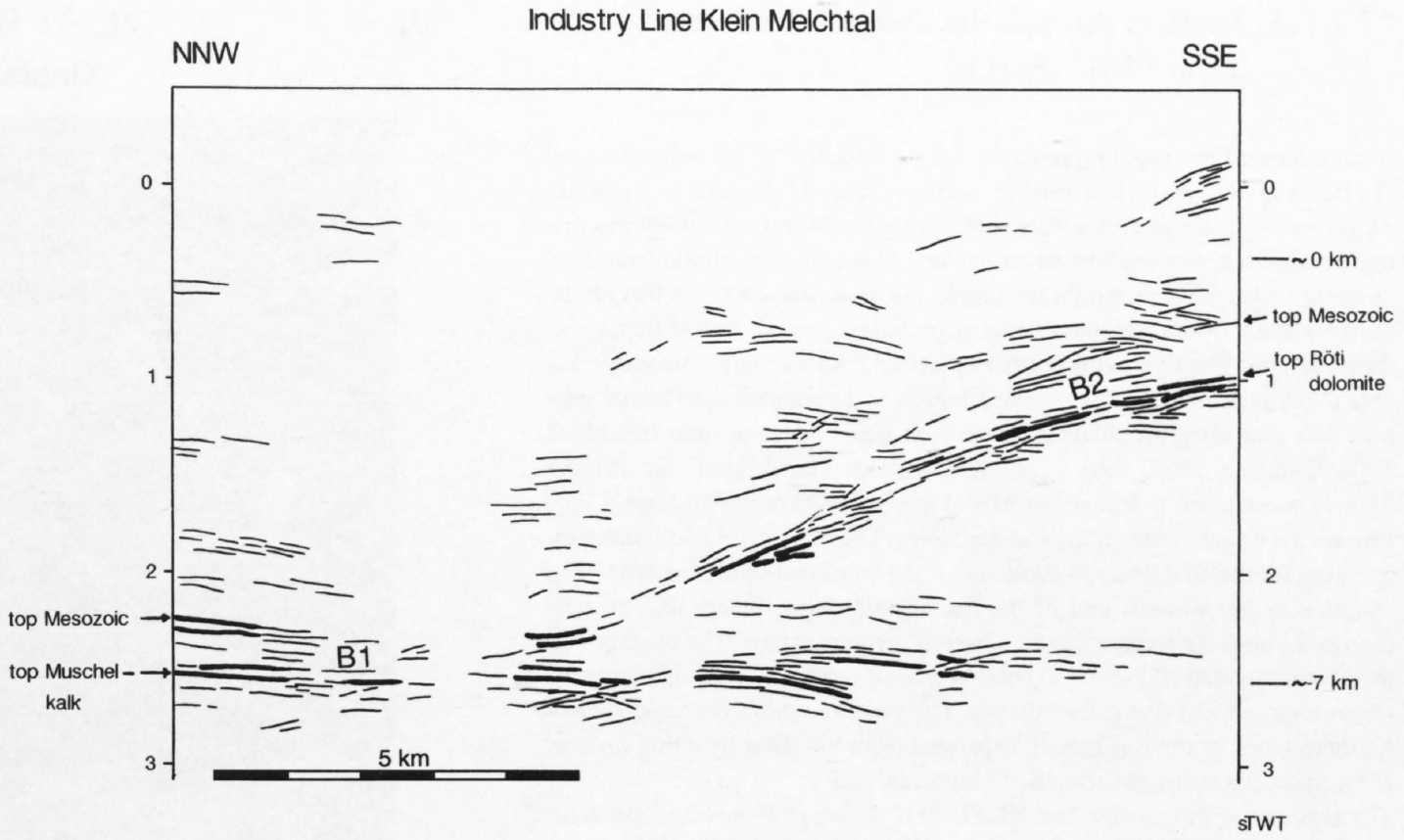

Figure 13.1-13b
Line drawing of an unmigrated stack of the Industry line (Klein Melchtal) covering northern flank of Aar massif and the adjoining foreland.

foreland is overridden by a thick wedge of Aar massif crystalline basement. The subsurface shape of the top-basement contact seems to be smooth and simple compared to Line E1. Surface geology, however, clearly shows that further south and up (e. g. Pfaffenchopf in Figure 13.1-14) this contact is folded in a quite complex way. The geometry of this deformation is described in detail in Rohr 1926, Müller 1938, Labhart 1966 and Kammer 1989. Figure 13.1-15 summarizes the observed structures. One of the characteristic features are the axial surfaces with a steep southern dip, which turn horizontal going northward and often end up northdipping within the sedimentary cover. Strangely enough the orientation of the planar fabrics within the crystalline basement remain constant across these structures. Kammer (1985, 1989) could show that the pervasive foliation evolved from a pre-Triassic structure. The Alpine overprint involved two sets of spaced cleavages: a shallow dipping one with "top to the north" movement, and a steeply dipping one with the hanging wall block moving down and southward. Combined movement on these shear surfaces was responsible for much of the internal strain of the large-scale fold structures. As is evident from Figure 13.1-15 (Wetterhörner section) some individual normal faults on the inverted limbs of recumbent anticlines offset the basement-cover contact and contribute to the rotation of the axial surface of the underlying syncline in the cover rocks into its present northern dip. In a general way the observed structures also suggest a mechanically strong basement, deforming as protrusion, i. e. a rigid northward indentation into the cover rocks. The cover rocks, as well as the outermost shell of the basement clearly show signs of an important rotational deformation with a "top to the north and down" shear sense. This rotational strain resulted in folded axial surfaces and thrust faults, including the basal thrust fault of the Helvetic nappes. Based on field work in the area west of line C1 Günzler-Seiffert (1941, 1943) distinguished an early Kiental phase, during which the structurally higher Axen thrust (Wildhorn thrust in the terminology of Günzler-Seiffert) was passively deformed during folding of the underlying Doldenhorn nappe (outcropping in the transect of line NEAT 9001; cf. Figure 13.1-17). In a later stage, the Grindelwald phase, the Doldenhorn thrust was deformed passively by folding within the underlying Aar massif. In any case it is difficult to conceive that the basal thrust faults of the Helvetic nappes were still active during the later stages of the internal deformation of the Aar massif. i. e. the latest stage of basement uplift was post-kinematic with respect to the Helvetic nappes. This scenario can be explained as "in-sequence" thrusting, whereby deformation proceeds downward and towards the external part of an orogen.

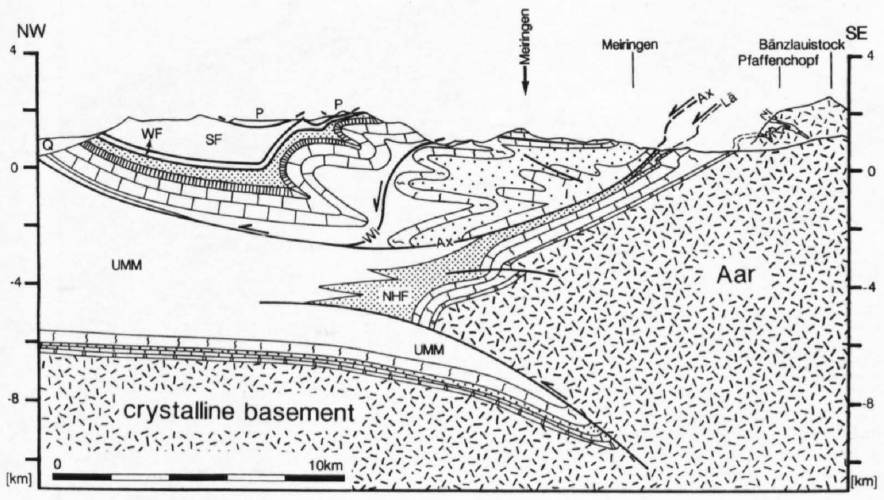

Figure 13.1-14
Geologic profile across the Aar massif along line C1. WF: Wildflysch; SF: Schlieren flysch; Ax, Lä, Wi: Axen, Läsistock, Wildhorn thrust. NHF: North Helvetic Flysch; UMM: Lower Marine Molasse

Figure 13.1-15
Detailed geologic profiles showing deformation style of the basement-cover contact on the northern flank of the Aar massif (Pfaffenkopf equivalent of Figure 13.1-4). Ax, Ho, Lä: Axen, Hohjägi, Läsistock thrust.

13.1.2.3 Transect through the western Aar massif (Line NEAT 9001)

In the course of investigating possible pathways for the NEAT railroad tunnel "Lötschberg-Basistunnel" a seismic section along the Kander and Gastern Valley and several short lines were shot. Although the seismic survey was primarily aimed at very shallow structures and thus only one vibrator was used as energy source, some insight relating to the basement-cover contact on the northern flank of the Aar massif was nevertheless gained. In addition an industry seismic line shot in the northern part of the Kander Vally became available (Vollmayr 1992). It thus seemed logical to summarize the various seismic data and integrate them together with new structural data (Burkhard 1988, Zwahlen 1993) into a geologic section. The section line (Figure 13.1-1) was chosen to follow km 618 of the Swiss National grid net, which follows the eastern flank of the Kander Valley. This transect is particularly interesting for the structure and evolution of the basement uplift, because of its situation at the western end of the Aar massif dome, where due to axial plunge a complete section can be observed at the surface. The section was therefore extended all the way across the massif, which is subdivided into the Gastern massif and Aar massif proper. The Gastern massif corresponds to a northern block of the Aar massif, separated from the latter by a thin layer of Mesozoic carbonates, the so-called "Jungfrau-Keil".

The segment of the seismic line NEAT 9001 shown in Figure 13.1-16 is located in the southernmost Kander Valley (Eggeschwand), follows the gorge Chluse and the Gastern Valley up to Gastere. Three reflection groups (1, 2 and 3 in Figure 13.1-16) can be recognized. Reflection 1 is interpreted to originate from the (top of) the Mesozoic carbonates overlying the Gastern massif basement beneath Eggeschwand. Reflection 2 lines up with the top of the Gastern massif outcropping at the SE end of the section. At Gastere the Gastern granite is overlain by Triassic Röti dolomite, followed by an inverted sequence of Jurassic limestones pertaining to the Doldenhorn nappe. The contact itself (4 in Figure 13.1-16) is marked by a thin calc mylonite. Reflection 1 and 2 do not line up. They are offset by reflection 3, which is interpreted to stem from a S-dipping thrust fault (associated with mylonites). In the interpretation given in Figure 13.1-17 this thrust fault does not dissect the Doldenhorn thrust. Rather it separates the southern Gastern massif, which has only remnants of Mesozoic cover sediments, from the northern Gastern massif, which has a more complete Mesozoic cover, comparable to the one observed in the industry line at the northern end of the geologic profile of Figure 13.1-17. The seismic data of this industry line suggests that the leading edge of the Aar massif consists of a stack of imbricates overriding the autochthonous foreland (Vollmayr 1992).

From the cross section in Figure 13.1-17 it follows that the Doldenhorn nappe consists of a series of recumbent folds whose axial surfaces are warped around the top of the Aar massif. The Doldenhorn nappe roots in the southern Aar massif, the latter forming the cores of its anticlines in the south of Figure 13.1-17. Here the crystalline basement deformed in a style which is in striking contrast to the one observed in the north: as discussed by Steck (1984) a penetrative foliation (S_2) is parallel to the axial surface of these folds and is overprinted by two spaced cleavages (S_2' and S_2''). S_2' is gently south dipping with "top to the north" movement, while S_2'' dips steeply north and has a "top to the south and up" shear sense. These structures also prove that the internal deformation of the Aar massif is coeval with folding within the Doldenhorn nappe. The Late Jurassic and Cretaceous carbonates were transported northward and a clear thrust fault marks the base of this nappe above the Gastern massif. Folding of the Doldenhorn nappe also affected the overlying Gellihorn and Wildhorn nappes, whose basal thrust faults were passively deformed in the process. The kinematic sequence in this transect was analyzed by Burkhard (1988) who defined the following deformation phases:

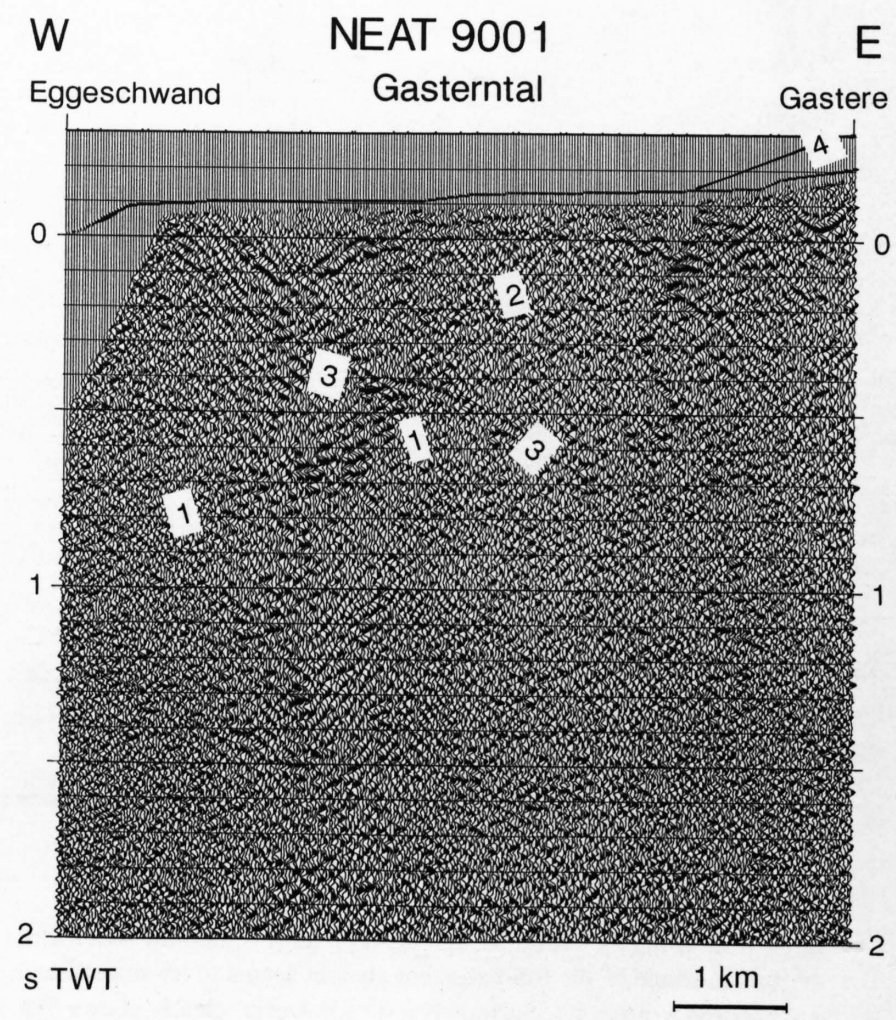

Figure 13.1-16
Detail of seismic line NEAT 9001 (Gasterntal). 1: Mesozoic cover of N Gastern massif, 2: Top of Gastern massif and Doldenhorn thrust, 3: thrust fault, 4: top Gastern massif and Doldenhorn thrust at surface.

1. Plaine Morte phase: Emplacement of detached, highly allochthonous cover strip sheets (Ultrahelvetic nappes).

2. Prabé phase: This phase corresponds to the main internal deformation of the Wildhorn and Gellihorn nappes, including imbrications and tight folding associated with an axial planar cleavage. These nappes were already thrust northward in this phase to rest on the future Aar massif.

3. Trubelstock phase: Local passive folding of the Wildhorn nappe due to activation of thrust faults in its footwall (Plammis and Jägerchrüz imbricates).

4. Kiental phase: Formation of the Doldenhorn nappe including pervasive internal deformation (and uplift) of the southern Aar massif and passive deformation of the overlying Gellihorn and Wildhorn nappes.

5. Grindelwald phase: This phase (considering the original definition by Günzler-Seiffert 1941 as well) is related to the rotation of the axial surfaces of the recumbent folds and the basal thrust of the Doldenhorn nappe in its northern part. It thus clearly relates to an episode of basement uplift.

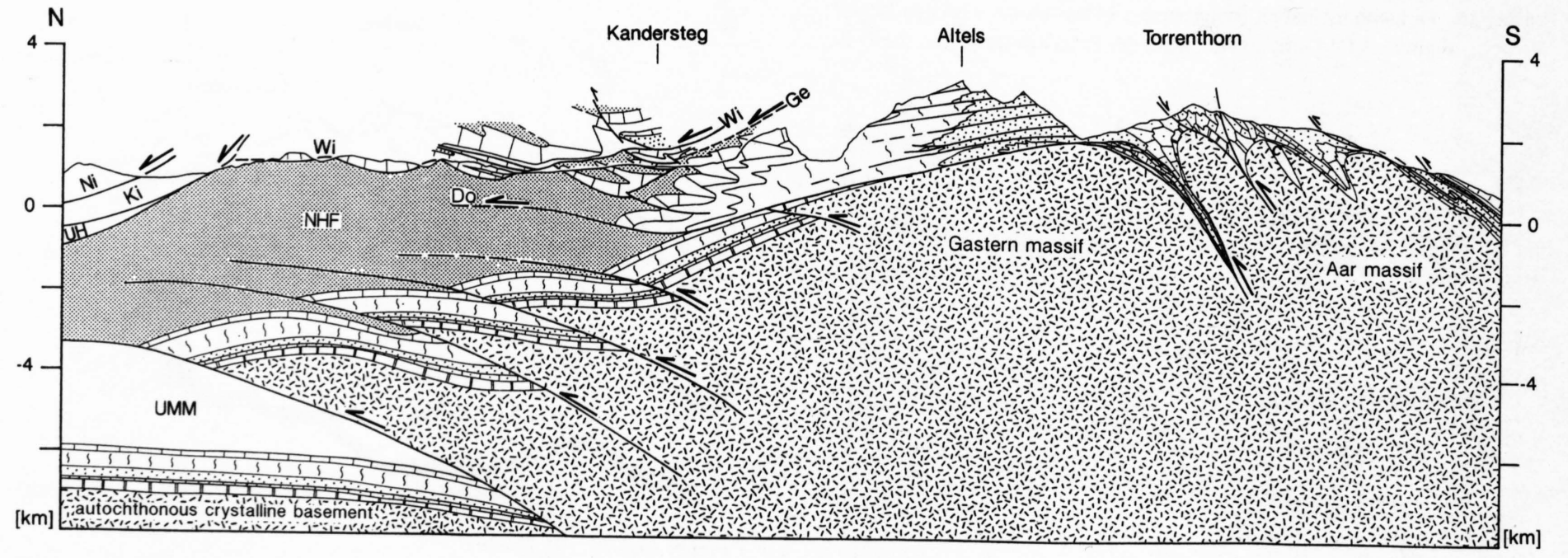

Figure 13.1-17
Geologic profile across the western end of the Aar massif drawn along km 718 and constrained seismic line NEAT 9001 and industry line. Do, Ge, Wi: Doldenhorn, Gellihorn, Wildhorn thrust, Ni: Niesen nappe (Penninic), Ki: Kiental flysch, UH: Ultrahelvetic, NHF: North Helvetic Flysch, UMM: Lower Marine Molasse.

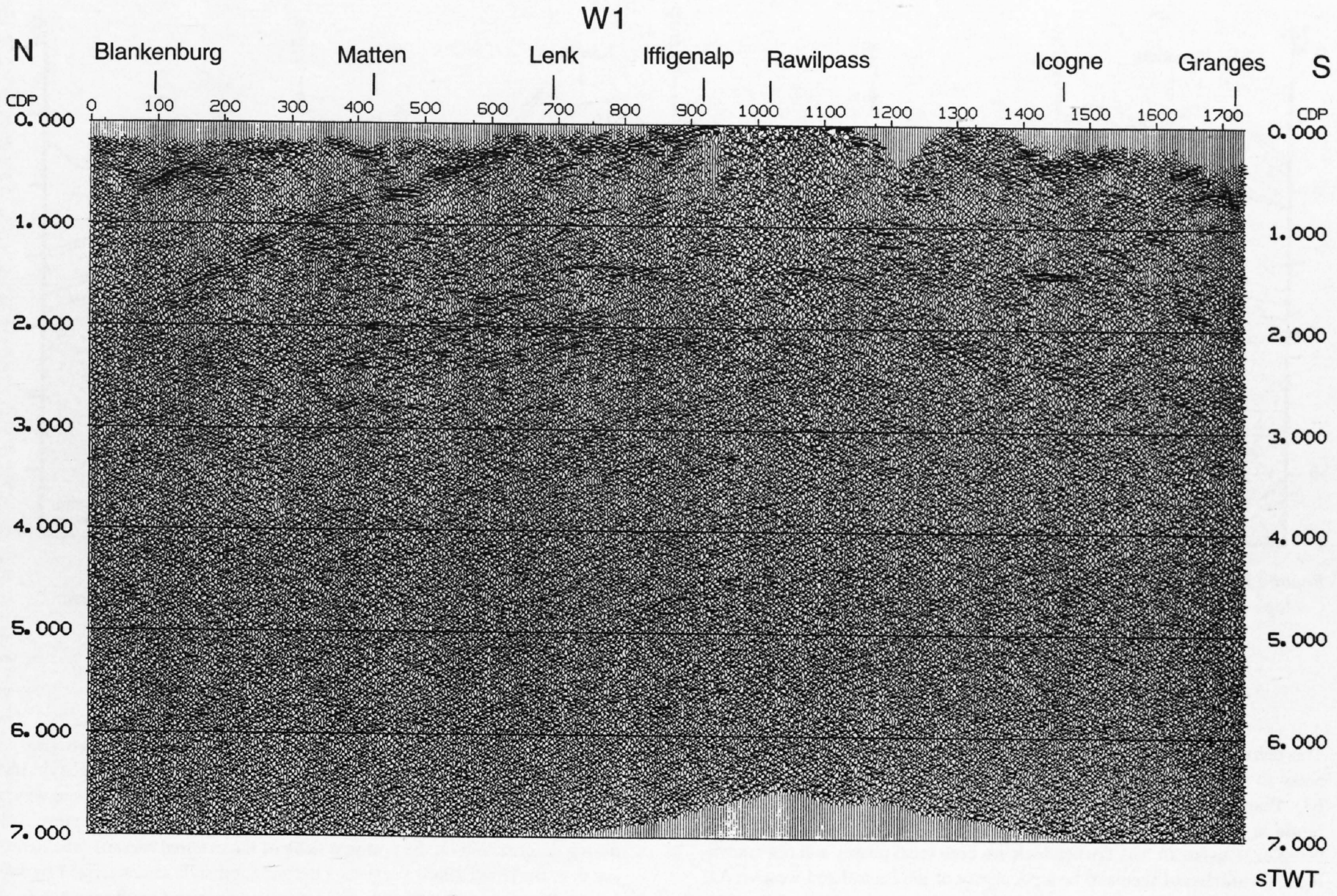

Figure 13.1-18
Seismic section W1 covering the basement uplift in the Rawil depression between Aar and Aiguilles Rouges/Mt. Blanc massif.

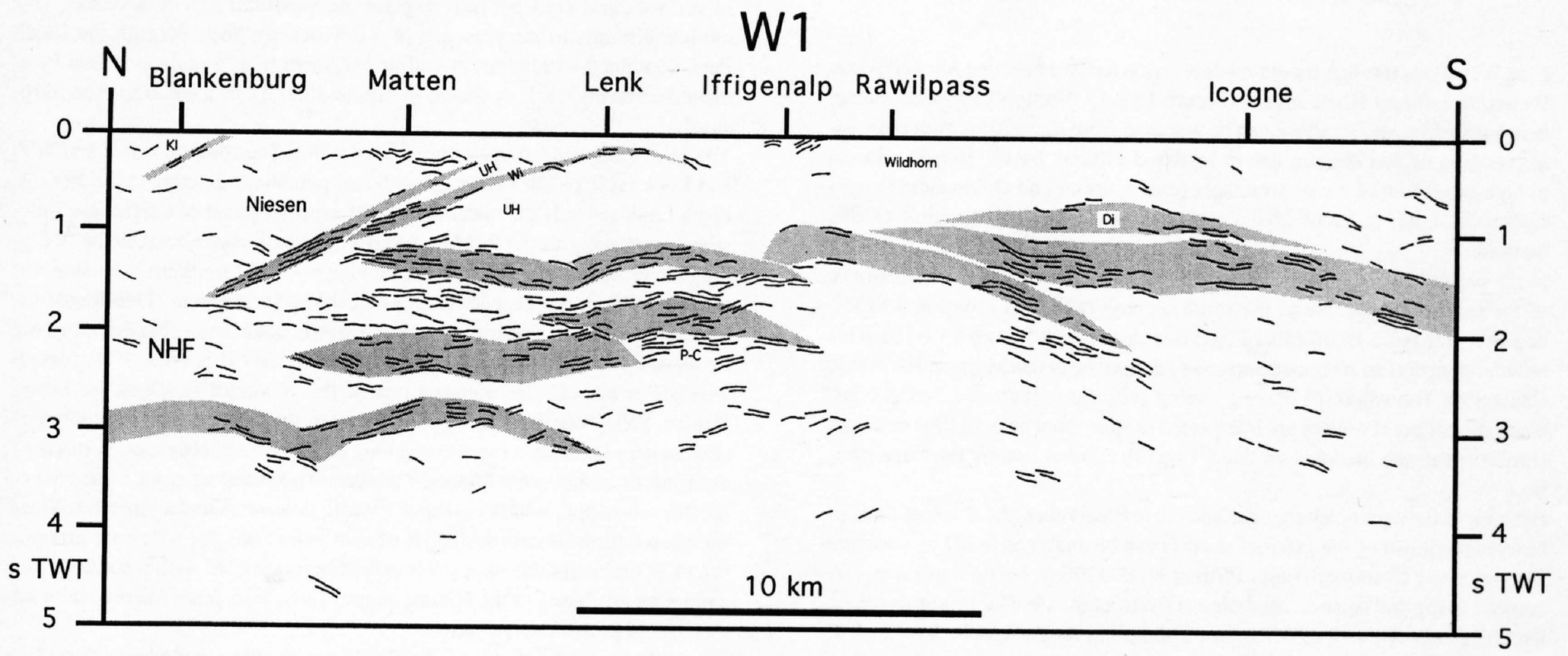

Figure 13.1-19
Line drawing of line W1. Gray shading: Mesozoic cover and panels of carbonates/evaporites representing potential reflectors discussed in text.
Di: Diablerets nappe (Helvetic)
Kl: Klippen nappe (Préalpes médianes, Penninic)
Wi: Wildhorn nappe (Helvetic)
NHF: North-Helvetic Flysch, UH: Ultrahelvetic nappes

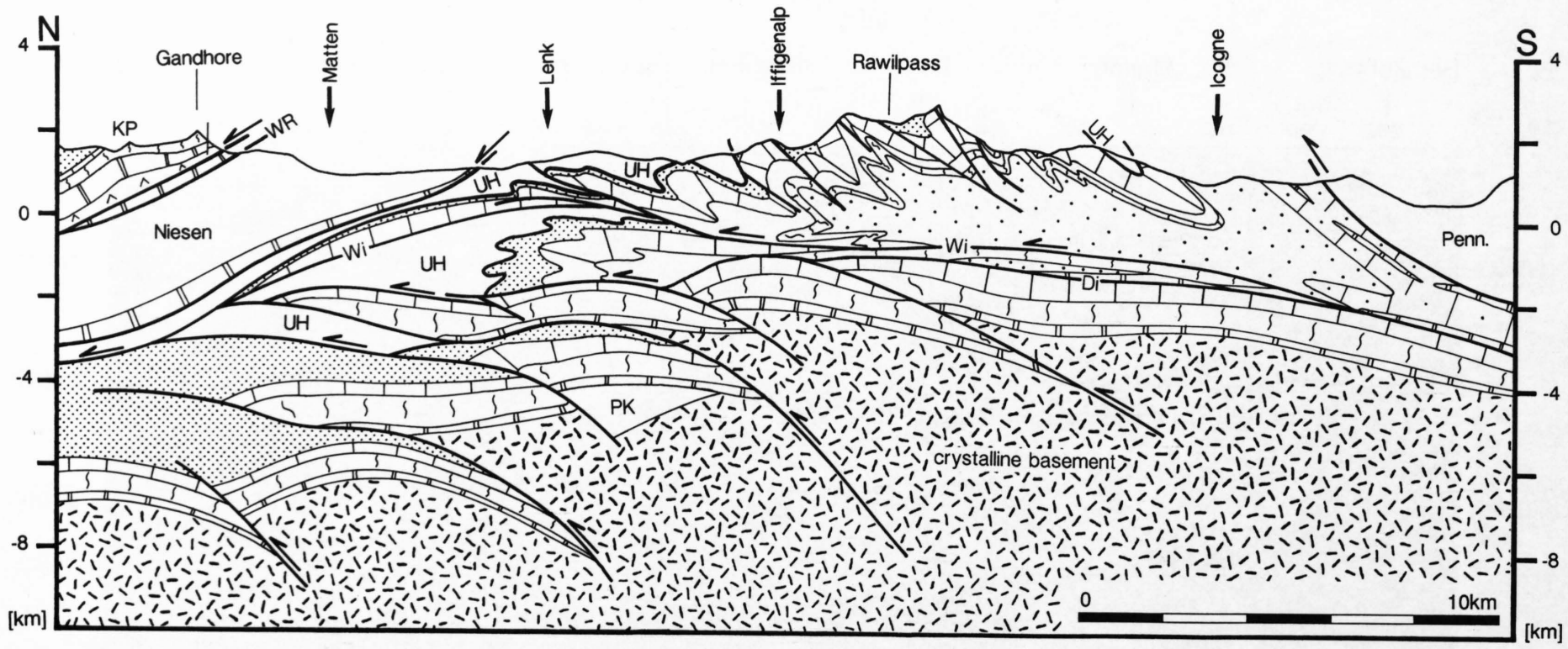

Figure 13.1-20
Geologic profile of line W1. KP: Klippen nappe, WR: Wierihorn slice, UH: Ultrahelvetic; PK: Permo-Carboniferous; Di, Wi: Diablerets, Wildhorn thrust.

This deformation sequence shows some striking similarities as well as differences to the one at the eastern end of the Aar massif described above (line E1). **Plaine Morte** and **Pizol** are equivalents. **Prabé** is comparable to **Calanda** in the Helvetic nappes, and **Kiental** to **Calanda** in the Infrahelvetic complex. **Cavistrau** and **Trubelstock** are both local phases and not equivalents. **Grindelwald** seems to be a pecularity of the central and western Aar massif! It has to be stressed again that the above mentioned correlations are kinematic and are not meant to be strictly chronological. Considering the deformations related to vertical uplift of the Aar massif and nappe transport of the Helvetic nappes, this western transect clearly shows a phase (**Grindelwald**, and to some extent **Kiental**) of post-kinematic uplift conspicuously absent in the eastern transect (E1). This point will be discussed further in section 13.1.4. In the kinematic interpretation of Steck (1984) the emplacement of the Wildhorn nappe onto the Doldenhorn nappe is largely post Doldenhorn folding (Kiental phase), which is however in contradiction to the findings of Günzler-Seiffert (1941, 1943), Burkhard (1988) and data discussed above.

13.1.2.4 Transect through the Rawil depression (Line W1)

Line W1 passes through the Rawil depression located between Aar and Aiguilles-Rouges/Mont Blanc massif (Figure 13.1-1). The top-basement contact is in subsurface and its shape can be assessed from the seismic data only. Interpretation of this seismic line is rendered difficult by the fact that downplunge projection of nappe structures (e. g. Morcles and Doldenhorn) imply distances of the order of 20 km which is at, or beyond the limit of this method.

In the seismic section shown in Figure 13.1-18 the autochthonous Mesozoic of the foreland gives rise to the south dipping reflection group at 3 sTWT beneath shot point Blankenburg (see line drawing in Figure 13.1-19). This reflection group can be traced northward across the entire Molasse Basin (see Chapter 8). The adjoining arcuate shaped reflections at around 3 sTWT just south of shot point Matten are interpreted to stem from an anticlinal structure similar to the one modeled on line E1 and situated at exactly the same position.

Because of the significant plunges and the vertical relief, the shape of the top-basement contact of the external massifs can be analyzed in 3D by structure contour maps (Burkhard 1988, Pfiffner et al. 1990a). Using these structure contour maps and seismic modeling (Levato et al. 1994) the prominent reflection group at 1.4–2 sTWT beneath shotpoint Icogne can be identified as autochthonous massif cover with some confidence. The south dipping reflections just to the north and beneath, extending from 1.5 to 2.5 sTWT can be attributed to a pinched-in layer of Mesozoic carbonates similar to the Jungfrau-Keil between Gastern and Aar massif in the transect of NEAT 9001 (Figure 13.1-17) observed in the old Lötschberg tunnel. Between shotpoint Lenk and the Rawil pass identification of the Mesozoic cover on the seismic section is much more difficult and ambiguous. In the interpretation shown in Figures 13.1-19 and 13.1-20 individual reflection packages were assigned to slabs of Mesozoic cover rocks. These were connected using the style observed farther east between lines C1 and E1, i. e. wedges of basement which are thrust northward. Moreover, an estimate of the p-T conditions prevailing during deformation on the northern flank of the external massifs (anchizone see e. g. Burkhard 1988) suggests a deformation style characterized by imbricate thrusting, rather than ductile folding as observed on the south side of the Aar massif (where deformation occurred under epizonal conditions).

The space between the massif's cover and the topographic surface devoid of reflections was filled with the Wildhorn nappe, whose geometry is quite well constrained by surface geology. Equivalents of the Morcles and Doldenhorn nappes, if at all, must be sought at different locations in this section because of the en échelon pattern of their hinge lines (Pfiffner 1993). The Morcles fold nappe projects to the space beneath shot points Iffigenalp and Lenk, while the Doldenhorn nappe must be sought – if at all – south of Rawil pass. In any case the basement top can be positioned at a maximum elevation of –3000 m to –4000 m in this transect, i. e. some 7 km lower as compared to the adjoining highs in the Aar and Aiguilles-Rouges/Mt. Blanc massifs. Gravimetric modeling by Klingelé (Chapter 13.2) suggests that a top basement contact at –2.5 km (taken from structure contour maps based on projection of surface data) does not fully explain the measured gravity anomaly. This modeling points to the presence of a low density body beneath the Rawil Pass, contained within the crystalline basement (e. g. a graben of Late Paleozoic sediments, such as shown in Figure 13.1-20, or a leuco-granite intrusion).

The N-dipping reflections between shot points Blankenburg (at 1.8 sTWT) and Lenk (at 0.2 sTWT) line up with two potential reflectors at the surface. From Lenk towards the north one might expect a panel of Cretaceous limestones pertaining to the Wildhorn nappe; it would correspond to the N-dipping Cretaceous linking the Wildhorn nappe with its northern extension, the so-called Randkette (border chain) of central Switzerland. This Randkette extends from Lake Lucerne (Pilatus) towards Lake Thun (Niederhorn), but its westerly continuation is uncertain. In particular it is open to discussion whether or not the Cretaceous strata of the Wildhorn nappe in the Lower Kander Valley continue to the NW beneath the Niesen. The interpretation chosen here includes a moderately long panel of Cretaceous strata reaching as far north as shot point Matten. The second potential reflector is the base of the Niesen nappe, which contains Triassic dolomites and evaporites. Since the Niesen thrust breaks surface N of shot point Lenk the reflection group at 0.2 sTWT beneath this shot point extending northward with a northerly dip cannot be attributed to the Niesen nappe. Thus, both potential reflectors are considered in this interpretation.

The N-dipping reflections at 0.4 sTWT beneath shot point Blankenburg line up with the evaporites and dolomites at the base of the Klippen nappe. As discussed in Chapter 8 these evaporites attain greater thicknesses further north (base of Klippen nappe in line W7).

An alternative interpretation of line W1 is given by Steck et al. in Chapter 12. In that interpretation the Niesen nappe is wrapped around a large recumbent fold (its inverted limb is taken to be represented by the gently S-dipping

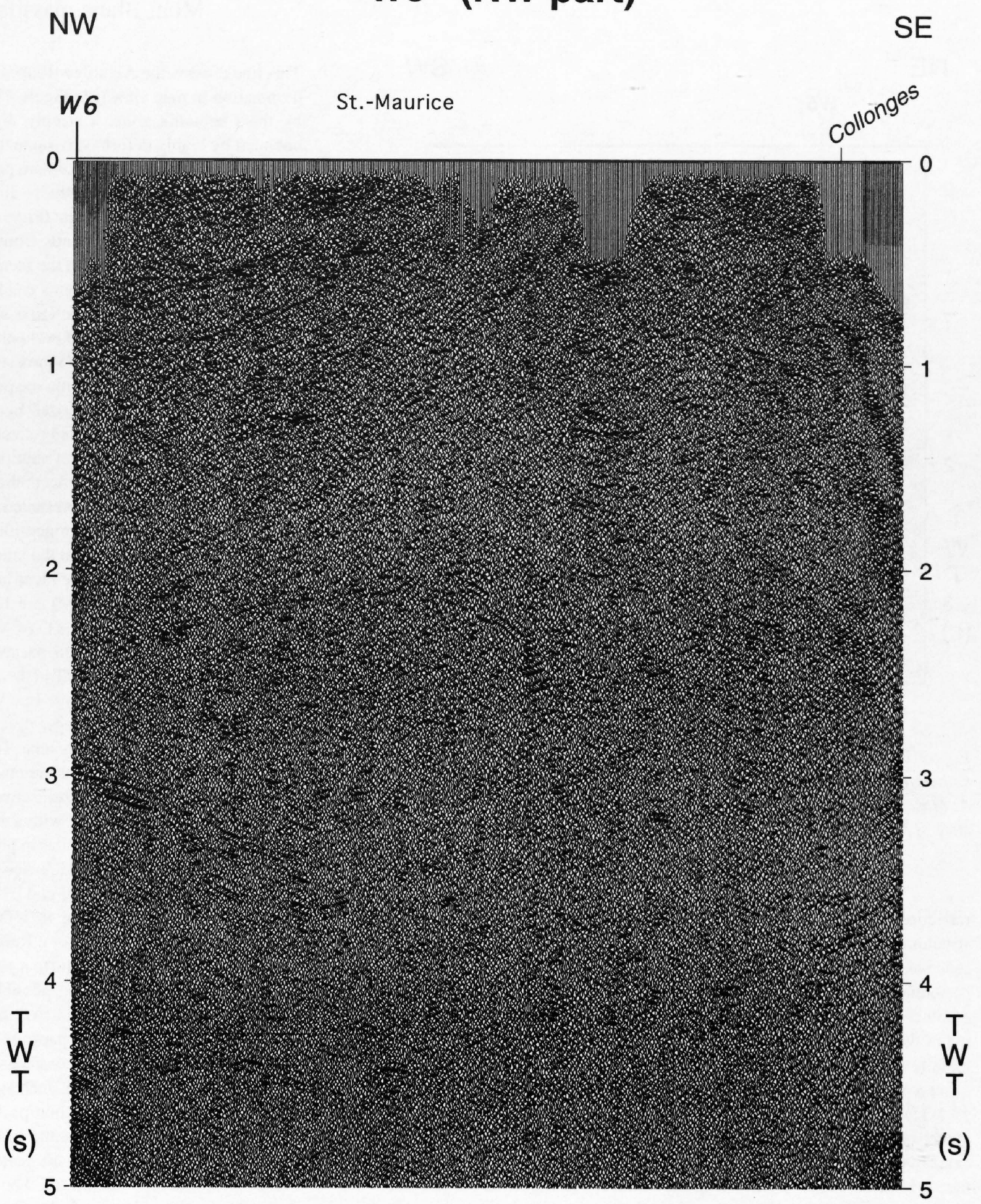

Figure 13.1-21a
Seismic section W5 (NW part) covering Aiguilles Rouges massif. Unmigrated Vibroseis stack.

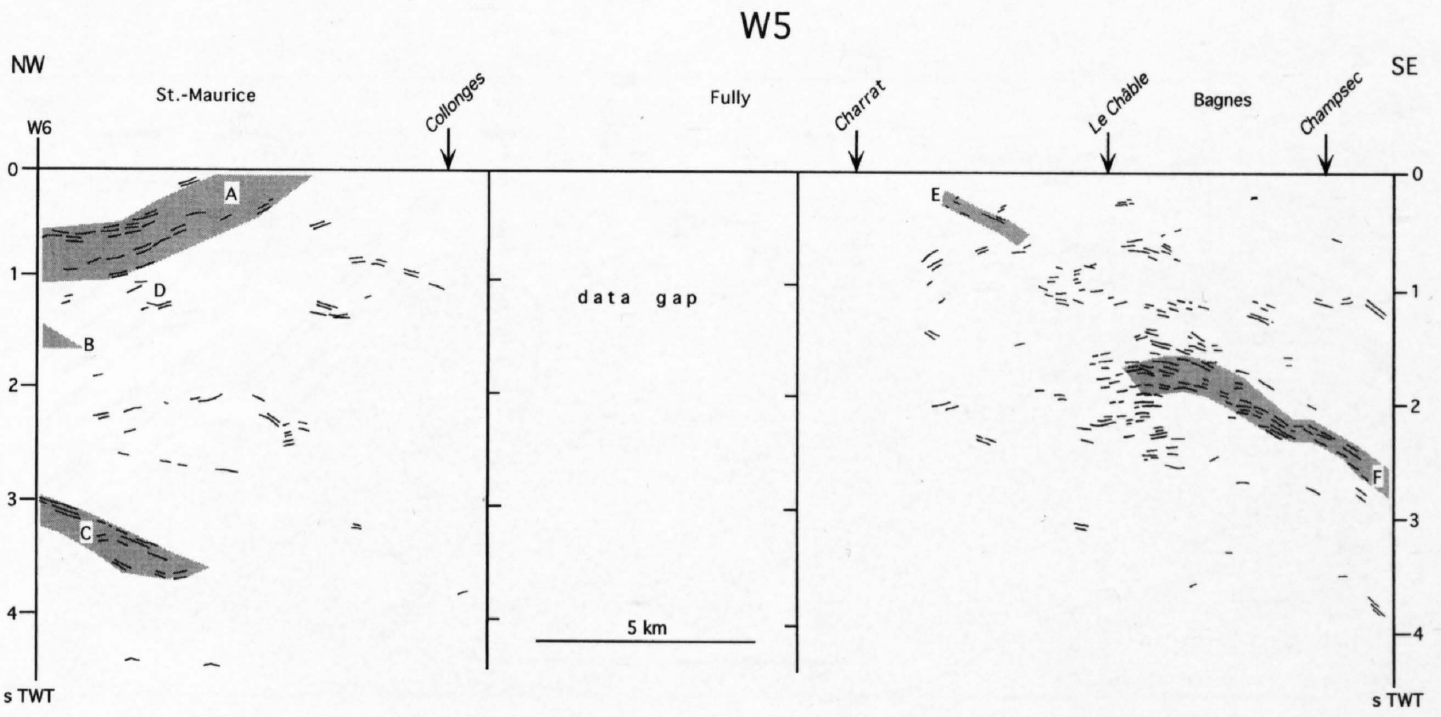

Figure 13.1-21b
Line drawing of unmigrated Vibroseis stack W5. Gray shading: Mesozoic cover representing potential reflectors discussed in text. A: Mesozoic cover of top of Aiguilles Rouges massif, B: Slice of Mesozoic inferred from line W6, C: Foreland Mesozoic cover, D: Permo-Carboniferous, E, F: Mesozoic cover of Mt Blanc massif.

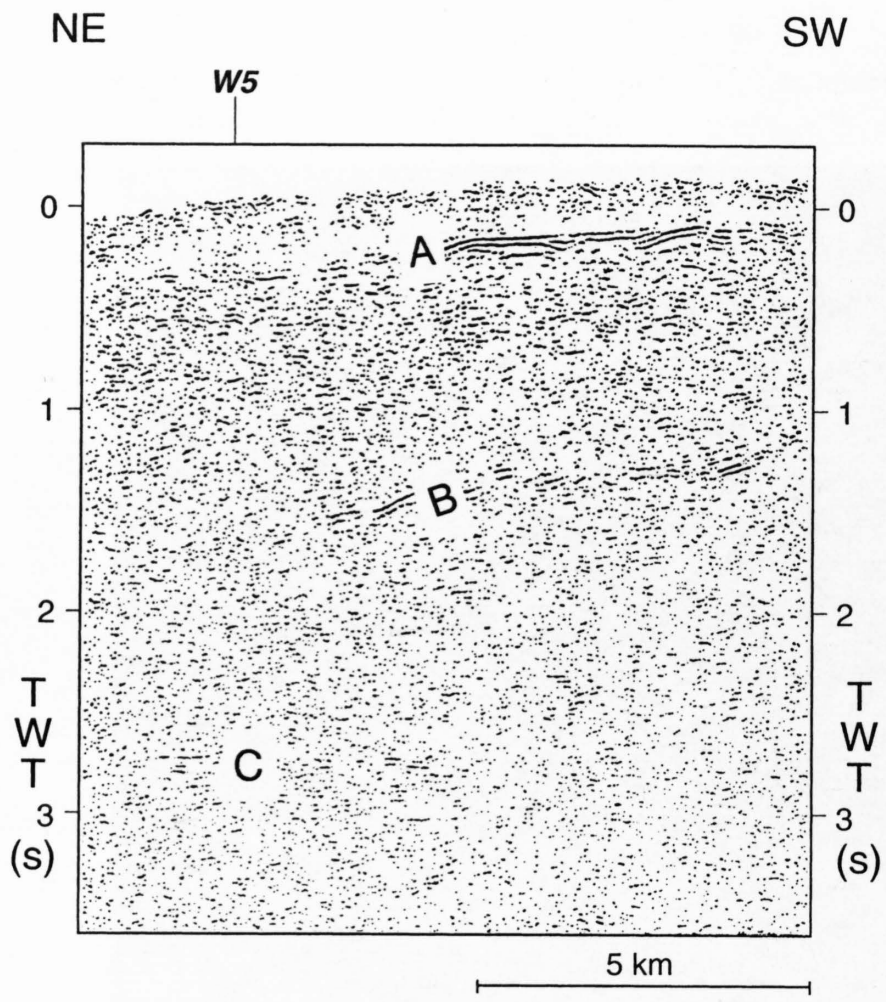

Figure 13.1-21c
Coherency filtered Vibroseis stack of strike line W6.
A: Mesozoic cover of top of Aiguilles Rouges massif, B: Mesozoic cover of a slice of Aiguilles Rouges massif, C: Foreland Mesozoic cover.

reflections at 1.5 sTWT beneath shot points Matten and Lenk). Given the structural style of the Niesen and overlying Klippen nappe, and given the absence of any sign of such a large scale fold in the area to the NW of line W1, preference is given to the solution presented in Figures 13.1-19a and 13.1-20. Another difference concerns the style of basement involvement. Ductile folding of the basement clearly can be recognized in the southern part of the Aar massif, where it occurred under greenschist facies conditions. The structures observed in the north cannot be described as "ductile folds" (see e. g. Figure 13.1-15). Also mapping of the overlying Mesozoic cover suggests a predominance of thrust faulting on the northern flank of the Aar massif. Furthermore extensive imbrications are indicated by seismic data (see Vollmayr 1992 and transect NEAT 9001). Considering the relatively low, anchizonal temperatures prevailing during formation of the basement-cover structures in the northern part of line W1, the structure style shown in Figure 13.1-20 seems more plausible.

13.1.2.5 Transect through the Aiguilles-Rouges and Mont Blanc massifs (Line W5)

This line crosses the Aiguilles-Rouges and Mont Blanc massifs at their NE termination in map view (see Figure 13.1-1). The two massifs are separated by the Chamonix zone, a steeply dipping layer of Mesozoic sediments bounded by highly deformed basement rocks.
The Vibroseis data from the northern part of line W5, covering the Aiguilles-Rouges massif, shows slightly N-dipping reflections at 0.4–0.8 sTWT leveling off towards the north (Figure 13.1-21a). Another coherent band of S-dipping reflections extends from 3 sTWT beneath the northern end southward. In the remainder of the section shown in Figure 13.1-21a, various incoherent short reflection events can be recognized. A hand-produced line drawing of this unmigrated section is shown in Figure 13.1-21b. Reflections were hand-picked based on an evaluation of their amplitude and lateral continuity. The southern part of (Vibroseis) line W5, crossing the Mont Blanc massif and some of the Penninic nappes, was also included in this analysis. This southern part is characterized by predominantly S-dipping reflections, some N-dipping reflections, and reflections defining an antiformal structure at around 2 sTWT just south of shot point Le Châble. We feel that this line drawing (Figure 13.1-21b) reflects the seismic data more closely than the hand-produced line drawing presented in Chapter 12 (Figure 12-12).
Figure 13.1-21c shows a coherency-filtered seismic section of line W6. This strike line intersects line W5 at the latter's northern end (see Figure 13.1-1). Two reflection packages can be identified in line W6, extending from the SW end at 0.2 (A in Figure 12-21c) and 1.2 sTWT (B in Figure 12-21c) to the NE. They are at 0.4 and 1.6 sTWT where lines W6 and W5 intersect. A deeper subhorizontal reflection package (C in Figure 12-21c) can be observed between 2.7 and 3 sTWT in the NE part of line W6. Reflections A and C can be correlated into seismic line W5, where they correspond to the N- and S-dipping reflection packages described above; in Figure 13.1-21b these packages are outlined by a gray tone. The equivalent of B has also be marked – although no actual reflections are observed in line W5. Reflection package A can be linked with the Mesozoic cover of the Aiguilles-Rouges massif that disappears into the subsurface with a northerly dip just S of St-Maurice. Reflection package C is very similar in position and character to the reflections from the Mesozoic foreland sequence observed in the other lines described in this chapter (namely W1, C1 and E1). Considering surface data the Mesozoic sediments corresponding to reflection package A form an anticline (located to the NW of Monthey). Reflection package B in line W6 (Figure 13.1-21c) is likely to correspond to a panel of Mesozoic strata, too, the strong double cyclic band originating possibly from the Triassic dolomites. Thus two thrust faults must be postulated, one between A and B, one between B and C. The fact that reflection package B is not observed in line W5 suggests that the upper fault has a southeasterly dip and cuts out the Mesozoic section corresponding to B in line W5, such as shown in the geologic profile in Figure 13.1-22. Missing of reflection package B in line W5 is in part possibly also due to the low coverage at the end of the seismic line. The scattered reflections D (Figure 13.1-21b) are tentatively interpreted as stemming from Permo-Carboniferous sediments. The latter are shown as pertaining to a Permo-Carboniferous graben whose inversion was associated with the upper of the two thrust faults discussed above. A similar inversion structure can be observed at the surface in the case of the Salvan-Dorénaz graben, which is

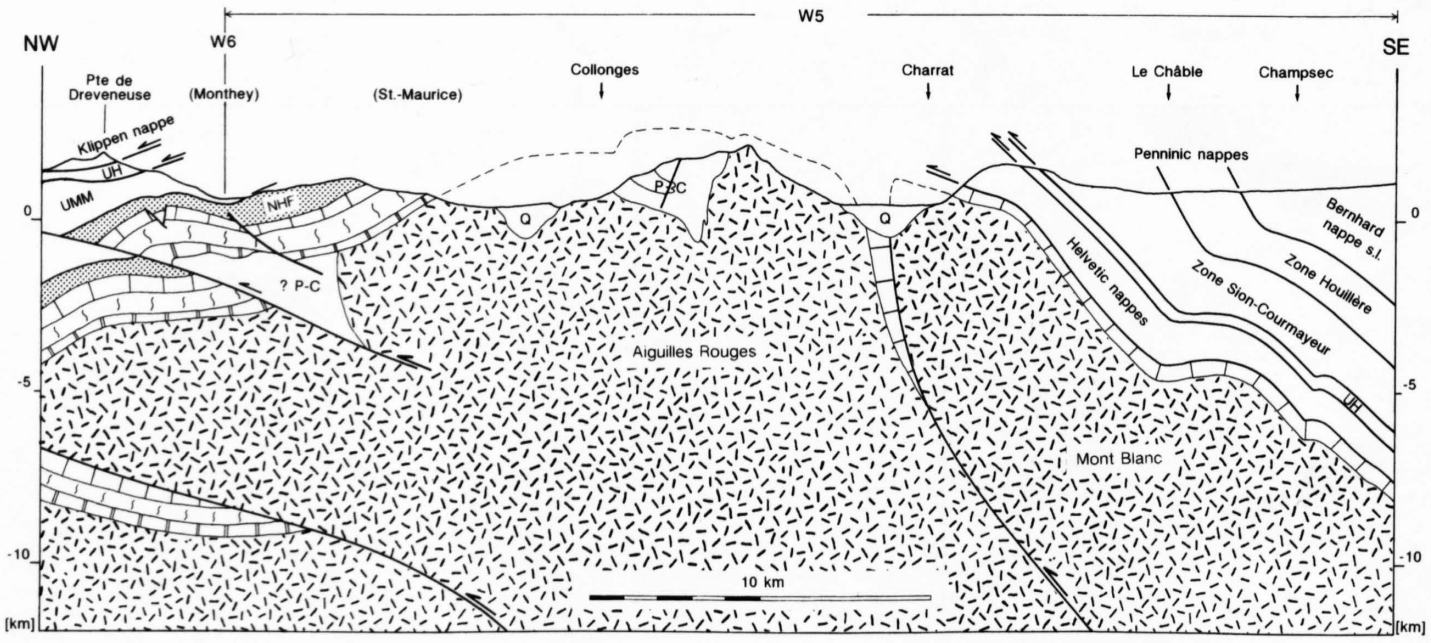

Figure 13.1-22
Geologic profile of line W5.
NHF: North-Helvetic Flysch, UMM: Lower Marine Molasse, UH: Ultra-Helvetic nappes, P-C: Permo-Carboniferous, Q: Quaternary

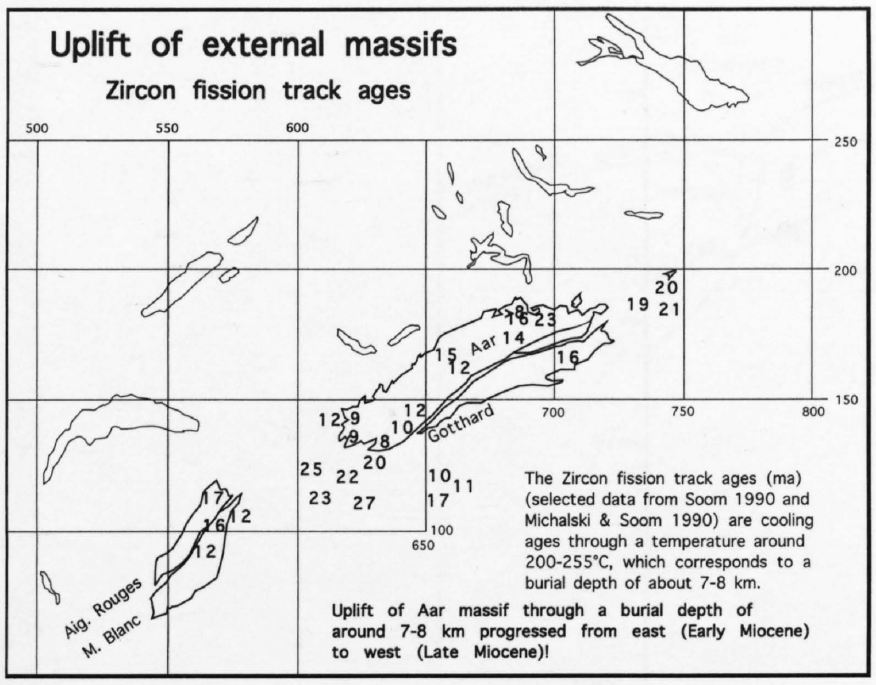

Figure 13.1-23
Zircon fission track ages of external massifs.

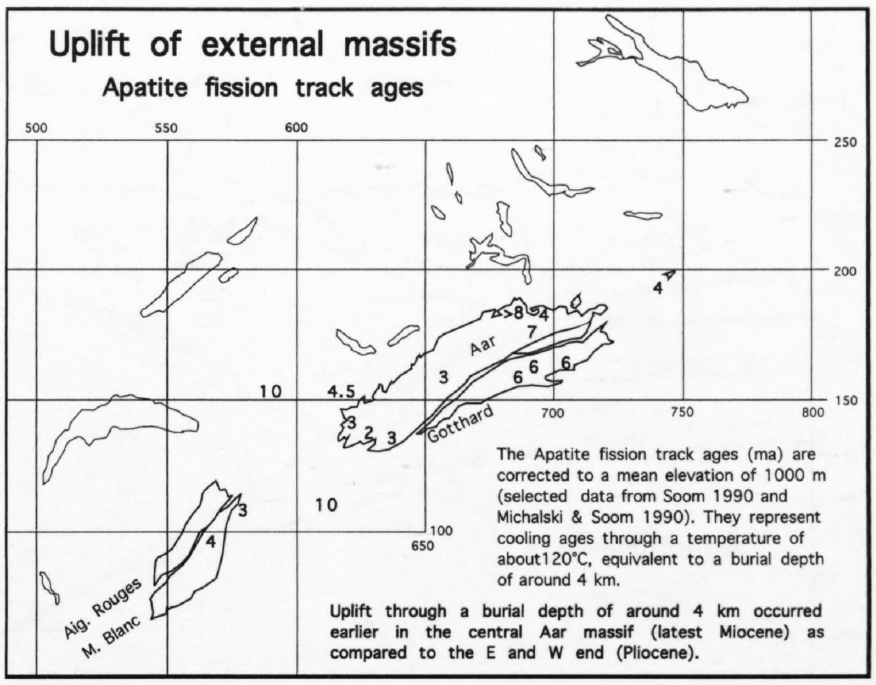

Figure 13.1-24
Apatite fission track ages of external massifs.

crossed by line W5 just south of shot point Collonges (see Figure 13.1-22). The SE-part of line W5 is more ambiguous to interpret. Surface data suggest that the SE dipping reflections between Charrat and Le Châble (marked E in Figure 13.1-21b) could stem from the Mesozoic carbonates overlying the Mt. Blanc massif. The continuation of these reflections to depth is not as straight as shown in Chapter 12 (Figure 12-12), although a general SW dip of the top basement contact must be assumed. In the interpretation drawn in the geologic profile of Figure 13.1-22, the reflection package marked F in Figure 13.1-21b, containing two antiformal structures was used as basis. Subhorizontal and slightly N-dipping reflections similar to the ones shown in Figure 13.1-21b have also been reported from the explosion seismic experiment of line W5 (line WBG in Levato et al. 1993). It is clear that the interpretation given in the geologic profile is not unique, in that not all of the numerous subhorizontal reflections at 1.5 and 2.7 sTWT are explained. Since the seismic line W5 is oblique to the structural trend of the top the Mt Blanc massif out-of-plane reflections are likely. In addition (doubly plunging) antiformal structures such as proposed in this interpretation could well give rise to multiple reflections. The shallower reflections beneath shot points Le Châble and Champsec might well originate from within the Helvetic and Penninic nappes. In any case the solution proposed in Chapter 12 (Figure 12-13 with a flat, SW-dipping top Mt Blanc basement does in our view not satisfactorily explain the seismic data.

The Chamonix zone between Aiguilles-Rouges and Mt Blanc massif reaches the surface within the data gap in line W5 (see Figure 13.1-21b). Its geometry in the geologic profile of Figure 13.1-22 reflects its subvertical orientiation at outcrop and in the deeper part a change to a steep SE-dip is compatible with a top-to-the-NW thrusting direction. Viewed at large scale, the two external massifs in this westernmost transect show imbrications with fault displacements of more than 5 km (? up to 10 km) along the basal thrust of the Aiguilles-Rouges and the Mt Blanc massif. Internal structures include thrust faulting and folding in the Aiguilles-Rouges massif and more ductile folding in the Mt Blanc massif. This difference in style could reflect the higher metamorphic grade of the Mt Blanc massif. Thrust faulting in the Aiguilles–Rouges massif might have been facilitated by pre-existing, Permo-Carboniferous graben structures.
An alternative interpretation of line W5 is presented by Steck et al. in Chapter 12.

13.1.3 Uplift history from cooling ages

The crystalline basement rocks of the external massifs were burried by crustal stacking in the course of the Alpine compression. Burial resulted in a metamorphism reaching greenschist facies conditions, i. e. temperatures up

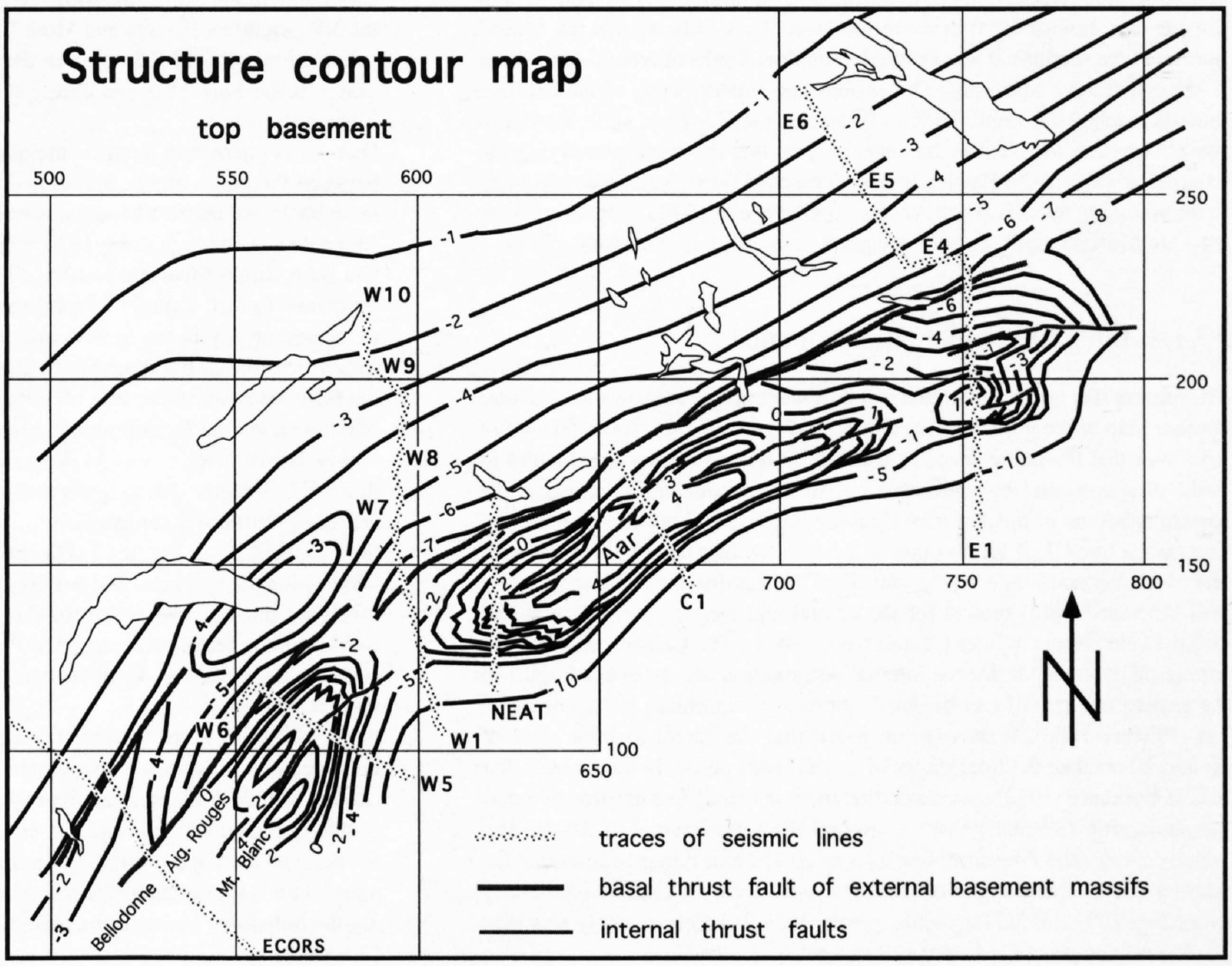

Figure 13.1-25
Structure contour map "top basement" covering N-Alpine foreland and external massifs.

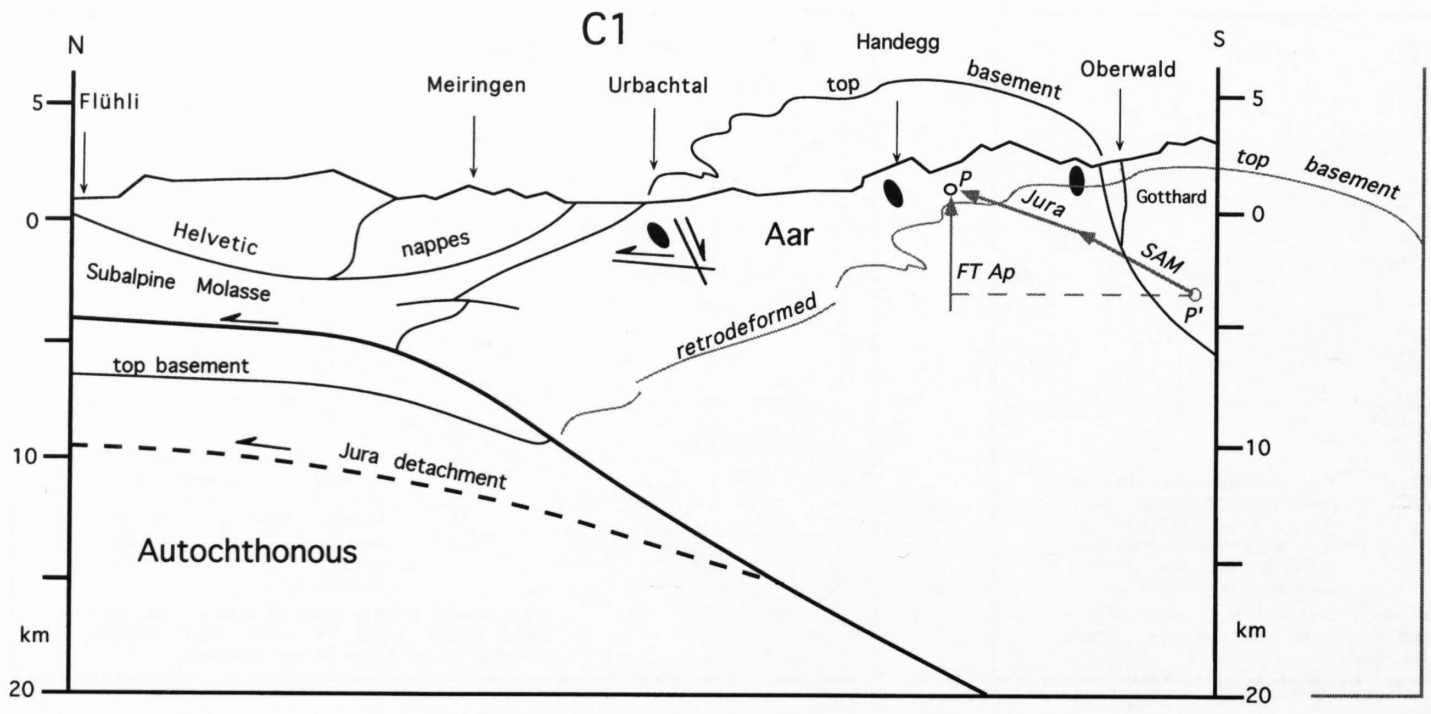

Figure 13.1-26

Kinematics of basement uplift along seismic line C1 (Haslital-Grimsel). Present-day shape of "top basement" is as determined from seismic and surface data, extrapolated across culmination. Black ellipses represent Alpine finite strain. Retrodeformation of material point P is by inversion of movements along the putative Jura detachment (5.5 km) and thrust fault at the base of the Subalpine Molasse (SAM, 6 km). Retrodeformed "top basement" was stretched horizontally in the southern Aar massif to account for ductile shortening in this part of the massif. FT Ap: Apatite fission-track data (uplift component).

to about 350 °C in the southern Aar massif. Subsequent uplift thus invoked cooling through the "closing temperatures" of the Zircon and Apatite fission track systems. Zircon fission tracks are thought to record cooling through the temperature interval of 200 – 255 °C which can be expected at depths of about 7-8 km. The Apatite fission tracks record cooling through a temperature around 120 °C, which is equivalent to a burial depth of around 4 km. Uplift and cooling ages are discussed in more detail by Hunziker et al. in Chapter 20.

One of the questions that was addressed by NRP 20 was the possible relation between axial plunges and cooling ages. The results of the investigations by Soom (1990) and Michalski & Soom (1990) are summarized in Figures 13.1-23 and 13.1-24, in which in some instances groups of measurements are represented by mean values. The Zircon data (Figure 13.1-23) suggest that the eastern Aar massif was uplifted earlier than the central and western Aar massif and the NE end of Aiguilles-Rouges/Mont Blanc. It reached shallow crustal levels of 7– 8 km depth about 20 Ma ago (Early Miocene) as compared to 10–15 Ma (Late Miocene) for the more westerly parts. The 20–27 Ma data in the Rawil depression are from overlying nappes and record their uplift in the course of nappe stacking. The Apatite data in Figure 13.1-24 are corrected to a mean elevation of 1000 m above sea level. They indicate that the central portion of the Aar massif was uplifted to shallow depths of around 4 km about 5 Ma ago (Latest Miocene). The eastern and western ends of the external massifs reached this depth later, in Pliocene times (2–4 Ma ago). Similar to the Zircon data, the Apatite data also suggest that the nappes overlying the external massifs in the Rawil depression reached these shallow depths prior to the adjoining massifs. Their Apatite cooling age of 10 Ma probably reflects the Late Miocene uplift episode recorded in the adjoining massifs.

13.1.4 Integrated kinematic sequence

The present day shape of the external basement uplifts is shown as structure contour map of the top-basement contact in Figure 13.1-25. From this figure it follows that the dome shape is affected by several substantial changes in strike directions and by faults that cut structure contours. Comparing the eastern subdome of the Aar massif (along line E1) and the central culmination (along line C1) it follows that in the east, the basement uplift is broader and of smaller amplitude. At the same time this eastern transect also lacks the post-kinematic uplift typical for the central and western part (Kiental and Grindelwald phases in lines C1 and NEAT 9001). The Calanda phase of deformation, responsible for the internal deformation and associated uplift of the eastern Aar massif can be dated as pre-metamorphic, i. e. Oligocene in age (Pfiffner 1986). It thus is concluded that the Zircon cooling ages of around 20 ma date the final stages of this Calanda phase. In the western Aar massif Burkhard (1988) speculated that the Aar massif was uplifted by internal shortening (Kiental phase) at around the time interval of 20–10 Ma, which contains the Zircon cooling ages of 10 – 15 Ma. It thus follows that the internal ductile deformation of the Aar massif occurred under temperatures exceeding 200 – 255 °C (or depths greater than 7– 8 km, probably less than 12–15 km) and proceeded from east to west.

Additional shortening and uplift of the massifs post-dating the emplacement of the overlying Helvetic nappes was restricted to the central and western Aar massif and the Aiguilles-Rouges/Mont Blanc massifs. It corresponds to the Grindelwald phase and was responsible for the following features:

(1) folding of the basal thrust of the Helvetic nappes (Axen thrust in Figures 13.1-14 and 13.1-15),
(2) rotation of the axial surfaces of recumbent folds within the massifs (see Figure 13.1-15),
(3) uplift of the massifs' crest lines to altitudes higher than in the ones observed in the east along line E1 (Figure 13.1-25), and
(4) the narrow width of the Central Aar massif (the massif suffered more horizontal shortening and was uplifted higher in the transect of line C1; see Figure 13.1-25).

This phase of uplift occurred at a rate of 0.5 mm/a in Late Miocene times (between 5 and 10 Ma ago) over the eastern and central Aar massif (Michalski & Soom 1990) and at a faster rate of 0.8–1 mm in Late Miocene-Pliocene times (2–7 Ma) in the western Aar massif and was coeval with shortening in the Subalpine Molasse and the Jura Mountains. In the case of the NW Aiguilles-Rouges and Mont Blanc massifs Soom (1990) determined exhumation rates of 0.5 mm/a in the Early Miocene, slowing down to 0.3 mm/a in the Late Miocene times, and accelerating to > 1mm/a since the Pliocene.

One of the interesting points is the question whether or not a kinematic link between the bulge of Aar massif and deformation in the foreland, the Molasse Basin and the Jura Mountains exists. In Chapter 8 it was argued that the Jura detachment has possibly to be sought within the basement and that a distant push with detachment restricted to the Triassic evaporites poses serious problems. In fact, a single detachment within the Triassic evaporites related to shortening within the Jura Mountains would require the entire Mesozoic-Cenozoic Molasse basin infill to be allochthonous (displaced conjunctly with the SE-most cover of the Jura Mountains). In this hypothesis the detachment horizon should be located near the base of the "authochthonous" Mesozoic within Triassic evaporites. As discussed in Chapter 8 such a detachment is difficult to imagine due to faults dissecting the evaporite horizon, the southerly disappearance of the evaporites, and for reasons of balancing. The reflections marked JD in Figures 11-2a and 13.1-12 might stem from a mylonite zone within the basement and possibly points to a deeper detachment horizon involving the topmost basement during Jura folding. Such a detachment would explain features like inverted Permo-Carboniferous grabens and associated folds, as well as depth-to-detachment, uplift and shortening estimates (see Chapter 8).

For a shortening in the basement related to shortening in the Subalpine Molasse one expects thrust faults remaining bedding parallel within the UMM (Lower Marine Molasse), ramping up through the USM (Lower Freshwater Molasse) at their leading edge, i. e. beneath the erosional front of the Helvetic nappes, and cutting down into crystalline basement at their trailing end. Such a geometry is suggested by the seismic data of lines E5/E1 and W7/W8 crossing the Subalpine Molasse and adjoining Helvetic and Penninic nappes (see Chapter 8).

In eastern Switzerland the Eocene-Oligocene Northhelvetic Flysch is partly detached from its substratum and this imbrication is directly comparable to the structure of the Subalpine Molasse (Vorstegstock thrust in Pfiffner 1986 figs. 3 and 4). The thrust faults in Figure 13.1-10 merging with the Glarus thrust towards the N on the other hand, cannot directly be linked kinematically to the Subalpine Molasse. In the central and western Aar massif, however, (Figures 13.1-14, 13.1-16 and 13.1-20) several thrust faults do not rejoin the base of the Helvetic nappes and can kinematically be linked to the Subalpine Molasse. Those faults are rotated into their actual, northerly dip in the course of the late, **Grindelwald phase**, a phase as discussed above, related to basement uplift.

In order to get insight into the effect of the (late) Grindelwald phase held responsible for the high amplitude doming of the Central (and probably western) Aar massif, a restoration of the youngest, thrust-related structures was attempted. The thrust fault in the northern flank of the Aar massif putting basement onto autochthonous Mesozoic foreland cover is only observed in Central and Western Switzerland. It is also likely to have formed late in the local sequence and was probably related to shortening within the Subalpine Molasse. The age of the movements on this fault can thus be estimated as post Mid-Miocene, i. e. younger than the tilting of the OSM sediments. Another possible fault is the suspected fault at –3 km beneath shot point Flühli, which is indicated by reflections JD in the seismic section C1 (see Figure 11-2a and 13.1-12) and which might stem from a mylonite zone associated with the detachment of the Jura Mountains. This thrust fault would be of Miocene-Pliocene age. Both thrust faults are thus likely to be responsible for the latest uplift. In Figure 13.1-26 the Aar massif is retrodeformed by inversion of movement along these thrust faults. For the Jura detachment ~5.5 km of displacement were assumed (based on shortening estimates of Noack 1989; see Laubscher 1992). The thrust fault imaged by the seismic line C1 (Figure 13.1-13.1 and 13.1-14) putting basement onto foreland cover has a displacement of around 6 km. Retrodeforming the top-basement contact of the Aar massif was done by sliding the Aar massif back on these thrust faults by the amounts mentioned and by extending the massif in the direction of the finite shortening indicated by the strain ellipses in Figure 13.1-26. Applying this retrodeformation results in a shape of the top-basement very similar to the one observed along the eastern traverse (line E1) with the crest line at a maximum elevation of around 2 km above sea level.

A control of this kinematic analysis can be gained from the Apatite fission-track ages (Figure 13.1-24). The latter suggest an uplift rate of 0.5 mm/a from 6 Ma to 4 Ma and an exhumation rate of around 4 km in the last 3 Ma (Michalski & Soom 1990). These uplifts occurred during the time interval when the (latest) Jura folds and the (latest) Subalpine Molasse thrust sheets formed. Considering a material point south of shot point Handegg in Figure 13.1-26, retrodeformation displaces that point 5.5 km on a shallow, and 6 km on a moderately dipping path back into the subsurface. If erosion is taken into account – about 2 km for the past 4 Ma – this material point can be placed at around 4 – 5 km beneath the paleo-land surface. Thus the estimated combined exhumation by erosion and uplift related to orogenic movements match the vertical movement inferred from fission-track data rather well.

In summary it is concluded that the younger uplift history of the central Aar massif, the Grindelwald phase, represents crustal shortening in response to thrusting and folding in the Molasse Basin and Jura Mountains.

Acknowledgments

This chapter benefitted from critical comments by J-L Mugnier.

13.2 2-D gravimetric study of the crystalline basement of the Rawil Depression

E. Klingelé

Contents

13.2.1 Introduction

In the framework of NRP 20, a gravimetric study, entitled "Exploration of the Geological Basement of Switzerland", has been carried out in the Rawil region in order to explore the depth to basement. For years the shape and the depth of this basement have been subject to many and controversial discussions. Even the most recent results (Burkhard, 1988; Dietrich, 1989; Steck et al., 1989; Pfiffner 1993), based on tectonic and stratigraphic studies show significant differences not only for the depth but also for the supposed morphology of the crystalline basement. From the stand point of gravimetry the determination of the depth to basement in this region is equivalent of finding the volume of less dense sediments filling a small basin laterally limited by two blocks of heavier crystalline material. In a simplified geological model these two blocks can be considered of anticline shape with displaced and asymmetric axial slope.

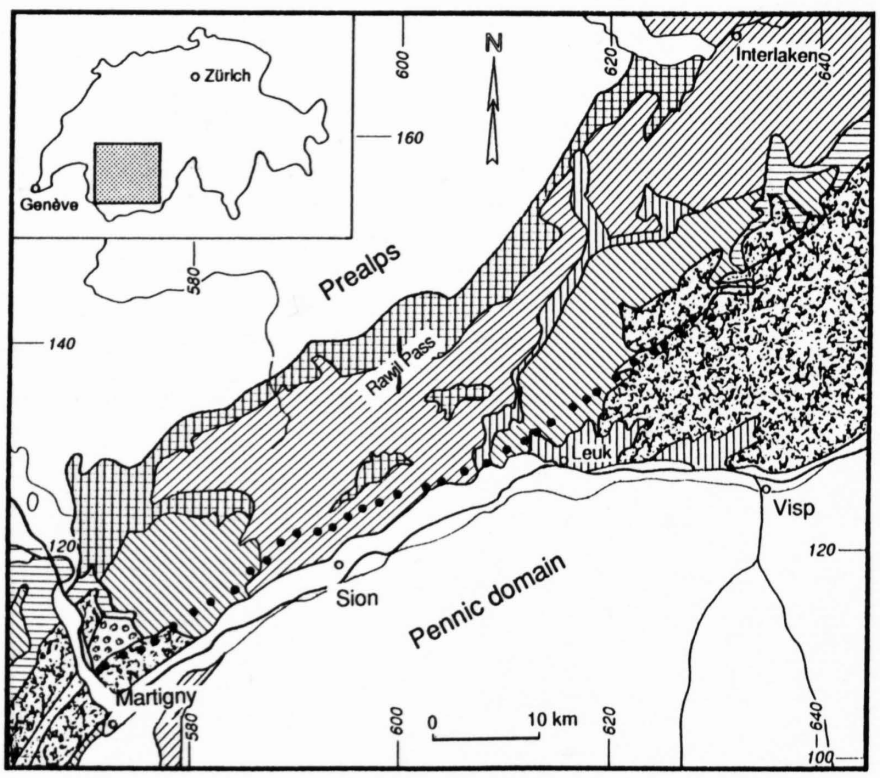

Figure 13.2-1
Geographic situation, geological sketch and location of the measuring points. The dots represent the locations of the measuring points.

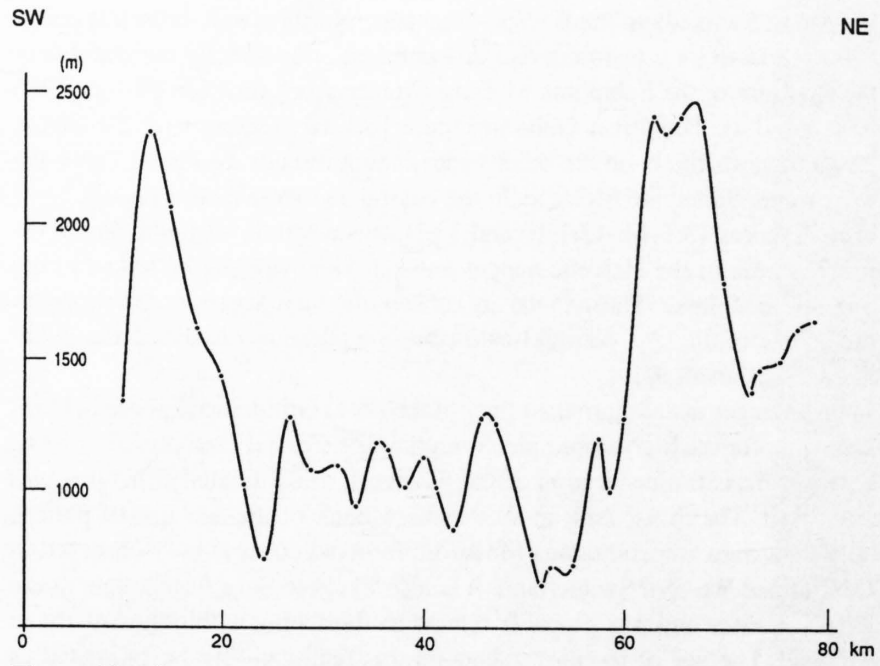

Figure 13.2-2
Diagram of the altitude along the gravimetric profile. The dots correspond to the location of the measurement points

13.2.2 Data acquisition and reductions

The above simplified geological model was taken as a constraint for the survey design. For economical reasons it was not possible to carry out a two dimensional survey, therefore the solution of a profile was adopted. The best solution would have been to have this profile along a line joining the two culminations of the lateral crystalline massifs. Due to difficult access and lack of reference points with good altitude determination it was decided to carry out the survey as close as possible to an ideal profile extending from the Lötschen Valley to a point situated NNW of the city of Martigny (Figure 13.2-1). The gravimetric stations were all situated on fourth-order trangulation points on which the coordinates accuracies are 10 cm for X and Y and 20 cm for H. The average stations spacing is 2 km and the mean altitude of the profile is around 1200 m, with station altitude ranging from 654 m to 2403 m (Figure 13.2-2). We will see later that the vertical positions of the stations lead to difficult problems for modelling.
The surveying, reduction and computation procedures to Bouguer anomalies are not described here. The reader interested in the technical details of these procedures can find a good description of them in the publications of Wagner (1970), Klingelé (1972), Olivier (1974), Klingelé et Olivier (1980). Figure 13.2-3 shows the Bouguer anomalies along the profile, calculated for densities 2.50, 2.60, 2.67, 2.70 and 2.73 $g \cdot cm^{-3}$.

13.2.3 Densities determination

The most critical point for the interpretation or for modelling is the choice of the appropriate density for the Bouguer reductions. Anomalies calculated for different densities, plotted as a function of the distance along the profile show a tendency to decrease whith increasing densities taken for the reduction (Figure 13.2-3).

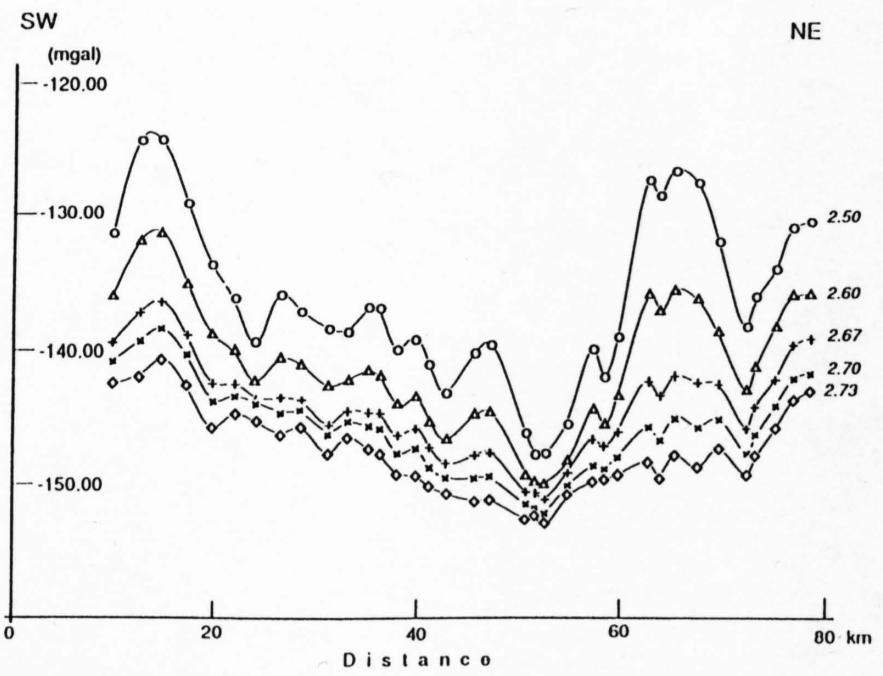

Figure 13.2-3
Bouguer anomalies along the profile for the densities 2.50; 2.60; 2.67; 2.70 and 2.73 [$g \cdot cm^{-3}$] . The values between the measurement points were interpolated by means of a spline function.

For values of 2.70 g·cm^{-3} or higher it is very difficult to see significant difference in these variations. In order to remove this ambiguity the linear regressions between altitudes and anomalies were computed for densities 2.50 g·cm^{-3} to 2.77 g·cm^{-3}. The parameters of these linear regressions are the following:

Densities	Slopes	Ordinate at the origin	Correlation coeff.
2.50	0.0115533	−151.64	0.918
2.60	0.00761324	−151.12	0.825
2.67	0.00485221	−150.74	0.667
2.70	0.00367144	−150.59	0.555
2.73	0.00248832	−150.43	0.406
2.75	0.00207923	−150.75	0.330
2.77	0.00130366	−150.66	0.212

A graphical analysis of these results is presented for densities 2.50 to 2.73 in Figure 13.2-4. The results for densities 2.75 and 2.77 are not presented in this figure because of the poor resolution of the diagrams. One can see that from density 2.73 g·cm^{-3} on there are no significant correlations any more between altitudes and anomalies.

In gravimetry it is very well known that it is not possible to determine both the density and the shape of a disturbing body. If the aim of a survey is the determination of the shape of a geologic structure then the interpretor has to assess the density of the body, either by compiling published data or by collecting rocks samples and measuring their densities in the laboratory. In the framework of a detailed gravimetric study in the region of Turtmann (Wallis), Bernauer and Geiger (1986) determined experimentally the densities of 14 different kinds of rocks. Wagner (1970) gives densities of seven different kinds of rocks taken from the western part of the profile (Permo-Carboniferous conglomerate, gneiss and granites of the Aiguilles-Rouges and Mt Blanc massifs). In order to further increase the number of available densities I also carried out some measurements on rocks of this region provided by A. Steck and H. Masson of the University of Lausanne. These measurements were done in the Petrophysics laboratory at the University of Geneva. The accuracy of these densities determinations can be estimated to be around 0.005 g·cm^{-3} . Table 13.2-2 give the results of these measurements.

Kind of rocks	Number of samples	Proportion in volume [%]	Density (g·cm^{-3})
Banded Gneiss with biotite	2	50	2.72
Microgranite, Gneiss Vallorcine Granite	5	18	2.67
Amphibolites	5	5	2.82
Migmatites	6	27	2.70
Taveyannaz Sandstone	19	1	2.72

Densities found in the literature and those determined for the purpose of this project suggest a small but significant difference between the densities of crystalline and sedimentary rocks. Based on the whole available data set the following average densities were adopted.

AAR:	2.72 [g·cm^{-3}],	(Bernauer & Geiger, 1986)
AIGUILLES-ROUGES:	2.73 [g·cm^{-3}],	(New determinations)
GASTERN:	2.73 [g·cm^{-3}],	(Bernauer & Geiger, 1986)
HELVETIC (nappes):	2.70 [g·cm^{-3}],	(Bernauer & Geiger, 1986)

Considering the results of the density determinations and the regression analysis I adopted for modelling the Bouguer anomalies computed with density value of 2.73 g·cm^{-3}. This density best corresponds to the densities of the two lateral crystalline blocks and simplifies the interpretation.

13.2.4 Computation of the residual anomaly

Two-thirds of the profile extend along the Rhone Valley and consequently the measured gravity values are influenced by the less dense Quaternary valley

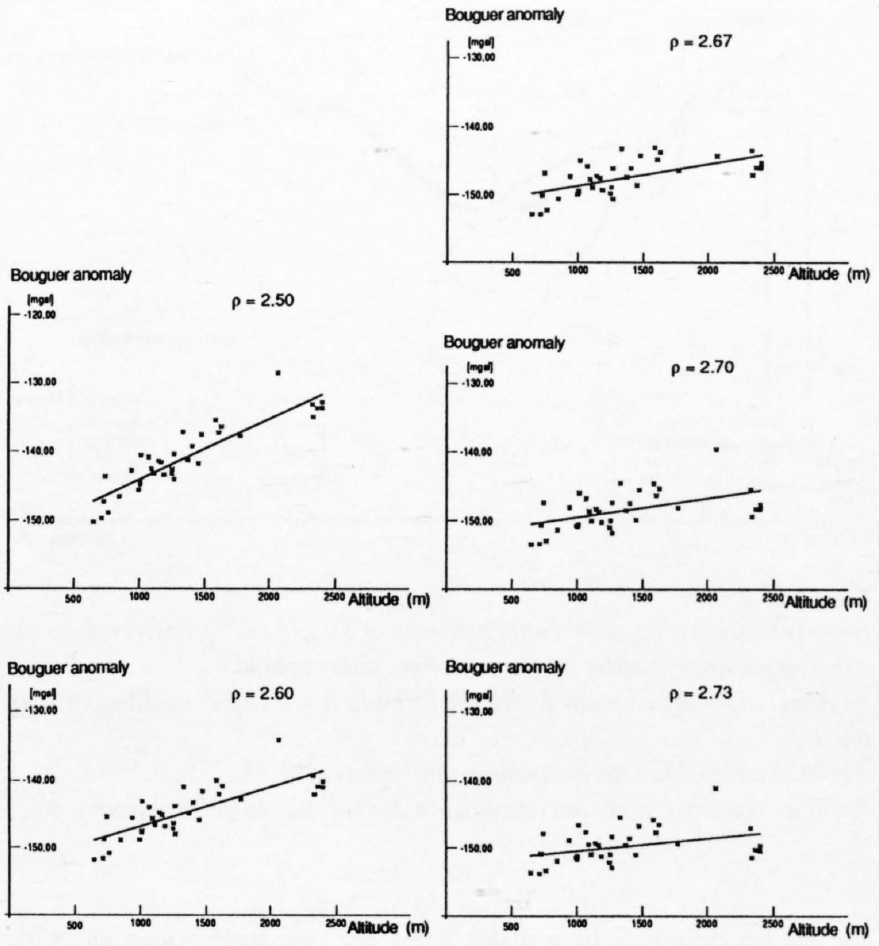

Figure 13.2-4
Diagrams of Bouguer anomalies versus altitude for different densities of reduction with the corresponding linear regression functions.

fill. In order to rid the anomaly values from influences other than those of the Rawil depression, the effects of the light sediments of the Rhone Valley, the Salgesch landslide and the Lötschen Valley were removed from the computed anomalies at the stations. For this purpose the volumes of these light sediments were approximated by blocks with polygonal cross-section. The shapes and the sizes of these blocks were determined from data given by Wagner (1970) and Bernauer & Geiger (1986) for the Rhone Valley and by geometrical prolongation of the slope of the topography for the Salgesch landslide and the Lötschen Valley. The computation was carried out in three dimensions by the method of Talwani and Ewing (1960) assuming a bulk density for the recent sediments of 2.0 g·cm^{-3}. These corrections on the 2.73 anomaly range from 5.65 mgal in the western part of the profile to 1.13 in the Lötschen valley, resulting in a shift and tilt of the Bouguer anomaly (Figure 13.2-5).

From this Figure 13.2-5 one can see that the anomalies of the easternmost part of the profile are strongly correlated with the altitude of the stations. This correlation could be explained by an inappropriate choice of the reduction density for this region. The geological map of the Lötschen Valley (Hügi et al., 1985) shows that most of the rocks forming the valley are of pre-Variscan

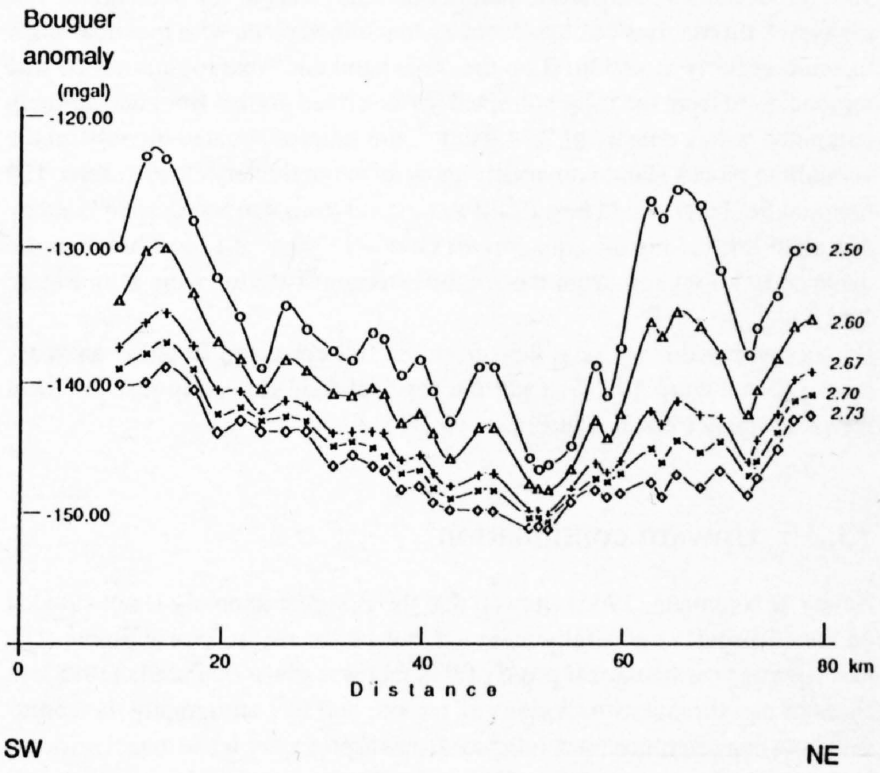

Figure 13.2-5
Bouguer anomalies for the densities of 2.50; 2.60; 2.67; 2.70 and 2.73 [g·cm^{-3}] corrected for the effects of the young sediments of the Rhone and Lötschent valleys and the Salgesch landslide.

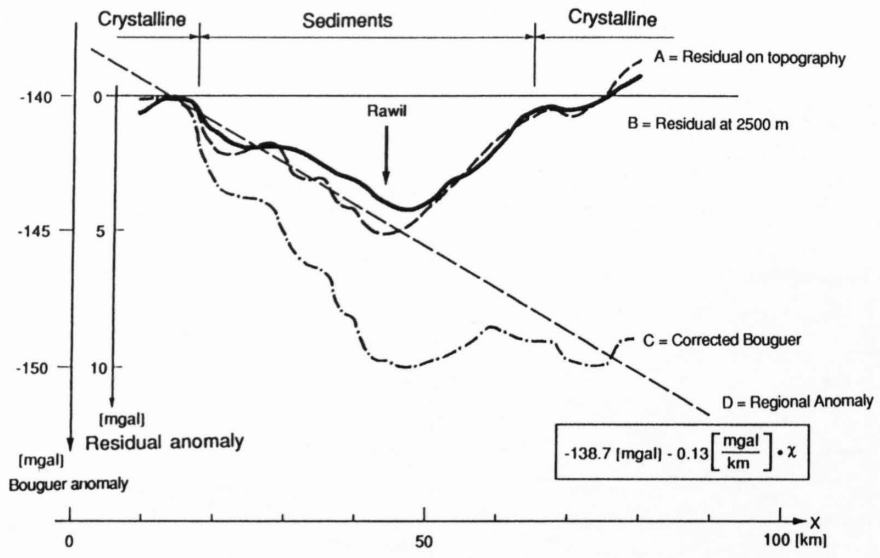

Figure 13.2-6
Bouguer anomaly computed with a density of 2.73 [g·cm^{-3}], corrected for the effect of the amphibolites of the Lötschen Valley (curve C).
Regional anomaly computed with the formula R = –138.7 – 0.13 x (straight line D).
Residual anomaly at the measurement points (curve A).
Residual anomaly upward continued to the altitude of 2500 m (curve B).

age and are chlorite-bearing shales, green gneisses, amphibolites etc. After Geiger & Bernauer (1986) the densities of this kind of rocks are around 2.83 g·cm^{-3}, which is 0.1 g·cm^{-3} higher than the density adopted for the Bouguer reductions.
In order to eliminate the anomaly-altitude correlation apparent in the eastern part of the profile a supplementary correction taking into account the difference between the average and the actual density was applied to the stations situated in the Lötschen Valley. This correction was calculated in two steps. First the effect of a vertical cylinder of 2.5 km radius (approximately equal to the width of the valley) and thickness equal to the altitude of the station with density of 0.1 g·cm^{-3} was removed from the Bouguer anomalies. Second the topographic correction up to 2.5 km radius from each station was recomputed with a density of 2.83 g·cm^{-3}. The final Bouguer anomaly computed for a density of 2.73 g·cm^{-3}, end corrected for young sediments and denser rocks, is represented by the dash-dot-dash line C in Figure 13.2-6.
All the computed anomalies show a value lower than –140 mgal. These values are too large to be explained by the effect of the sediment fill in the Rawil depression. The major component is due to the combined effect of the Alpine roots or to the depth of the Moho discontinuity. These effects have to be removed from the Bouguer anomaly in order to give a residual anomaly that can be attributed specifically to the Rawil depression. Removing the effects of the depth variation of the Moho can lead to uncertain results because the density difference at the discontinuity is not known to sufficient accuracy. To avoid this problem I considered a different way for determining the correct regional field. The Bouguer anomaly map of Switzerland (Klingelé & Olivier, 1980) shows straight and parallel anomaly curves for this region. The regional field can thus be considered as an inclined plane with maximal slope in south-easterly direction. If on the other hand one were to remove the true regional field from the fully corrected (as described above) Bouguer anomaly computed with a density of 2.73 g·cm^{-3}, the stations situated directly on the crystalline blocks should obviously show an anomaly very close to zero. The regional field that would best fulfill these conditions can be approximated by a straight line having the equation $R(x) = -137.0 - 0.13x$, where x is the distance in kilometers from the southwesternmost station (line D in Figure 13.2-6).
By subtracting this regional field from the full corrected Bouguer anomaly (curve C in Figure 13.2-6) I got the residual field reflecting just the local Rawil anomaly (curve A in Figure 13.2-6).

13.2.5 Upward continuation

Naudy & Neumann (1965) showed that the Bouguer anomaly is not situated on the ellipsoid, as generally assumed, but on the measurement points. The first rigorous mathematical proof of this fact was given by Patella (1988). In cases of measurements in regions of smooth and low topography the confusion between reference level (ellipsoid) and topography leads to insignificant inaccuracies for interpretation. This is not the case in the Alps where the altitude difference between stations a few kilometres apart can reach more than thousand meters. It is therefore essential to carry out an upward continuation of the residual field to a horizontal plane situated higher than the highest station.

A very elegant method to carry out this upward continuation using the property of multiplicity of the solutions of the gravity field was given by Dampney (1969). This author remarked that the value of an anomaly g at any point with co-ordinates x, y, z, situated outside the disturbing body can be written as:

$$g(x, y, z) = G \int_{-\infty}^{+\infty} \int_{-\infty}^{+\infty} \frac{\sigma(\alpha, \beta, h) \cdot (z - h) \cdot d\alpha \cdot d\beta}{[(x-\alpha)^2 + (y-\beta)^2 + (z-h)^2]^{3/2}}$$

where $\sigma = (\alpha, \beta, \gamma)$ is a density contrast and **G** the universal gravity constant. This equation shows that from a given anomaly it is possible to compute a density or mass distribution on any surface, which give a gravity effect equal to that produced by the real disturbing body ("equivalent source"). Following this it is possible to use this density or mass distribution to recompute the anomaly to any desired surfaces .
In his technique Dampney (1969) used a horizontal plane as a support surface for the equivalent source and showed that the anomaly can be synthetised with the help of a discontinuous and finite distribution of masses situated on this plane.
Calling g_i the value of the anomaly at the point i and m_i the elementary mass situated on the support surface just below the point i one can write, using the superposition property of potential fields :

$$g_1 = a_{11}m_1 + a_{12}m_2 + \ldots + a_{1i}m_i + \ldots + a_{1M}m_M$$
$$g_2 = a_{21}m_1 + a_{22}m_2 + \ldots + a_{2i}m_i + \ldots + a_{21M}m_M$$

$$g_N = a_{N1}m_1 + a_{n2}m_2 + \ldots + a_{ni}m_i + \ldots + a_{NM}m_M$$

and M = N
M = number of masses
N = number of measurement points

The coefficients a_{ik} are calculated by :

$$a_{ik} = \frac{G \cdot (z - h)}{[(x_i - \alpha_k)^2 + (y_i - \beta_k)^2 + (z_i - h)^2]^{3/2}}$$

This leads to a linear system of M equations of N unknowns which in principle allows the computation of the masses m_i. Unfortunately the practical application of this method leads to numerical difficulties because the heterogeneous values of the coefficients $a_{i,k}$ result in ill-conditioned matrices.
Starting from the same idea as Dampney (1969), Graber et al. (1992) developed an upward continuation technique which is practically applied for the first time here. This method differs from the one of Dampney (1969) in the fact that the support surface is not a horizontal plane but a surface parallel to the topography, situated at a depth l and with a finite thickness e (Figure 13.2-7a). In this case the equivalent layer is formed of elementary mass elements. Each element produces a gravity effect, g_i, on each measurement point equal to the product of its density by its effect computed for a density equal to one. It follows that

$$g_1 = s_1 g^*_{11} + s_2 g^*_{12} + \ldots + s_i g^*_{1i} + \ldots + s_n g^*_{1n}$$
$$g_i = s_1 g^*_{11} + s_2 g^*_{i2} + \ldots + s_i g^*_{ii} + \ldots + s_n g^*_{in}$$

$$g_n = s_1 g^*_{n1} + s_2 g^*_{n2} + \ldots + s_i g^*_{ni} + \ldots + s_n g^*_{nn}$$

with g^*_{ik} = effect of the block k on the point i, and s_k the density of the block k. It is easy to see that in this case the system has to be solved for the densities s_i instead for the masses m_i.
The finite geometry of the layer and the sizes of the elementary blocks lead to a very stable linear system which can be solved easily by any standard matrix method. In the case of very rugged topography this method gives acceptable results, but the accuracy is not totally satisfactory. Inaccuracy arises from the fact that blocks corresponding to the lowest stations give a relatively too weak contribution to the highest points. To reduce this disadvantage Graber et al. (1992) developed an iteration method. Instead of computing directly the prolonged field on the horizontal plane they use an intermediate prolongation surface situated between the equivalent layer and the final prolongation surface. From the field obtained on this intermediate surface they compute a second equivalent surface which is less rugged than the first one. This second equivalent layer then serves either for the final prolongation or for a supplementary iteration (Figure 13.2-7b). The number of computation steps depends on the ruggedness of the topography, but usually only two iterations are necessary. The iteration procedure allows the use of equivalent layers less and less rugged and consequently practically eliminates any numerical instabilities.

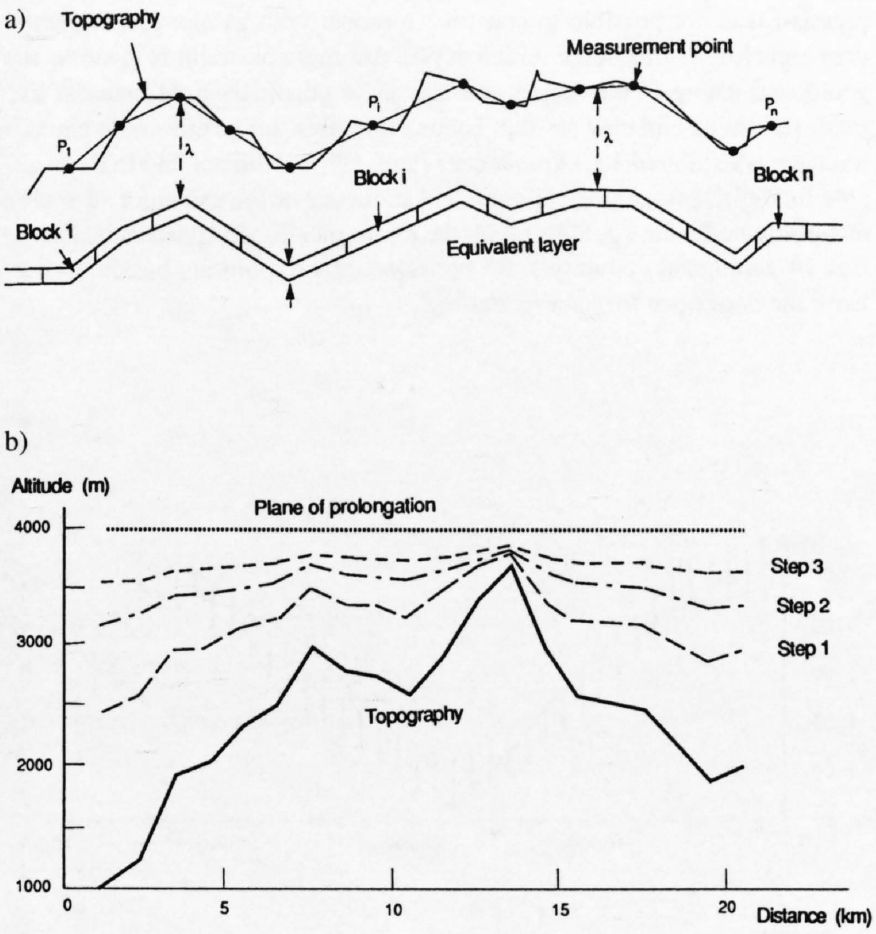

Figure 13.2-7
a) Sketch showing a cross section of the equivalent layer. The lateral extension of the equivalent layer can be finite (3-D case) or infinite (2-D case).
b) Sketch showing the iteration procedure used during the prolongation.

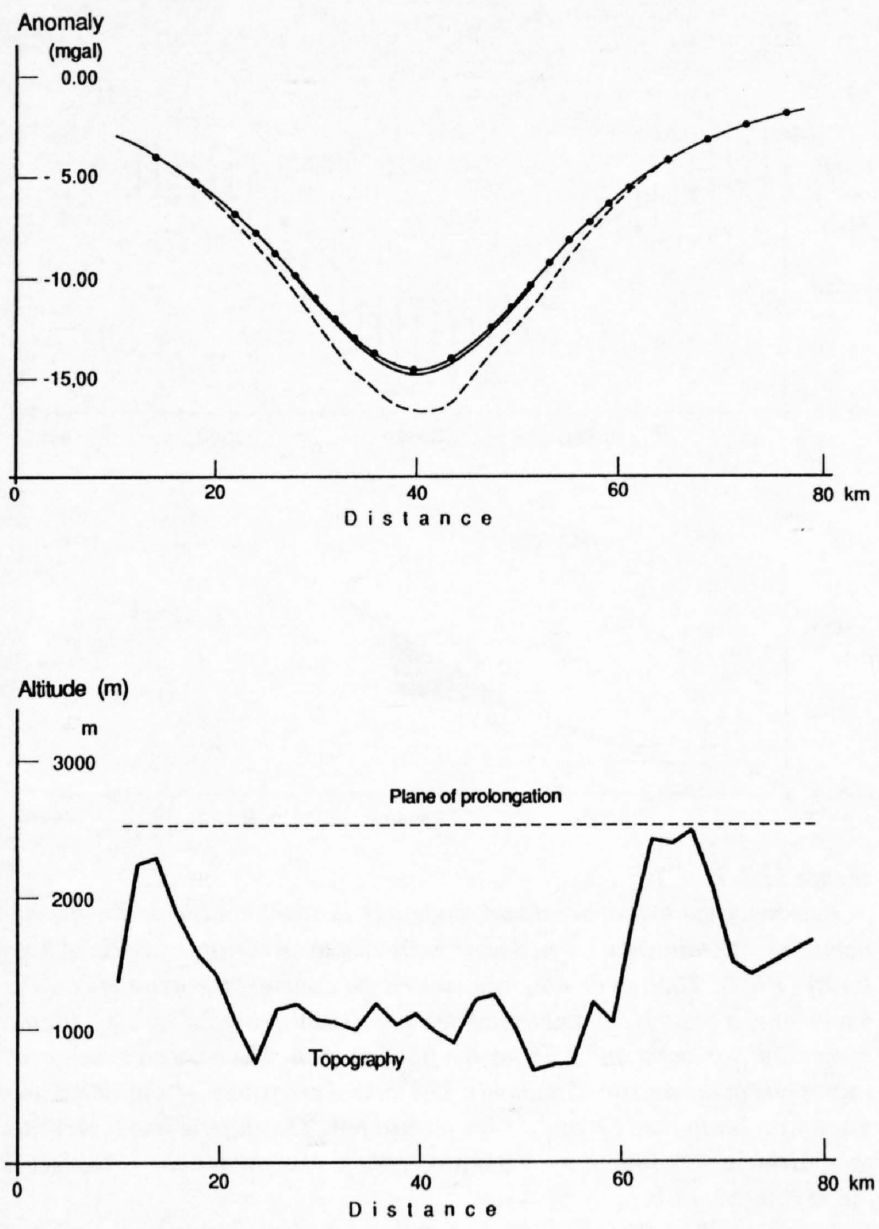

Figure 13.2-8
Example of the upward continuation of a synthetic anomaly.
The upper figure shows the synthetic anomaly computed on the topography (dotted line), the same anomaly computed directly on the prolongation plane (dash-dot-dash line) and the prolonged anomaly (continuous line).
The lower figure shows the topography used and the situation of the prolongation plane.

The parameters l, e , depth and thickness of the equivalent layer can be optimally determined by synthetic disturbing bodies placed below the real topography and by computing their theoretical and prolonged effects. Figure 13.2-8 shows an example of a synthetic anomaly produced by a disturbing sphere on the Rawil profile and its theoretical and practical prolongation on a plane situated at the altitude of 2500 meters. The mass of the disturbing sphere is $1.1 \cdot 10^{15}$ kilograms and the centre is placed in the middle of the profile at 20 km depth. The size and the location of the disturbing body has been chosen in such a manner that it produces an anomaly similar to the observed one. It is easy to see that the difference between the theoretical and the prolonged anomaly is very low and therefore the method can be applied without restriction. The procedure described above was applied to the smoothed observed anomaly (Figure 13.2-6, curve C) to continue it upward to an altitude of 2500 meters (Figure 13.2-6, curve B).

13.2.6 Three-dimensional modelling

The structural models of Burkhard (1988) and Steck et al. (1989) were taken as initial models for the three-dimensional modelling with the hope that some arguments could be found in favour of one of these models. For computation the study area was divided into vertical prisms of 2 km by 2 km cross-section; the top of each prism corresponding to the topography and the bottom to the depth of the crystalline basement given by Burkhard (1988) or Steck et al. (1989). A mean density was assigned to each prism taking into account the volume proportion of each kind of rock forming the prism. For this purpose some synthetic lithological cross sections were constructed with the help of the available geological information. (Bernauer & Geiger, 1986; Jäckli, 1950; Burkhard, 1988; Steck et al., 1989; Escher et al., 1989). The density distributions obtained from this compilation show a homogenous density of 2.70 $g \cdot cm^{-3}$ for all the sediments situated north of the Rhone–Simplon line and a density varying from 2.71 $g \cdot cm^{-3}$ to 2.72 $g \cdot cm^{-3}$ from those blocks situated south of the same line, whereas the density of the crystalline basement is 2.73 $g \cdot cm^{-3}$.
The structural model of Steck et al. (1989) gives only the depth of the Aiguilles-Rouges and Gastern massifs. Therefore it was necessary to combine the two different models in order to be able to model the part above the Aar massif. The depth of the two gravimetric three-dimensional models are given in Figures 13.2-9a and 13.2-9b. The computation was carried out by means of the formula of Nagy (1966) on each experimental point prolongated to 2500m altitude.
The results of the computations, presented in Figure 13.2-10, show little difference between these two models. Both fit the residual anomaly well in the western part of the profile up to the Rawil pass and in the eastern part from the contact between crystalline and sedimentary rocks to the NE end of the profile. Between these two limits the results show a deficit in anomaly up to two milligals.

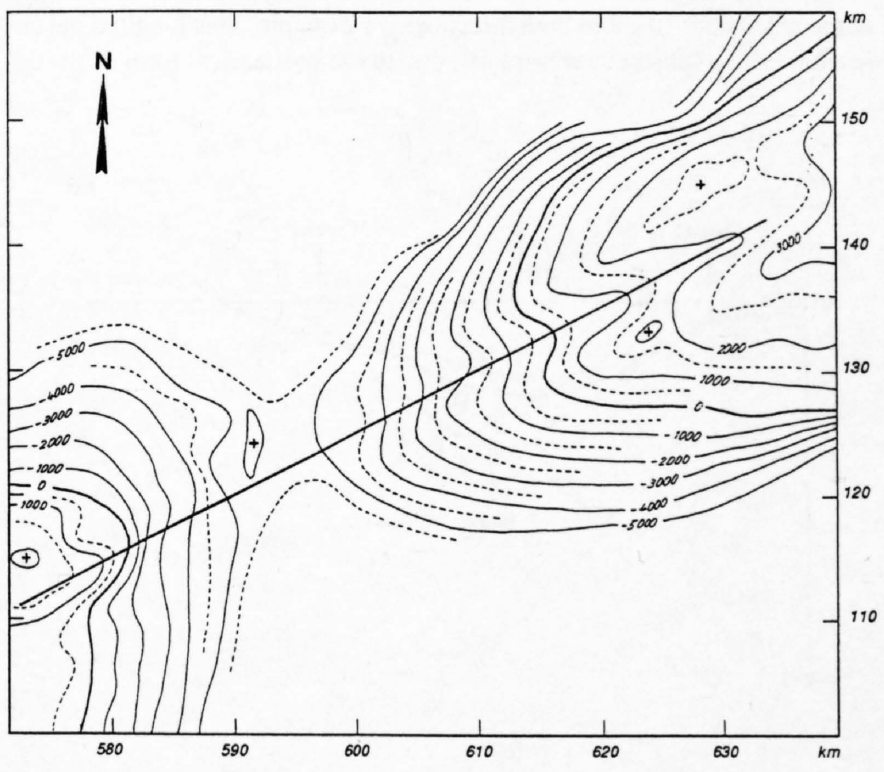

Figure 13.2-9a
Depths of the crystalline basement, referred to sea level, obtained by the combination of the structural models of Burkhard (1988) and Steck et al. (1989). Contour interval : 1000 m.
These depths were used as first initial model for the three dimensional gravimetric modelling

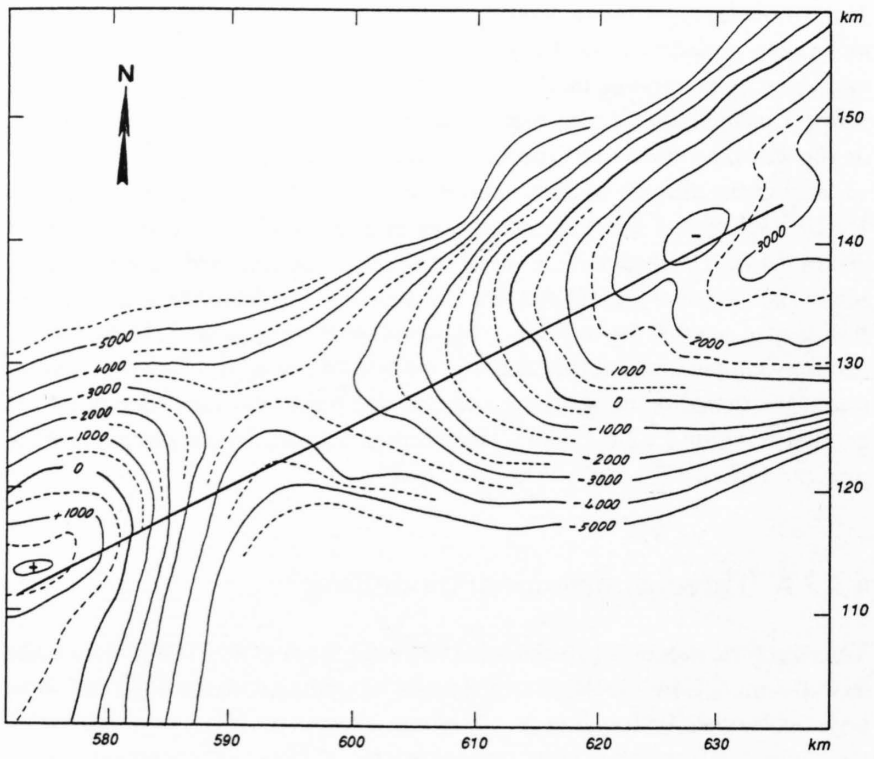

Figure 13.2-9b
Depth of the crystalline basement, referred to sea level, of Burkhard (1988) used as second initial model in the three dimensional gravimetric modelling. Contour interval: 1000m.

13.2.7 Interpretation

To explain the misfit between the residual anomaly and the results of the modelling in this part of the profile one can formulate four hypotheses.
The first (and simplest) hypothesis would be to explain this difference by an inappropriate choice of the density used for the Bouguer reduction and/or for the three-dimensional modelling. In our opinion this hypothesis can be rejected because the results of the modelling fit very well the residual anomaly along seventy percent of the profile. It can also be rejected because the misfit has a too long wave length to be due to a systematic error in the densities and/or altitude determinations (The accuracy of the altitude is around 20 cm which cause an maximal inaccuracy of 0.06 mgal of the anomaly).
The second hypothesis would be to attribute this effect to a heterogenous body situated within the sediments. After Bernauer & Geiger (1986) the lightest sediments found in the study area are quartzitic rocks of Triassic age. Their mean density is around 2.64 $g \cdot cm^{-3}$, consequently constraining the density contrast to be not higher than $-0.07\ g \cdot cm^{-3}$. The shape of a heterogenous body would be strongly influenced by its vertical position: if situated above 500 m (level of the Rhone valley), its lateral extensions cannot exceed 1 km toward SE and 10 km toward NW because of the geometry of the mountains. If situated below the level of the Rhone valley it could have a much larger extension, 10 km in both directions for example. This longitudinal extension is also subject to constraints: due to the geometrical form of the depression it is not possible to construct a model with an elongation greater than eight kilometres in the direction NE. Another constraint is given by the geological nature of the region: the masses of potentialy light material like marl, sandstone and clay are thin layers (1km at most) or piles with a maximum cross section of 1 x 1 km (Escher et. al. 1987). I did not find in the available literature any geological argument in favour of the existence of such a disturbing body that could fulfill all the above mentioned constraints. Due to lack of geological certainty I did not reject this hypothesis but decided to leave the door open for later modelling.

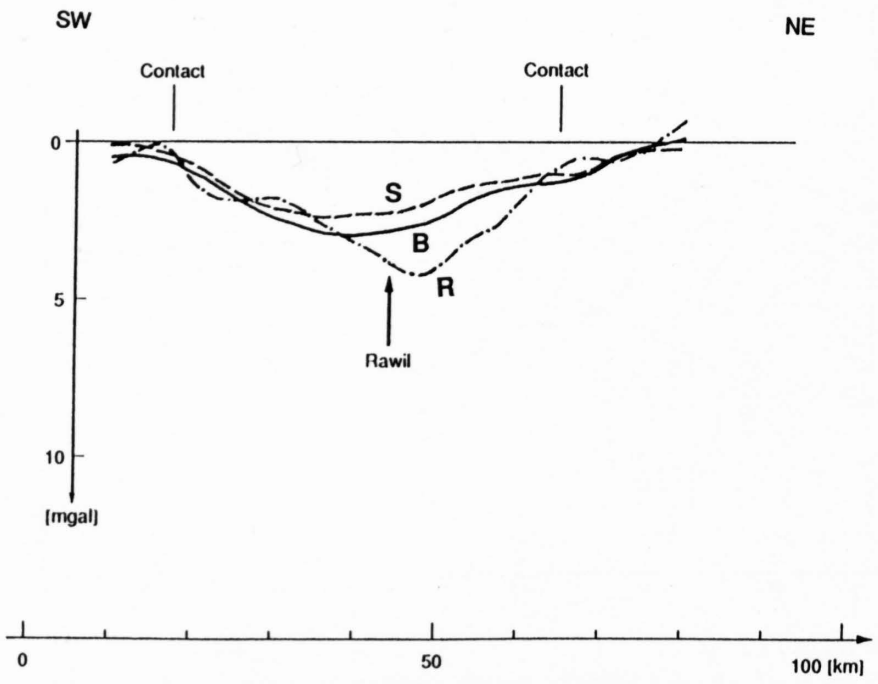

Figure 13.2-10
Residual anomaly at 2500 m (curve R) and effects of the three dimensional models one and two at the same altitude. Curve S is for the model of Steck et al. (1989); curve B for the model of Burkhard (1988).

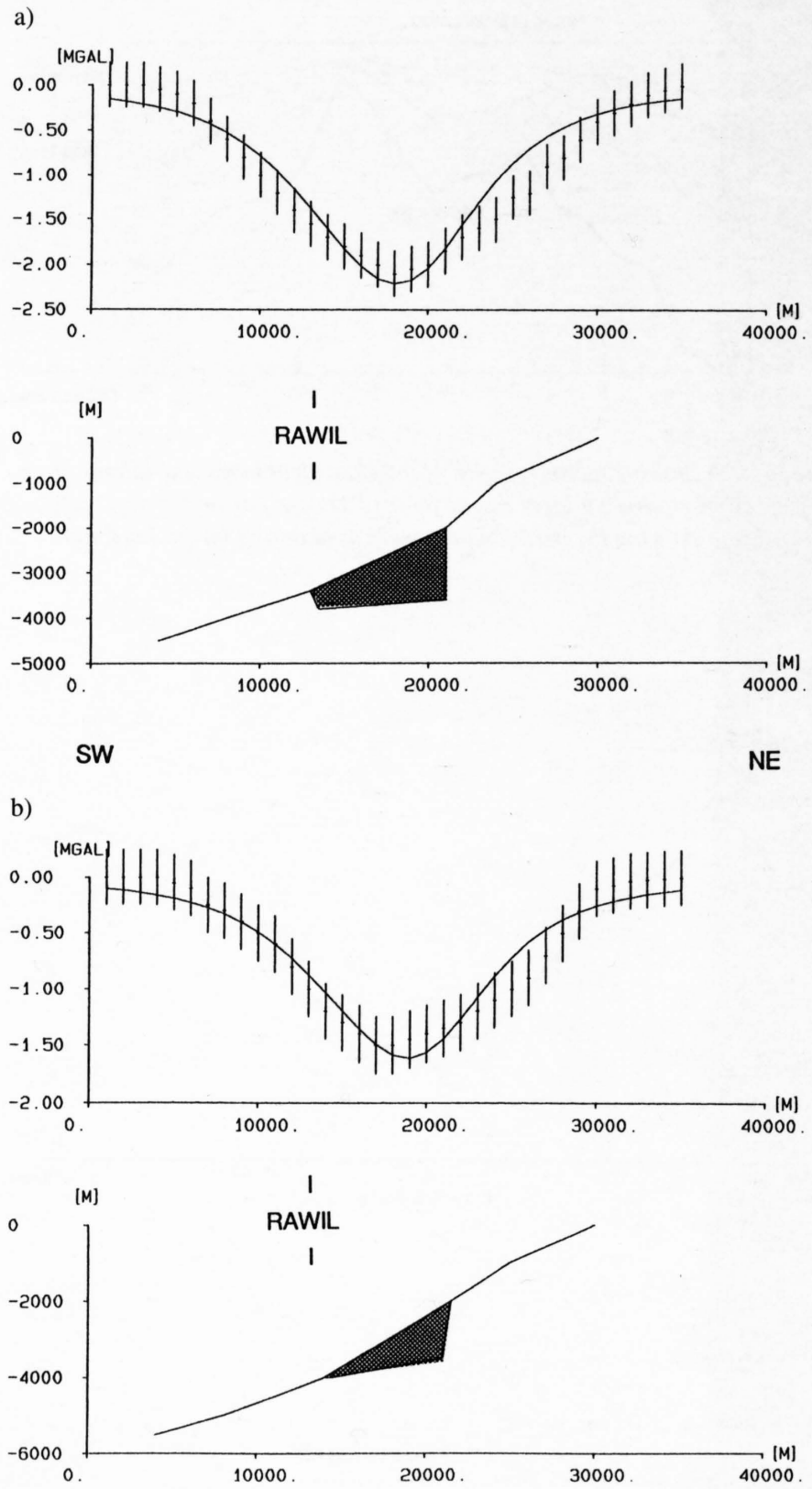

Figure 13.2-11
a) Results of the two-dimensional modelling at 2500 m altitude for the hypothesis of a sedimentary syncline or graben in the structural models of Burkhard (1988). The upper diagram shows the computed gravity effect, the lower one, a cross section of the model. The densities are 2.73 $g \cdot cm^{-3}$ for the crystalline basement and 2.55 for the filled graben. The bars give the accuracy limits of the measured anomaly. The lateral extensions of the model was taken as 5 km toward SE and 15 km toward NW. The sloping line represents the basement interpreted by Burkhard (1988). The shaded area represents the hypothetic graben.
b) Results of the two-dimensional modelling at 2500 m altitude for the hypothesis of a sedimentary syncline or graben in the structural models of Steck et al. (1989). The upper diagram shows the computed gravity effect, the lower one a cross section of the model. The densities are the same as used in Figure 13.2-11a The bars give the accuracy limits of the measured anomaly. The lateral extensions of the model was taken as 5 km toward SE and 15 km toward NW. The sloping line represents the basement interpreted by Steck et al. (1989). The shaded area represents the hypothetic graben.

The third hypothesis consists of assuming a basement below this part of the profile deeper than that given by Burkhard (1988) or Steck et al. (1989). The additional depth necessary to cancel the misfit can be estimated by computing the depth of the bottom of a vertical cylinder of density 0.02 g·cm^{-3}, with a diameter of 24 km. The top of such a body would be situated at 5000 m depth. The result of this calculation give a depth to bottom of 12000 m. This would mean that the depth of the basement should be around seven kilometers deeper than presently supposed. In my opinion this result is completely unreasonable and therefore this hypothesis has to be rejected.
The fourth hypothesis would be to assume the presence of a lighter structure having its top at the depth given by both structural models. In that case the morphology of the basement would correspond to the structural models of Burkhard (1988) or of Steck et al. (1989) but either a part of the crystalline material would have a different petrological composition (like a leuco-granite with a lower density) or a sedimentary structure would occur within the basement (syncline or graben for example).
Let us first examine the possibility of a Permo-Carboniferous graben suggested by Pfiffner in his interpetation of the seismic reflection line W1 (Chapter 13-1). Results of borehole logging from the NAGRA deep well of Weiach in NE Switzerland (Weber et. al. 1986) show a density contrast of around 0.18 g·cm^{-3} between the gneiss forming the crystalline basement (2.73 g·cm^{-3}) and the Premo-carboniferous sediments filling a deep graben discovered in this region (2.55 g·cm^{-3}). If we take this density contrast as a possible value for our models, and putting as a constraint that the top of this structure has to be at the depth of the basement, then it is possible to compute a very simple and schematic two-dimensional model of the disturbing body. For both models the lateral extensions were taken as 5 km toward SE and 15 km toward NW. Figure 13.2-11 shows the results of this modelling for the gravity anomalies produced by the basement models of Burkhard (Figure 11a) and Steck et. al. (Figure 13.2-11b). In both cases the thickness of the sediments does not exceed 1.5 km.
In the case where the disturbing body would be a lighter crystalline volume we can take the same working hypothesis from the previous modelling, except that the density contrast would be of the order of 0.08 g·cm^{-3}. Figure 13.2-12a and 13.2-12b show the results obtained in this case for the structural models of Burkhard (1988) and Steck et. al. (1989). The maximum thickness of the bodies are not higher than those of the graben, but the longitudinal extension is almost double in both cases.

a)

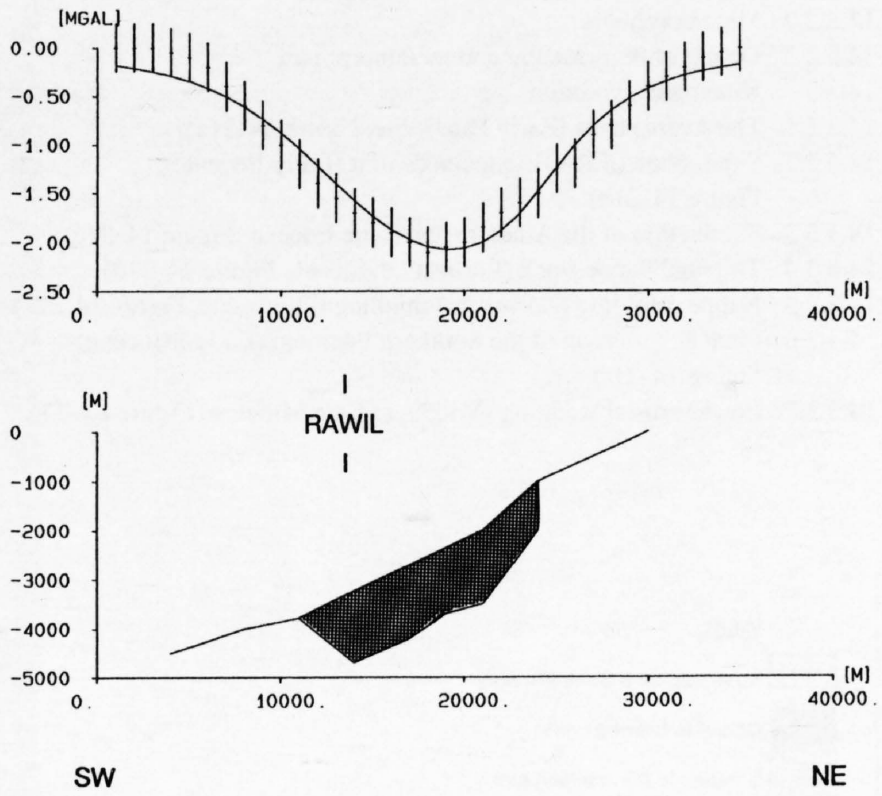

b)

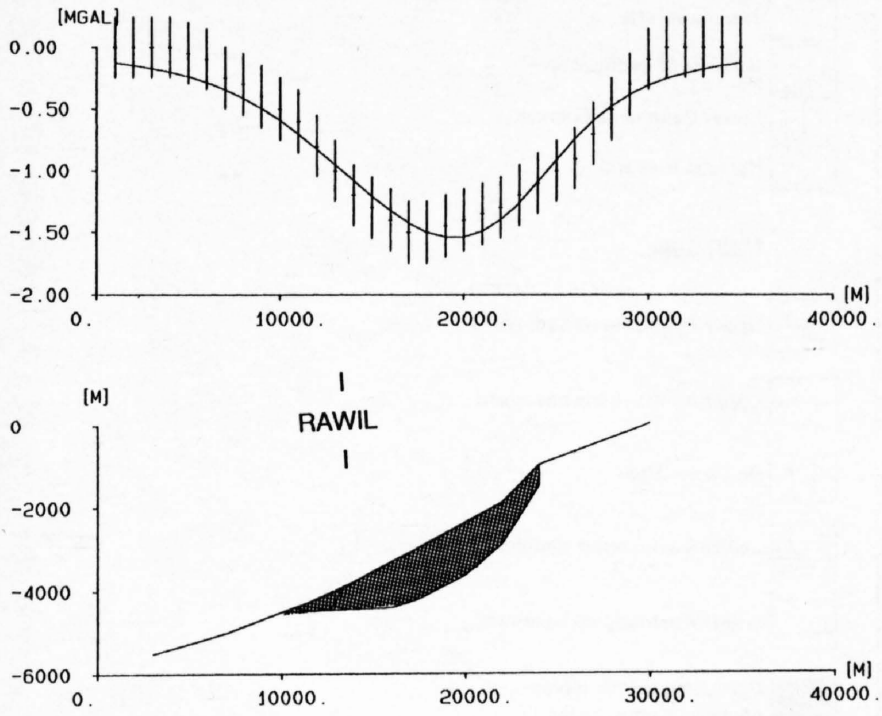

Figure 13.2-12
a) Results of the two-dimensional modelling at 2500 m altitude for the hypothesis of a lighter crystalline body in the structural models of Burkhard (1988). The upper diagram shows the computed gravity effect, the lower one a cross section of the model. the densities are 2.73 g·cm^{-3} for the crystalline basement and 2.65 g·cm^{-3} for the lighter crystalline disturbing body. The bars give the accuracy limits of the measured anomaly. The lateral extensions of the model was taken as 5 km toward SE and 15 km toward NW. The sloping line represents the basement interpreted by Burkhard (1988). The shaded area represents the hypothetic light crystalline body.
b) Results of the two-dimensional modelling at 2500 m altitude for the hypothesis of a lighter crystalline body in the structural models of Steck et al. (1989). The upper diagram shows the computed gravity effect, the lower one a cross section of the model. The bars give the accuracy limits of the measured anomaly. The lateral extensions of the model was taken as 5 km toward SE and 15 km toward NW. The sloping line represents the basement interpreted by Steck et al. (1989). The shaded area represents the hypothetic light crystalline body.

13.2.8 Summary and conclusions

The shape and the depth of the Rawil depression situated between the Aar massif and the Mt. Blanc/Aiguilles-Rouges massifs was modelled in three dimensions by means of a gravimetric profile carried out and interpreted in terms of depth to basement.
Before interpretation the measured anomalies were first corrected for the influence of the quartenary sediments and of the pre-Triasic crystalline rocks of the Lötschen Valley, then continued upward to a constant altitude of 2500 m by means a newly developed method.
A two-dimensional gravimetric study of a profile crossing the Rawil depression shows that the two basement models of Burkhard (1988) and Steck et al. (1989) are not very different from a gravimetric point of view. The model resulting from the synthesis of both seems to better fit the experimental anomalies. However neither of them can explain the 2 mgal, 24 km halfwavelength negative residual anomaly situated just east of the Rawil pass. The possibility of a disturbing body situated within the sedimentary cover cannot be supported (even if it cannot be formally rejected) because of the constraints imposed to the geometry and density of a supposed disturbing body, by the shape and the amplitude of the anomaly, and by the geology of the region. This anomaly can be explained by a lighter structure situated in the basement such as a leuco-granite body or a graben filled by Permo-Carboniferous sediments (such as shown in the geological interpretaions by Steck et al. in Figure 12-4 and Pfiffner et al. in Figure 13-20). In the frame of the accuracy of the experimental anomaly both models give comparable results.

Acknowledgements

The author is greatly indebted to Prof. Henri Masson and Prof. Albrecht Steck, both of the University of Lausanne, for helpful discussions and for providing the material for the density determinations. A special and warm thanks to Prof. Martin Burkhard of University of Neuchâtel who provided me many unpublished geological data and spent hours of his time to an attempt to furnish me with a basic geological feeling. I further wish to thank my colleague Dr. Nazario Pavoni for helpful information about the landslide of Salgesch. This paper was critically reviewed by my colleague Dr. Roy Freeman. His helpful suggestions an those from two anonymous reviewers, are gratefully acknowledged.

14 Rifting and collision in the Penninic zone of eastern Switzerland

S. M. Schmid, O. A. Pfiffner & G. Schreurs

Contents

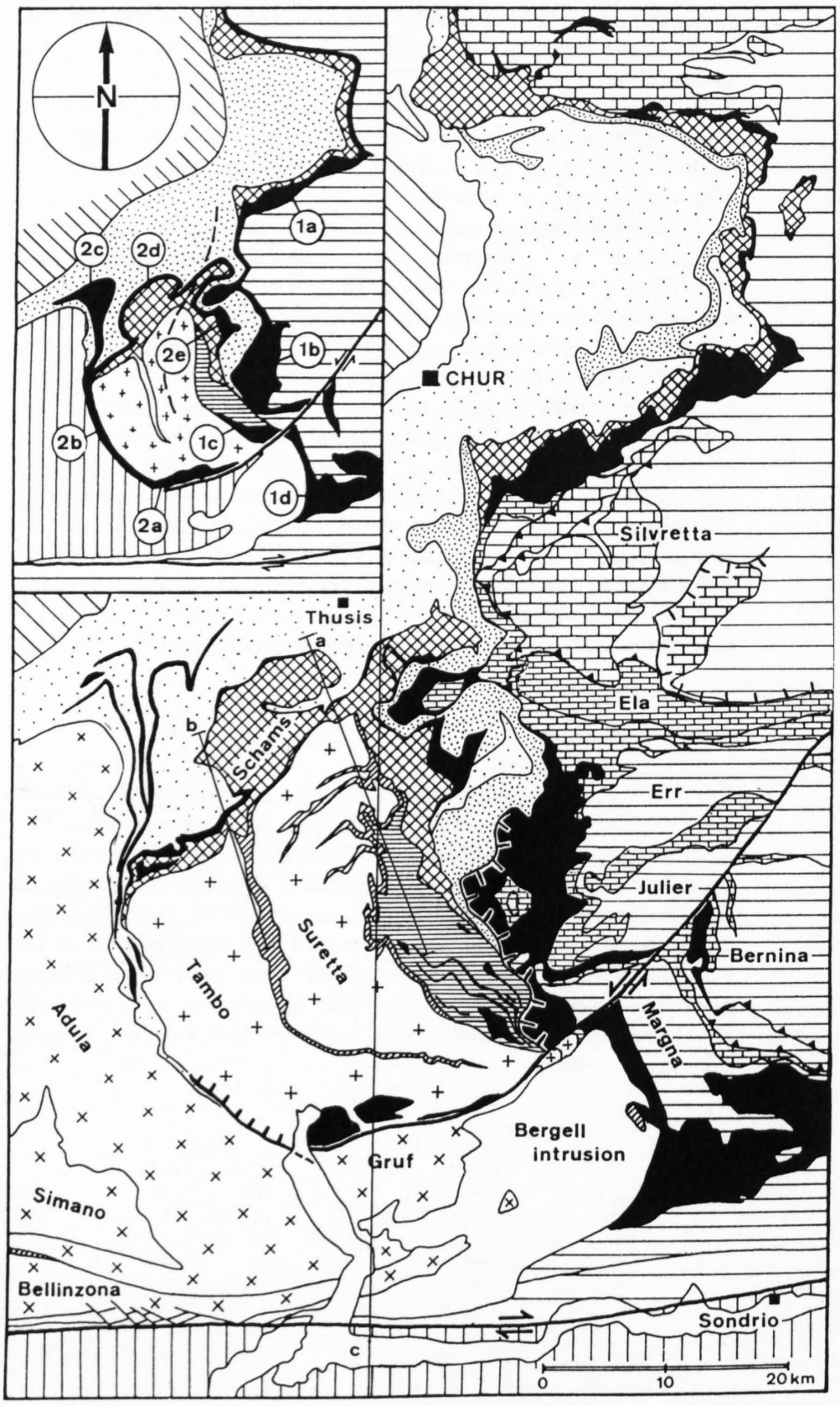

Figure 14-1
Tectonic map of eastern Switzerland, modified after Schmid et al. (1990). Encircled numbers in inset refer to ophiolite-bearing units (black) derived from the S-Penninic or Piemont-Liguria ocean (units labelled "1" and from the N-Penninic or Valais ocean (units labelled "2"). 1a: Arosa; 1b: Platta; 1c: Lizun and Avers; 1d: Malenco; 2a: Chiavenna; 2b: Misox zone; 2c: ophiolites within N-Penninic Bündnerschiefer; 2d: Areua-Bruschghorn; 2e: Martegnas. Profile traces a and b refer to Figures 14-10a and 14-10b, respectively. Profile trace c refers to Figure 14-2.

14.1 General geological introduction

The southern part of the eastern traverse of the NRP 20 reflection profile E 1 (see chapter 9) crosses the Penninic domain of eastern Switzerland (Figure 14-1). The following brief introduction into the geological setting intends to familiarize the reader with the study area. Inevitably, such an introduction is partly based on new findings presented in more detail later on.

Compositionally, the Penninic structural domain comprises:

(1) A stack of pre-Triassic crystalline basement units consisting of the Adula, Tambo and Suretta nappes within our area of interest. The two higher amongst these three basement nappes largely preserved their autochthonous to parautochthonous Mesozoic cover (Tambo cover or Splügen zone, Suretta cover) and contain relics of pre-alpine (Variscan and Late Paleozoic) magmatism, deformation and metamorphism. Hence they basically represent basement-cover flakes derived from upper continental crust, albeit strongly overprinted by Alpine deformation and metamorphism (mostly greenschist facies). The Misox zone definitely does not simply represent the cover of the Adula nappe but forms the telescoped southern continuation of detached sedimentary units described under (2). The Adula basement nappe, in contrast to Tambo and Suretta nappes, is very intensely sliced into sheets of quartzo-feldspathic basement interleaved with very thin eclogite facies mafics and Mesozoic metasediments.

(2) Allochthonous cover sheets are found in front of, above and below the Tambo-Suretta pair. The Middle Penninic or Briançonnais cover slices are characterized by carbonate-rich platform sediments with reduced thickness (Schams, Falknis-Sulzfluh nappes). The bulk of the rather monotonous calcareous shales and arenites (N-Penninic Bündnerschiefer and Flysch, deposited in the Valais trough) are found in front of the Tambo-Suretta pair. Their extension into the footwall of the Tambo nappe forms the major part of the Misox zone while the extension into the hangingwall of the Suretta nappe is known as Arblatsch flysch.

(3) Ophiolite-bearing units shown in Figures 14-1 and 14-2 contain, amongst other rock types, rocks which unambiguously represent former oceanic crust (e.g. Platta, Martegnas). Mafic and ultramafic lithologies whose origin is not entirely clear occur as components of mélange zones (Areua-Bruschghorn mélange) between N-Penninic Bündnerschiefer and Schams nappes or as imbricates, preferably at the base of individual tectonic-stratigraphic subunits within the N-Penninic Bündnerschiefer (Figure 14-2).

Parts of the Tambo and Suretta basement nappes suffered pre-Alpine as well as Alpine metamorphism (polycyclic basement). Post-Variscan (Permo-Carbonifereous) granitoids and volcanics (Truzzo granite, Rofna porphyry) underwent one (Alpine) metamorphic event only (monocyclic basement). Judging from their Mesozoic cover, the Tambo and Suretta basement flakes represent the uppermost few kilometers of continental crust, paleogeographically part of the Briançonnais platform (Middle Penninic). This rise started to individualize in the early Middle Jurassic as the result of oblique rifting and drifting. A more external basin, the Valais or N-Penninic trough is characterized by very thick Jurassic and Cretaceous turbiditic sequences (Bündnerschiefer) grading into Late Cretaceous to Eocene flysch. Interlayered prasinites and serpentinites are interpreted here as tectonically emplaced remnants of oceanic crust. Classically, they have been described as stratiform intrusions into the Bündnerschiefer, which were deposited onto continental crust ("Adula"-Bündnerschiefer). While in the latter view the Briançonnais simply represents distal European margin, the former interpretation results in a more complicated paleogeographic scenario with two oceanic domains separated by the continental Briançonnais platform. An oceanic origin for the S-Penninic or Piemont-Liguria basin (e.g. Platta unit) is undisputed.

Alpine convergence presumably started in "Mid"-Cretaceous times in the S-Penninic domain. Upper Cretaceous W to WNW-directed thrusting and metamorphism is documented within the Austroalpine nappes (Thöni 1986, Schmid & Haas 1989, Froitzheim et al 1994), synchronous with the suturing of the Austroalpine nappes with the Arosa-Platta ophiolitic unit (Ring et al. 1988). However, the extent of deformation at the southern margin of the Briançonnais platform during the Cretaceous as well as the timing of collision between the Austroalpine and the Briançonnais will have to be discussed.

The main deformation affecting the more external mid-Penninic rise, the Valais trough and the distal European margin (hence the entire nappe pile below the Platta unit of Figure 14-2) did not occur before the Tertiary according to our results (for differing point of views, calling for Cretaceous deformation and metamorphism in this nappe pile, particularly for the Adula nappe, see Hunziker et al. 1989, Ring 1992 a & b). Hence, the present day structure of the Penninic structural zone depicted in Figure 14-2 is essentially the result of Tertiary orogeny. Late Cretaceous uplift and cooling, associated with severe extension (Froitzheim 1992) rendered the Austroalpine units virtually undeformable during Tertiary orogeny: Austroalpine and Platta units behaved as an orogenic lid and were thrusted N-wards over the viscously deforming Middle and North Penninic units (Schmid et al. 1990, Froitzheim et al. 1994). Stacking into basement and cover nappes is the result of foreland tectonics in the distal European margin, and (if the N-Penninic domain represents former oceanic crust), accretionary wedge formation leading to collision of the distal European margin with the Briançonnais platform.

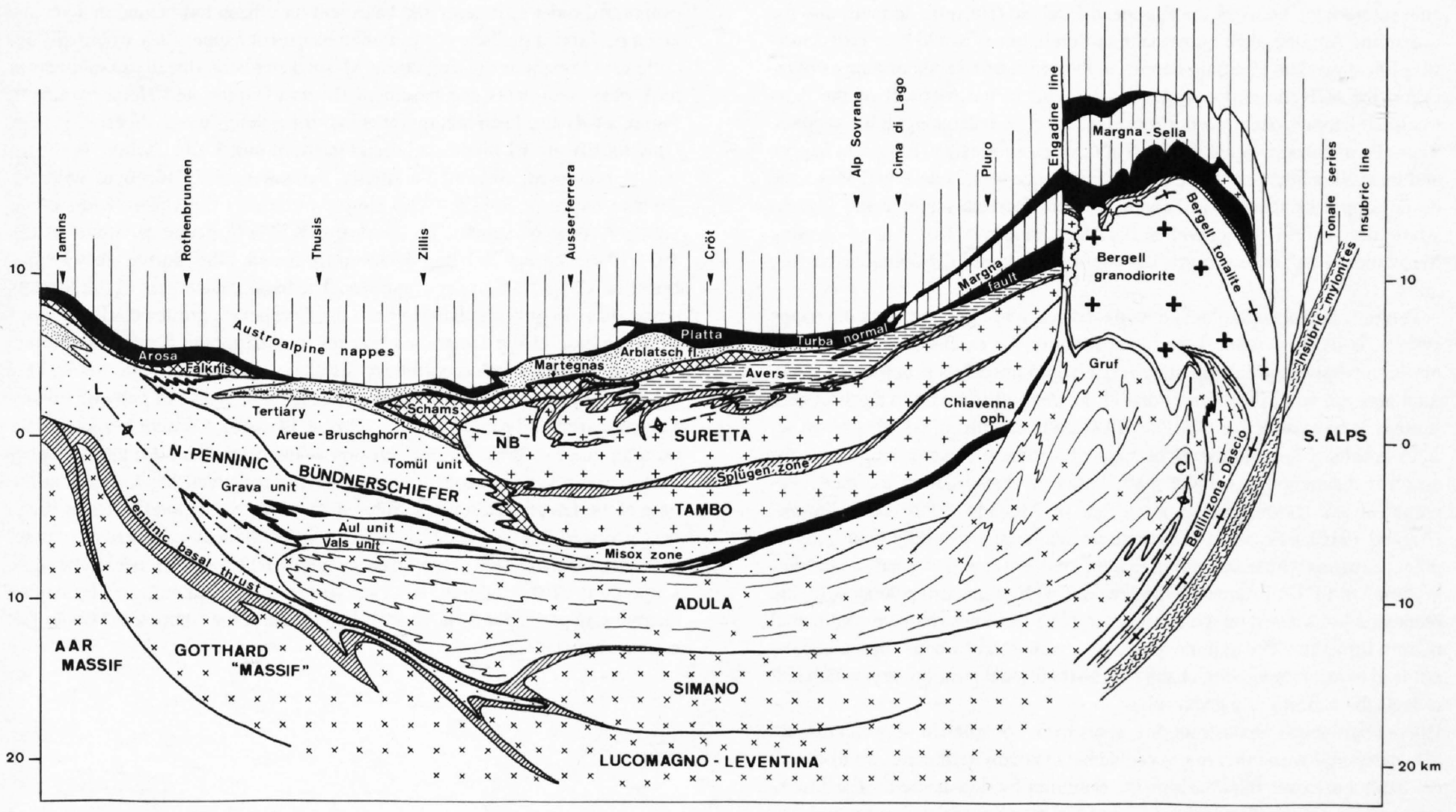

Figure 14-2

N–S profile through the Penninic zone of eastern Switzerland, drawn after the seismic line E1 and the integrated cross section of the Eastern Traverse fully presented and discussed in Chapters 9 and 22. Axial traces indicated refer to the Lunschania antiform (L), the Niemet-Beverin fold (NB) and the Cressim antiform (C). Profile trace indicated in Figure 14-1, trace c.

Intense post-nappe folding locally inverted the stacking order of previously detached units. This strong overprint is associated with post-collisional shortening starting in the Oligocene. It is important to stress the fact that in the external zones (Helvetics, Southern Alps) substantial post-collisional shortening went on at least until the end of the Miocene, while our area of interest was largely consolidated by the end of the Oligocene.

The foregoing introduction showed that a palinspastic reconstruction of the Penninic domain in its paleographical sense is crucial for a better understanding of tectonic processes such as rifting and collision. An answer to the following two questions is fundamental for understanding the tectonic evolution along the NRP 20 Eastern Traverse: What is the original position of the Schams nappes in the nappe pile before post-nappe refolding, and, what is the nature of the Valais trough (oceanic or distal European margin)?

The results of detailed studies carried out in conjunction with the NRP 20 project concentrated on an area occupied by the frontal part of the Tambo and Suretta nappes, including the allochthonous Schams cover slices wrapped around the front of these basement nappes. Since stratigraphic-sedimentological and structural-tectonic arguments are not independent from each other a combined interdisciplinary approach was chosen. For clarity of presentation, however, the results on the rifting and drifting stage will be presented before the results on Alpine convergence. But the reader should bear in mind that the stratigraphic-sedimentological data presented first heavily rely on the results of the structural analysis and vice versa. For details on the work carried out in connection with NRP 20 the reader is referred to the results of three PhD theses (Mayerat 1989, published in modified form under Mayerat Demarne 1994, Rück 1990, published1995, Schreurs 1990, published 1995) and unpublished diploma theses (Adler 1987, Schegg 1988, Pauli 1988 at ETH Zürich, and Hitz 1989, Dalla Torre 1991, Christen 1993 at the University of Berne). Previous summaries have been published by Pfiffner et al (1990), Schmid et al. (1990) and Schreurs (1993). This summary will additionally make an attempt to place these detailed studies into a larger context by comparing them with published and ongoing work in neighbouring areas in order to arrive at a larger scale paleogeographic and kinematic picture.

14.2 Mesozoic rifting and drifting

14.2.1 Introduction

Amongst the major paleogeographical domains found in the Alps (Helvetic, Penninic, Austroalpine-Southalpine) the Penninic domain is the most problematic one. To regard the Penninic domain as simply representing an oceanic suture zone between the European foreland (Helvetic domain) and the overriding Apulian plate (Austroalpine-Southalpine) would be a gross oversimplification. The Penninic nappes in the sense of a series of nappes overriding the Helvetic nappe system and found in the footwall of the Austroalpine nappe system do not represent a single paleogeographic domain. These Penninic nappes are made up of three categories: (1) basement nappes and their autochthonous to parautochthonous cover, (2) detached Mesozoic cover nappes or slices (e.g. Schams nappes, Bündnerschiefer and Flysch) whose derivation from individual basement nappes or from nappe-dividing Mesozoic thrust zones ("roots") is controversial, and (3) ophiolite-bearing units.

A Penninic paleogeographical domain, corresponding to the Penninic nappe system, is hard to define for several reasons. An extension of the former northern passive continental margin (Helvetic) into units occupying a structural position within the lower parts of the Penninic domain in the structural sense is to be expected (e.g. Milnes 1974, Subpenninic units). This raises serious problems in terminology because of historical reasons. Unfortunately, no clear distinction is usually made between "Penninic" in the paleogeographical and tectonic sense, a heritage of Argands "Embryonaltektonik" (Argand 1916), associated with extreme cylindrism regarding paleogeographical domains which, according to him, predetermine future nappes in "embryonic" form. Unfortunately, the breakthrough of modern paleogeographic reconstructions based on the concepts of plate tectonics (passive continental margin formation, ocean floor spreading, accretionary wedge formation) did not lead to a corresponding change in the traditional terminology, which still reflects the concept of a geosyncline.

Paleogeographical reconstructions, apart from nomenclatural problems, are also hampered with other major problems: (1) many sediments are ill-dated; (2) basement-cover relationships are obscured by décollement of sedimentary cover slices whose position in respect to basement nappes is often a matter of debate (e.g. the "Schams dilemma", see Trümpy and Haccard 1969, Trümpy 1980), in some cases corresponding basement units are missing altogether; (3) polyphase penetrative deformation often associated with large scale refolding of a previously emplaced nappe pile (e.g. Milnes 1974) prevents simple paleogeographic reconstructions; (4) intense deformation associated with metamorphism makes stratigraphical and sedimentological studies extremely difficult.

This chapter reports some progress made regarding the paleogeographical evolution of an important part of the NFP 20 Eastern Traverse. In the framework of the NFP 20 project stratigraphic-sedimentological investigations primarily aimed at (1) rocks of the Schams nappes (Rück 1990, Schmid et al. 1990), in close conjunction with structural work (Schreurs 1990) and (2) similar cover rocks presently found at the front of the Tambo nappe investigated by combined structural and stratigraphic work (Mayerat 1989, Pfiffner et al. 1990). The results of these investigations will be discussed in the context of older investigations (e.g. Falknis-Sulzfluh nappes, Gruner 1981) and very recent investigations (e.g. Bündnerschiefer; Steinmann et al. 1992, Steinmann 1994) in neighbouring sedimentary realms with the aim of deriving a larger scale paleogeographical reconstruction crucial for understanding the Alpine orogeny.

14.2.2 Stratigraphy and sedimentology of the Schams nappes

14.2.2.1 Paleogeographic and tectonic units in the Schams nappes

In order to discuss stratigraphy and sedimentology of the Schams nappes, or better the Schams cover slices, it is convenient to subdivide the paleogeographical realm covered by the Schams slices into roughly E-W trending units and subunits depicted in Figure 14-3 a and b (Rück 1990). This subdivision is based on a combined structural and sedimentological approach (Schmid et al. 1990). Units and subunits primarily denote paleogeographical entities, but abrupt facies changes control the position of décollement horizons and, consequently, the structural subdivision of the Schams nappes (Figure 3c and d). These facies changes are most pronounced in the Middle Jurassic to Lower Cretaceous strata. The reconstruction along a N–S paleogeographical profile is based on a detailed structural analysis (Schreurs 1990).

Presently, subunit 1b (hemipelagic basin) may be directly linked with subunit 1a (proximal slope characterized by the Vizan breccia) around a F1 fold hinge whose location is predetermined by an abrupt facies change (Figure 14-3). Both subunits 1b and 1a roughly correspond to the Gelbhorn nappe of Streiff (1939, 1962), Jäckli (1941) and Neher in Streiff et al. (1971/1976). Over large distances the Gelbhorn unit 1 has been detached along the Carnian evaporites, older sediments and basement have been left behind in a yet unkown position at the base of the Tambo basement nappe. Only where this décollement horizon is missing due to Mesozoic erosion (locally in subunit 1a) have older sediments and basement slivers (Taspinit and Nolla basement, Figure 14-4) also been incorporated into the Schams cover slices.

Only locally are F1 hinges between Gelbhorn unit 1 and Tschera-Kalkberg unit 2 preserved. Subunit 2a (partly but not entirely identical with the Tschera nappe of Streiff, 1939) simply represents the Upper Triassic and younger cover of subunit 2b (Gurschus-Kalkberg nappe of Streiff et al., 1971/1976), 2a and 2b being detached from each other during early F1 imbrication along the Carnian evaporites. The basal detachment of the Schams cover slices in general changes from the Carnian evaporites (Gelbhorn unit 1) to the base of the Triassic carbonates (unit 2b), both décollement levels being at a similar depth according to the reconstruction in Figure 14-3c. This geometry is strongly controlled by the paleogeography: in parts of subunit 1a, and particularly in subunit 2c (Figure 14-3a,b), Carnian evaporites are missing due to predepositional erosion at the base of the Middle to Upper Jurassic breccia formations; consequently, décollement has to occur at the base of the Triassic carbonates. Subunit 2c (partly corresponding to the Wissberg nappe of Kruysse 1967, see also Pauli 1988) locally exposes a coherent sequence from the base of the Triassic carbonates into the Upper Cretaceous. Large parts of this subunit, however, are strongly dismembered by Alpine tectonics, in particular by large scale boudinage of the competent Middle Triassic carbonates.

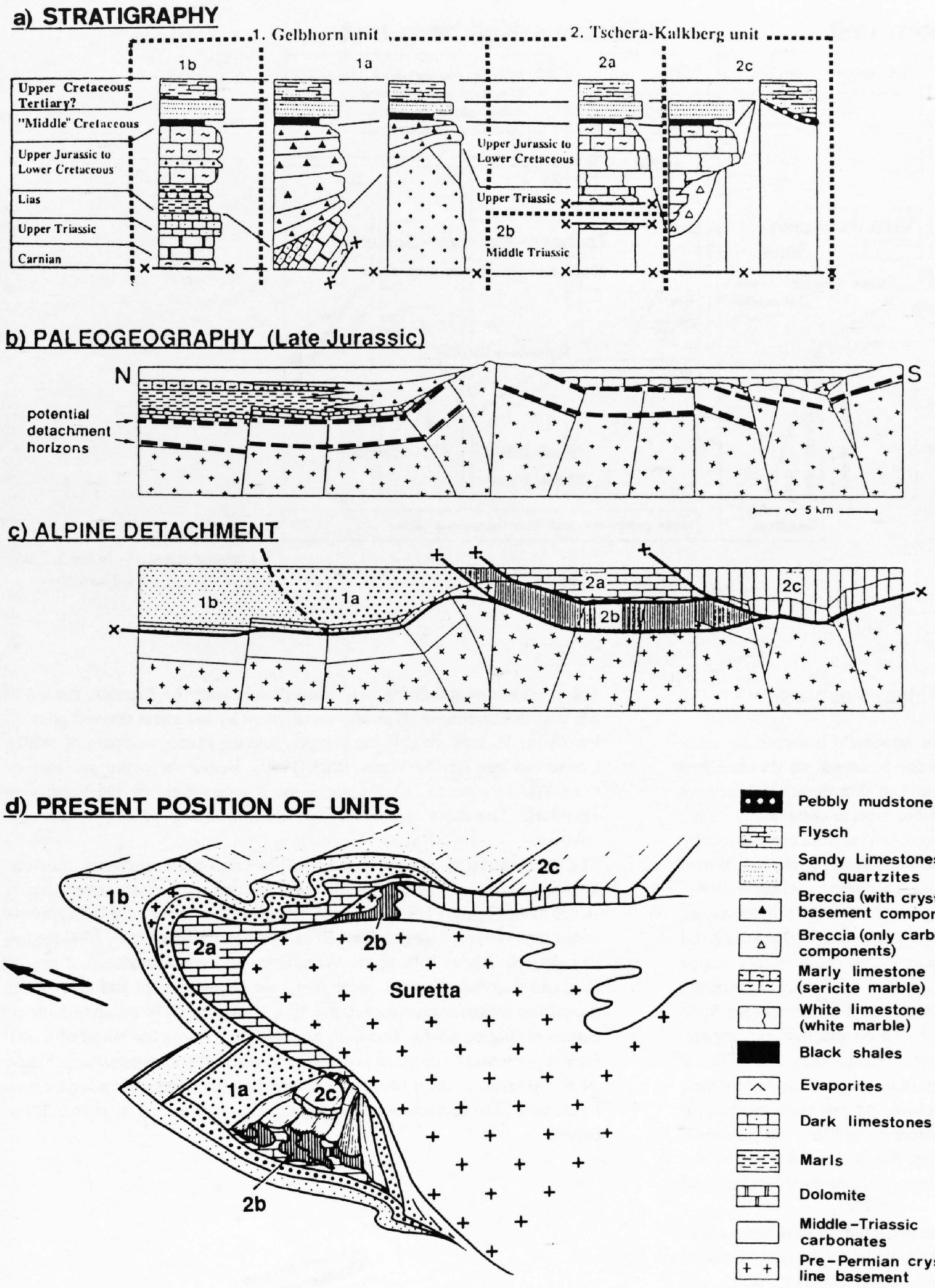

Figure 14-3
Schematic overview of stratigraphy and structure of the Schams nappes after Rück (1990).
a) Stratigraphy of the Schams units.
b) Sketch of the paleogeography during the Late Jurassic epoch.
c) Position of future Alpine detachments.
d) Sketch of the present day cross section through the Schams nappes.

14.2.2.2 Lithostratigraphy of the Schams nappes

Correlations of the formations and series schematically illustrated in Figure 14-4 are mainly based on lithologies which at least locally occur in all the subunits. These are in particular the Tumpriv-Serie reaching from the Carnian evaporites into the Lower Jurassic (fossil occurrences in the Rhaetian and the Pliensbachian, Wilhelm 1933) and, additionally, the Ölquarzit and Plattensandstein (erroneously referred to as Platten-"quarzit" by Streiff et al. 1971/1976) embedded in anoxic black shales. The latter lithologies exhibit a high content in organic carbon and show striking lithological similarities to well dated formations in the Falknis nappe (Allemann 1957 dated the top of the Plattensandstein, locally referred to as "Gault", to be of Cenomanian age). Rück (1990) correlates these lithologies with the "Mid"-Cretaceous anoxic event (Jenkyns 1980). There are no further age determinations for the intervening formations. Continuation of sedimentation into the Tertiary is to be expected for parts of the Schams nappes from the presence of dated Tertiary sediments in the neighbouring Arblatsch flysch (Lower Eocene, Ziegler 1956, Eiermann 1988) and in the Falknis nappe (Paleocene, Allemann 1957).
Correlations across subunits 1a and 1b are facilitated by the presence of distal turbidites of the Vizanbrekzien-Serie in subunit 1b. Similar interfingering is also observed across the boundary between subunits 1a and 2a (Figure 14-4). The Untere Sericitmarmor is common to subunits 1a and 2a. Its age is probably Latest Jurassic to Early Cretaceous because it overlies the Tschera-Marmor-Serie (white marbles and carbonate breccias) found in subunits 2a,b and c, considered to be of Upper Jurassic age (based on facies analogies to the Sulzfluhkalk of the Sulzfluh nappe and Upper Jurassic limestones in the Préalpes Médianes), and because it is covered by "Mid"-Cretaceous formations. The Vizanbrekzien-Serie locally encompasses the entire age bracket between Early Jurassic (post-Pliensbachian) and Mid-Cretaceous times. It locally cuts down section due to pre-depositional erosion, in places by more than 600 m (maximum thickness of the Middle Triassic carbonates) and down to the pre-Triassic basement. The actual thickness of the Vizanbrekzien-Serie is extremely variable and may reach 250 m (corresponding to 500 m after retrodeformation according to a strain analysis carried out by Schreurs 1990). The minimum thickness of the post-Carnian cover in subunit 1b amounts to about 400 m, intensive layer-parallel cleavage suggests that this is only a fraction of the original thickness. In subunit 2 the thickness of the post-Triassic sediments is highly variable and may reach about 100 m, this again being an absolute minimum (due to intensive cleavage formation). Because of these large uncertainties the thicknesses in Figure 14-3 and14-4 are only approximately scaled. The horizontal scale in Figure 14-3 is estimated according to an area balance (24 km^2 are occupied by Schams nappes and related units at the front of the Tambo nappe in a N–S section) and a very rough estimate of the average thickness of the Schams cover (800m). According to this estimate the extreme facies variations across the various subunits occur over a lateral distance of only some 30 km.

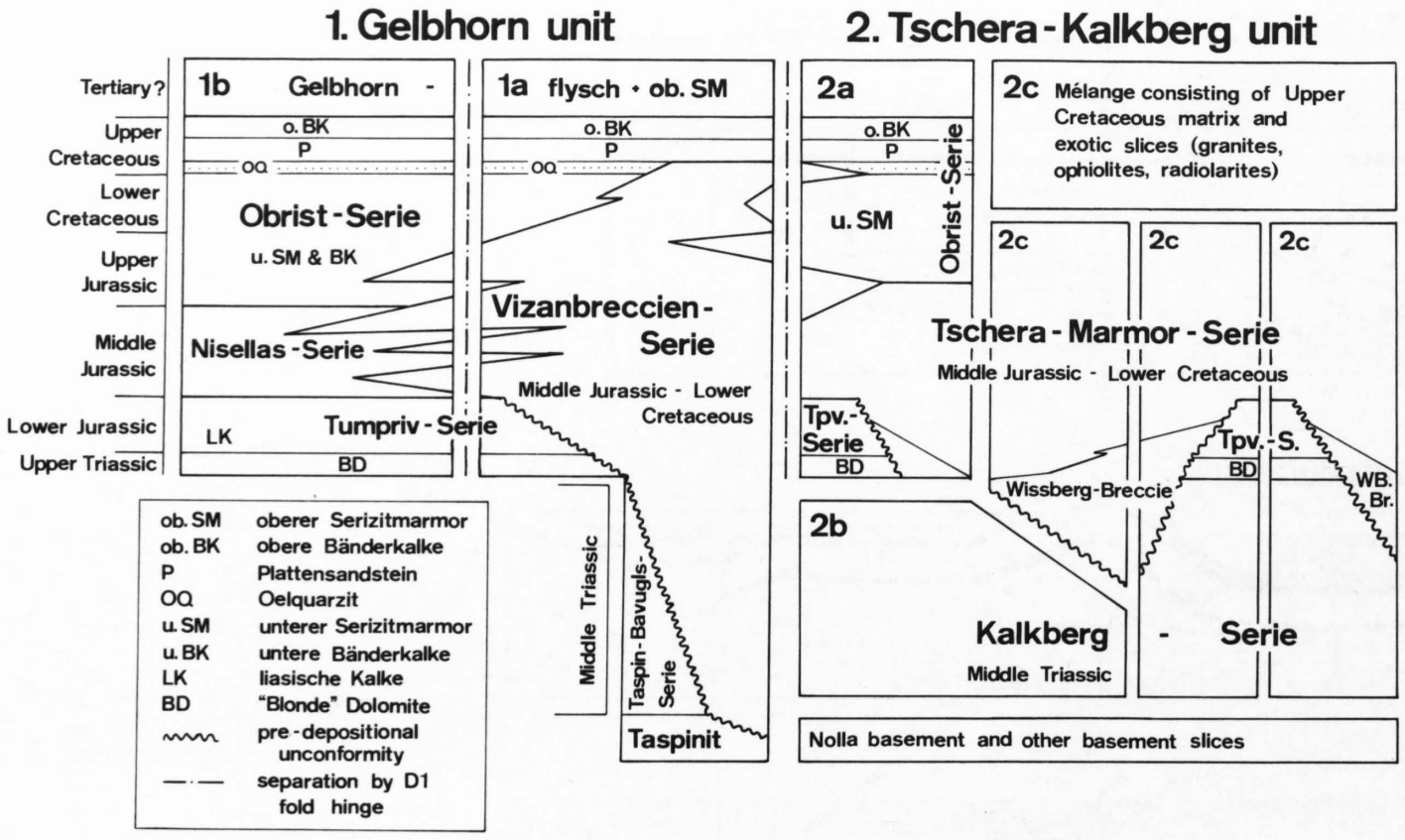

Figure 14-4
Lithostratigraphy of the Schams nappes, after Rück (1990)

14.2.2.3 Basin evolution of the Schams nappes

Information on the nature of the **pre-Triassic basement** is crucial for speculations about the present-day position of the basement of the detached Schams sediments. Such information is found in thin detached basement slivers (Taspinit and Nolla basement) and from breccia components in the Vizanbrekzien-Serie. Microstructural investigations indicate that the locally preserved pre-Alpine foliation in the Taspinit and Nolla basement formed under upper-greenschist to amphibolite grade conditions (Schreurs 1990). Hence the Rofna porphyry, typical for the entire front of the Suretta nappe, and similar "monocyclic" basement lithologies (i.e. lithologies which did not undergo a pre-Alpine tectonometamorphic event) in the Tambo nappe can be excluded to have formed the "homeland" of the Schams sediments. The erroneous statement in Schmid et al. (1990), that Vizanbrekzien-Serie pebbles resemble the Rofna porphyry was based on macroscopic appearance. Also excluded as source area for crystalline pebbles is the top of the Suretta and Tambo nappes since they are in most places sealed by their own Mesozoic cover. Detachment of the Schams nappes from the base of the Tambo and Suretta thrust sheets is extremely unlikely for structural reasons. The Adula nappe is separated from the Schams nappes by the N-Penninic Bündnerschiefer of the Misox zone and can therefore be ruled out as well.
In conclusion, it seems that most of the sediments of the Schams nappes have been originally deposited on polycyclic continental basement (i.e. basement which underwent pre-Alpine deformation and metamorphism) which was almost completely subducted during Alpine orogeny. This basement is only preserved in the form of thin slivers within the Schams nappes and it is unlikely that the large basement nappes depicted in Figure 14-2 (Adula, Tambo, Suretta) can be considered as representing the homeland of the detached Schams sediments.

The **early stages of subsidence** led to the deposition of a thick (max. 600 m) Middle Triassic carbonate platform, the Upper Triassic dolomites above the Carnian evaporites exhibiting a very reduced thickness and intercalations of clay formations identical with the Helvetic Quartenschiefer ("Carpathian" facies). In contrast to the Upper Austroalpine and part of the Lower Austroalpine passive continental margin the Lower Jurassic limestones indicate a transition from neritic to open marine hemipelagic conditions and evidence for extensive rifting of pre-Toarcian age is missing.

The **rifting and/or transcurrent faulting stage** starts immediately after the Pliensbachian, possibly in the Toarcian represented by black shales containing the first distal turbidites of the Vizanbrekzien-Serie in subunit 1b. These black shales grade into carbonate bearing shales and marls, virtually undistinguishable from the N-Penninic Bündnerschiefer (Nisellas-Serie). In subunit 1a, however, the base of the Vizanbrekzien-Serie, where conformable on the Tumpriv-Serie, immediately overlies Liassic limestones. Locally, these Liassic limestones are Gryphäa-bearing and covered by a thin veneer of black shales (Toarcian?). It is important to note that while conformable parts of the base of the Vizanbrekzien-Serie indicate the initiation of rifting and/or transcurrent faulting in or immediately after the Toarcian, the top of the Vizanbrekzienserie (typically represented by basement derived arkoses) locally grades conformably but abruptly into the Plattensandstein of "Mid"-Cretaceous age (at Piz Vizan, Rück 1990). Hence the entire age interval from Mid-Jurassic to "Mid"-Cretaceous is represented by the Vizanbrekzien-Serie. The exact age of intermediate lithostratigraphic levels remains unkown.
The depositional geometry of the Vizanbrekzien-Serie, sediment transport directions and the geometry of the basal unconformity (only schematically sketched in Figure 14-5) have been interpreted in terms of a transpressive rather than distensive regime (see Rück 1990 and Schmid et al. 1990 for further details). About 50% of the Vizanbrekzien-Serie is made up of gravity flow and rock-fall deposits, indicating a very strong relief and near-source deposition almost exclusively to the N of a roughly E–W trending fault escarpment (Figure 14-6). This fault escarpment delimits the N end of a platform represented by unit 2. It is depicted as sinistrally transpressive in Figure 14-6, the sense of shear being purely based on the large scale plate tectonic framework. The remainder of the resediments is made up of proximal turbidites.

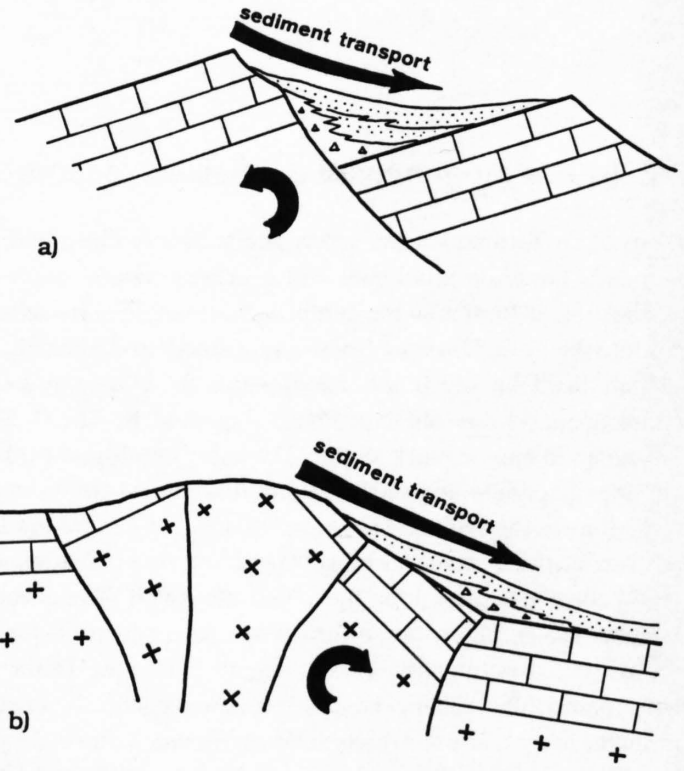

Figure 14-5
Sketch visualizing relations between tilt-direction of pre-rift sediments and sediment transport direction of syn-rift sediments for the case of (a) extension or transtension and b) transpression. After Rück (1990), for discussion see text and Rück (1990).

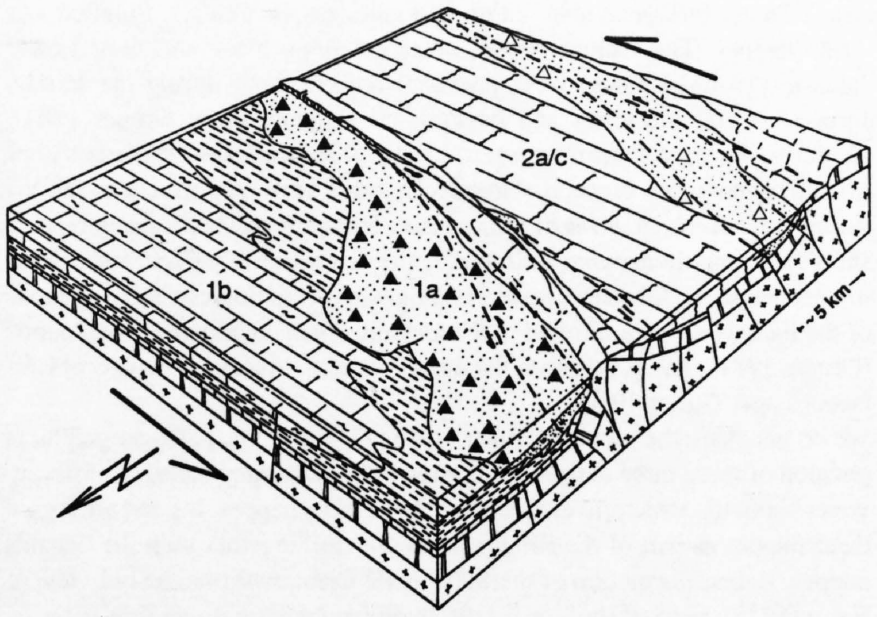

Figure 14-6
Block diagram of the paleogeography of the Schams nappes during Late Jurassic times, after Rück (1990). For symbols and numbers see Figure 14-3a.

Sedimentological data indicate that the fault escarpment remained active untill "Mid"-Cretaceous times (Rück 1990). Clast abundance generally indicates a tendency for upwards increasing amounts of crystalline basement and generally a thinning-fining-upward tendency is observed, occasionally in two cycles (Piz Vizan, Piz Tschera, Rück 1990). Contemporaneous tectonic activity is responsible for continuous supply of pebbles, almost exclusively derived from a local source (basement, overlying Middle Triassic carbonates and Tumpriv-Serie). This ongoing tectonic activity is directly manifested by Mesozoic cataclasites within the Taspinit basement (Bavugls area, see Rück 1990). Abundant neptunian dykes in basement and pre-breccia cover indicate extension and illustrate that this tectonic activity was not of a transpressive nature for the entire time interval covered by the Vizanbrekzien-Serie (Mid- Jurassic to "Mid"-Cretaceous). Large scale considerations also indicate that the Schams nappes were part of a passive continental margin setting associated with substantial crustal thinning in the Early to Middle Jurassic. It is not clear during which time interval the transpressive regime inferred from the depositional geometry (Figure 14-6) prevailed. Also, transpression may only be a local phenomen, restricted to the Schams area.
Contemporaneous sediments in unit 2 are typical platform sediments (Tschera-Marmor-Serie topped by local occurrences of Unterer Sericitmarmor and locally with the Wissberg breccia at the base). The Wissberg breccia is entirely composed of reworked Triassic and Jurassic carbonates and is, in contrast to the Vizanbrekzie, devoid of basement clasts. Direct transgression onto Middle Triassic carbonates and erosion of intervening lithologies (Tumpriv-Serie) is reminiscent of the Préalpes Médianes Rigides. In subunit 1b the already described Nisellas-Serie is topped by impure carbonates (mainly Unterer Sericitmarmor and untere Bänderkalke of the Obrist-Serie, identical with the so-called "Nivaigl-Serie" mapped in the E-Schams by Streiff et al. (1971/1976).

A **tectonically quiescent phase** before the onset of Alpine convergence is indicated by the "Mid"-Cretaceous lithologies which are identical in all subunits. Obviously, the ongoing tectonic activity which is responsible for the preservation of the extreme facies variations characteristic for older formations within the Schams nappes came to a halt by "Mid"-Cretaceous times. The resediments found in the Ölquartzit and Plattensandstein are very mature and are widespread over the entire Tethys (Weissert 1981, 1989).

The **Alpine convergence and accretionary stage** is represented by the illdated Gelbhorn "flysch" which contains the Obere Sericitmarmor, probably representing the Couches Rouges. Thin-bedded limestones, intercalated with shales form the remainder of this "flysch". Unit 2 is characterized by mélange formations, embedded in a Late Cretaceous matrix of pebbly mudstones (planktonic foraminifera described by Pauli 1988 and Neher in Streiff et al. 1971/1976). This mélange locally contains exotic slices of granite, ophiolites and radiolarites (subunit 2c), indicating the proximity to and/or accretion of the southernmost Briançonnais to the S-Penninic oceanic domain at this time. While it is possible that accretion and mélange formation started in Late Cretaceous time within the southernmost subunit 2c, it is possible that relatively undisturbed sedimentation (which does not exclude coeval accretionary wedge formation) continued into the Tertiary within unit 1b.

14.2.3 Stratigraphy of neighbouring sedimentary units

14.2.3.1 The sediments at the front of the Tambo nappe

Mayerat (1989) showed that large parts of these sediments, referred to as Areua-, Vignone- and Knorren-Zone by Gansser (1937) are made up of Schams cover slices and that the Schams nappes near Splügen may be directly traced across the Hinterrhein valley and into the area in the front of the Tambo nappe. The Areua basement slice, not being part of the Schams nappes, has a very reduced autochthonous cover (Permo-Carboniferous, basal Triassic) and is part of the Areua-Bruschghorn mélange (Schmid et al. 1990) enveloping the Schams nappes and continuous with the Martegnas mélange in the E-Schams. The Schams sediments in front of the Tambo nappe are in tectonic contact with the Areua mélange and have been detached within the Carnian evaporites. The lithologies found are diagnostic for both subunits 1a and 1b: Tumpriv-Serie, Vizanbrekzien-Serie (predominantly dolomitic and rarely with basement pebbles), Unterer Sericitmarmor, Plattensandstein, Oberer Sericitmarmor and Gelbhorn "flysch". Hence, only elements of subunits 1a and 1b are present, while subunit 2 is completely missing (no Middle Triassic nor Tschera-Marmor-Serie).

Mayerat (1989) somewhat artificially separated these Schams cover slices from a dismembered unit referred to as Knorren mélange. This mélange largely consists of Schams lithologies and is in direct tectonic contact with the front of the Tambo basement nappe. In Val Vignone (Motta da Caslasc) this mélange contains a gneissic breccia directly overlying a basement slice, consisting of Permo-Carboniferous breccias and paragneisses. The analogies with similar contacts at coordinates Bavugls (E-Schams, Rück 1990) are striking and indicate the presence of slices of subunit 1a in the Knorren mélange at the front of the Tambo nappe.
Recent field work (Schmid unpublished) revealed that the Andrana zone (topmost cover slice of the Misox zone, Strohbach 1965) contains typical Tumpriv-Serie, Unterer Sericitmarmor and Plattensandstein (along the San Bernardino motorway at 736 600 / 144 400). This suggests that the Schams nappes can be traced southwards and along the base of the Tambo nappe as far as near the village Mesocco. On the one hand this excludes the front of the Tambo nappe as a possible site of detachment for the Schams cover slices. On the other hand it makes the hypothesis for rooting the Schams nappes in the Splügen zone (Mayerat 1989), i.e. at the top of the Tambo nappe, virtually impossible.

14.2.3.2 Splügen zone and Suretta cover

Most previous workers considered the age of the autochthonous cover of the Suretta nappe (excluding the Avers Bündnerschiefer) and of the sediments of the Splügen zone to be of pre-Jurassic (Triassic) age. In the case of the Splügen zone, however, Baudin et al. (1993) suggest that part of this cover, represented by carbonate breccias (similar to the Wissberg breccia in the Schams nappes), white calcite marbles, yellow sericite marbles, black shales and calcareous schists is of Jurassic and Cretaceous age. These authors found that Permo-Triassic conglomerates ("Verrucano"), volcanoclastics ("Rofna"-type) and basal Triassic sandstones are widespread at the base of the Splügen zone, representing the parauthochthonous cover of the Tambo nappe (partly identical with the Bardan zone of Strohbach 1965). These basal slices, together with the Andossi zone in the hangingwall, containing the post-Triasssic lithologies mentioned above, form the Splügen zone as a single unit characterized by complex imbrication of the cover of the Tambo nappe.
The Triassic quartzite of the Suretta Mesozoic cover is transgressive on a polycyclic basement (Timun unit) or on monocyclic basement (Rofna porphyry and "Verrucano"-type sediments). While parts of the dolomite and calcite marble alternations topping the basal quartzite are undoubtedly of Triassic age (close facies analogies to the Middle Triassic of the Tschera-Kalkberg unit in the Schams nappes) there is strong evidence for the presence of younger sediments. At several locations in the Suretta nappe, breccias contain angular components of dolomite and calcite marbles and, locally, crystalline basement overlies Triassic carbonates. To the south (Val Madris) these breccias contain large boulders and can be interpreted as (submarine) rock fall breccias (Hitz 1989). At some localities these breccias are in direct contact with the pre-Triassic basement and contain meter-size fragments of basement rocks (Dalla Torre 1991) suggesting that the Triassic quartzites and carbonates had been eroded locally and/or that the breccia-basement contact is a synsedimentary normal fault associated with Jurassic rifting. A peculiar relationship between basement, carbonates and breccias can be studied on the E side of Val Ferrera. In the Piz Grisch area (Christen 1993) and E of Campsut (Pfiffner unpublished, Figure 14-7), large (100m size) blocks of pre-Tri-

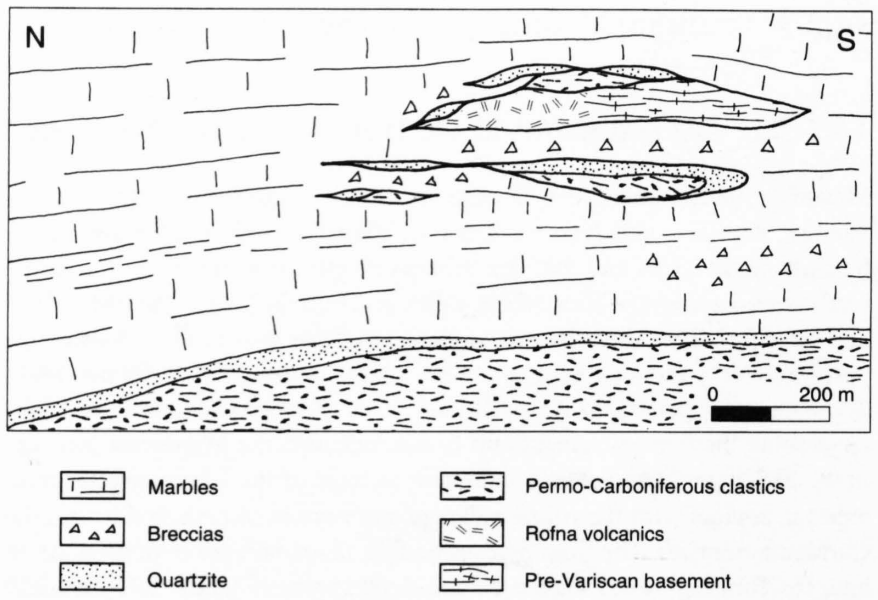

Figure 14-7
Evidence for Jurassic normal faulting in the Suretta nappe.
Lenses of pre-Triassic basement and Triassic quartzites are embedded in Jurassic breccias and Triassic carbonates (geologic sketch of the slope E of Campsut).

assic basement and quartzites embedded in a matrix of breccias occur as elongate lenses within Triassic carbonates. Alpine imbrication alone, even if considering the polyphase structural evolution, cannot be responsible for the observed structures. The large elongate basement blocks are more likely the result of synsedimentary faulting, which was subsequently obliterated by polyphase Alpine folding and thrusting.
The local unconformities leading to the direct transgression onto basal Triassic quartzite or pre-Triassic basement indicate substantial predepositional erosion caused by emersion following rifting. The large blocks of pre-Triassic basement and Triassic quartzites embedded in Jurassic breccias point to synsedimentary normal faulting and, associated, high relief. Both features are typical for the rifting and/or transcurrent faulting stage during the Jurassic and the Early Cretaceous as also found in the Schams nappes.
Hence, it appears that the cover of both Tambo and Suretta nappe exhibits strong similarities to the Tschera-Kalkberg unit of the Schams nappes, where the Tschera-Marmor-Serie (including the Wissberg breccia) is often transgressive onto the Middle Triassic. In many places the Tumpriv-Serie is missing due to post-Triassic erosion and hence lithologies typical for the Lower and Middle Jurassic are frequently absent. Tectonically emplaced cargneule horizons (presumably of Carnian age) and yellow dolomites are the only relics of the Tumpriv serie in the Tambo and Suretta cover. In view of the paleogeographic reconstruction of the Schams nappes (Figure 14-3) and the derivation of the Schams nappes below the Tambo basement nappe it is suggested that the cover of the Suretta and Tambo nappes represents the direct southern continuation of the Schams nappes, analogous to the Barrhorn Serie in the Western Swiss Alps which represents a paleogeographical equivalent of the Médianes Rigides, still autochthonous on the pre-Triassic basement (Sartori 1990).
The Avers Bündnerschiefer must be considered allochthonous with respect to the underlying Triassic carbonates and Jurassic rift breccias. Milnes & Schmutz (1978) considered the local occurrence of the Jurassic breccias, which they interpreted as having a tectonic origin, to be indicative of a thrust separation. However, recent mapping (Hitz 1989, Christen 1993 and field work by Pfiffner) showed that (Triassic) cargneules overly in places (Jurassic) breccias at this contact. In other places small scale imbrications of Bündnerschiefer and basement or Triassic carbonates point to a tectonic contact. The Avers Bündnerschiefer unit has been accreted to the Austroalpine orogenic lid and thrusted over the Suretta cover during an early stage of Alpine convergence. The presence of radiolarian cherts (Nievergelt pers. comm.), together with ophiolitic slivers within the Avers Bündnerschiefer (Oberhänsli 1977) suggests a S-Penninic origin of the Avers Bündnerschiefer. They should no longer be considered to represent the post-Triassic cover of the Suretta nappe.

14.2.3.3 Falknis, Sulzfluh and Tasna nappes

The Cretaceous sediments of the Falknis, Sulzfluh and Tasna nappes, in particular the Gault of "Mid"-Creaceous age, show close similarities to their equivalents in the Schams nappes. The Jurassic lithologies, however, differ substantially from those found in the Schams nappes (Gruner 1981 and references therein). Only the Upper Jurassic Sulzfluh-Kalk of the Sulzfluh nappe (Allemann 1957, Ott 1969) is virtually identical with the Tschera-Marmor-Serie of the Schams nappes. The Jurassic sediments are subject to strong facies variations also within and amongst the Falknis, Sulzfluh and Tasna nappes. The Falknis nappe, detached along black shales of Lower Jurassic (Toarcian?) age, lacks proximal breccia input during the Middle Jurassic (distal turbidites and background sedimentation, Gruner 1981). However, during a short time interval (Late Kimmeridgian? to Early Tithonian) basement-rich breccias (Falknis-Brekzie), very reminiscent of the Vizanbrekzien-Serie in terms of sedimentary transport mechanisms, indicate a short-lived important pulse, followed by the deposition of pelagic and detrital limestones at the Jurassic-Cretaceous boundary. Lithologies similar to those of the Falknis nappe are found in the tectonically dismembered Tasna nappe (Gruner 1981). There, however, the most important breccia horizon is of Cretaceous age (Gürler 1982).
We do not share the view of Gruner (1981) regarding the paleogeographical position of these three nappes at the Austroalpine margin, based on differing views about the structural evolution of the Schams nappes. Instead we regard these nappes as part of the Briançonnais domain, together with the Schams nappes. Retrodeformation of the Schams F2 event confirms the old view of Haug (1925), revived by Streiff (1962), and suggests a direct link between Falknis-Sulzfluh nappes and E-Schams nappes due to a S-closing fold in the Avers valley. The facies arguments proposed by Gruner (1981), based on the differing petrology of pre-Alpine basement components in the breccias, are not conclusive for deriving the paleogeographical position during the Jurassic and merely imply petrologically different basement sources for the Falknis and the Vizan breccia. The close neighbourhood of the Falknis and Sulzfluh nappes with their contrasting lithologies is very reminiscent of the rapid facies changes in the Schams nappes. The stacking order (Sulzfluh over Falknis nappe) is that of the W-Schams nappes (Tschera-Kalkberg over Gelbhorn unit), supporting the notion of a S-closing megafold between E-Schams (inverted stacking order) and Falknis-Sulzfluh nappes. The southern continuation of the Falknis-Sulzfluh nappes into the Avers valley is strongly disrupted and thinned and the hinge in the Avers valley is affected by subsequent normal faulting along the Turba mylonite zone (Nievergelt et al. 1996). The thickness of Jurassic-Cretaceous sediments reaches about 1000m in the Falknis nappe but is substantially less in the Sulzfluh nappe. Assuming an average thickness of the Mesozoic cover of about 800m for both Falknis and Sulzfluh nappes and measuring the area occupied by these two nappes in a N–S-section (31 km^2), i.e. subparallel to the movement direction during Tertiary orogeny, gives a width of 39 km for the depositional area of the Falknis-Sulzfluh sediments measured in a N–S-direction. Since the Falknis-Sulzfluh nappes structurally represent the N continuation of the Schams nappes (their depositional width in a N–S direction was earlier estimated to some 30km), the width of the Briançonnais platform (not including the Tambo- and Suretta sediments) in a N–S-direction may be estimated to be in the order of 70 km.

14.2.3.4 N-Penninic Bündnerschiefer and ophiolites

In the W-Schams and in front of the Tambo nappe the Areua-Bruschghorn mélange zone (Mayerat 1989, Rück 1990, Schmid et al. 1990) forms the basal thrust zone of the Schams cover slices, overriding the N-Penninic Bündnerschiefer. Around a large scale post-nappe fold (Niemet-Beverin fold) this mélange zone directly connects with the Martegnas mélange (Figure 14-2), which is part of an overturned stack of tectonic units in the E Schams (Rück 1990, Schmid et al. 1990). There, the Martegnas mélange separates the Schams nappes from the Tertiary Arblatsch flysch, originally part of the N-Penninic flysch zone. Only due to post-nappe refolding is the Arblatsch flysch at present in a structurally higher position in respect to the Schams nappes (Figure 14-2).
The continuous Areua-Bruschghorn-Martegnas mélange zone consists of ophiolitic remnants whose derivation from oceanic crust is, contrary to other mafic and ultramafic units within the N-Penninic Bündnerschiefer, beyond any doubt. Serpentinites, gabbros, pillow lavas, radiolarian cherts, pelagic limestones are widespread near Piz Martegnas (Streiff et al. 1971/1976, Eiermann 1988, Schmid et al. 1990) and imbricated with basement slivers (i.e. Areua basement) and sediments of the Schams nappes (i.e. Tumpriv-Serie, Vizanbrekzien-Serie, Tschera-Marmor-Serie). While the ophiolitic remnants are virtually undistinguishable from S-Penninic ophiolites (Platta-Arosa) the non-ophiolitic constituents are different in these two mélange zones (Schams lithologies in the Martegnas mélange versus Austroalpine lithologies in the Platta-Arosa mélange).
The bulk of the N-Penninic Bündnerschiefer and flysch sediments is structurally below the Areua-Bruschghorn-Martegnas mélange and the Schams nappes. These Bündnerschiefer are imbricated into four major units (Nabholz 1945, Steinmann et al. 1992, Steinmann 1994) which are, from top to bottom (Figure 14-2): the Tomül unit (equivalent to the backfolded Arblatsch flysch reaching into the Lower Eocene (Ziegler 1956, Eiermann 1988), the Grava unit (probably continuous with the Prättigau Bündnerschiefer and flysch also reaching into the Tertiary (Nänny 1948), the Aul marble unit (pre-

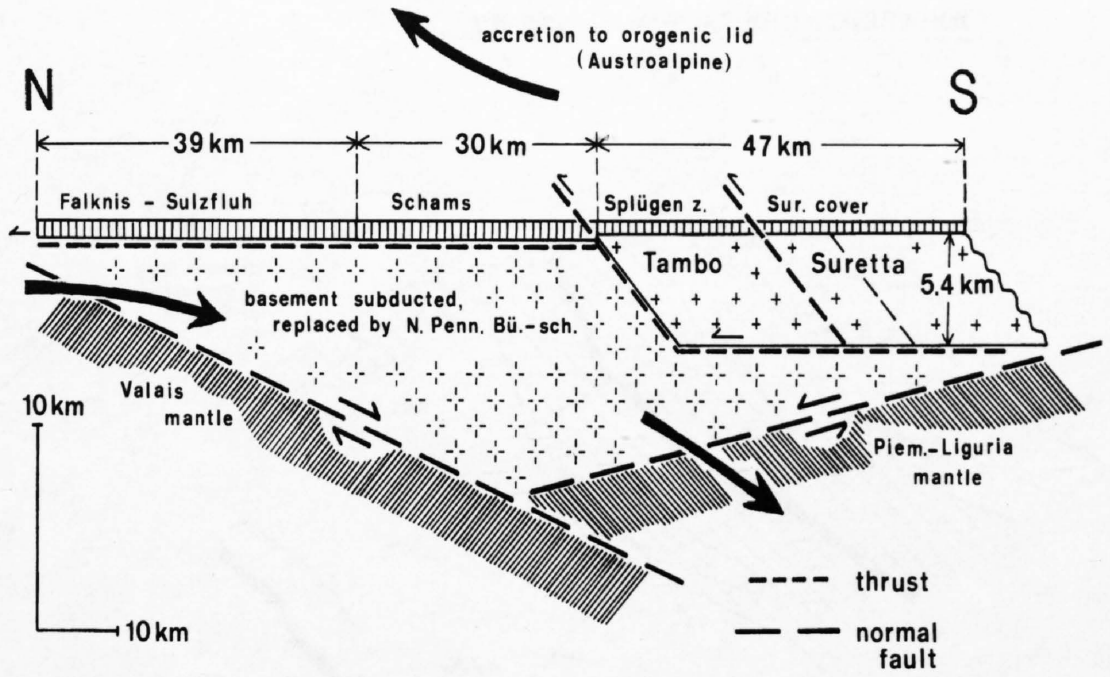

Figure 14-8
Very schematic restoration showing (1) the dimensions of crustal flakes derived from the Briançonnais domain now incorporated into the present day cross section and future detachment horizons related to Alpine collision (thrusts); (2) a minimum estimate of crustal thickness arrived at by assigning an upper plate margin position to the Briançonnais domain during two subsequent events of passive margin formation (compare Figures 14-9a and 14-9b); (3) subduction of excess crustal material being replaced by Valais Bündnerschiefer in an accretionary wedge scenario.

dominantly impure carbonates) and the Valser Schuppen (highly variable lithologies, imbricated with the Adula basement). Steinmann (1994) reports ophiolite-bearing mélange zones, also containing slivers of continental basement, Permo-Triassic cover and in particular Liassic Gryphea-bearing limestones (Nabholz 1945), at the base of the Grava and Tomül units. The Aul marble unit and the Valser Schuppen also contain ophiolitic slices. Typical Bündnerschiefer lithologies, however, are largely missing within these two lowermost units. Instead the Aul marble represents an impure marble presumably representing a platform area N of the Bündnerschiefer.

It appears that the Areua-Bruschghorn-Martegnas mélange and Schams cover slices represent the topmost elements of a large accretionary wedge mainly consisting of the four Bündnerschiefer units mentioned above. It will be argued later that this accretionary wedge formed during the Tertiary. It roots in the Misox zone and on top of the Adula high-P unit. Interestingly, the age of the Bündnerschiefer in Grava- and Tomül units is predominantly Cretaceous (with possibly some Late Jurassic sediments at the base). Moreover, parts of these N-Penninic Bündnerschiefer appear to have been deposited onto oceanic rather than on continental crust (see Steinmann 1994).

In summary, the N-Penninic ophiolites, and at least parts of the Bündnerschiefer are likely to represent a domain of oceanic crust, as proposed by Frisch (1979), Rück (1990), Schmid et al. (1990) and Stampfli (1993), situated to the N of the Schams paleogeographical domain. The Areua-Bruschghorn-Martegnas mélange would have formed at the N boundary of the Briançonnais platform. This platform, represented by the Schams and the Falknis-Sulzfluh cover nappes and, additionally, the Tambo-Suretta basement nappes with their own Mesozoic cover, separates the Valais (N-Penninic Bündnerschiefer) oceanic domain from the S-Penninic or Piemont-Liguria ocean.

14.2.4 Paleogeographical setting in a larger context

In order to discuss basement-cover relationships in the Penninic nappes and in order to sketch large scale paleogeographical maps it is important to have some estimate on the original width of the Briançonnais platform. The foregoing discussions showed that the original width of the Falknis-Sulzfluh and Schams cover nappes amounts to about 70 km measured in a N-S-direction. Admittedly, this estimate is very crude. It is based on area balancing applied to a N-S oriented cross section (see chapter 22, plate 1), assuming plane strain deformation within the profile plane. While the thrusting direction cannot have been far off from N (see discussion of structural data in section 14.3.1.2), out of plane deformation during orogen-parallel extension is a more serious problem. The assumed thickness of the Mesozoic cover is an additional source of error.

While these cover nappes are completely detached from a basement which is no longer preserved in the present-day cross section, the situation is different for the southernmost part of the Brianconnais platform comprising basement flakes (Tambo and Suretta basement nappes). The affiliation of these basement nappes to the southernmost Briançonnais platform was deduced earlier from the nature of their autochthonous to parautochthonous cover (Suretta cover and Splügen zone). Taking again the area of both Suretta cover (12 km^2) and Splügen zone (16 km^2) in the present-day N–S-section and assuming an original thickness of 600m for the Suretta and Tambo cover, another 47 km have to be added to the N–S width of the Briançonnais platform. Hence the total original width of this platform is in excess of 100 km (Figure 14-8). While this figure may be considered an overestimate due to an underestimate of the original thickness of the cover, those parts of the Suretta cover intruded by the Bergell batholith and possible extensions of the Suretta cover into the southern steep belt were not included in the area balance and would add extra length to our estimate. Evidence for orogen parallel late stage stretching discussed later also results in an underestimate of the area occupied in the profile plane and, consequently, also the total N–S-width of the Briançonnais platform.

It is obvious that the present-day cross sectional area occupied by Tambo nappe (111 km^2) and Suretta nappe (145 km^2) can only represent a fraction of the continental crust formerly underlying the cover of the Briançonnais platform (Figure 14-8). Together with the original width of the Tambo-Suretta part of the Briançonnais platform an original depth of about 5.5 km can be calculated for the basal décollement of the Tambo and Suretta crustal flakes. The depth to detachment within the Tambo basement has been independently estimated to be around 8 km by Mayerat (1989), who restored the present day thickness to the pre-Alpine geometry considering the intensity of Alpine overprint. With the same procedure the base to detachment within the Suretta nappe was found to be at about 4 km beneath the Triassic quartzites. All these estimates are within 4–8 km and compare to the ones obtained in the Southern Alps (Schönborn 1992) and the Aar massif (chapter 13), i.e. areas lacking substantial ductile overprint modifying the original depth to detachment.

The numbers discussed so far have been used for the very simple paleogeographic profile depicted in Figure 14-8. This crude sketch primarily serves for illustrating a dramatic problem concerning basement-cover relationships during Alpine orogeny. Even given extreme amounts of crustal thinning predating convergence, the conclusion that much of the basement originally underlying the Briançonnais cover must have been eliminated by subduction is unavoidable. The structurally lower Adula nappe cannot be regarded to represent a crustal flake derived from the Briançonnais. It is separated from higher tectonic units by the Misox zone, representing the oceanic suture between the Briançonnais and the European foreland. The Adula nappe therefore must represent the southernmost edge of this European foreland.

It is interesting to note that Menard et al. (1991) came to the conclusion that subduction of a significant amount of "European" continental crust (including the Briançonnais platform) is not required. While these authors based their estimate on a bulk mass budget which includes the entire profile across the French-Italian Alps, our conclusion (which is valid for the cross section in Eastern Switzerland) is essentially based on the recognition that most of the basement nappes of the Penninic structural domain (with the exception of the Tambo-Suretta pair) are part of the European distal margin N of the Valais suture. Hence all the area occupied by the Adula and structurally lower nappes down to the Moho cannot represent continental crust belonging to the Briançonnais. As pointed out earlier, the Schams and Falknis-Sulzfluh cover nappes lack their basement (except for thin basement slivers) in the present-day cross section while the Tambo and Suretta basement slices are covered by their own sediments.

The paleogeographic reconstruction proposed by Schmid et al. (1990, their Figure 11), sketching the en-echelon arrangement of two oceanic domains (Valais and Piemont-Liguria) simultaneously forming to the N and S of the Briançonnais platform during the Middle Jurassic was arrived at in order to explain the existence of a continental fragment (Briançonnais) caught between two oceanic spreading centers but at the same time firmly attached to the European foreland in front of the Western Alps. Classically, the Valais zone is considered to blindly end within the Western Alps. Lemoine et al. (1986) kinematically linked the Valais zone to the Piemont spreading center. This "classical" reconstruction cannot explain the ongoing paleotectonic activity until "Mid"-Cretaceous times, as recorded by the Vizanbrekzien-Serie in the Schams nappes. Additionally, it does not explain the short-lived Late Jurassic rifting pulse recorded in the Falknis nappe. If both continental margins, N and S of the Briançonnais, are interpreted to have become passive

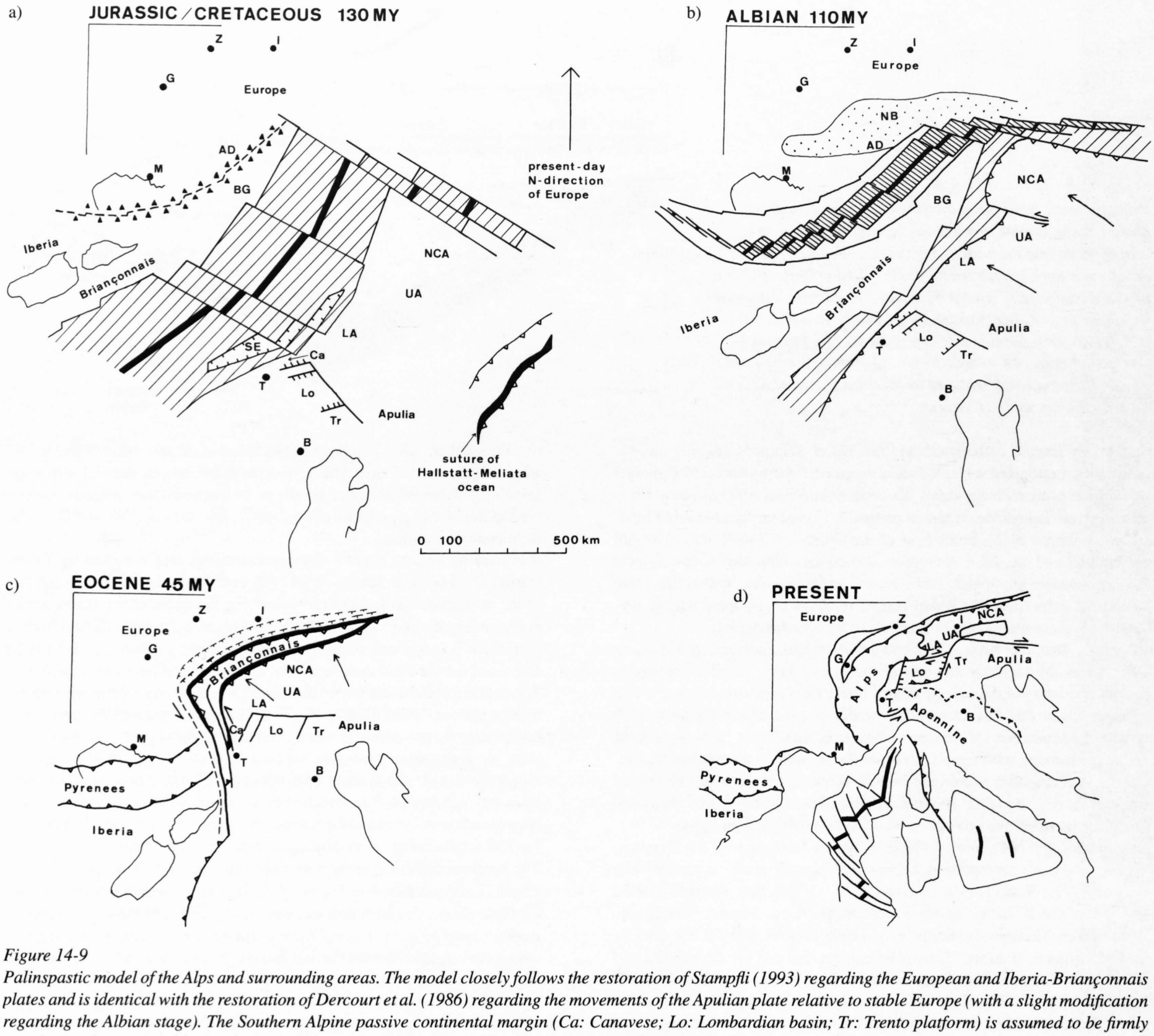

Figure 14-9

Palinspastic model of the Alps and surrounding areas. The model closely follows the restoration of Stampfli (1993) regarding the European and Iberia-Briançonnais plates and is identical with the restoration of Dercourt et al. (1986) regarding the movements of the Apulian plate relative to stable Europe (with a slight modification regarding the Albian stage). The Southern Alpine passive continental margin (Ca: Canavese; Lo: Lombardian basin; Tr: Trento platform) is assumed to be firmly attached to the Apulian block (after retrodeformation of Neogene S-directed thrusting in the Southern Alps).

Other geological units indicated are: AD: Adula nappe; NB: part of the N-Penninic Bündnerschiefer deposited on continental crust and Vocontian trough; Sch: Schams, Falknis, Sulzfluh and Tasna nappes; BR: Breccia nappe; SE: Sesia-Dentblanche and Margna-Sella extensional allochthon; LA: Lower Austroalpine nappes; UA: Upper Austroalpine nappes excluding the Northern Calcareous Alps; NCA: Northern Calcareous Alps.

Geographical reference: I: Innsbruck; Z: Zürich; G: Geneva; M: Marseille; T: Torino; B: Bologna.

a: Jurassic-Cretaceous boundary. Spreading in the Piemont-Liguria ocean linked to the Gibraltar transform system and rifting along the future break-up between Europe and the Iberia-Briançonnais block (stippled line, triangles refer to syn-rift breccia deposits). The Hallstatt-Meliata ocean already closed in the Late Jurassic (see discussion in Chapter 22).

b: Albian. Spreading in the Valais ocean linked to the Pyrenean fracture zone and active margin between the Piemont-Liguria ocean and Apulia, leading to subduction of the Sesia extensional allochthon.

c: Eocene. Closure of the Valais ocean, head-on collision in the Central and Eastern Alps, oblique collision associated with major sinistral strike-slip motion (Ricou and Siddans 1986) in the Western Alps separating the Briançonnais from Iberia (including Corsica-Sardinia) and Pyrenees.

d: Present day configuration, largely resulting from W-directed indentation of the „Insubric" plate during the Neogene (see Laubscher 1971, 1991).

during mid-Jurassic times, both margins ought to behave passively after the final break-up. Finally, the predominantly Cretaceous age of the N-Penninic Bündnerschiefer in the Grava and Tomül units (Steinmann 1994) argues for a later rifting and drifting event in the Valais trough.

An alternative palinspastic sketch is presented in Figure 14-9, largely based on a new model proposed by Stampfli (1993), a somewhat similar model having been proposed much earlier by Frisch (1979). Both these authors proposed a two-stage break-up. The Briançonnais first represented the passive continental margin of the Europe-Iberia block in respect to the Piemont-Liguria oceanic crust starting to form during Early to Middle Jurassic times (Figure 14-9a). Rifting along the future break up of the Valais ocean initiated later and during the Oxfordian (Figure 14-9a). Late Jurassic to "Mid"-Cretaceous drifting of the Briançonnais-Iberia block (Figure 14-9b) is responsible for the opening of the Valais ocean, partly accompanied by closure of the Piemont-Liguria ocean starting in the Cretaceous. According to this model, the Briançonnais platform, in particular its northern part represented by the Schams, Falknis, Sulzfluh and Tasna nappes suffers a second episode of rifting corresponding to large-scale sinistral transtension. A transition from rifting to drifting in the N-Penninic Valais domain during the Early Cretaceous has indeed been confirmed by recent field work in the N-Penninic Bündnerschiefer (Steinmann 1994) and at the northern margin of the Briançonnais (Tasna nappe, Florineth and Froitzheim 1994).

Because of dating problems it is hard to decide how much of the Vizanbrekzien-Serie could have formed during each rifting stage. The very long time interval covered by the Vizanbrekzien-Serie suggests that both rifting stages may be represented by these breccias. Tentatively local sinistral transpression indicated by the work of Rück (1990) in the Schams nappes could be attributed to the second rifting cycle whereas the extensional scenario in the Suretta cover discussed above might be related to the first rifting cycle. The main rifting episode recorded by the Falknis-Brekzie, however, is well dated (Latest Jurassic) and has to be related to the second rifting event associated with the opening of the Valais ocean.

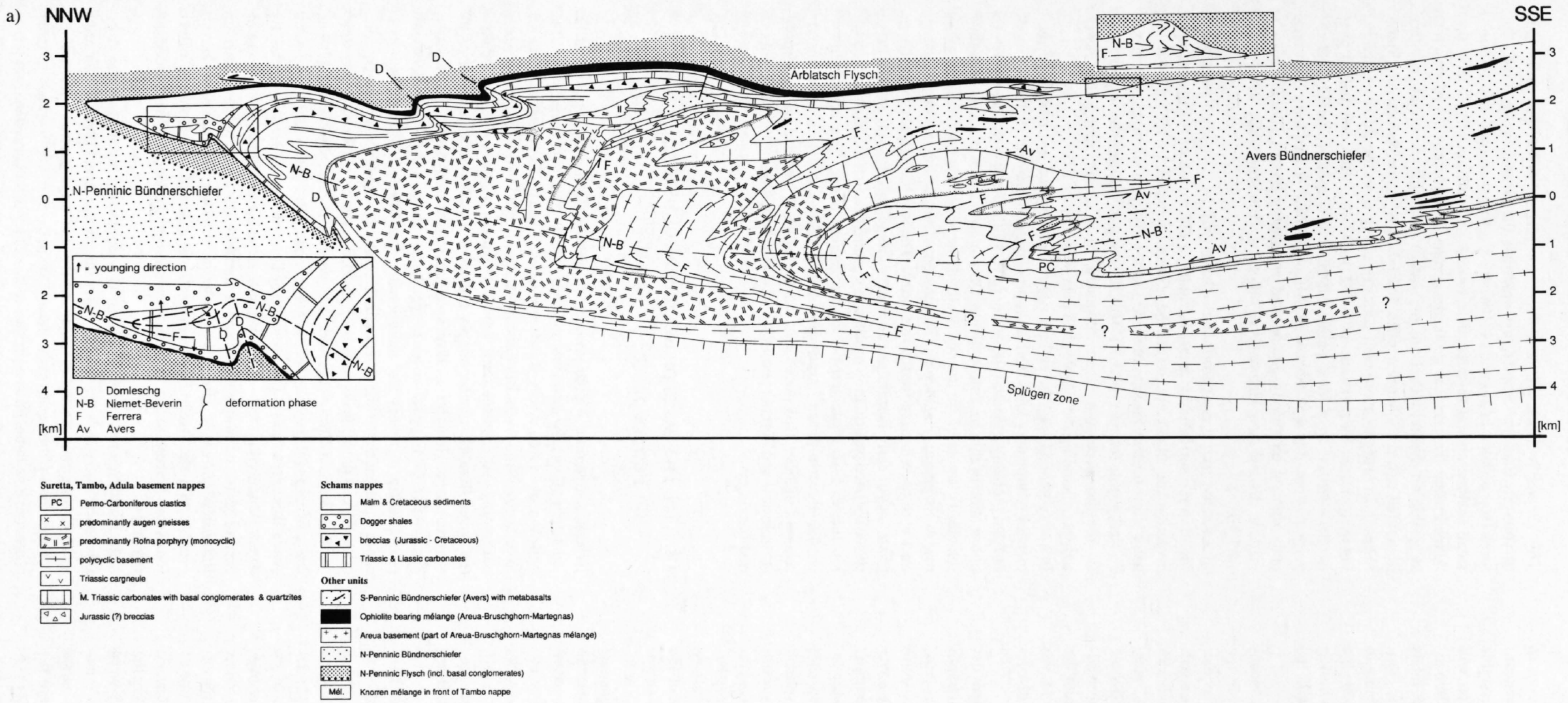

Figure 14-10
NNW–SSE-oriented detailed geological profiles. Profile traces are indicated in Figure 14-1 (traces a and b)
a: Suretta nappe and E-Schams nappes
b: front of Tambo nappe and W-Schams nappes.

According to the reconstructions of Stampfli (1993) the Valais ocean was directly connected to the Pyrenean fracture zone (Figure 14-9b). Hence the Valais ocean does not end blindly within the European foreland according to this model. Instead, it is kinematically linked to the Pyrenean fracture zone through an oceanic domain formerly present in the Western Alps. In present day map view the Valais zone in the sense of a tectonic unit terminates in the Upper Val d'Isère. The reasons for this are still unclear. Sinistral strike-slip motion parallel to the N–S trending part of the W Alps (Late Cretaceous to Eocene "décrochement Briançon-Ligurie" of Stampfli, 1993, "Subbriançonnais strike slip fault" of Ricou and Siddans,1986) might have obscured this important suture. According to this reconstruction strike-slip motion will produce a relative displacement of the Adriatic wedge over some 500km towards the N (Figure 14-9c) contemporaneous with the closure of the Valais ocean in the Central and Western Alps during the Eocene. During the Neogene this strike-slip fault must have been overprinted by E–W-shortening in the Western Alps, related to the W-ward indentation of the Adriatic wedge (Laubscher 1971, 1991). Oceanisation in the western Mediterranean during the Neogene obscured the former connections of the Valais ocean with the Pyrenees (Figure 14-9d).

Clearly, the paleotectonic evolution depicted in Figure 14-9 remains speculative and, admittedly, it also meets with some difficulties. For example, the radiolarian cherts and pelagic limestones of the N-Penninic Martegnas mélange are identical to those found in the S-Penninic ocean. Hence these sediments must have been deposited contemporaneously in both oceanic domains, in contrast to Figure 14-9a and in agreement with the "classical" view saying that both oceans formed during the Middle Jurassic. It is also possible that the Briançonnais already formed a ribbon continent during the Mid-Jurassic break-up, a ribbon continent which was further removed from the European margin during the later opening of the Valais trough (Figure 14-9b) during the Early Cretaceous (see Steinmann 1994 for an extensive discussion)

Returning to the area of investigation and the basement-cover problem depicted in Figure 14-8, the two-stage rifting model proposed by Stampfli (1993) offers a viable model for eliminating much of the continental crust underlying the Briançonnais before the onset of convergence. Uniform-sense simple shear rifting (Wernicke 1985) is in fact able to eliminate all the lower and much of the upper crust of the passive margin referred to as the upper plate margin (see Stampfli et al. 1991). Upper plate margins are characterized by large-scale updoming related to initial uplift caused by the isostatic response to replacing subcontinental mantle by less dense asthenospheric mantle, while lower plate margins are characterized by strong initial subsidence due to extreme thinning of the crust. For Jurassic times such an asymmetry is in fact indicated by the strongly contrasting subsidence history between the northern passive margin (Briançonnais) and the southern passive margin (Austroalpine and Southern Alps) situated on opposite sides of the Piemont-Liguria ocean (Lemoine et al. 1987). This strongly supports an upper-plate margin setting of the Briançonnais, as proposed by Lemoine et al. (1987) and Stampfli (1993). Following Stampfli (1993) the Briançonnais again formed an upper-plate margin during the second rifting event near the Jurassic-Cretaceous boundary which led to the opening of the Valais ocean. Hence the uppermost crust of the Briançonnais microcontinent may be envisaged as being extremely thin and directly juxtaposed onto mantle rocks along low angle detachments, as depicted in Figure 14-8. It must be noted, however, that Florineth and Froitzheim (1994) postulate a lower plate scenario for the northern margin of the Briançonnais during the second rifting event.

However, even given the most "optimistic" scenario depicted in Figure 14-8 (an upper plate margin was chosen N and S of the Briançonnais) leading to the omission of large volumes of continental crust during rifting and drifting, substantial amounts of upper crust must have been subducted during the Eocene. All the basement formerly underlying the Schams and Falknis-Sulzfluh nappes must have been subducted and replaced by the cover slices of the Valais Bündnerschiefer, currently underlying these Briançonnais cover nappes. Décollement of these cover nappes and juxtaposition with the Valais Bündnerschiefer may be readily explained in a context of accretion of the extremely thin Briançonnais cover slices, followed by in-sequence accretion of the four Bündnerschiefer units described earlier onto an upper plate formed by the N-wards advancing orogenic lid of the Austroalpine nappes during the Eocene. This accretion would have occurred in conjunction with S-ward directed subduction of the distal European lower plate margin of the Valais ocean leading to Tertiary high pressure metamorphism in the Adula nappe (Becker 1992 and 1993, Gebauer et al. 1992, Gebauer 1996), in spite of the fact that dating of the Adula high pressure metamorphism (Cretaceous versus Tertiary) is still controversial (for a different view see Hunziker et al. 1989).

14.3 Alpine convergence: from early imbrication to exhumation

14.3.1 Structural analysis and nappe geometry

This chapter will discuss the deformation phases, proceeding from older to younger. Each subchapter first describes the large-scale tectonic structures (see profiles in Figure 14-10a and b), followed by a description of small scale structural features. The various deformation phases have been defined using the classical geometrical rules of superposition of structures as visible on the individual outcrop and/or in profile view within an area of limited extent (Schams nappes, frontal parts of the Suretta and Tambo nappes). In order to avoid confusions resulting from the different numbering system used by previous authors (D1, D2 etc.) each defomation phase is characterized by a local name referring to a specific locality where a particular phase is well developed. Although these phases have been originally defined on strictly geometrical arguments an attempt will also be made to discuss their kinematic significance within the study area (chapter 14.3.3.).

In a second step these deformation phases will be correlated with phases found in the surrounding areas, including a discussion of the metamorphic evolution and an attempt to date these phases (chapter 14.3.2.). This will finally allow for a discussion of the kinematic evolution along the entire NRP 20 East profile (chapter 14.3.3.). This last chapter will form an important basis for the discussion of an integrated cross section along this eastern transect, including the geophysical data (see chapter 22).

In a very general way the earliest Alpine deformation involved the detachment of sedimentary units from their pre-Triassic basement (Schams nappes) or from probably oceanic lithosphere (Avers Bündnerschiefer) as well as the imbrication of thin basement slivers. Only in the case of the Avers Bündnerschiefer is it possible to unequivocally define a separate deformation phase (the Avers phase) related to this detachment event, which is probably associated with accretionary wedge formation. The resulting thrust faults (Avers phase and/or early Ferrera phase) were subsequently folded, and the pervasive associated deformation resulted in a prominent first foliation and stretching lineation so characteristic for the Ferrera phase. The next following Niemet-Beverin phase implies post-nappe folding and locally produced a second foliation. This phase was in turn followed by local later overprints (Domleschg and Forcola phases) related to exhumation by thrusting and normal faulting.

14.3.1.1 The Avers phase: precursor of the Ferrera phase?

Evidence regarding Alpine pre-Ferrera-phase deformation stems from the paleogeographically most internal unit, the Suretta nappe and its contact with the overlying Avers Bündnerschiefer. Clearly, the interface between Suretta cover and Avers Bündnerschiefer is affected by Ferrera phase isoclinal folding and cleavage formation. This led many authors to conclude that the Avers Bündnerschiefer simply represent the post-Triassic cover of the Suretta nappe. However, as discussed previously, such a view is untenable. The so-called "Triassic" cover of the Suretta turned out to also encompass post-Triassic members and, additionally, the lithological composition of some components of the Avers Bündnerschiefer (radiolarian cherts, ophiolitic slivers) preclude deposition on the Briançonnais platform. Direct structural evidence for thrusting along this contact is given by the local occurrence of cargneule or other sedimentary or basement lenses at the base of the Avers Bündnerschiefer. The presence of numerous mafic boudins within the Avers Bündnerschiefer – some of them at the basal contact – suggests pre-Ferrera phase intense imbrication or mélange formation within the Avers Bündnerschiefer unit. The only mesoscopic evidence for such a pre-Ferrera event within the Avers Bündnerschiefer is reported by Hitz (1989) who found pre-Ferrera phase folds in prasinites, embedded in Avers Bündnerschiefer.

Milnes and Schmutz (1987) suggested S-directed movement of the Avers Bündnerschiefer over the Suretta cover during the Avers phase. Their argument for a tectonic contact is based on the seemingly chaotic structure of the contact zone ("torn-apart rock masses of mappable size") which in many places are now believed to represent sedimentary breccias and megabreccias. Evidence for S-directed thrusting was based on a different scenario of these authors regarding the reconstruction of the nappe pile formed during Avers and Ferrera phases (in contrast to our results regarding post-nappe refolding, they reconstructed the Ferrera phase folds as having been originally formed in a S-facing orientation).

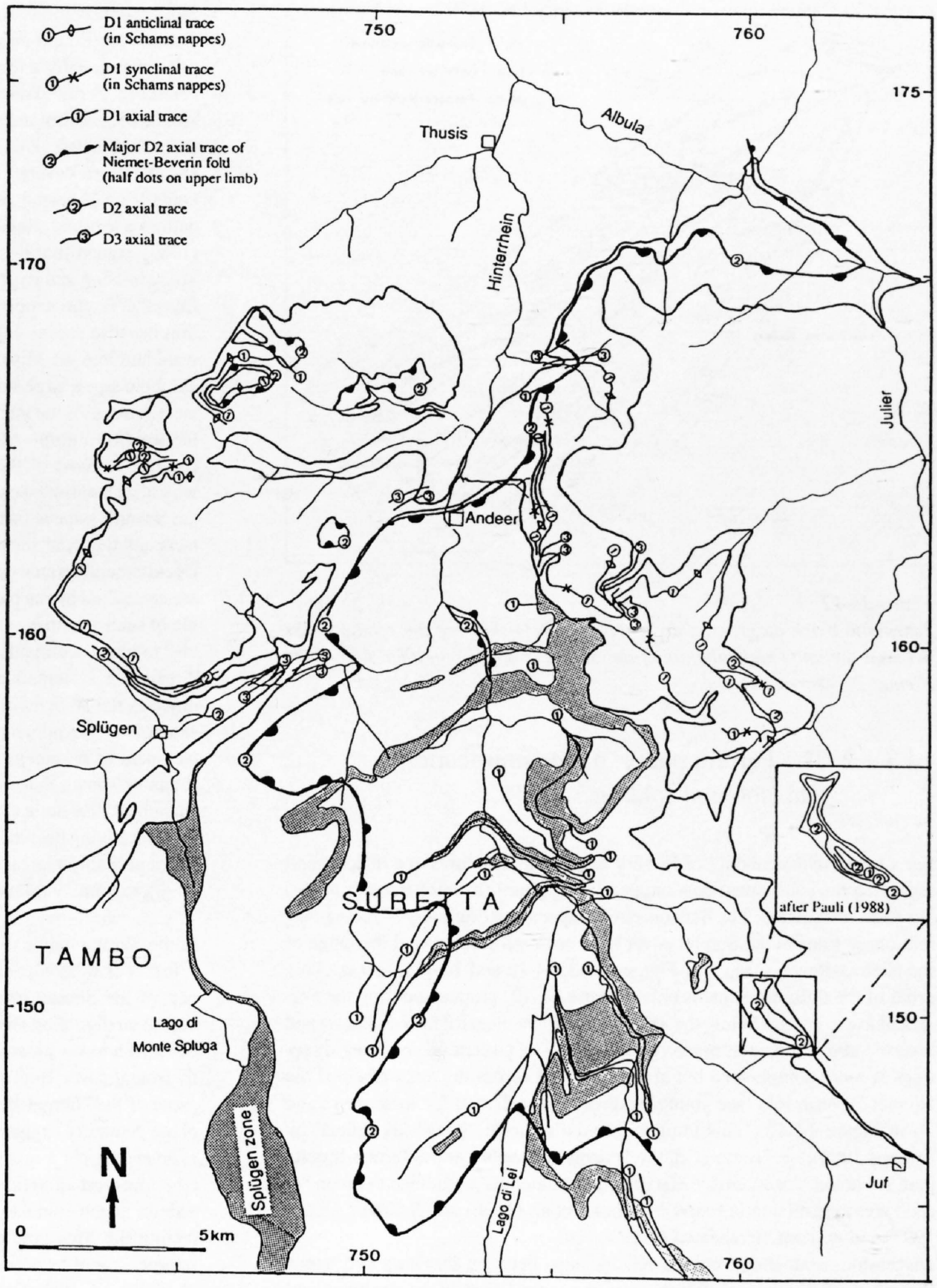

Figure 14-11
Axial plane of traces of the Ferrera (D1), Niemet-Beverin (D2) and Domleschg (D3) phase folds within the frontal Suretta nappe and the Schams nappes.

Pre-Ferrera phase foliations can be observed in pre-Triassic basement and Triassic cover rocks of the Suretta nappe and in the Avers Bündnerschiefer (Hitz 1989, Schreurs 1990, and own work). However, such older mesoscopic structures are extremely scarce and their tectonic significance remains unclear.

Ring (1992a, b) reports E–W lineations associated with high pressure metamorphism and top to the W shear senses of supposedly Cretaceous age in both Tambo and Suretta basement. If correct, these findings would indicate that the Briançonnais realm would have been deeply involved in the Cretaceous (Eoalpine) orogeny, a conclusion that would be completely incompatible with the palinspastic model previously derived for the rifting and drifting stage. These E–W lineations are conspicuously absent in the Adula basement nappe and in the case of the Suretta and Tambo nappes they turn out to be reoriented Ferrera phase lineations and/or lineations formed during the Niemet-Beverin post-nappe folding event (Baudin et al. 1993, Mayerat 1989, Schreurs 1990). Furthermore, shear sense indicators indicate top to the E movement where observable (Marquer 1991, Mayerat 1989 and own work). Regarding the age of high pressure or pressure dominated metamorphism radiometric evidence suggests considerably younger ages, a point that will be discussed in section 14.3.2.

In the Schams nappes, Carnian cargneule, representing the principal detachment horizon, occasionally occurs in the core of Ferrera phase folds. Strictly, this implies that Ferrera phase folding post-dates detachment. However, we interpret these structures as detachment folds, with detachment and folding in terms of a continuous process during the Ferrera phase deformation.

In the case of the Schams nappes located at the front of the Tambo nappe, however, isoclinal Ferrera folds also fold thrust faults delimiting the Areua and Vignone basement slivers (see Figure 14-10b, inset, and Mayerat 1989). Considering the large displacement that occurred along these detachment thrust faults, the large amplitude of the subsequent Ferrera phase fold, and the analogy to the basal thrust of the Avers Bündnerschiefer, it is more logical, in this case, to associate these thrust faults with the precursor, the Avers phase.

In summary, a distinct separate Avers phase can only be clearly defined in case of the detachment of the Avers Bündnerschiefer. There are considerable difficulties in assigning detachment events elsewhere to either the Avers phase or to an early stage of the Ferrera phase. Therefore we consider the Avers phase (where well defined) as a precursor of a continuous evolution from early detachment (Avers phase) to isoclinal folding and penetrative ductile deformation (Ferrera phase) as a result of steadily increasing burial and metamorphism during the Paleogene. According to our work there is no structural evidence for a separate Cretaceous (Eoalpine) tectonic event below the Platta and Austroalpine teconic units. In profile view the Avers Bündnerschiefer, unlike the Schams nappes and N-Penninic Bündnerschiefer and Flysch, are not wrapped around the front of the Suretta nappe. Instead they wedge out S of the Suretta front. Southwards they can be followed into the direct footwall of the Lizun and Forno ophiolitic units until they are cut by the Bergell intrusion (Liniger 1992). This suggests thrusting of the S-Penninic Avers Bündnerschiefer onto the most internal Briançonnais platform in a direction with a northerly component during the Avers phase.

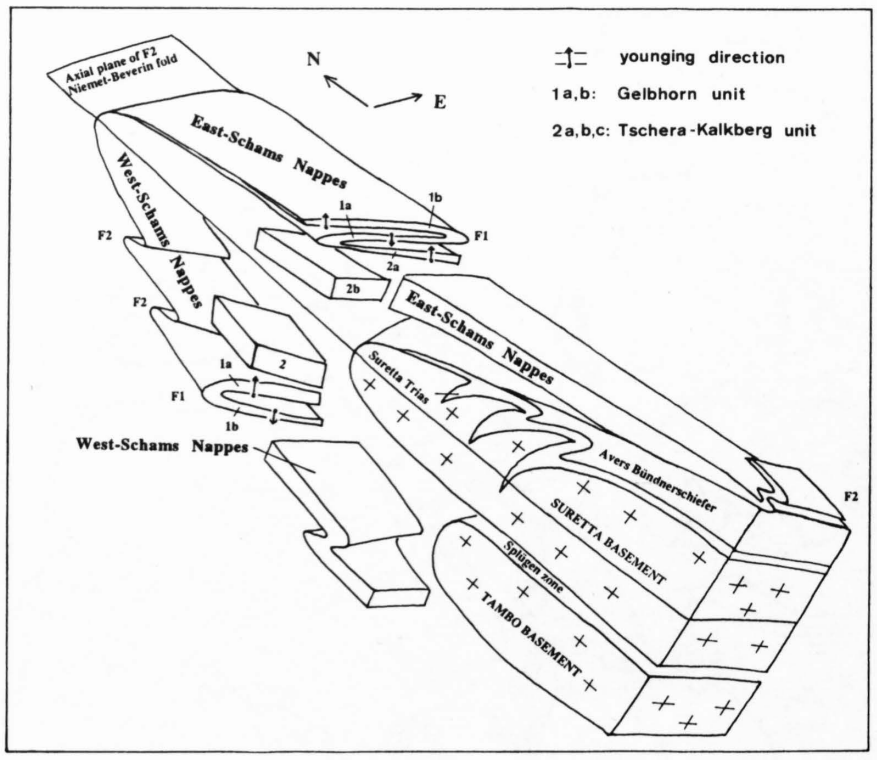

Figure 14-12
Schematic block diagram after Schreurs (1993) showing the relationships between the units and subunits of the Schams nappes on either side of the Niemet-Beverin axial trace.

14.3.1.2 The Ferrera phase: nappe imbrication and isoclinal folding

For a better understanding of Ferrera large scale structures one major result regarding the subsequent post-nappe folding phase (Niemet-Beverin phase) has to be anticipated: The Schams cover nappes and originally N-facing Ferrera phase folds in the Suretta cover have been refolded around the hinge of the Niemet-Beverin fold (see Figures 14-2, 14-10 and 14-11). The stacking order of the different Schams units (Figure 14-12) produced during the Ferrera phase is upright below the axial plane of this megafold (W-Schams) and inverted above the axial plane (E-Schams). The pattern of younging directions is more complicated but also is reversed across the axial plane of the Niemet-Beverin fold (see younging directions indicated for subunits 1a and 1b in Figure 14-12). This implies that the solution "infra" (as defined by Trümpy 1980), i.e. "rooting" of the Schams nappes below the Tambo-Suretta pair, is correct. An extensive discussion of numerous arguments in favour of such a reconstruction is found in Schmid et al. (1990) and Schreurs (1990, 1993) and will not be repeated here.

Discussions concerning mutual relationships between thrusting and nappe formation (discontinuous deformation on a large scale) on the one hand, and folding associated with pervasive straining, leading to a first generation of folds, planar and linear fabrics on the other hand, are very typical for the Penninic structural domain. Some authors envisage a foreland-type thrust-and-fold belt geometry being overwhelmed by subsequent penetrative deformation. This clearly would imply a two-stage scenario. Others envisage continuous progressive deformation with overlapping events of detachment and penetrative strain.

Ferrera phase deformation in the Schams cover nappes (Schreurs 1990) strongly argues for the second view. Ferrera phase thrusting of the Schams cover nappes over the N-Penninic Bündnerschiefer was accommodated by a mélange zone composed of gneissic material, Schams cover sediments and ophiolites: the Areua-Bruschghorn and Martegnas mélange zones (Figure 14-10). However, before juxtaposition with this mélange zone the Schams cover nappes must have been detached from their substratum first (see reconstruction of principal décollement horizons in Figure 14-3). In case of the Gelbhorn unit 1b this décollement horizon is made up of Upper Triassic cargneules which are frequently but not always found in the core of isoclinal Ferrera phase folds. In most places (an exception discussed later is found in front of the Tambo nappe) these folds do not affect the underlying mélange zone and could well be interpreted as detachment folds which developed coeval with thrusting over the mélange zone.

The tectonic contacts between the Schams subunits (in a paleogeographical sense) also argue for a continuous scenario: The limits between individual subunits may be defined by still visible Ferrera phase isoclinal fold hinges in one place (between units 1a/1b and 1a/2a, see Figure 14-12) or marked by thrusts in other places (occasionally between 1a/1b and 1a/2a, always at contacts of subunits within the Tschera-Kalkberg unit). Furthermore, Ferrera phase foliations (S1), axial planar to D1 isoclinal folds, are parallel to D1 thrust contacts which often but not always remain unfolded by D1 folds.

Similar observations are reported from the thin basement and cover slices in front of the Tambo nappe (Figure14-10b) by Mayerat (1989). There, a very thin (occasionally a few m) basement slice (Areua gneiss, covered by a thin veneer of Permo-Triassic clastics), which can be traced E-wards into the Areua-Bruschhorn mélange, can be continuously followed over a distance of more than 10km. This slice was thrusted onto N-Penninic Bündnerschiefer and is in turn covered by allochthonous Schams cover slices. Another mélange zone (Knorren zone, predominantly made up of Schams cover rocks) defines a tectonic contact in respect to the front of the Tambo nappe. Mayerat (1989) argued that this Knorren mélange extends a short distance into the Splügen zone and hypothesized that the Schams nappes could have derived from the Tambo nappe. As reported earlier, we disagree with this interpretation because recent field work enables us to trace Schams elements southward and into the Misox zone beyond the village of Mesocco. In front of the Tambo nappe a large scale isoclinal Ferrera fold locally affects the thrust contact between Areua gneiss and Schams slices and is probably responsible for the westward termination of the Schams nappes (Mayerat 1989). This is in contrast to most of the other Ferrera phase thrusts in the Schams nappes which, as mentioned earlier, remain unfolded during the Ferrera phase. As in the Schams nappes further to the N and E, S1 is parallel to these thrust contacts and the axial surface of the isoclinal fold.

Décollement horizons and, occasionally, the position of (Ferrera) fold hinges are controlled by the paleogeography (see Figure 14-3). A spectacular example of such a control is the position of fold hinges at the transition from breccias to basin sediments between subunits 1a and 1b (note that the younging direction is systematically inversed across the boundary between these subunits, in the W-Schams as well as in the E-Schams, Figure 14-12). Another example of the influence of the paleogeographic geometry concerns the detachment of basement slivers such as the Taspinit, Nolla and Areua slivers. It can be shown that the Taspinit basement sliver is directly covered by the Vizanbrekzien-Serie (Rück 1990), the potential décollement horizons in the Triassic having been eliminated by pre-depositional erosion. These basement slices probably represent "decapitated" horsts (Mayerat 1989, Schmid et al. 1990), extremely thinned out by subsequent straining.

In the Suretta nappe, Ferrera phase thrusting and folding occurred coevally (Pfiffner et al. 1990, Schreurs 1990). A major thrust fault occurs in the frontal part of the Suretta nappe (Figure 14-10a). This thrust emplaces an upper basement digitation (with polycyclic basement at its base) onto the Mesozoic cover of a lower basement digitation (largely made up of Rofna porphyry in its frontal part). Both imbricates are in an upright position below the axial plane of the Niemet-Beverin fold (Figure 14-10a). The pre-Niemet-Beverin phase geometry suggests that the thrust – although following a flat within Triassic evaporites – cuts up section towards the N, possibly indicating a northerly transport direction during the Ferrera phase. The central part of the Suretta nappe contains a number of tight, more or less symmetric folds affecting the Mesozoic cover of the Suretta nappe and the Avers Bündnerschiefer, cored by polycyclic basement (immediately SSE of the central part of Figure 14-10a). The contrast in style of this nappe-internal deformation may well reflect the mechanical stratigraphy involved: the mechanically stiffer monocyclic Rofna porphyry reacted by brittle thrust faulting, whereas the polycyclic basement containing more schistose lithologies deformed by ductile folding. It is important to note that the pervasive Ferrera foliation in basement and cover is parallel to both the thrust fault and the axial surfaces of the folds, and that the thrusts remain unaffected by Ferrera phase folding (of course except for the basal thrust of the Avers Bündnerschiefer). This suggests that the two structures (thrusts and folds) are more or less coeval. These large scale Ferrera phase folds, as well as subsequent Niemet-Beverin folds, involve the previously emplaced Avers Bündnerschiefer but not the E-Schams nappes. Milnes & Schmutz (1978) concluded from this, that the Schams nappes had been emplaced onto the Suretta nappe and Avers Bündnerschiefer at some later, post-Ferrera stage.

In the Tambo nappe the autochthonous cover is completely missing at the front of the nappe and at the base, whereas in the Suretta nappe relics of a thin autochthonous cover (basal quartzites) are locally preserved at the front of the nappe. For both, Tambo and Suretta nappe the contact with the Schams slices is tectonic everywhere. Hence, on a very large scale these basement nappes represent right way up thrust sheets which, on a smaller scale, are internally sliced by thrusts and penetratively deformed by folding and pervasive strain. The basal thrusts of both basement nappes, however, are often overprinted by post-Ferrera movements discussed later.

The Ferrera phase nappe stack consists of (from bottom to top): (1) N-Penninic Bündnerschiefer and flysch; (2) Areua-Bruschghorn-Martegnas mélange; (3) Schams units with subunits 1b, 1a, 2, occasionally linked by isoclinal folds; (4) mélange zones such as the Knorren zone; (5) Tambo nappe including Splügen zone; (6) Suretta nappe including its Mesozoic cover and previously emplaced Avers Bündnerschiefer. Note that these elements are of

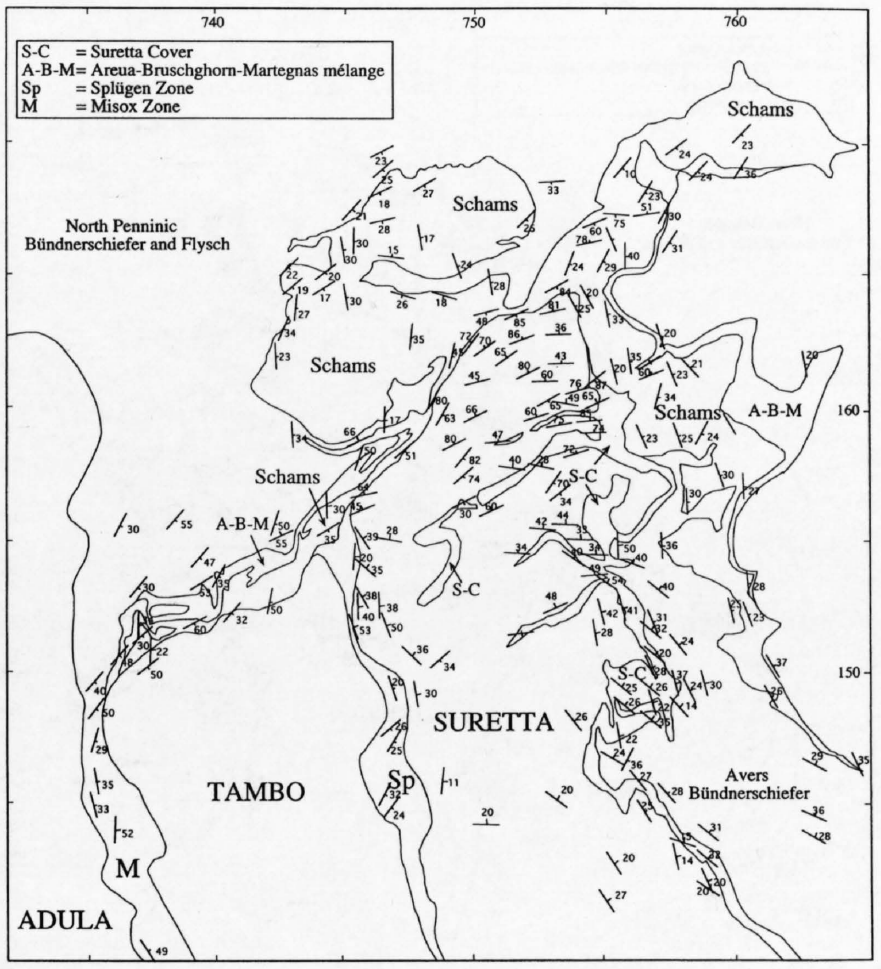

Figure 14-13
Strike and dip of Ferrera phase foliations.

extremely heterogeneous nature and include thick basement thrust sheets, detached and isoclinally folded cover sheets, extremely thin basement slices and mélanges containing ophiolitic elements. The pre-Triassic basement of the Schams cover nappe is missing apart from a few basement slivers.

Due to the regional axial plunge, Ferrera phase foliations mostly dip towards the E. Deflections from this direction are clearly visible in Figure 14-13 at the front of the Suretta and Schams nappes positioned in the hinge zone of the later Niemet-Beverin fold. Foliation, schistosity or cleavage is penetrative in all lithological units except in dolomites and in parts of Rofna porphyry and Truzzo granite, the latter deforming by networks of shear zones (Marquer 1991). A strain analysis regarding Ferrera phase straining was carried out in the Vizanbrekzien-Serie (Schreurs 1990) and the Tambo basement (Mayerat 1989). Axial ratios indicate plane strain deformation producing a thickness reduction of around 50%, assuming constant volume. This is a more or less representative strain measurement regarding basement and limestone lithologies but certainly an underestimate regarding less competent lithologies (basin sediments of Schams subunit 1b, post-Mid-Cretaceous sediments).

Surprisingly, the Ferrera phase stretching lineations exhibit a reasonably well developed preferred orientation trending NNW–SSE in the Schams nappes, despite of intense post-Ferrera folding (Figure 14-14a). Rare occurrences of reliable shear indicators and intense post-Ferrera phase folding prevent an unambiguous determination of the overall sense of movement related to this stretching lineation.

In contrast, the stretching lineations in the Schams units in front of the Tambo nappe and within the Tambo nappe (Figure 14-14a,b) are very variably oriented (Mayerat 1989, Baudin et al. 1993 and new work by Pfiffner and Schmid). Examples of variably oriented stretching lineations from the Misox zone and the top of the Suretta nappe are given in Figure 14-15 (c and d). The stretching lineations from these areas are seen to form a girdle along a great circle whose pole coincides with the average foliation poles (S1 or S2). This scatter is due to two effects which cannot always be separated: (1) reorientation of earlier formed Ferrera stretching lineations L1 during near-isoclinal Niemet-Beverin F2 folding due to non-parallelism between L1 and F2, and, (2) formation of a new stretching lineation L2 during the Niemet-Beverin phase. Mayerat (1989) finds both stretching lineations L1 and L2 straddling a complete great circle on a stereoplot (see Figure 14-15b). At the same time, a clear preference of E–W orientations is found. The great circle distribution argues for reorientation of L1. However, there is also clear evidence for finite E–W stretching from L2 stretching lineations found within axial planar S2 schistosities (Mayerat 1989, Baudin et al. 1993 and own work), supported by strain determinations (Mayerat 1989). Therefore it is impossible to separate L1 and L2 at many localities, especially when S2 completely transposes S1. Mayerat (1989) assigned a third deformation phase to be responsible for what we (and Baudin et al. 1993) refer to as F2 (Niemet-Beverin phase) E–W stretching, but this will be discussed later. At this point it is important to re-emphasize that E–W stretching very clearly postdates NNW–SSE stretching during the Ferrera phase, contrary to the findings of Ring (1992 a and b) who claims E–W-stretching to be followed by NNW–SSE stretching. At some locations it can be clearly seen that the Ferrera phase stretching lineation is folded around Niemet-Beverin folds reorienting the stretching lineations from a more N–S orientation on the lower limb to a more easterly dip on the upper limb.

NNW–SSE trending Ferrera phase lineations not affected by D2 with unambiguous sense of shear are found in the contact zone to the Splügen zone in the mylonitized top of the Tambo basement (at Splügen-Pass: Mayerat 1989, Schreurs 1990) and at the base of the Tambo basement and within the Misox zone (Schreurs 1990). A kinematic analysis of shear zone networks within

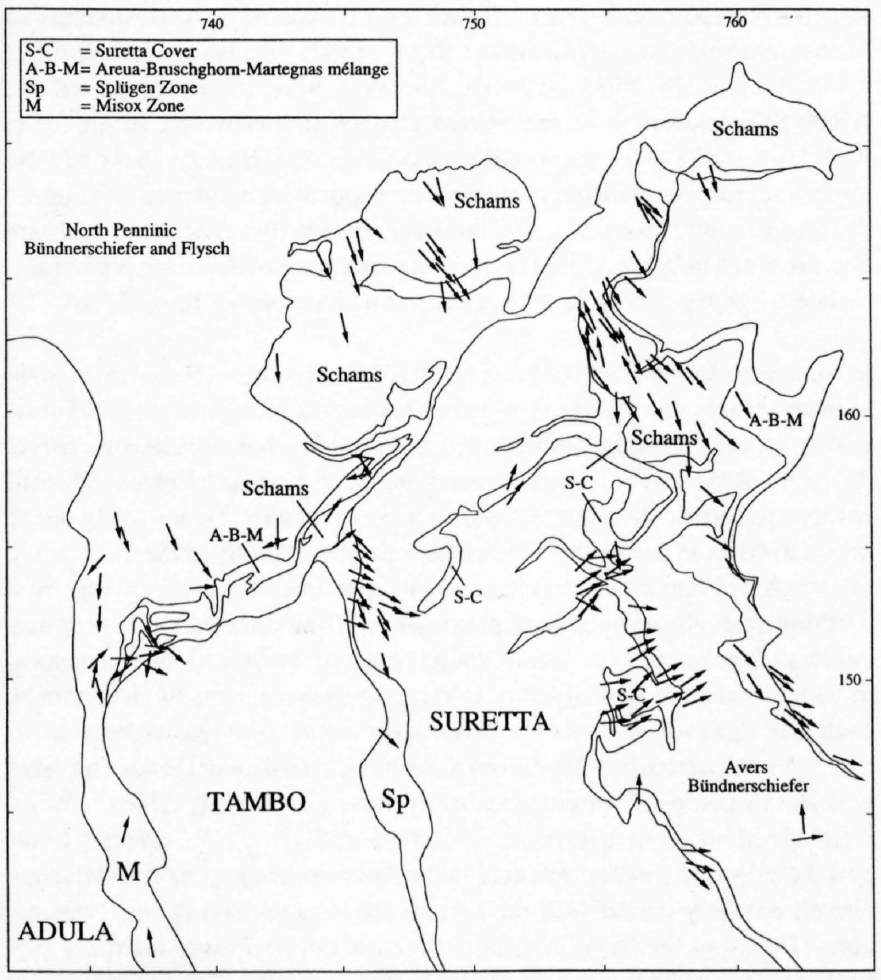

Figure 14-14a
Ferrera phase stretching lineations in the Schams nappes.

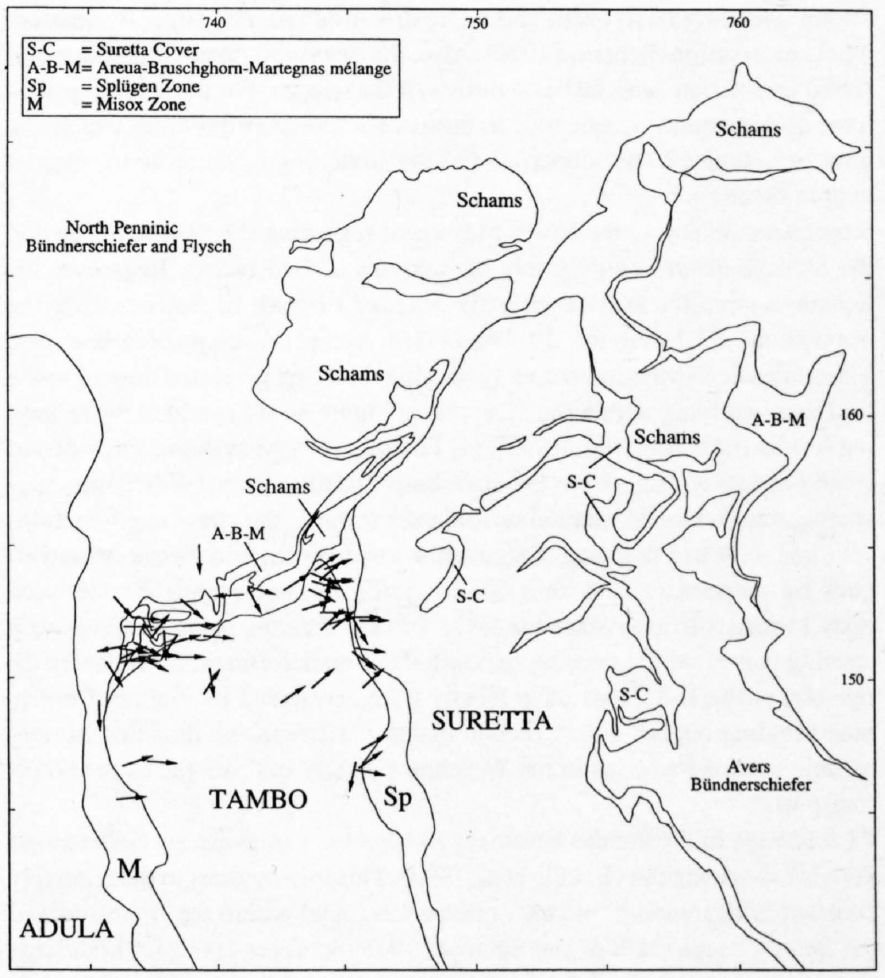

Figure 14-14b
Ferrera and/or Niemet-Beverin phase stretching lineations (where assignment to one or the other deformation phase is impossible) in Suretta and Tambo nappes and in the Schams units in front of the Tambo nappe.

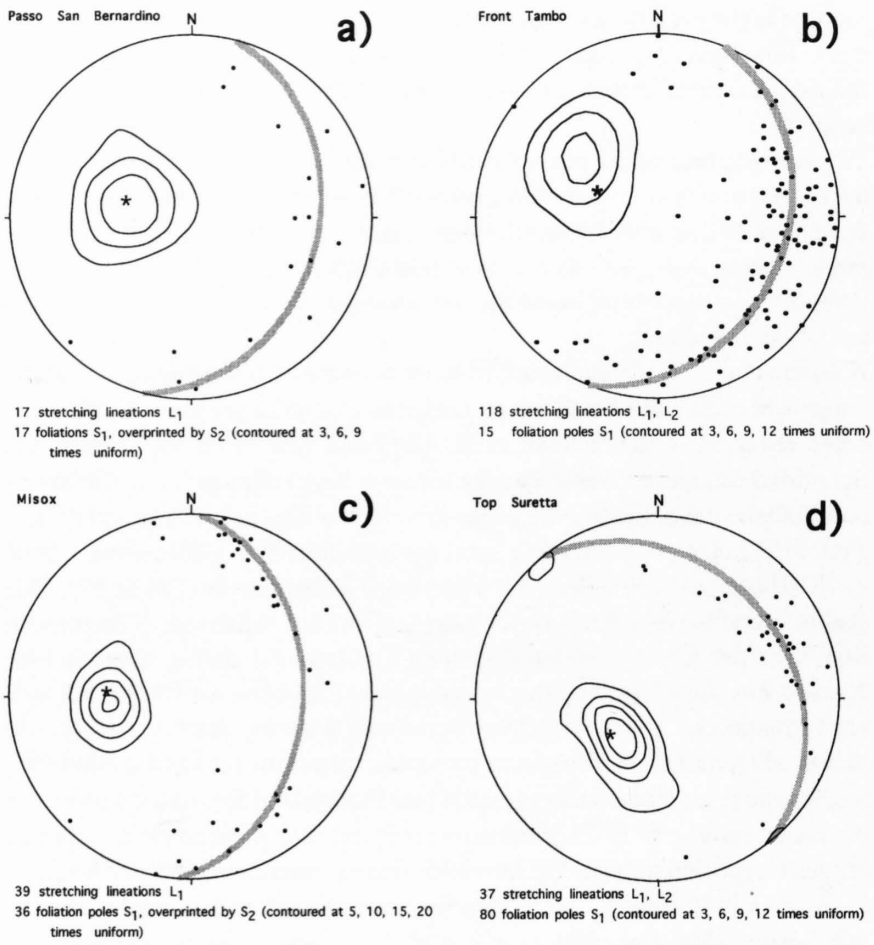

Figure 14-15
Stereograms showing foliation poles (contoured) and stretching lineations (points). Stretching lineations scatter on a great circle (best fit shaded) which is identical with the average orientation of the foliation (pole to best fit great circle for lineations (star) lies within maximum of foliation poles); a: Schams units near Passo San Bernardino; b: front of the Tambo nappe (from Mayerat Demarne 1994); c: Bündnerschiefer of the Misox zone; d: top of the Suretta nappe.

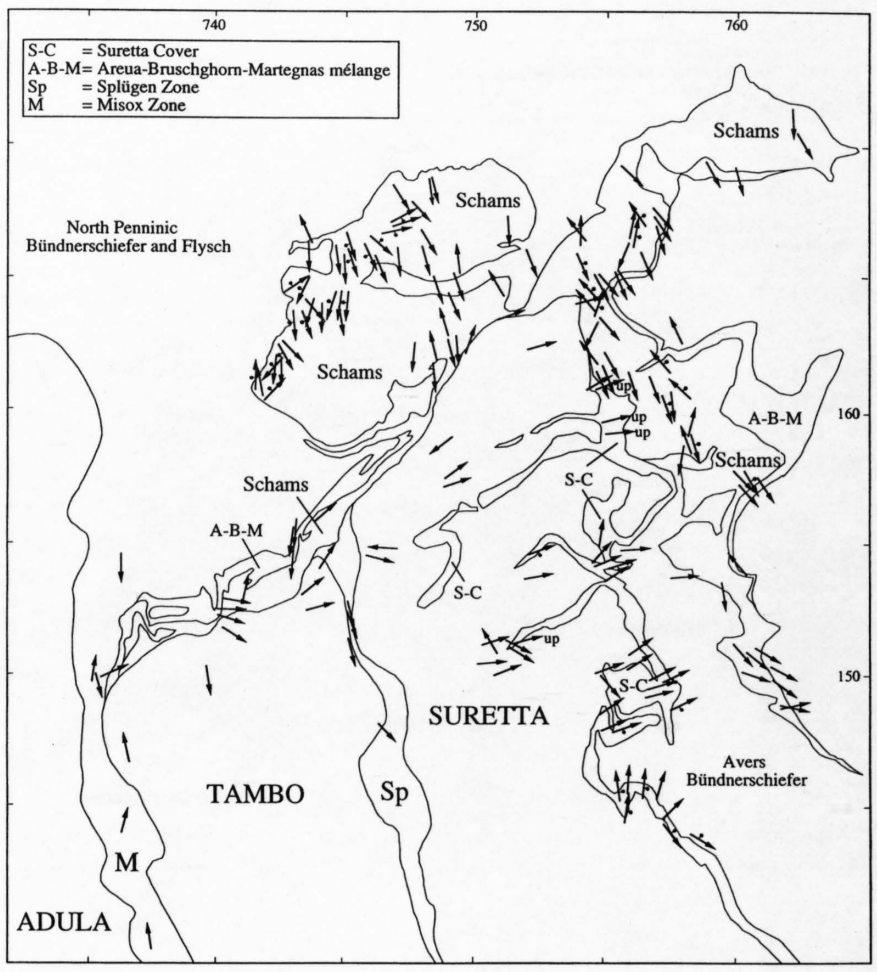

Figure 14-16
Orientation of subhorizontal Ferrera phase folds (arrows) and structural facing direction (indicated by short tick with dot; up = upward directed facing direction)

the Truzzo granite (Marquer 1991) documents top NNW sense of shear within the Tambo nappe.

Stretching lineations in the Suretta nappe, discernible as stretched deformed pebbles, are invariably parallel to Ferrera phase fold axes and intersection lineations (compare Figure 14-14a with Figure 14-16). Strictly, they only represent finite elongation during the Ferrera phase and they do not necessarily have a kinematic signification. In fact, strain measurements indicate a strong flattening component and microstructural analysis suggests near-coaxial deformation (Schreurs 1990). Also, the lineations do not turn into a preferred orientation near the basal thrusts of the nappes. For these reasons they have no kinematic significance in terms of a transport direction which can only be assumed to be subparrallel to the stretching lineation in the case of simple shearing.

Arguments for top to the NNW movement regarding the Suretta nappe and the Schams nappes entirely rely on analyses of fold facing. Regarding the Schams nappes the axes of perfectly isoclinal F1 folds lie fairly close to the orientation of L1 (Figures 14-14a,14-16), except for competent horizons. The analysis of structural facing (younging direction projected normal to the fold axis and lying within the axial plane, Figure 14-16) yielded the following results (Schreurs 1990, 1993): (1) Facing azimuths systematically depart in one direction away from the stretching lineation in the W-Schams, suggesting unidirectional rotation of fold axes towards the stretching lineations resulting in W to SW facing. This excludes true sheath fold formation and argues for rotation of fold axes due to systematic non-parallelism between early formed fold axes of buckle folds with the shearing plane, progressively rotating these fold axes during ongoing shearing deformation. (2) Facing directions in the E-Schams have locally been reoriented by Niemet-Beverin phase folding but NE-facing predominates. (3) The facing direction of non- or little rotated fold axes in the W-Schams clearly indicate top to the NNW transport.

F1 fold axes in the Tambo basement and Splügen zone are curviplanar and variable in orientation (Baudin et al. 1993). This is in contrast to the relatively constant ENE trending fold axis orientation found within the frontal part of the Suretta nappe (Milnes and Schmutz 1978, Schreurs 1990) for both large and small scale isoclinal folds affecting the Suretta cover (Figure 14-16). Since these folds have been coaxially folded around a large scale F2 fold (Niemet-Beverin fold) their present day facing (up or SSW, Figure 14-16) restores into NNW-facing after retrodeformation, again compatible with NNW-directed transport during D1. The stretching lineation, if in fact acquired during D1, suggests finite elongation perpendicular to the transport direction. However, a D2 stretch accidentally parallel to earlier formed F1 fold axes cannot be ruled out.

Orientations of fold axes in the Suretta cover dramatically change in the area of Val Madris going south (see southernmost data in Figure 14-16; Hitz 1989, Schreurs 1990). The large scale Ferrera phase fold axes prefer a NW–SE trend but small scale intersection lineations and fold axes straddle a complete great circle in S1 (Hitz 1989). Facing is variable but predominantly NE directed, resulting in apparent N-facing when projected into a N–S-section (Figure 14-10a). Stretching lineations, where observable in the form of pebble stretches, are mostly NW–SE to NNW–SSE oriented and close to large scale F1 folds. This change in orientation of D1 structures occurs across the trace of the Niemet-Beverin fold surface trace which leaves the Suretta basement across Lago di Lei, running into the Suretta cover and Avers Bündnerschiefer (southernmost part of Figure 14-11), contrary to the findings of Milnes and Schmutz (1978). Hence, this southerly area being situated in the lower limb of the Niemet-Beverin fold may have largely preserved the NNW–SSE-orientation of the Ferrera phase lineation which, in this case, would be parallel to the supposed transport direction (contrary to the stretching lineations near the front of the Suretta nappe which are perpendicular to the transport direction). Locally, however, Niemet-Beverin phase folds are also observed in Val Madris. Therefore a reorientation of Ferrera phase folds by later straining during the Niemet-Beverin phase cannot be excluded.

In summary, the Ferrera phase represents at the same time (i) the major event of nappe imbrication and (ii) the main phase of ductile penetrative deformation in the area. Penetrative deformation follows earlier detachments during the Avers phase and/or during the early stages of the Ferrera phase. The orientation pattern of stretching lineations is very complex. This is partly due to later deformation during the Niemet-Beverin phase, partly to the fact that not all stretching linations can be inferred to have formed subparallel to the transport direction. Arguments for approximately NNW directed movement during this phase can only be locally found (base of Tambo and Suretta nappes) or be inferred from an analysis of fold facing (Schams nappes). It cannot be excluded, however, that this NNW transport direction may have been reoriented to some extent by later deformation phases. In fact, neighbouring areas with less intense post-Ferrera phase overprint exhibit slightly different movement directions. Froitzheim et al. (1994) inferred a N to NNE directed transport direction for Tertiary thrusting in the Austroalpine nappes (their Blaisun phase), probably coeval with the Ferrera phase as defined for the Penninic units. Therefore the NNW transport direction inferred from our study area may be of rather limited precision and in fact may have been deflected from strictly N to NNW due to later strains.

14.3.1.3 The Niemet-Beverin phase: nappe refolding and vertical shortening

On a large scale the D2 Niemet-Beverin fold clearly overprints Ferrera phase thrust contacts and isoclinal folds (Figures 14-10,14-11). Large scale folding inverts the nappe pile presently found in the upper limb of the Niemet-Beverin fold axial trace consisting of (from top to bottom in its present position): (1) N-Penninic Bündnerschiefer and flysch (mainly Arblatsch flysch); (2) ophiolitic mélange zones (Martegnas); (3) part of the Schams nappes (E Schams); (4) the top of the frontal Suretta nappe with its spectacular backfolds. The axial trace of the Niemet megafold discovered by Milnes and Schmutz (1978) can be followed into the frontal Beverin fold (Figures 14-10a and b) in the Schams nappes (Schreurs 1990, 1993) and as far N as the Stätzerhorn (Figure 14-2, above Rothenbrunnen) into a S-facing isoclinal fold (Jäckli 1941). Inversion of Ferrera phase imbricate thrust sheets occurs over a distance as long as 40km (measured in a N–S section from Rothenbrunnen to the S end of the Schams nappes and the Arblatsch flysch near Alp Sovrana; see Figure 14-2). Large scale Z-shaped parasitic folds (viewed towards the E, Figure 14-10b) are observed to refold the imbricates at the front of the Tambo and Suretta nappes (W-Schams, Schreurs 1990, Mayerat 1989). Parasitic folds are also observed above the front of the Suretta nappe, where they affect the E-Schams nappes, the overlying Martegnas slice and the Arblatsch flysch (Schreurs 1990). These Niemet-Beverin phase folds are not visible in Figure 14-10a since their fold axes run parallel to the plane of the section. The Z-shaped folds in the front of the Tambo nappe may be treated as parasitic folds in respect to the Niemet-Beverin megafold. Most of the "backfolds" found within the northern part of the Suretta nappe (new work by Pfiffner, DallaTorre 1991 and Christen 1993), however, represent formerly N-facing Ferrera-phase megafolds reoriented by the Niemet-Beverin phase. The large backfold at Piz Grisch is a notable exception and has formed (or was at least amplified) during the Niemet-Beverin phase. On the other hand, the Z-shaped folds found above the trace of the Niemet-Beverin megafold (Figure 14-10a, above the frontal part of the Suretta nappe) formed during the Domleschg phase. On a mesoscopic scale the Niemet-Beverin cleavage, S2, can be continuously traced through the Niemet-Beverin fold axial trace from lower limb to upper limb.
Interestingly, the basal "backthrust" of the E-Schams nappes over the Suretta cover and Avers Bündnerschiefer (Figure 14-10a, central part) is seemingly planar (where not affected by D3 folding discussed later) and suggests that post-nappe (re)folding is associated with some amount of "backthrusting" in the upper limb of the Niemet Beverin fold. We will discuss later that "backthrusting" and megafold formation probably both result from N to NW-directed differential movement of the Suretta and Tambo nappes in respect to the orogenic lid.
Pauli (1988) showed that the southern termination of the E Schams nappes (Figure 14-10a, inset near southern end of the profile) is caused by isoclinal Niemet-Beverin folding associated with a S-closing (in N–S profile view) megafold (Wissberg fold). This confirms the early views of Haug (1925) and Streiff (1962) and shows that the Middle Penninic Falknis-Sulzfluh nappes (northern part of Figures 14-1, 14-2) in principle represent the N continuation of the E-Schams nappes in the hangingwall of the Arblatsch flysch. A mega-scale Z-shaped fold affecting all the Briançonnais units of Graubünden appears in a large scale cross section (cross-hatched in Figure 14-2): The Falknis-Sulzfluh nappes form the upper right-way-up limb, the E-Schams nappes the overturned short middle limb, and the W-Schams nappes the lower right-way-up limb in respect to Niemet-Beverin phase mega folding.
How can such mega-scale folding lead to the overturning of a 40km long (measured in N–S-direction) "short" middle limb possibly have formed? The only feasible model we know of is that proposed by Merle and Guillier (1989), extensively discussed in Schmid et al. (1990). In brief: Post-collisional shortening in the root zone near the Insubric line during the Early Oligocene led to the vertical extrusion of the southern Penninic units in the Bergell area. Due to the presence of a rigid orogenic lid vertical flow within the ductile Penninic units was deflected into a near-horizontal direction and towards the N at shallower levels immediately below the lid. This led to a horizontal differential movement towards the N of the Tambo-Suretta pair both in respect to the overlying units (Austroalpine) and the underlying units (Adula nappe). It is this differential movement which is responsible for the apparent back-folds in the Suretta cover which simply represent originally N-facing Ferrera phase folds reoriented by the Niemet-Beverin phase strain. However, the second and structurally higher (in respect to the Niemet-Beverin-fold) megafold (Wissberg fold) is severely overprinted by a later, ESE directed normal fault, the Turba mylonite zone (Liniger 1992, Nievergelt et al. 1996) running along the base of the Platta nappe and cutting down section from N to S (from top Arblatsch flysch to top Avers Bündnerschiefer, Figure 14-2). Hence, omission by out of section normal faulting is responsible for the complete lack of Briançonnais tectonic units in the upper limb of the Wissberg fold along our N–S profile which runs approximately parallel to the

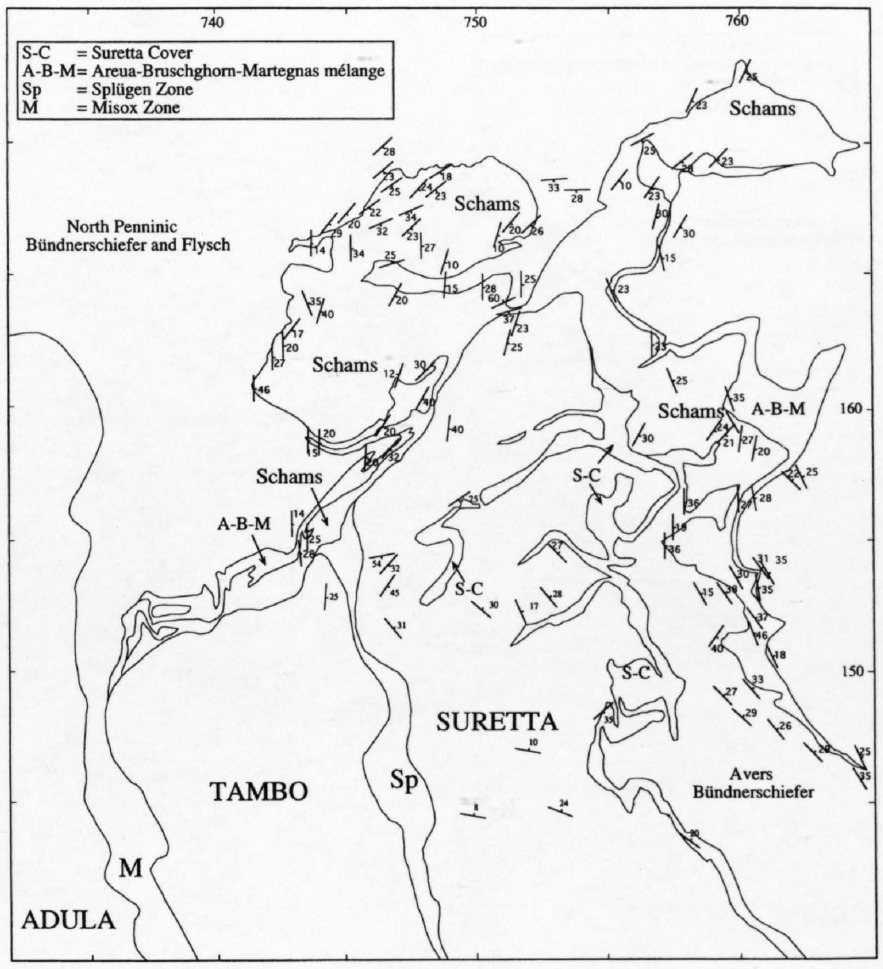

Figure 14-17
Strike and dip of the Niemet-Beverin phase foliation.

Turba normal fault (Figure 14-2). Between the Wissberg fold and the S termination of the Falknis nappe near Lenzerheide, only a very thin lens of Briançonnais units is found near Tiefencastel and in the hangingwall of the Arblatsch flysch (Streiff 1962).
In the surroundings of the frontal Tambo nappe, Mayerat (1989) attributed a local E-dipping lineation ("L3") with top to the E shear sense to an E–W extension. Marquer (1991) and Baudin et al. (1993) also described top to the E shearing in the Tambo nappe associated with a stretching lineation. These authors, however, correlated this E–W-extension with their second phase (the Niemet-Beverin phase). Thus, it appears that Niemet-Beverin folding is coeval with E–W extension. This E–W stretch, which we attribute to the Niemet-Beverin phase following Marquer (1991) and Baudin et al. (1993), leaves no trace in terms of large scale structures in a N–S profile except for the above mentioned omission at the Turba normal fault. Large scale parasitic folding in front of the Tambo nappe could be the combined effect of megafold formation largely related to N-directed differential movement of the Suretta-Tambo pair accompanied and/or immediately followed by E–W extension. Interestingly, no E–W extension was recorded in the Schams nappes further to the N where such Z-shaped parasitic folds also occur in the lower limb of the Niemet-Beverin axial trace.
Strains associated with the Niemet-Beverin phase vary in space. In the Mesozoic cover of the frontal Schams nappes (Schreurs 1990) the associated foliation is usually only well developed as a discrete or zonal crenulation cleavage in pelitic rocks. Limestones, even when isoclinally folded, only rarely exhibit a weak planar fabric. Penetrative fabrics in pelitic rocks are restricted to the Schams slices in front of the Tambo nappe and to the southern part of the E-Schams nappes, where strains are markedly higher. In spite of the generally weak axial planar fabrics, Niemet-Beverin folds are often near isoclinal on all scales in the cover.
In the basement strain intensity is in general weaker, but may be high locally. In the frontal Suretta nappe the early Ferrera foliation is gently wrapped around the very broad hinge of the Niemet-Beverin megafold, contrasting with the isoclinal megafold at Piz Beverin in the Schams nappes (along the same axial trace, Figure 14-10). On a small scale strain within the Rofna porphyry, as well as the Tambo nappe (according to Baudin et al. 1993) is pervasive but heterogeneous. The axial traces of the Niemet-Beverin large scale parasitic folds developed in the cover slices in front of the Tambo nappe cannot be traced into the Tambo basement (Mayerat 1989). This disharmonic structure again suggests a considerable contrast in mechanical behaviour between basement and cover during the Niemet-Beverin phase.
Axial planes of Niemet-Beverin folds and foliations are generally E-dipping (Figure 14-17), subparallel to the Ferrera foliation and they appear subhorizontal in a N–S cross section. Fold axes orientations are highly variable (Figure 14-18) although an ENE–WSW trend predominates in many places. An E to ENE strike characterizes the hinge line of megafolds such as defined by the front of the Suretta nappe and the basal D1 thrust of the Schams nappes. These hinge lines can be followed over a considerable distance along strike.

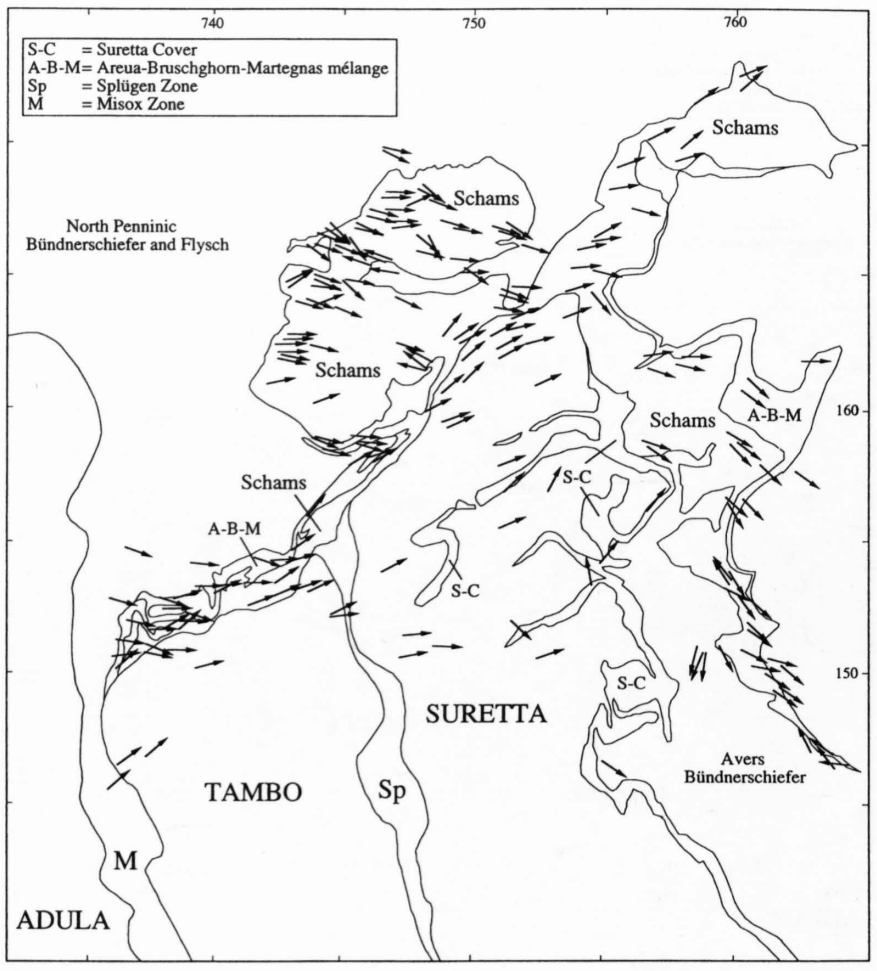

Figure 14-18
Niemet-Beverin fold axes (subhorizontal)

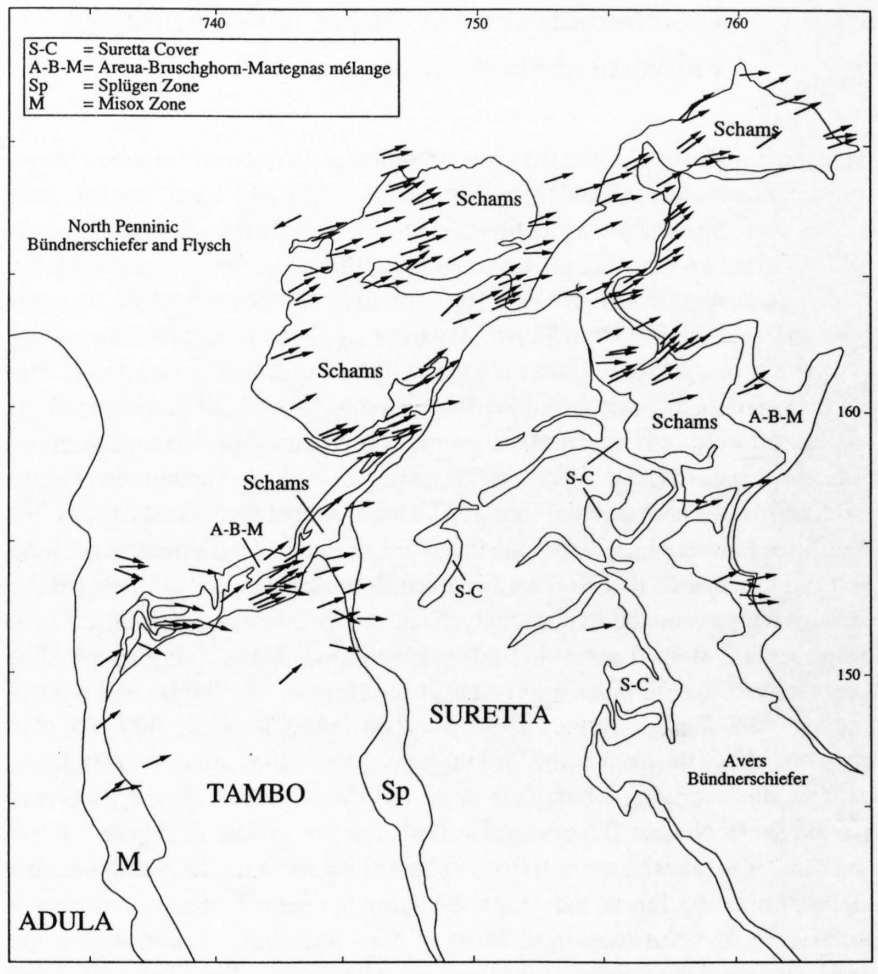

Figure 14-19
Domleschg phase fold axes (subhorizontal)

A systematic departure in orientation is observed in Figure 14-18 regarding the E Schams nappes where fold axes continuously swing into a NW–SE orientation towards the S. The rotation of these fold axes in the cover nappes away from the Niemet-Beverin hinge zone seems to indicate that the front of the Suretta nappe acted as a relatively rigid indenter producing a zone of high shearing strain on top of the Suretta nappe. This shearing strain, increasing southwards and associated with top to the SSE shear sense indicators, rotated the fold axes into a direction parallel to the local Niemet-Beverin transport direction. A SSE directed transport direction was also constructed by Schreurs (1990), based on deformed Ferrera phase lineation patterns around Niemet-Beverin folds, occupying a great circle on a stereogram.
In general, Niemet-Beverin phase stretching lineations and sense of shear indicators are only developed locally and are of variable orientation. Stretching lineations are absent in the frontal Schams nappes. In the E-Schams nappes shear bands indicating a top to the SE movement are widespread and also affect the overlying Arblatsch flysch, and the underlying Avers Bündnerschiefer (Schreurs 1990, Pauli 1988). Approaching the Turba mylonite in the hangingwall of the Arblatsch flysch the transport direction changes into the more easterly direction characteristic of the Turba mylonite normal fault formed during the closing stages of the Niemet-Beverin phase (Liniger 1992).

In summary, the Niemet-Beverin phase is associated with large scale post-nappe megafolding visible in a N–S cross section (Niemet-Beverin and Wissberg folds). Vertical shortening during the final stages of the Niemet-Beverin phase substantially thinned the pre-existing nappe pile. During the closing stages this vertical shortening was taken up by E–W extension, restricted to certain areas only (Turba mylonite zone, Schams nappes in front of the Tambo nappe and Tambo basement).

14.3.1.4 The Domleschg and Forcola phases: overprint related to final exhumation

The entire region is overprinted by a regionally consistent NW to NNW fold vergence with steeply inclined SE-dipping axial planes and NE to ENE plunging fold axes (Figure 14-19). This deformation also affects the N-Penninic Bündnerschiefer and flysch where it has been described as the Domleschg phase by Pfiffner (1977). This phase, although locally well developed as an intense crenulation, does not significantly alter the large scale geometry. Closely spaced large scale antiform-synform pairs produce a staircase geometry in the E-Schams nappes above the Niemet-Beverin axial trace (Figure 14-10a), affecting underlying units (backthrust of the Schams nappes over the Avers Bündnerschiefer) and, in particular, overlying units (up to the Austroalpine). Such large scale folds also concentrate near the front of the Suretta nappe, where they affect the axial trace of the Niemet-Beverin fold (Figure 14-10a). Staircase folds are again widespread in the Tambo basement (Baudin et al. 1993) where they increase in intensity towards the S and are, at least partially, responsible for the steeper northern dip of the Tambo nappe towards the S, observable in a N–S section (Figure 14-2).
The orientation of small scale fold axes (F3 of Schreurs 1990, 1993 and Schmid et al. 1990, F4 of Mayerat 1989) is amazingly constant, plunging NE to ENE (Figure 14-19), vergence being invariable towards the NW. Domleschg phase crenulations are easily distinguished from flat-lying Niemet-Beverin folds, because the former generally exhibit a more steeply inclined SE dipping axial plane. NE to ENE trend and plunge of small and large scale Domleschg folds is subparallel to most of the older large scale structures characteristic for the entire area situated E of the Ticino culmination of the Lepontine dome. This axial plunge is variable, as revealed by large scale contouring of Penninic basement nappes (Pfiffner et al. 1990 and Chapter 9, Steck et al., Chapter 12) and tectonic units in the hangingwall of these basement nappes, and locally varies between 10° and 35° to the ENE. On the other hand, the plunge of the Domleschg phase folds is only gentle to the ENE or near-zero (Pfiffner 1977, Schreurs 1990, Mayerat 1989, Baudin et al. 1993). This suggests that the large scale axial plunge between 10° and 35° is partly due to E-side-down offsets on later normal faults formed during the Forcola phase. SSE-dipping lineations, related to the Domleschg phase are only found in the southern Tambo nappe (Baudin et al 1993).
Normal faulting during the Forcola phase clearly overprints Domleschg phase folding and is only well developed in the S and in lower structural levels (Tambo nappe and base Suretta nappe, cf. Baudin et al. 1993). These authors describe NNW–SSE-striking steeply inclined E-dipping normal faults with a systematic downthrow towards the ENE, documented by stretching lineations. The largest of these faults, the Forcola normal fault, has not yet been investigated systematically and is situated at the base of the Tambo nappe. It is held responsible for the wedging out of the Misox zone towards the SE in map view (Figure 14-1) and can be followed as a retrograde greenschist facies mylonite into the Valle della Mera near Chiavenna (A. Berger, pers. comm.). Schreurs (1990) describes very low grade quartz mylonites with top to the E shear sense at the base of the Tambo nappe in Val Mesocco, overprinting higher grade top to the N or NNE mylonites related to earlier phases. However, the Forcola normal fault dies out northwards and cannot be traced further within the Bündnerschiefer. This retrograde and often brittle, steeply inclined normal faulting represents a later stage of E–W-extension in respect to the Turba low angle normal fault, as will be discussed later. In the upper and southern part of the Suretta nappe, E–W extension is documented by (brittle) shear bands, kink bands and joints and is associated with a top to the east shear sense (Hitz 1989).

In summary, the Domleschg phase moderately shortens the entire nappe pile in a SSE–NNW direction without producing significant décollement or large scale nappe folding. The systematic axial plunge to the ENE suggests that uplift of the Lepontine dome at its eastern margin postdates the Domleschg phase. Axial plunge is most likely related to final uplift and tilting of the nappe units, related to E–W extension manifested by the Forcola phase normal faults.

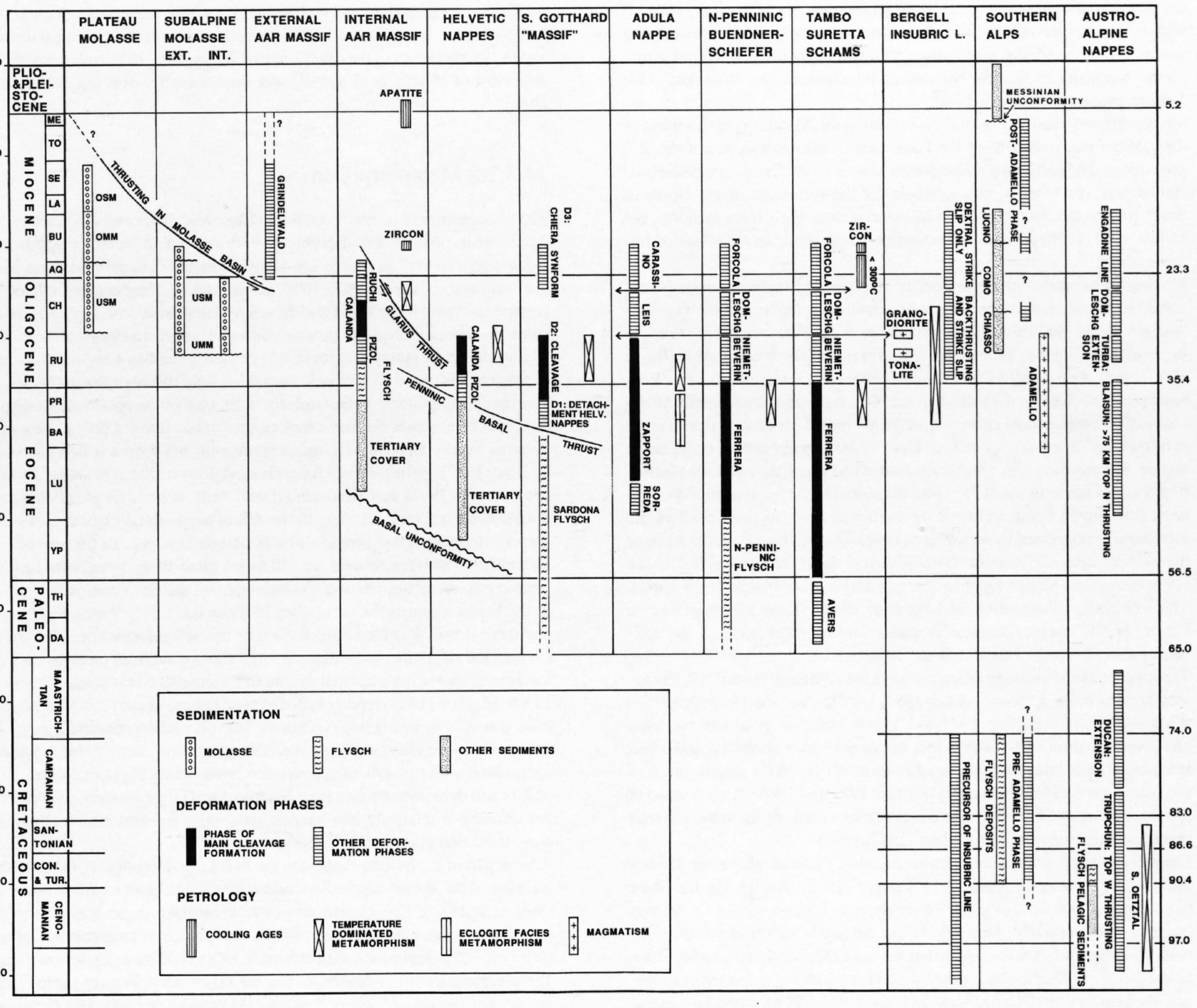

Figure 14-20
Correlation table attempting to date deformation phases and stages of the metamorphic evolution along the Eastern Traverse. Time scale according to Harland et al. (1989). See text for further explanations. Information concerning the Bergell area, the Insubric line, the Austroalpine nappes and the Southern Alps is added for convenience, but will be discussed in Chapter 22.

14.3.2 Regional correlation, metamorphism and dating of deformation phases

So far deformation phases were primarily based on structural superpositions analysed on all scales but within an area of limited extent. The tectonic and kinematic significance of such phases can only be further assessed after an attempt is made (1) to correlate these phases with those found in neighbouring areas, (2) to evaluate metamorphic conditions during deformation, and, (3) to date these phases with geochronological methods. As long as deformation phases are entirely defined by locally observed structural superpositions they simply represent a classical methodological tool. The correlation table given in Figure 14-20 summarizes the interpretation given in this chapter.

14.3.2.1 Regional correlation of deformation phases

In the units below the Tambo-Suretta pair, four deformation phases have been recognized by Löw (1987) for the frontal sector and by Meyre and Puschnig (1993) for the middle sector of the Adula nappe. The first phase (Sorreda phase of Löw 1987) predates eclogite facies overprint and is related to intense slicing of the quartzo-feldspatic basement with Mesozoic slivers. The Zapport phase, as defined by Löw (1987) represents the principle phase of penetrative cleavage formation in the Adula nappe. This longlasting phase sets in under eclogite facies conditions and spans a wide interval of pressures during near-isothermal decompression. Two stages of this Zapport phase have recently been distinguished by Meyre and Puschnig (1993) and Partzsch et al. (1994). An earlier deformation stage D2a, related to eclogite facies conditions, produced an early penetrative foliation and subsequent isoclinal folding of this foliation. Stage D2a structures are preserved in mafic boudins only. Outside these boudins the dominating penetrative Zapport phase foliation corresponds to stage D2b. This stage, prevalent outside the mafic boudins, is clearly post-eclogitic and associated with an alteration of the rims of the eclogite facies boudins under amphibolite facies conditions.
The post-eclogitic D2b stage foliation (formed during the closing stages of the Zapport phase in the sense of Löw, 1987) carries a N–S oriented stretching lineation associated with top to the N shearing according to numerous sense of shear criteria (Meyre and Puschnig 1993, Partzsch et al. 1994). Recent field work (M. Frey, J.Partzsch, S.Schmid, work in progress) shows that this main schistosity related to stage D2b can be followed without a structural break across the entire Misox zone (N-Penninic Bündnerschiefer). As described below, this Misox zone is characterized by a composite Ferrera and Niemet-Beverin phase foliation. From these field relations we conclude that the closing stages of the Zapport phase in the Adula nappe (stage D2b) are contemporaneous with the Niemet-Beverin phase of the higher tectonic units.
The subsequent Leis phase in the Adula nappe (Löw 1987), however, cannot be correlated with the Niemet-Beverin phase of our working area. This Leis phase corresponds to a large scale antiform in front of the Adula nappe, the Lunschania antiform (Löw 1987, Probst 1980) found in the N-Penninic Bündnerschiefer. According to Steinmann (1994) this antiform is equivalent to the Domleschg phase as defined by Pfiffner (1977). The correlation between Leis and Domleschg phase (Figure 14-20) confirms that the Niemet-Beverin phase has to be roughly contemporaneous with the closing stages of the Zapport phase in the Adula nappe. In the Bündnerschiefer of the Misox zone near the base of the Tambo nappe, Niemet-Beverin phase deformation is extremely intense and completely transposes the Ferrera phase first penetrative cleavage. There, Ferrera phase lineations, strongly deformed during

the Niemet-Beverin phase, straddle an entire great circle due to "in-plane" folding (see Figure 14-15c). This indicates very strong syn-Niemet-Beverin strains across the Misox zone, which represents a telescoped section across all the four major units of the N-Penninic Bündnerschiefer, with relics of the Schams nappes in its hangingwall.
The Carassimo phase (Löw 1987) is related to the Alpettas synform north of the Adula front, overprinting the Lunschania antiform and, therefore, also post-dating the Domleschg phase. No equivalent of the Carassimo phase (and similar late synforms so characteristic for the formation of the Northern Steep Belt of the Penninic structural zone such as the Chiera synform, see Milnes 1974, 1976) seem to have overprinted our working area situated further to the E.
Moving further down the nappe pile, the N-Penninic Bündnerschiefer are observed to be thrust onto the largely allochthonous "cover" of the Gotthard "massif" (Etter 1987) along what we refer to as the Penninic Basal Thrust, to be correlated with the "Frontal Penninic Thrust" of the Western Alps (Bayer et al. 1987). According to Steinmann (1994), this thrusting post-dates the main phase of cleavage formation in the N-Penninic Bündnerschiefer attributed to the Ferrera phase. However, we do not regard his structural arguments to be conclusive in this respect. In analogy to the findings in the Suretta nappe and the Schams units we regard detatchment and penetrative cleavage formation (Ferrera phase in the N-Penninic Bündnerschiefer) as a continuous process, detachment being followed by ductile penetrative overprint and not vice-versa as postulated by Steinmann (1994). Therefore we prefer to attribute detachment along the Penninic Basal Thrust to the Ferrera phase. Steinmann (1994) observes Domleschg phase overprinting of the Penninic Basal Thrust. This overprint is also seen in the large scale profile (Lunschania antiform in Figure 14-2). Intense Domleschg phase folding (equivalent to the Leis phase) also affects the Penninic Basal Thrust.
The main phase of cleavage deformation in the Gotthard "massif" and its autochthonous cover remnants (Etter 1987, his D2) and the Helvetic nappes (Calanda phase of Pfiffner 1977 and 1986), however, post-date the main cleavage formation in the N-Penninic Bündnerschiefer, attributed to the Ferrera phase (Dreibündenstein phase of Pfiffner 1977) and the emplacement of the latter onto the Helvetic nappes (Pfiffner 1977 and 1986). A correlation of the Domleschg phase with movement along the Glarus thrust in the Helvetic realm has been suggested by Pfiffner (1977, 1986).
Correlations with deformation phases found in the units above the Tambo-Suretta pair have been provided by Liniger (1992). During his D1 phase (equivalent to our Ferrera phase) a nappe pile, formed during Cretaceous orogeny, was passively transported over viscously deforming underlying units (orogenic lid in the sense of Laubscher 1983, Merle & Guillier 1989, Schmid et al. 1990). Eoalpine deformation is considered to represent a separate orogenic event ("Cretaceous orogeny") because an important extensional phase (Froitzheim 1992, Froitzheim et al. 1994) separates Cretaceous WNW-directed convergence from the Tertiary (Meso- and Neoalpine) orogeny characterized by NNE to N directed convergence (the Blaisun phase of Froitzheim et al. 1994, see Figure 14-20). In regard to the dating and kinematics of Cretaceous deformation the reader is referred to data and discussions provided by Liniger (1992), Froitzheim (1992), Thöni (1986), Schmid & Haas (1989), Deutsch (1983) and Froitzheim et al. (1994). Cretaceous deformation will also be briefly discussed in chapter 22 of this volume. Tertiary age structures have been observed in the orogenic lid by Liniger (1992) Froitzheim (1992) and Froitzheim et al. (1994), but their importance is minor N of the Engadine line and they certainly are not related to the formation of the main schistosity in this orogenic lid, which is of Cretaceous age.
This upper nappe pile, already formed during the Cretaceous, represented an orogenic lid during the Tertiary. It consists of (from top to bottom) the Austroalpine nappes, the Arosa-Platta ophiolite units, the Margna nappe and the Lizun-Forno-Malenco ophiolitic units. This suturing of the remnants of the Piemont-Liguria oceanic domain (ophiolitic units) with the Apulian plate (Austroalpine) during Cretaceous orogeny predates all deformation phases observed in our working area. The Avers Bündnerschiefer represent the only derivatives of the Piemont-Liguria ocean which are in a structural position below the orogenic lid and which have consequently been penetratively deformed by Tertiary age deformation. Unfortunately, no structural correlation of the Avers phase with phases found in the orogenic lid can be made. If we propose that this Avers phase is related to an early phase of Tertiary convergence, this is based on their present-day structural position in the footwall of the orogenic lid, and additionally, on the large scale configuration in a N–S profile discussed earlier, suggesting roughly N-directed transport of the Avers Bündnerschiefer over the Suretta cover.
The basal thrust of the orogenic lid is severely overprinted by normal faulting during the closing stages of the Niemet Beverin phase in the Turba mylonite zone. This Turba mylonite zone forms an extremely valuable time marker: Liniger (1992) was able to follow this mylonite zone into the contact aureole of the Bergell intrusion where it is cut by the well dated Bergell granodiorite.
A subsequent event of NNW–SSE compression (D3 of Liniger 1992) folds the Turba mylonite zone and underlying Avers Bündnerschiefer. This D3 of Liniger (1992) is associated with differential uplift of the Bergell intrusion and the southern part of the Suretta nappe. It can easily be correlated with D3 structures of Baudin et al. (1993) and, consequently, with our Domleschg phase.

14.3.2.2 Metamorphism

The discussion will be restricted to the Mesozoic cover and the monocyclic basement in order to avoid problems with pre-alpine metamorphism. The Adula nappe, where an Alpine age of high pressure metamorphism has been demonstrated by Löw (1987), forms an exception. Temperatures related to metamorphism will be discussed first. Problems arise with regard to pressures discussed thereafter, because different interpretations are possible. Classically, high pressure metamorphism is regarded as Cretaceous in age (Eoalpine), followed by Tertiary Barrowian type metamorphism (Meso- to Neoalpine, "Lepontine metamorphism"). In view of the previous discussion on Cretaceous versus Tertiary orogeny, this would imply a polyphase metamorphic history. In contrast to this, a continuous p-T-loop was first proposed by Löw (1987). A Tertiary age for such a p-T-loop has been proposed by Gebauer et al. (1992) and Gebauer (1996) while Schmid et al. (1990) cast doubts about a Cretaceous age in the Adula nappe purely based on the inferred paleogeographic position of this basement nappe. In the absence of undisputable radiometric ages we will assess these alternatives based on data concerning interactions between metamorphism and deformation.
In the Schams nappes the occurrence of white mica, stilpnomelane, chlorite and epidote indicates lower greenschist or blueschist facies conditions (discussion and references in Schreurs, 1990). These conditions prevailed during the Ferrera phase but persisted during the Niemet-Beverin phase (Schreurs 1990). Mayerat (1989) reports syn- and post-Ferrera phase growth of amphibole, followed by retrograde conditions, but still within greenschist (or blueschist) facies conditions during the Niemet-Beverin phase. This evidence agrees well with the style of deformation observed during both deformation phases and demonstrates that both basement and cover may undergo ductile deformation at relatively low temperatures. Final exhumation clearly postdates these two phases of deformation.
A large part of the Suretta nappe and the Avers Bündnerschiefer, but only the NE edge of the Tambo nappe, are situated N of the stilpnomelane-out isograd (Frey et al. 1983). New occurrences of stilpnomelane in the Schams nappes have been mapped by Schreurs (1990). This indicates temperatures below about 450°C (experimental data of Nitsch, 1970, valid for a pressure of 4 kb). Temperatures are better constrained in the Misox zone with regard to "Lepontine metamorphism" where Teutsch (1982) indicates 500–550°C around Mesocco and 600–660 °C near the Forcola pass. In this context "Lepontine metamorphism" is not used in the sense of a metamorphic event. Instead, this term refers to a final equilibration under moderate pressures (around 6 kb in this case) leading to the famous pattern of isograds in the Lepontine dome. Teutsch (1982) reports growth of staurolite during and after his second deformational phase which corresponds to either the Ferrera or the Niemet-Beverin phase. In the light of the pressure estimates by Baudin and Marquer (1993) from the Tambo nappe discussed later, equilibration during the Niemet-Beverin phase is more likely. This agrees well with the classical picture of NW–SE-running isograds in the E part of the Lepontine dome, suggesting that final equilibrium related to Lepontine metamorphism overprints all major tectonic contacts formed during the Ferrera and Niemet-Beverin phases. The strike of these isograds indicates final exhumation related to differential uplift and erosion of the southern Penninic region during the Domleschg phase (N–S gradient), in combination with the axial plunge to the E, associated with E–W extension during the Forcola phase (E–W gradient).
Metamorphism related to the Lepontine isograds postdates D2 in the cover of the Gotthard massif (Etter 1987). Since we found this D2 to be roughly contemporaneous with our Niemet-Beverin phase, peak temperatures must have been reached at some later stage in this area.
Mafic eclogites of the Adula nappe (Heinrich 1983) indicate temperatures around 450–550°C in the extreme north, increasing to 550° to 650°C at Trescolmen in a middle sector E of Mesocco (Trescolmen). These temperatures agree with those obtained outside mafic boudins by Heinrich (1983) and Löw (1987). Hence eclogite facies related temperatures (and pressures) are not restricted to mafic lithologies and presumably prevailed all across the Adula nappe. Interestingly, these temperature estimates are above those reported for Lepontine equilibration in case of the northern Adula nappe. This implies that the Lepontine equilibration, as for example indicated by the staurolite "isograd" (Frey et al. 1980), established primarily within Mesozoic cover rocks, does certainly not apply to the northern Adula nappe situated a long way outside this "isograd", indicating temperatures of around 500°C. In fact, Klein (1976) reports staurolite north of this "isograd" and within the northern Adula nappe, while Koch (1982) inferred temperatures in excess of 500° C

for the middle part of the Adula nappe. This is important since it indicates that the rocks in the northern Adula nappe must have cooled considerably before they were equilibrated during the Lepontine stage. Löw (1987) reports that temperatures and pressures compatible with Lepontine zonation were reached only after his Zapport and Leis phases, while Meyre & Puschnig (1992) find that Lepontine p-T conditions where established at the end of the Zapport phase (during their stage D2b) but before the Leis phase.
This confirms that Lepontine isograds postdate the major nappe contacts, formed during the early stages of the Ferrera phase. However, some difficulties still arise with regard to the timing of the higher or similar temperatures reached during the eclogitic stage. Strictly speaking, only D2b of Meyre & Puschnig (1993) can directly be correlated with the Tertiary aged Ferrera and Niemet-Beverin phases, the eclogitic event D2a being only detectable within mafic boudins. However, D2a and D2b probably have to be viewed as two stages during a continuous tectonic evolution associated with near-isothermal decompression (Löw 1987) and top to the N senses of shear documented for the later stages (D2b). This evolution is viewed to be contemporaneous with the Ferrera and Niemet-Beverin phases. The two stages D2a and D2b do in fact correspond to the Zapport phase of Löw (1987) who found this Zapport phase to straddle a range of decreasing pressures, starting at peak pressures. If this eclogitic stage is of Tertiary age indeed, as suggested by the correlation of D2a and D2b with the Ferrera and Niemet-Beverin phases, respectively, a high pressure overprint in the tectonic units overlying the Adula nappe would be expected. The following discussion on pressures will show that this is the case indeed.
The peak pressures reported for the Adula nappe increase from 10–13 kb (northern Adula nappe) to 15–22 kb (Trescolmen) according to Heinrich (1983, 1986). Eclogites are also found at the base of the Misox zone, but no Alpine age eclogites are known from the upper portions of the Misox zone or higher tectonic units. This suggests a drop in pressure and/or temperature across the Misox zone towards the E.
In basement slices of the Misox zone (Gadriolzug) Teutsch (1982) reports that phengitic white mica related to the Ferrera phase foliation are preserved in the N. His Si-contents reach values of around 3.5 (based on 11 oxygens per formula unit), indicating pressures of around 10 kb. This is compatible with a more recent study by Baudin & Marquer (1993) on the monocyclic Tambo basement. These authors analysed white mica in different microstructural sites corresponding to their deformation phases. Pressures in the order of 10–13 kb during the Ferrera phase are followed by pressures of around 5-10 kb recorded during the Niemet-Beverin phase. In spite of considerable difficulties concerning the applicability of the geobarometer provided by Massone and Schreyer (1987), pressures in excess of those reported for the Lepontine stage nearby (6 kb near Mesocco according to Teutsch, 1982) must have been reached. The results of Baudin & Marquer (1993) also suggest, at least qualitatively, a substantial pressure drop during the Niemet-Beverin phase. Temperatures dropped only insignificantly. This is analogous to the near-isothermal decompression reported for the Adula nappe by Löw (1987) and Meyre & Puschnig (1993).
Data on a possible pressure dominated overprint of higher tectonic units are scarce and no evidence for such an event is reported yet from the Schams nappes. Ring (1992 a) reports pressures in excess of 10 kb, also based on the Si-content of white mica, from the Suretta nappe and the Avers Bündnerschiefer. Oberhänsli (1986), who studied blue amphiboles in the Avers Bündnerschiefer, concludes that glaucophane and crossite indicate "pressure-accentuated" greenschist facies overprint but gives no estimate of pressure. Goffé & Oberhänsli (1992) found pseudomorphs in the Avers Bündnerschiefer which resemble carpholite, which indicates minimum pressures of around 7 kb.
Regarding the N-Penninic Bündnerschiefer, Goffé & Oberhänsli (1992) found carpholite preserved in the Lugnez valley, near the Basal Penninic Thrust. They estimate pressures to be in excess of 7 kb. There, chloritoid formed as a break-down product of carpholite when temperatures rose to about 350°C. Since carpholite pseudomorphs are also found near Thusis, these authors suggest that high-p low-T relics in the Bündnerschiefer are only preserved at the periphery of the Lepontine isograds. In the light of the common deformation history this strongly suggests that the Schams nappes were also affected by such a high-p event before the temperature rose to somewhere above 350°C but below about 450°C, as indicated by the stability of stilpnomelane.
In conclusion it appears that the entire studied area has been affected by high-pressure metamorphism as originally suggested by Frey et al. (1983) based on the occurrence of 3T white mica polymorphs. The decrease in pressure across the Misox zone is substantial but cannot be quantitatively assessed yet. The relations between mineral growth and deformation phases carefully established by a number of workers (e.g. Baudin & Marquer 1993, Löw 1987, Meyre & Puschnig 1993) exclude an Eoalpine age for this high pressure overprint which prevailed during the initial stages of the Ferrera phase. Near-isothermal decompression is indicated during the late stages of the Zapport phase in the Adula nappe (D2 of Meyre & Puschnig, 1993) and during the Niemet-Beverin phase in the Tambo nappe. In the N-Penninic Bündnerschiefer and Schams cover slices decompression from more moderate pressures must have been associated with increasing temperatures during the final stages of the Ferrera phase. The conclusion regarding a single p-T evolution of Tertiary age will have to be confronted with radiometric data discussed in the following section.

14.3.2.3 Dating of deformation and metamorphism

Deformation phases which can be correlated between different areas do not need to be strictly synchronous. If an attempt is made to date a particular deformation phase at a certain localitiy in the following discussion, summarized in Figure 14-20, such dating is only strictly valid at this particular locality. The same, of course, applies to the dating of metamorphic "events", or better, certain stages of a metamorphic evolution. Only in the absence of clear indications for migrating deformation phases do we assume contemporaneity (for example in case of the Domleschg phase, see Figur14-20). In other cases (for example the Calanda phase, see Figure 14-20) the available data point to the heterochroneity of the same deformation phase (in a strictly structural sense) in different tectonic positions.
Solid stratigraphical constraints for the earliest onset of deformation in parts of the Valais domain are only available for the Arblatsch and Prättigau flysch (Early Eocene, about 56–50 Ma) and the Falknis nappe (Paleocene). Sedimentation in the remainder of the Briançonnais and Valais domains may theoretically have stopped at some earlier stage because no fossils younger than Late Cretaceous in age have been found. Hence these constraints do not exclude the onset of collision at some earlier stage regarding the southern Briançonnais realm (Avers phase) nor do they exclude tectonic and metamorphic events in the basement while sedimentation continues in the cover. However, for the Tomül unit of the N-Penninic Bündnerschiefer the Ferrera phase is constrained to be younger than Early Eocene.
Regarding the more external Helvetic units (Glarus flysch), sedimentation continued well into the Early Oligocene below the Glarus thrust (Herb 1988, Pfiffner 1986), constraining the local maximum age of the Pizol and Calanda phase in the Infrahelvetic complex to substantially postdate the Eocene-Oligocene boundary (about 35 Ma). In the Helvetic nappes, however, sedimentation stopped earlier (Herb 1988, Lihou 1995) and synchronously with the emplacement of exotic cover sheets of S-Helvetic origin (Pizol phase) near the Eocene-Oligocene boundary. These data confirm the classical view of orogenic foreland propagation from S to N. Both the Pizol and the Calanda phases are not contemporaneous in the Helvetic nappes and the units below the Glarus thrust, as depicted in Figure 14-20.
Radiometric dating of the intrusion of the Bergell granodiorite at 30.13 ± 0.17 Ma (von Blanckenburg 1992) provides an absolutely reliable and extremely useful time marker. As discussed earlier, this intrusion constrains the end of the Niemet-Beverin phase to predate 30 Ma.
Radiometric dating of metamorphism is less straightforward and is a misnomer in that metamorphism also has to be viewed as an evolution in time and space which, strictly, has no fixed age. Additionally, numerous problems are inherent to the method used, such as to know wether isotopic compositions record cooling, formation or mixed ages.
Evidence, often quoted in favour of Eoalpine or Cretaceous metamorphism below the orogenic lid, stems from the Suretta nappe (Hanson et al. 1969, Steinitz and Jäger 1981). A Rb-Sr whole rock isochron age of 118 Ma was obtained for the northern Suretta nappe. This age, however, is in contrast to Tertiary phengite mineral ages, and, according to Hurford et al. (1989), the possibility of an artifact due to partial rejuvenation of pre-Alpine ages has to be considered. The second piece of evidence for Eoalpine ages comes from eclogites of the Adula nappe where Hunziker et al. (1989) quote a time bracket of 76–180 Ma based on work by Muralt (1986). This contrasts with Tertiary U-Pb zircon ages reported from the Cima Lunga unit, a western continuation of the Adula nappe (Gebauer et al. 1992, Gebauer 1996). Recent Sm-Nd mineral data by Becker (1992, 1993) are controversial too, in that they indicate both Tertiary (Cima Lunga) and Cretaceous (Adula) ages within the same tectonic unit. All this shows that radiometric evidence for the age of high-pressure metamorphism in the Adula nappe is still contradictory. Based on stratigraphic and structural arguments we prefer a Tertiary age for high pressure metamorphism. In accordance with the Tertiary ages given by Becker (1993) and Gebauer (1996) we place the age of this high pressure event in the Adula nappe somewhere between 42 and 36 Ma (Figure 14-20).
Radiometric evidence for Tertiary metamorphism in the Suretta, Tambo and Schams nappes has been compiled by Schreurs (1990, 1993). For the Ferrera phase cleavage in the Schams nappes K-Ar ages between 45 and 30 Ma are obtained for the <2 mm fraction (analyses by S.Huon and J. Hunziker reported in Schreurs 1990, 1993). An age bracket of 41–38.4 Ma is indicated for phengites in the Suretta cover by K-Ar dating (Steinitz and Jäger 1981,

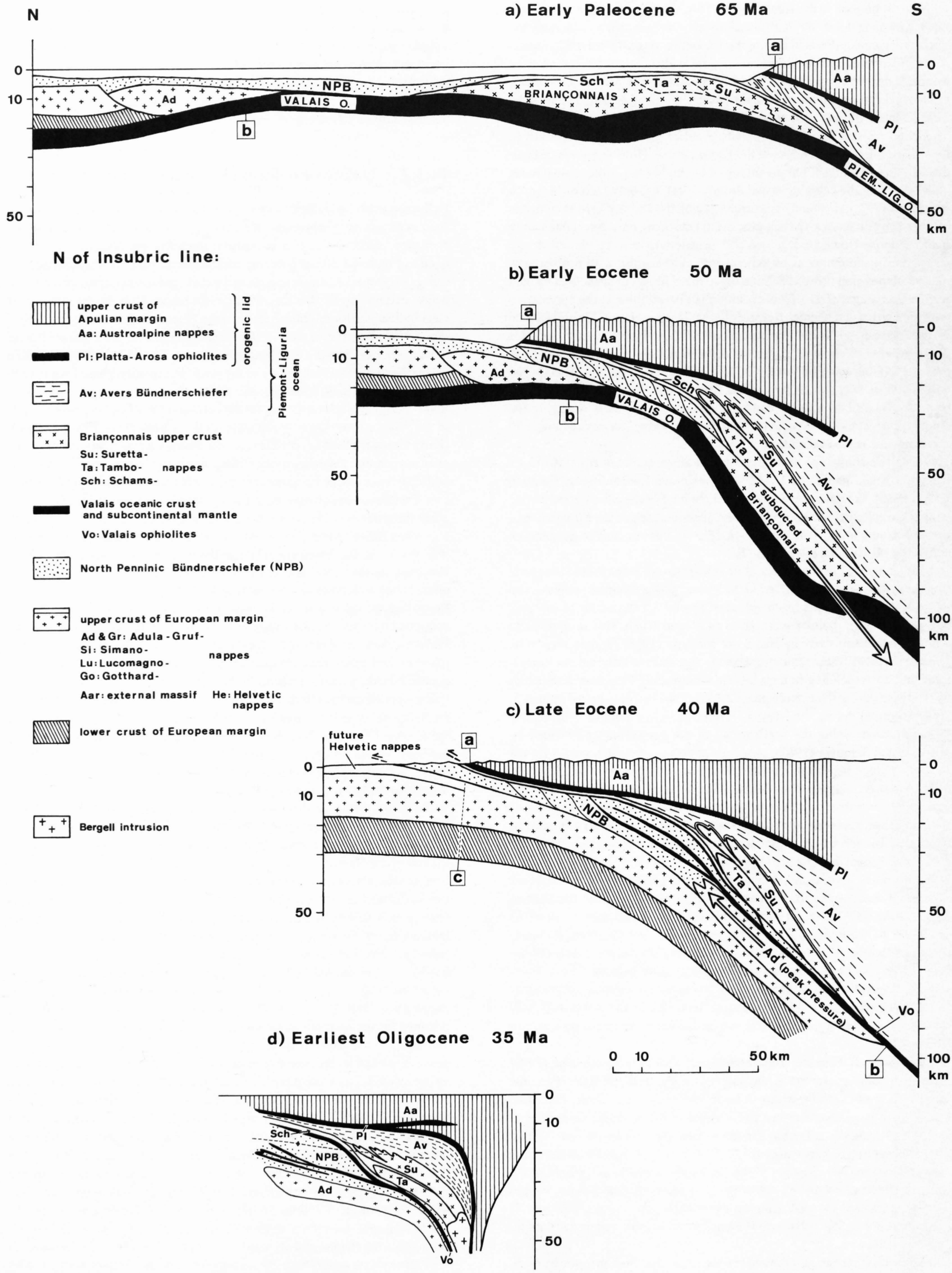

Figure 14-21
Scaled and area-balanced sketches of the kinematic evolution from early convergence and subduction (stages a and b) to collision (stage c) and postcollisional shortening (stages d to g).

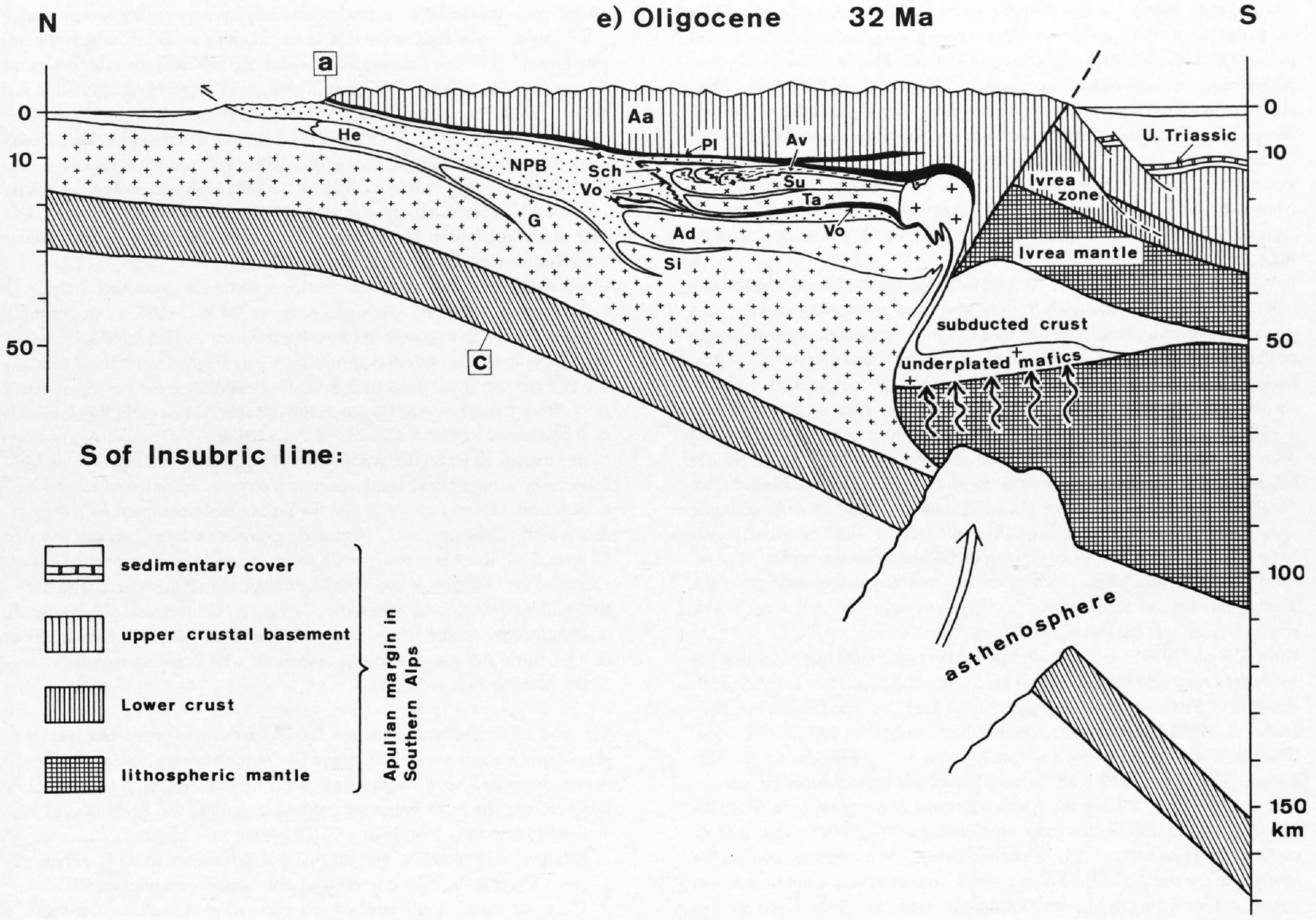
N
e) Oligocene 32 Ma
S
a
c
Aa
He
Pl
Av
NPB
Sch
Vo
Su
Ta
G
Ad
Si
U. Triassic
Ivrea zone
Ivrea mantle
subducted crust
underplated mafics
asthenosphere
0
10
50
100
150
km
S of Insubric line:
sedimentary cover
upper crustal basement
Lower crust
lithospheric mantle
Apulian margin in Southern Alps
f) Early Miocene 19 Ma
Insubric line
Gonfolite Lomb.
future thrust
Aar
Go
Lu
50
km
g) Present
Engadine line
Gr
0 10 50 km

Hurford et al. 1989). Similar phengite ages (36.6–37.6 Ma) are reported for the Rofna porphyry by Baltzer (1989) but phengite ages may be older in other places within the Suretta basement (up to 49.6 Ma, Hurford et al. 1989). Amphibole ages are still older (maximum age of 55 Ma, Hurford et al. 1989). All minerals dated are related to the main schistosity formed during the Ferrera phase and do not date the Niemet-Beverin phase, as erroneously reported by Steinitz and Jäger (1986). The dated amphiboles are aligned within the Ferrera stretching lineation, but also broken and stretched, possibly by late Niemet-Beverin E–W extension. Given the possibility of excess or inherited argon, Hurford et al. (1989) consider the age of 49–55 Ma as being maximum formation ages.

In view of the large spread of K-Ar mineral ages from the Suretta and Schams units (35–55 Ma, excluding Rb-Sr ages which are in part younger) an exact age for the Ferrera phase deformation and associated metamorphism cannot be deduced. Hurford et al. (1989) conclude that the age bracket of 35–40 Ma, encompassing concordant Rb-Sr and K-Ar ages, is the most realistic estimate for the age of metamorphism associated with the Ferrera phase (Figure 14-20). However, we provided evidence that the pressure peak probably predates the temperature peak in this area. Hence we consider the 35–40 Ma bracket to date the temperature peak postdating the onset of early pressure dominated stages of the Ferrera phase. Taking the spread of K-Ar phengite ages to reflect a spread in their age of formation, 50 Ma (Early Eocene) seems to be a good estimate for the beginning of the high-P metamorphic stage related to the Ferrera phase. Hence, the Ferrera phase deformation in the Tambo, Suretta and Schams area is inferred to have started before 50 Ma, somewhere around the Paleocene-Eocene boundary.

Hurford et al. (1989) use the 35–40 Ma bracket as the most likely age interval for evaluating the cooling history of the Suretta nappe, starting between 350° and 450°C. Fission track zircon ages for the Suretta nappe (20–21 Ma, Hurford et al. 1989), together with a temperature estimate of 400°C at 37.5 Ma, result in a slow average cooling rate (around 10° C/ Ma) during the Oligocene. This agrees well with the conclusion that temperatures did not decrease significantly during the Niemet-Beverin phase, ending in Mid-Oligocene times. Apatite fission track ages between 10–16 Ma indicate a more rapid cooling rate during Early Miocene times. Since accelerated cooling fits nicely into the context of the Forcola phase, related to final exhumation, this phase, and consequently also the Domleschg phase, are likely to predate this 10–16 Ma age interval (Figure 14-20). However, the Suretta cooling data do not have enough resolution to date the onset of rapid cooling related to final exhumation more precisely.

An attempt to date the Domleschg and Forcola phases more precisely has to use data from the more internal Penninic zone around the Bergell intrusion. The southern Tambo nappe cooled to below 300° C during Early Miocene times (biotite Rb-Sr and K-Ar ages between 21 and 25 Ma, KAW 105 and KAW 281 of Jäger et al. 1967, and Purdy and Jäger 1976). The greenschist facies mylonites related to the Forcola line found near Chiavenna (recent field work by A. Berger, Basel) can therefore not have formed substantially later than this time interval. Younger biotite cooling ages in the southern Misox valley (around 18–19 Ma, Purdy and Jäger, 1976, Wagner et al. 1977) show that the axial plunge of the eastern Lepontine area already existed at around 18–19 Ma. An age interval somewhere between 21 and 25 Ma (Oligocene-Miocene boundary) is therefore realistic for the Forcola phase (Figure 14-20).

The Domleschg phase, related to northward tilting of the southern Tambo nappe, is intimately related to uplift of the Bergell region. According to Giger (1991) and Giger and Hurford (1989), cooling and exhumation of the Bergell region immediately postdates the Bergell intrusion (30–32 Ma, von Blankenburg 1992). Work in progress (Rosenberg et al. 1994 & 1995) even suggests that backthrusting along the Insubric line already initiated during the intrusion of the Bergell tonalite (32 Ma, Blanckenburg 1992). It appears that the Domleschg phase initiated immediately after the final stages of the Niemet-Beverin phase. Liniger (1992) in fact argues that normal faulting along the Turba mylonite may even be contemporaneous with his D3 (correlated with the Domleschg phase). A scenario for contemporaneous E–W extension and N–S compression was recently proposed along the Simplon line by Mancktelow (1992) and, for Early Miocene times, for the region between Engadine line and Tonale line (Schmid & Froitzheim 1993). The Glarus thrust in the adjacent Helvetic zone, whose final stages can be correlated to the Domleschg phase, leads to a locally inverse metamorphic zonation and can be dated as Late Oligocene to Early Miocene (Groshong et al. 1984). In conclusion then, the Domleschg phase is inferred to have been active within the 30–25 Ma time interval (Figure 14-20).

Concerning deformation phases in the Helvetic units radiometric dating has to rely on illite-muscovite data discussed in Hunziker et al. (1986) and on stratigraphic evidence (Pfiffner 1986). Hunziker et al. (1986) conclude that Calanda phase deformation within the Helvetic nappes above the Glarus thrust occurred at around 35–30 Ma ago, a time interval also given in the reconstruction of Pfiffner (1986). Figure 14-20, however, depicts a somewhat younger time interval for Calanda phase deformation and associated metamorphism in the Helvetic nappes because, as discussed earlier, sedimentation did occur up to the Priabonian (i.e. in the Blattengrat unit of S-Helvetic origin, Lihou 1995). The Calanda phase within the Infrahelvetic units below the Glarus thrust is still younger (post 30 Ma, see Figure 14-20, "Internal Aar massif"). Final movements along the Glarus thrust related to the Ruchi phase (Milnes & Pfiffner 1977, Schmid 1975) offset the metamorphic zonation indicated by illite crystallinity data (Frey 1988 and Groshong et al. 1984). Pfiffner (1986) suggests that movement on the Glarus thrust causing the inverse metamorphic zonation stopped at around 20 Ma. From this time onwards further shortening within the Aar massif is related to thrusting in the Molasse basin (Grindelwald phase of Figure 14-20).

Geochronological data from areas further to the N along the NRP 20 have recently been provided by Michalski & Soom (1990). They are discussed in Chapter 13.1 of this volume in more detail. Zircon fission track ages around 20–21 Ma from the eastern Aar massif (Vättis window), the Ilanz area and the N-Penninic Bündnerschiefer near Rothenbrunnen do not significantly differ from those reported for the Suretta nappe. At first sight this implies a near-horizontal isotherm at 20 Ma ago in relation to the present-day position of these units. However, the assumption of horizontal isotherms during Miocene times is unjustified and N-dipping isotherms are inferred for the Helvetic nappes (Frey et al. 1973) and the Infrahelvetic complex, including the Aar massif (Groshong et al. 1984 and references therein). As discussed in Chapter 13.1, the Aar massif zircon fission track ages of around 20 Ma are related to the initiation of uplift of this external massif associated with the initial stages of shortening within the Aar massif (Grindelwald phase). Uplift, documented by apatite fission track ages, continued until the Late Miocene in the Central Aar massif and was associated with thrusting within the Subalpine Molasse Figure 14-20).

The most important conclusions on dating deformation phases and metamorphic stages are summarized in Figure 14-20, together with events within the Austroalpine and South-Alpine units which are discussed in Chapter 22 of this volume. The most important features regarding the Penninic and Helvetic units emerging from Figure 14-20 are the following:

1. Youngest sedimentation ages suggest that the onset of tectonic activity migrates towards the northern foreland over a time span of about 40 Ma.
2. The main phase of deformation related to nappe imbrication, associated with the development of a first penetrative cleavage also migrates towards the foreland. The same applies to the activity of the major thrusts: The Penninic Basal Thrust is followed by the Glarus Thrust and finally by thrusting within the Subalpine Molasse.
3. Thrusting along the Glarus thrust is preceded by early décollement of exotic strip sheets of S-Helvetic and Penninic origin during the Pizol phase. This Pizol phase is not associated with cleavage formation but is, in case of the Helvetic nappes, contemporaneous with the closing stages of Ferrera phase deformation and thrusting along the Penninic Basal Thrust. Similarly, the Ferrera phase deformation and associated thrusting follows earlier phases of detachment and imbrication within more internal units (Sorreda phase of the Adula nappe, Avers phase).
4. Metamorphic isograds drawn across the Penninic-Helvetic tectonic boundary (between cover of the Gotthard massiv and N-Penninic Bündnerschiefer) must be heterochronous. Peak temperatures were reached in the Suretta and Tambo nappes at around 40–35 Ma. This predates the peak temperatures inferred for the Gotthard massif and the Helvetic nappes at 35–30 Ma.
5. Lepontine equilibration at moderate pressures in the Adula, Tambo and Suretta nappes immediately follows and is intimately related to a high pressure event of Tertiary age. This is not the case with respect to the Gotthard region, where indications of an earlier pressure dominated stage are missing.
6. Cooling due to exhumation started relatively early (around 35 Ma) in the Eastern Lepontine units. This exhumation is locally associated with E–W extension (Niemet-Beverin and Forcola phases), but contemporaneous with ongoing N–S to NW–SE compression in the external zones, and differential uplift of the Bergell region related to backthrusting along the Insubric line.

14.3.3 Kinematic evolution

The following synthesis of the kinematic evolution also makes use of data provided in other chapters of this volume in order to arrive at a more synthetic view. This particularly concerns the geophysical infomation on the present day deep structure of the Alps contained in Figure 14-21g (compare Chapters 9 and 22) and geological data on the northern (see Chapter 13.1) as well as the southern (see Chapter 15) foreland of the Alps. On the other hand, this following discussion forms an important basis for Chapter 22, where some of the features discussed here will be further discussed with the help of

an integrated present day cross section of the eastern transect, forming the base of the sketch presented in Figure 14-21g. Some overlap between the present discussion and Chapter 22 could not be avoided and we recommend the reader to also consult parts of Chapter 22 while reading this discussion of the kinematic evolution (in particular the integrated cross section, Plate 22-1).

Any attempt to sketch different stages of the kinematic evolution, such as the one proposed in Figure 14-21, is of course highly speculative. Nevertheless, construction of these sketches respects constraints, including all the uncertainties, which evolve from the previous discussions. In fact many constraints turned out to be more severe than anticipated during preparation of the sketches. On the other hand retrodeformation needs to be performed more rigorously in the future. Figure 14-21 only represents a first attempt. The most important guidelines and constraints need to be briefly outlined: The stages a,b and c in Figure 14-21 are constructed on the basis of the palinspastic restoration as given in Figures 14-8 and 14-9 and propose stages of convergence leading to final collision in the Late Eocene arrived at by forward modelling. Stages d, e, f and g in Figure 14-21, on the other hand, represent stages obtained by backwards modelling based on the present day profile along the NRP 20 Eeastern Traverse (Figure 14-21g) integrating geological and geophysical evidence further discussed in chapter 22. These last stages represent the result of successive retrodeformation of post-collisional deformation stages. All profiles are scaled and area-balanced in a semi-quantitative way. The area occupied by the Avers Bündnerschiefer has been enlarged for the stages represented in Figures 14-21a,b,c,d in order to take account for out of profile movements associated with E-W extension related to the Turba mylonite zone. The depth of several tectonic units (e.g. Aar massif, Suretta nappe, Bergell intrusion) respects data on the P-T-t evolution discussed previously, and, in the case of the Bergell intrusion, data found in Rosenberg et al. (1994 & 1995) Reusser (1987), von Blanckenburg (1992) and in Giger & Hurford (1989). The position of the Helvetic foreland in respect to the Insubric line in Figures 14-21e,f is based on the curvimetric retrodeformation of the present-day N–S-extension of the orogenic lid (Austroalpine units), which was only insignificantly strained during Tertiary deformation.

14.3.3.1 The Avers phase (Early Paleocene, Figure 14-21a)

The exact timing of the Avers phase is ill-constrained. The Early Paleocene was chosen for dating the sketch of Figure 14-21a because the Avers phase must substantially predate the final closure of the Valais ocean during Early to Middle Eocene times. Given the total width of the Briançonnais domain (about 115 km, Figure 14-8) and a minimum width of the oceanic part of the N-Penninic domain (only 50 km of oceanic lithosphere were chosen in Figure 14-21a), any time later than 65 Ma for the onset of subduction of the Briançonnais domain would lead to unrealistically high convergence rates when compared to large scale plate reconstructions (e.g. Dewey et al. 1989).

The parts of the Avers Bündnerschiefer still preserved in a present-day cross section are interpreted to represent the frontal shallow parts of an accretionary wedge which is going to be underplated by the Briançonnais units during the Avers phase. The upper plate is represented by the Austroalpine units and the previously sutured Platta and Lizun-Forno-Malenco ophiolites. The future decollement horizons within the Briançonnais platform, related to the initial stages of the Ferrera phase, are sketched according to Figure 14-8.

14.3.3.2 Subduction of the Briançonnais unit (Early Eocene, Figure 14-21b)

This sketch represents early stages of the Ferrera phase deformation affecting the Tambo, Suretta and Schams nappes, as well as parts of the N-Penninic Bündnerschiefer. The part of the N-Penninic realm which is characterized by oceanic lithosphere has already been closed. However, marine sedimentation continues in those parts of the N-Penninic Valais domain (Arblatsch and Prättigau flysch), which are underlain by continental lithosphere. Alternatively, the Eocene flysches may be assumed to have been deposited on parts of the N-Penninic realm characterized by oceanic lithosphere. In this case a wider N-Penninic oceanic lithosphere (more than the 50 km assumed) would not have closed yet at the stage depicted in Figure 14-21b. However, in this alternative case the convergence rate between the stages depicted in Figure 14-21 b and c would have to be very high (more than 1.5 cm per year).

Peak pressures in the Suretta-Tambo pair are assumed to have been reached by Early Eocene times in order to allow enough time for the subsequent subduction of the Adula unit, placed at the southern distal continental margin of Europe still during the early stages of the Ferrera phase, i.e. during the Early Eocene. Even so, the rate of convergence during Eocene times must have been relatively high and in the order of 1.5 cm per year in order to allow subduction of some 150 km of lithosphere necessary to arrive from the stage depicted in Figure 14-21b to that of Figure 14-21c (compare the relative positions of the 2 reference points marked "a" and "b" in the profiles).

As proposed in Figure 14-8, large parts of the continental crust of the Briançonnais will be subducted during this stage without subsequent exhumation. Southern parts of the N-Penninic Bündnerschiefer, the Schams nappes and the Tambo-Suretta pair have been accreted to the orogenic lid. Hence nappe formation during this and subsequent stages of the Ferrera phase is interpreted to be related to accretionary processes at great depth. This would explain the contemporaneity of decollement and isoclinal folding so typical for the Ferrera phase.

14.3.3.3 Subduction of the Adula nappe (Late Eocene, Figure 14-21c)

Compared to the Briançonnais units, deformation and high pressure metamorphism must be younger in age in the case of the Adula nappe if the palinspastic scenario depicted in Figure 14-21a and Figure 14-9, postulating a N-Penninic ocean between Briançonnais and Adula unit, is correct. Heterochroneity in regard to the onset of Ferrera phase and Zapport phase deformation and high pressure metamorphism in regard to Briançonnais and Adula units (Figure 14-20) is primarily a corrolary of the paleogeographic and tectonic reconstruction and is still ill-constrained by the geochronological constraints discussed earlier.

Figure 14-21c depicts the Adula nappe at its position corresponding to the peak pressures as determined for its northernmost part (11.5 kb) and at Alpi Arami in the southernmost part (27 kb in the Cima Lunga unit, corresponding to the southernmost Adula nappe) as given by Heinrich (1986). The total length of the Adula nappe would be about 85 km at the particular ill-constrained subduction angle chosen in Figure 14-21c. This figure is not unrealistically high when compared to the present day N-S extension of the Adula nappe: 45km in map view, about 60 km in profile view due to backfolding and steepening into the southern steep belt (see profile in Figure 14-2).

Unfortunately, there still is no adequate model available in order to explain the subsequent early phases of exhumation which bring the Adula unit back to more moderate pressures of typically around 6–8 kb, prevailing during equilibration at the temperature dominated so-called Lepontine stage reached at around 35 Ma (see Figure 14-20 and the next stage represented in Figure 14-21d). This exhumation is very rapid since it occurs over a time span of only 5 Ma. This pressure drop corresponds to uplift rates between 3 and 14 mm per year for a pressure drop from 11.5 and 27 kb, respectively.

A corner flow model such as proposed by Cowan & Silling (1978) and Cloos (1982) would be unlikely to have preserved the very substantial and systematic pressure gradient as presently observed from N to S within the eclogites of the Adula nappe. The widely accepted extensional model proposed by Platt (1986) is only applicable for parts of the later stages of exhumation, related to the Niemet-Beverin and Forcola phases, when E–W extension does occur. The rise of a delaminated rock pile as a buoyant sheet along the shear zone formed by the proces of subduction, representing a zone of greatest weakness, was recently proposed by von Blanckenburg & Davies (1995) for the case of the Central Alps. This model meets with difficulties because the Adula nappe is not surrounded by high-density mantle rocks according to the reconstruction given in Figure 14-21c. A mechanism of forced extrusion parallel to the subduction shear zone (arrow in Figure 14-21c) seems to be the most likely mechanism. Such a mechanism was recently proposed for the Western Alps (Michard et al. 1993). This mechanism is analogous to the subsequent differential movement of the Tambo-Suretta pair, as postulated during the subsequent Niemet-Beverin phase by Merle & Guillier (1989) and Schmid et al. (1990).

Unfortunately, such a model of forced extrusion is not supported by the field data. Kinematic indicators at the base and top of the Adula nappe suggest top to the N movement, while top to the S movement sense would be expected at the top of the Adula nappe according to this model. However, the top to the N movements reported to have been active during the late stages of the Zapport phase (D2b of Meyre & Puschnig 1993, Partzsch et al. 1994) in the structurally higher parts of the Adula nappe are likely to have overprinted earlier top to the S movements. These late stages of the Zapport phase are considered to be contemporaneous with the Niemet-Beverin phase (Figure 14-20), when top N thrusting of the Tambo-Suretta pair over the previously exhumed Adula nappe did occur (between the two stages represented in Figures 14-21d and 14-21e, as discussed below).

14.3.3.4 The final nappe stack (Earliest Oligocene, Figure 14-21d)

The scenario depicted in Figure 14-21d is arrived at by retrodeformation of the Niemet-Beverin phase as proposed by Schreurs (1990, 1993). The marked southerly dip of the Penninic nappes depicted in Figure 14-21c must have been preserved until the Eocene-Oligocene boundary in order to allow for backfolding of the units in the upper limb of the Niemet-Beverin axial plane. Top to the N to NW shearing of the Tambo-Suretta pair in respect to the underlying Adula unit (Schmid et al. 1990) during the subsequent Niemet-Beverin phase results in a more southerly position of the Tambo-Suretta front in respect to the front of the previously exhumed Adula nappe in Figure 14-21d when compared to Figure 14-21e.

14.3.3.5 Nappe refolding and vertical thinning (Oligocene, Figure 14-22e)

The kinematic model based on the work of Merle & Guilier (1989) regarding megafold formation associated with the inversion of a Ferrera phase nappe stack over a N–S distance of some 40 km in the hangingwall of the Niemet-Beverin axial trace has been extensively discussed earlier and in Schmid et al. 1990 and Schreurs (1993). This model implies relatively slow differential movement of those parts of the deforming Penninic units which were in close contact to the Austroalpine orogenic lid during overall NW to NNW transport of the Tambo-Suretta pair. Hence backfolding in the Suretta nappe is only apparent and not related to backthrusting of the orogenic lid in respect to some fixed point of reference in the lower crust. Differential NW to NNW-directed flow of the Tambo-Suretta pair in respect to the underlying Adula nappe occurred contemporaneously. The intense Niemet-Beverin phase overprint in the Misox zone and top to the N shearing during the closing stages of the Zapport phase in the Adula nappe are related to this differential movement of the Tambo-Suretta pair.

However, the relative velocity profile proposed by Schmid et al. (1990) has to be modified for the effects of simultaneous vertical shortening during the closing stages of the Niemet-Beverin phase. As pointed out correctly by Schreurs (1993) the plane strain heterogeneous simple shear model proposed by Schmid et al. (1990) cannot adequately explain shortening of the Schams units in front of the Tambo nappe. Simultaneous vertical shortening, however, may easily place the originally S-dipping Schams nappes into the shortening field of an oblate strain ellipsoid.

On the large scale depicted in Figure 14-21e, one of the major effects of the Niemet-Beverin phase concerns the relative uplift of the southern Penninic units which leads to the subhorizontal attitude of the Ferrera phase nappe stack in Figure 14-21e. In Figure 14-21e the Lombardic Southern Alps of the present-day profile (Figure 14-21g) are replaced by the Ivrea cross section after Zingg et al. (1990) in order to account for retrodeformation of some 50 km dextral strike slip motion along the Insubric line after Early Oligocene times (Schmid et al. 1989). The southern steep belt (and consequently a precursor of the present-day Insubric line) must have already existed during the intrusion of the Bergell pluton, as indicated by intrusive relationships found in the lower Val Masino (Rosenberg et al. 1994 & 1995). Hence this tilting of the Penninic units into a subhorizontal attitude is intimately related to early stages of movement along a precursor of the Insubric line and final emplacement of the Bergell intrusion.

The final stages of the Niemet-Beverin phase overlap with the final emplacement of the Bergell tonalite, but predate the intrusion of the Bergell granodiorite. The ascent of the Bergell pluton along a pre-existing Insubric line is facilitated by the overall relative uplift of the entire southern Penninic zone with respect to the Southern Alps along a pre-existing southern steep belt. Following von Blanckenburg & Davies (1995) we relate the ascent of the Bergell batholith to slab breakoff which results as a consequence of continental collision. It has to be emphasized, however, that final exhumation of the Bergell intrusion from the considerable depth of intrusion indicated in Figure 14-21e, associated with backthrusting along the present-day Insubric mylonite belt (Rosenberg et al. 1994), post-dates the Niemet-Beverin phase. Only the ascent of magma and the final emplacement of the Bergell pluton (except for parts of the granodiorite which intrudes the Turba mylonite zone at the NE corner of the Bergell intrusion) are associated with the Niemet-Beverin phase.

The modelling work of Merle & Guillier (1989) proposes that upwards directed viscous flow in the southern steep belt results in N-directed viscous horizontal flow of the Tambo-Suretta pair and the Schams nappes indicated by nappe refolding. In principle we still regard this model to adequately describe flow during the Niemet-Beverin phase. However, part of this horizontal flow may also be due to vertical shortening. Consequently, upwards directed flow in the southern steep belt may be less dramatic than suggested by these authors.

In the northern part of the section, palinspastic reconstructions (Pfiffner 1986, 1992) suggest that the Helvetic nappes must be considered as being detached from their crystalline substratum (the Lucomagno-Leventina and Gotthard nappes) at this time. The latter was internally shortened, leading to the detachment of the allochthonous Gotthard "massif". Some 200 km of European crust must have been subducted below the higher Penninic units and the orogenic lid by this time. This distance is measured between points "b" and "c" in Figure 14-21 b and c, a distance which needs to be subducted in order to have the Adula nappe at its depth required for eclogite facies metamorphism. Together with the previously subducted parts of the Briançonnais domain this length is compatible with an absolute minimal length of 200 km inferred to have been subducted until present into the lithosperic mantle beneath the Southern Alps by Pfiffner (1992) and Stampfli (1993).

14.3.3.6 Final exhumation of the Southern Penninic (Early Miocene, Figure 14-21f)

Comparing Figures 14-21e and 14-21f illustrates the effects of the Late Oligocene Domleschg phase because the effects of the Forcola phase (installment of an axial plunge and E-W extension) are not visible in a N-S section. Insubric backthrusting along the Insubric mylonite belt sets in immediately after the Niemet-Beverin phase and results in amazingly rapid exhumation and erosion of the deep-seated parts of the Bergell intrusion (Giger & Hurford 1989). In fact, exhumation of the southern Penninic region may be seen as a continuous process between the stages represented in Figure 14-21d and 14-21f. Tilting of the southern Penninic nappes continues and results in the presently observed northerly dip.

Oblique block rotation along the Engadine line (Schmid & Froitzheim 1993) results in differential uplift of the Bergell region also in respect to Penninic and Austroalpine units N of the Engadine line. The activity of the Engadine line certainly postdates the Late Oligocene Domleschg phase but is likely to be Early Miocene in age and contemporaneous with dextral strike slip movement along the Insubric line (see discussion in Schmid & Froitzheim 1993).

N–S shortening during the Domleschg phase is rather moderate across the Penninic and Austroalpine units. Major components of N–S shortening are now taken up by the Helvetic foreland where the Glarus thrust accommodates some 25 km displacement between the stages represented in Figures 14-21e and 14-21f (Pfiffner 1986). Thus, as pointed out by Pfiffner (1985), a major part of the deformation in the Helvetic foreland is contemporaneous with backthrusting along the Insubric line. In the footwall of the moving Helvetic nappes the upper crust is involved in shortening, as evident from the initiation of bulging in the Aar massif. This deformation eventually leads to a broad antiformal structure depicted by the Austroalpine orogenic lid. Effects of Late Oligocene to Early Miocene shortening in the Southern Alps, in contrast, are rather moderate or even absent according to Schönborn (1992).

14.3.3.7 Lower crustal wedging (Middle and Late Miocene, Figure 14-22g)

It is interesting to note that this spectacular event, profoundly shaping the deep structure of the Alps as revealed by geophysical work, left little trace of internal deformation in the transect of the Alps of eastern Switzerland. Roughly speaking, the Central Alps float as an undeformed area above S and N dipping deformation zones confined to the northern and southern Alpine foreland, similar to a pop-up structure. However, the Central Alps were subjected to differential uplift in the order of 10 km during this time interval.

Shortening within the Aar massif in the eastern transect amounts to about 27 km, but is higher in the transect of central Switzerland. This uplift and shortening progressed from east to west as discussed in Chapter 13.1. During the Miocene time interval considered here, shortening concentrated mainly to the west, i.e. in the central and western transects. Miocene shortening in the Southern Alps is more substantial and amounts to 56 km in respect to the post-Adamello phase which does not set in before Middle Miocene (Burdigalian) times according to Schönborn (1992).

Contrary to early interpretations of lower crustal wedging (e.g. Bernoulli et al. 1990) this Miocene phase clearly postdates Insubric backthrusting and strike slip motions, as already proposed by Laubscher (1990) and confirmed by Schönborn (1992). Hence, it is not admissible to kinematically link the lower crustal wedge with backthrusting along the Insubric line. Instead, the Insubric line is cut by this lower crustal wedge beneath the Central Alps.

On the other hand, balancing of shortening in the Southern Alps demands excess volume of crustal material below the Central Alps (Pfiffner 1992, Schönborn 1992). This volume cannot be provided by the crustal material below the N-dipping Insubric line alone but has to include the area occupied by the lower crustal wedge. Hence lower crustal wedging and shortening in the Southern Alps are kinematically linked. As a consequence the Insubric line is part of the hangingwall and allochthonous in respect to the major thrusts formed during Miocene-Pliocene shortening in the Southern Alps (Lombardic phase of Laubscher 1990). The exact shape of this wedge, as well as its composition (exclusively lower crustal material vs. "mélange") remains unknown. Figure 14-22g merely presents a possible geometry which is area balanced against Figure 14-22f in terms of Southern Alpine upper and lower crustal material.

Acknowledgements

The reviews by J. Platt and G. Stampfli have been extremely useful for improving a first draft. Both reviewers are thanked for their enormous patience in having worked through a very preliminary form of the manuscript. M. Frey, N. Froitzheim and J. Lihou also helped to improve earlier versions of the manuscript. Conclusions regarding the stratigraphy of the Schams nappes heavily rely on the work of our friend Ph. Rück. We are also thankful to our colleagues in Neuchatel, D. Marquer and T. Baudin, who contributed very much towards a better understanding of the study area and with whom we had many fruitful discussions. G. Schönborn is thanked for interesting information and discussions about the Southern Alps. Much of the conclusions are influenced by ongoing work at the University of Basel in the Adula nappe (C. Meyre and J. Partzsch) and in the Bergell area (A. Berger, C. Davidson, R. Gieré and C. Rosenberg). M. Steinmann, who finished his Ph. D.-work during the writing of this contribution contributed very much towards a better understanding of the Bündnerschiefer. He is thanked for many interesting discussions and for his generosity in providing new data which are essential for the topic of this contribution.

15 Rifting and collision in the Southern Alps

M. E. Schumacher, G. Schönborn, D. Bernoulli & H. P. Laubscher

Contents

15.1 Setting and role of the Southern Alps in the Alpine system

The Southern Alps are a 500 km long and 50 to 150 km wide fold-and-thrust belt forming the southern orogenic wedge of the Alps (Figure 15-1). This overall west-east trending, south-vergent frontal belt is separated from the Western and Central Alps to the west and north by the Canavese line and the Insubric line, respectively. At their eastern end, the Southern Alps interfere with the Dinarides (Cousin 1981, Doglioni & Bosellini 1987, Doglioni and Siorpaes 1990). The southwestern end of the Southern Alps is covered by the young deposits of the Po plain, and their relation with the Western Alps and the Apennines is still controversial (Roure et al. 1990, Castellarin 1992, Piana & Polino 1995, Schumacher & Laubscher 1996). To the south, the frontal half of the South-Alpine wedge is also buried below the Messinian to Plio-Quaternary deposits of the Po plain (Pieri & Groppi 1981). The internal basement part of the Southern Alps represents a transitional area between the central part of the orogenic lid and the southern frontal wedge (Laubscher 1994). In this transitional area various observations point to an Alpine high anchigrade to lower greenschist metamorphism (e. g. illite crystallinity, Cassinis et al. 1978, Schönborn 1992b; growth of stilpnomelane, Crespi et al. 1982) and deformation took place near the brittle-plastic transition for quartz. However, the exposed parts of the Southern Alps were deformed essentially under brittle conditions.

Prior to Alpine deformation the area was part of the Mesozoic passive continental margin on the western and northern side of the Adriatic (Apulian) microplate or African promontory (Biju-Duval et al. 1977, Channell & Horvath 1976, Laubscher & Bernoulli 1977). With convergence between Adria and Europe from the Late Cretaceous to the Recent, polyphase deformation of this margin has resulted in the formation of the Southern Alps and the Austroalpine nappes. The Austroalpine nappes with transport directions to the west and north originate from the northern area of this margin and became mainly part of the central portion of the orogenic lid, whereas the geological units of the frontal, southern wedge, with south-directed thrusting, come from a more southern area (Weissert & Bernoulli 1985).
The overall northwest-directed movement of Adria relative to stable Europe during Alpine orogeny (Dewey et al. 1973, 1989) implies two different kinematic systems: a dextrally transpressive one along the northern boundary of the Adriatic indenter and a sinistrally transpressive one along the western boundary (compare Laubscher 1991). Where both joined, near the northwestern corner of the indenter, their interference resulted in extremely complex structural patterns, as it is the case for the South-Alpine area studied by the NRP 20 reflection seismic program (Schumacher 1990 and Chapter 10).
The Adige embayment and the Giudicarie are a first order transverse zone dividing the Southern Alps into a western and eastern part (Figure 15-1). Our discussion of the structural evolution in the Southern Alps focuses on the western Southern Alps (Figure 15-2) and particularly on the area crossed by the NRP 20 seismic lines between Lago Maggiore and Lago di Como (cf. Figures 15-10 and 15-11).

15.2 Pre-Alpine history

15.2.1 Late Precambrian to Variscan basement evolution

Alpine tectonic structures are clearly defined in the late Palaeozoic and Mesozoic sediments, whereas in the crystalline basement rocks they are superimposed on pre-Alpine, particularly Variscan deformations. For a clearer picture of the purely Alpine deformations these earlier structures ought to be recognized. Inasmuch as the age and tectonic position of important structural features in the crystalline basement rocks, such as the Taverne-, the Tesserete- and other lines as well as the Gneiss Chiari bodies are controversial, a brief discussion of basement evolution is called for.

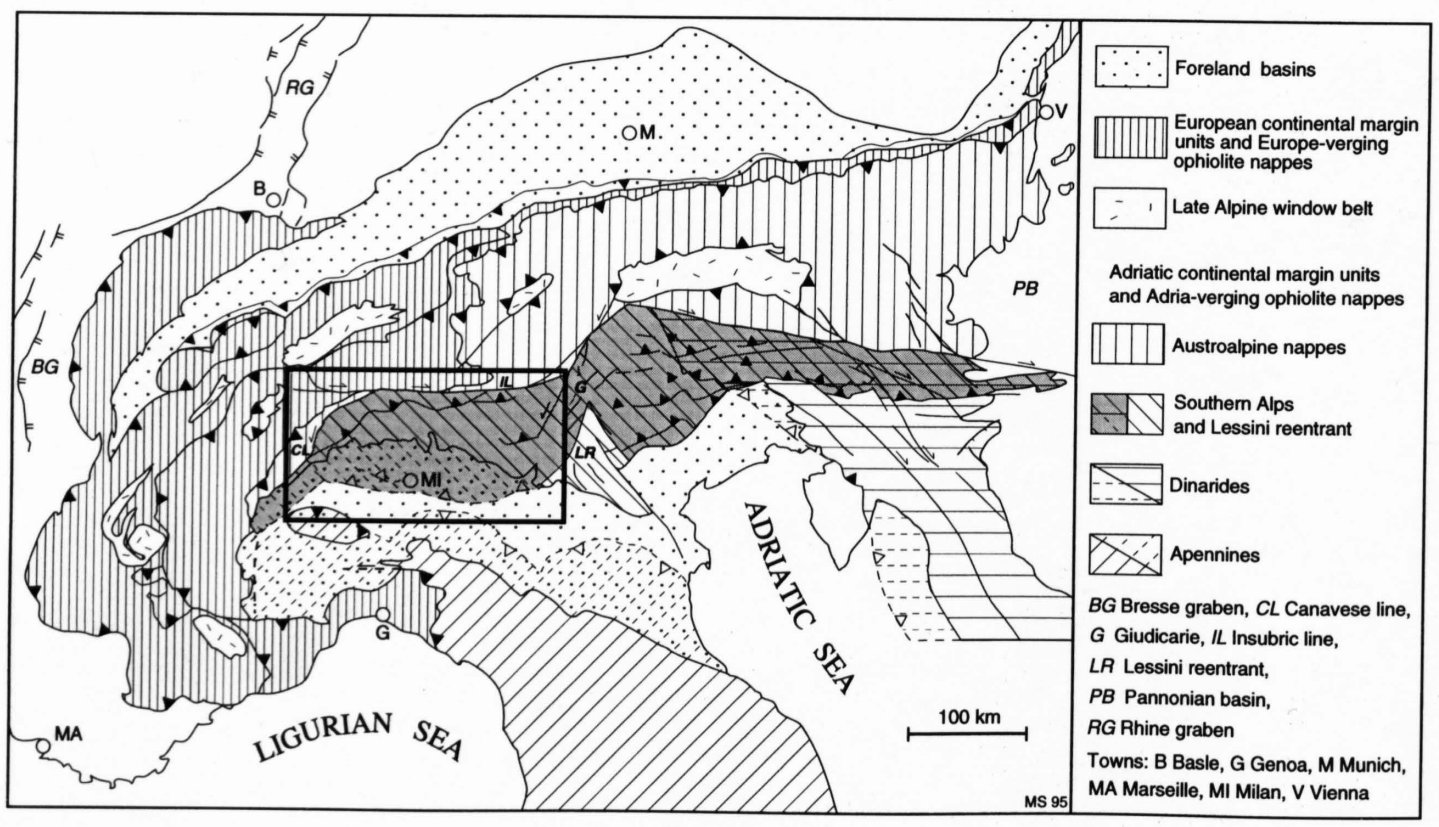

Figure 15-1
Location of the Southern Alps (grey shaded) and Figure 15-2 (rectangle) within the Alpine arc. The present-day Southern Alps form mainly the southern orogenic wedge of the Neogene Alpine system; they are separated by the Giudicarie (G) and the Lessini reentrant (LR) into the western and eastern Southern Alps. The Canavese line to the W and the Insubric line s.s. to the N separate the western Southern Alps from the Western and Central Alps, respectively.

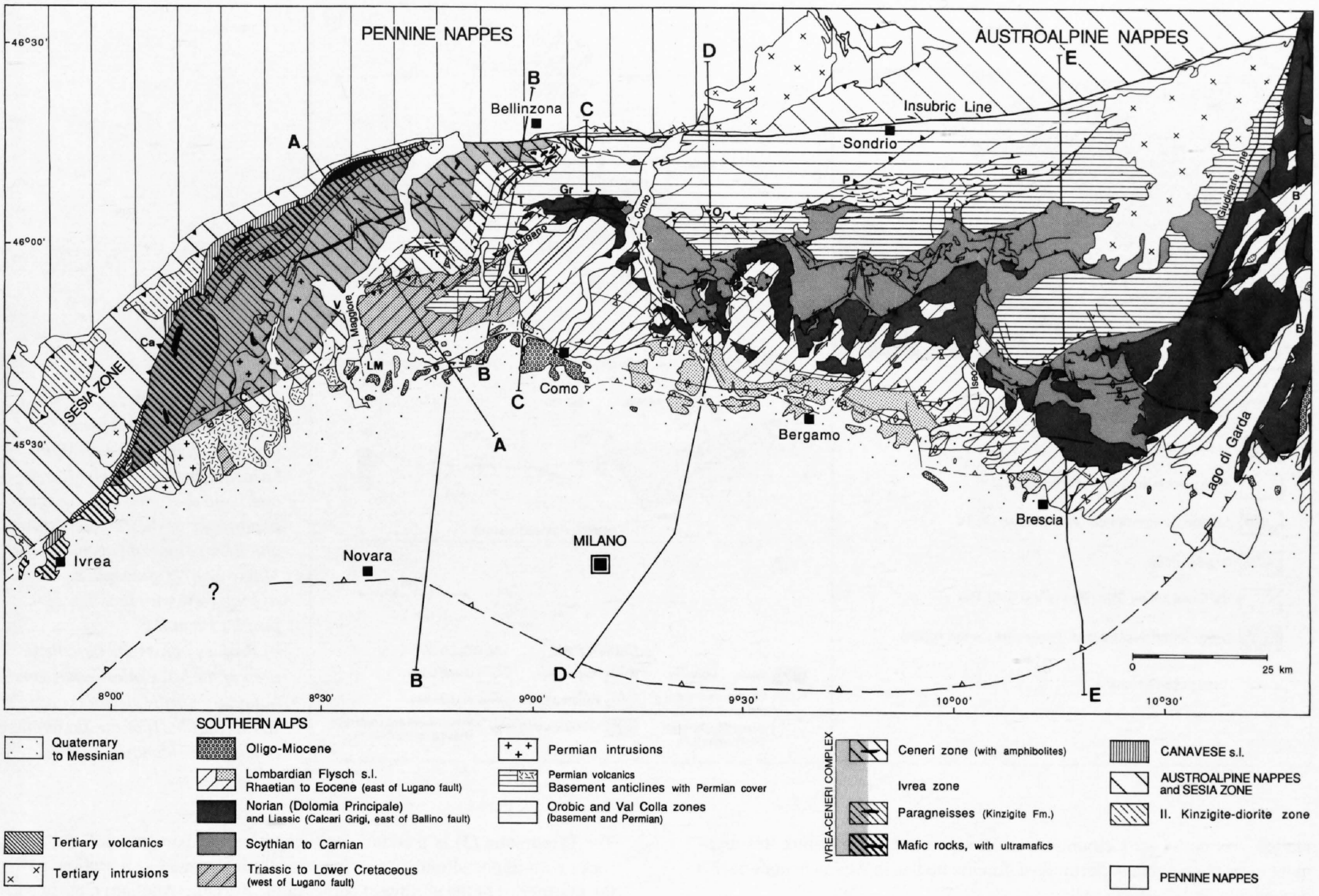

Figure 15-2

Tectonic map of the western Southern Alps with location of cross sections A to E (Figures 7, 9, 13 and 15). The western end of the Southern Alps curves into the arc of the Western Alps, and between Lago Maggiore and Lago di Como the thick-skinned Ivrea-Ceneri complex interferes with the thin-skinned Orobic nappe system. To the south the approximate location of the Middle to Late Miocene front of the Milan belt (Pieri & Groppi 1981) under the Po plain is indicated, except for the westernmost part where the most frontal thrusts may have a Late Oligocene to Early Miocene age (Roure et al. 1990, Schumacher & Laubscher 1996). C: Cremosina line, Ca: Canavese line, Ga: Gallinera line, Gr: Grona line, Le: Lecco line, Lu: Lugano line, LM: Lago Maggiore line, O: Orobic line, P: Porcile line, T: Tesserete line, Tr: Tresa line, V: Verbania line.

In the Southern Alps, a pre-Upper Carboniferous (Variscan), folded basement underlies the Upper Palaeozoic and Mesozoic formations. The post-Variscan, non- or only anchimetamorphic sediments unconformably overly different levels of the Variscan edifice: The metamorphic grade of the rocks underlying the Upper Carboniferous unconformity (Westphalian B/C, Jongmans 1960) increases from east to west, i.e. from deep burial diagenesis and anchimetamorphism in the Carnian Alps to amphibolite grade west of Lago di Lugano (Figure 15-2, e.g. Castellarin & Vai 1981, Vai et al. 1984). This regional metamorphic pattern of Variscan (Early Carboniferous) age in the South-Alpine crystalline basement could suggest a westward transition from the external to internal zones of the Variscan orogen (Vai et al. 1984). Although this seems to be the case, the situation may be more complicated: the deep-crustal rocks of the Ivrea zone are nowhere in direct contact with Upper Palaeozoic sediments; consequently, a large portion of the exhumation process must be the product of Permian to Mesozoic crustal extension and/or Alpine thrusting (Schmid 1993). In any case, the depositional age of the pre-Upper Carboniferous metasediments is still poorly known and some controversy exists about the signatures of earlier, "Caledonian" or Precambrian ("Cadomian") metamorphic events in the South-Alpine basement (e.g. Hunziker & Zingg 1980, Boriani et al. 1985, 1990b).

West of Lago di Como (Figure 15-2) different segments can be distinguished in the Variscan basement of the Southern Alps: (1) an eastern segment, the Val Colla zone, comprising micaschists and phyllites with granitic gneisses (Gneiss Chiari) and subordinate amphibole-bearing gneisses, (2) an intermediate zone, the Strona-Ceneri zone, consisting of various amphibolite facies granitic gneisses, paragneisses and lesser amphibolites and ultramafics which form large-scale folds with subvertical axes (Reinhard 1953) and (3) the high-grade, amphibolite to granulite facies metamorphic rocks of the Ivrea zone, separated from the Strona-Ceneri Zone over a distance of about 12 km by an early Mesozoic low-angle extensional fault, the Pogallo line (Hodges & Fountain 1984, Handy 1987, Handy and Zingg 1991). Elsewhere the Cossato-Mergozzo-Brissago line, a Paleozoic mylonite, forms the boundary between the two zones (Boriani et al. 1990a). However the relations between these two lines, particularly in the NE are unclear.

The rocks of the **Val Colla zone** (1) are metamorphosed under amphibolite and (retrograde?) greenschist conditions. In its eastern continuation, the Orobic Alps, Gansser and Pantic (1988) dated greenschist facies schists and quartz-phyllites by palynomorphs as Ordovician to Silurian. However, Milano et al. (1988) reported also retrograde greenschist facies after amphibolite facies metamorphic conditions in this general area. A typical lithology of this zone are the Gneiss Chiari (Bernardo Gneiss, Reinhard 1953). They invariably occur in a high tectonic position and have been interpreted as metagranites (Reinhard 1953), meta-arkoses (El Tahlawi 1965), migmatites (Liborio & Mottana 1971, Köppel & Grünenfelder 1971) or meta-rhyolites (Boriani & Colombo 1979). They yield highly discordant zircon ages ranging from 140 to 580 Ma which suggest a minimum crystallization age of 300 Ma but defy a more precise interpretation due to inheritant heterogeneities of the mineral substance (Köppel & Grünenfelder 1971).

Reinhard (1953) considered the Gneiss Chiari to form a Variscan nappe as there is no intrusive contact. So far there is no plausible alternative explanation for their position on top of the metasediments. As the Gneiss Chiari are covered with a stratigraphic contact by Upper Permian Verrucano, a pre-Late Permian age is documented for their emplacement; more specifically the occurrence of pebbles of Gneiss Chiari in the Upper Carboniferous Manno Conglomerate (Reinhard 1953) would seem to point to a pre-Late Carboniferous age. This age is in agreement with the general characteristics of Variscan tectonics in western Europe where shortening with nappe formation is found in the "Asturian phase", whereas tectonics from the Late Westphalian on is dominated by dextral transtension and transpression (Arthaud & Matte 1977). This view is in contrast with that of Reinhard (1953) who had observed apparently undeformed Gneiss Chiari in the pebbles of the Upper Carboniferous Manno Conglomerate and therefore concluded that their defor-

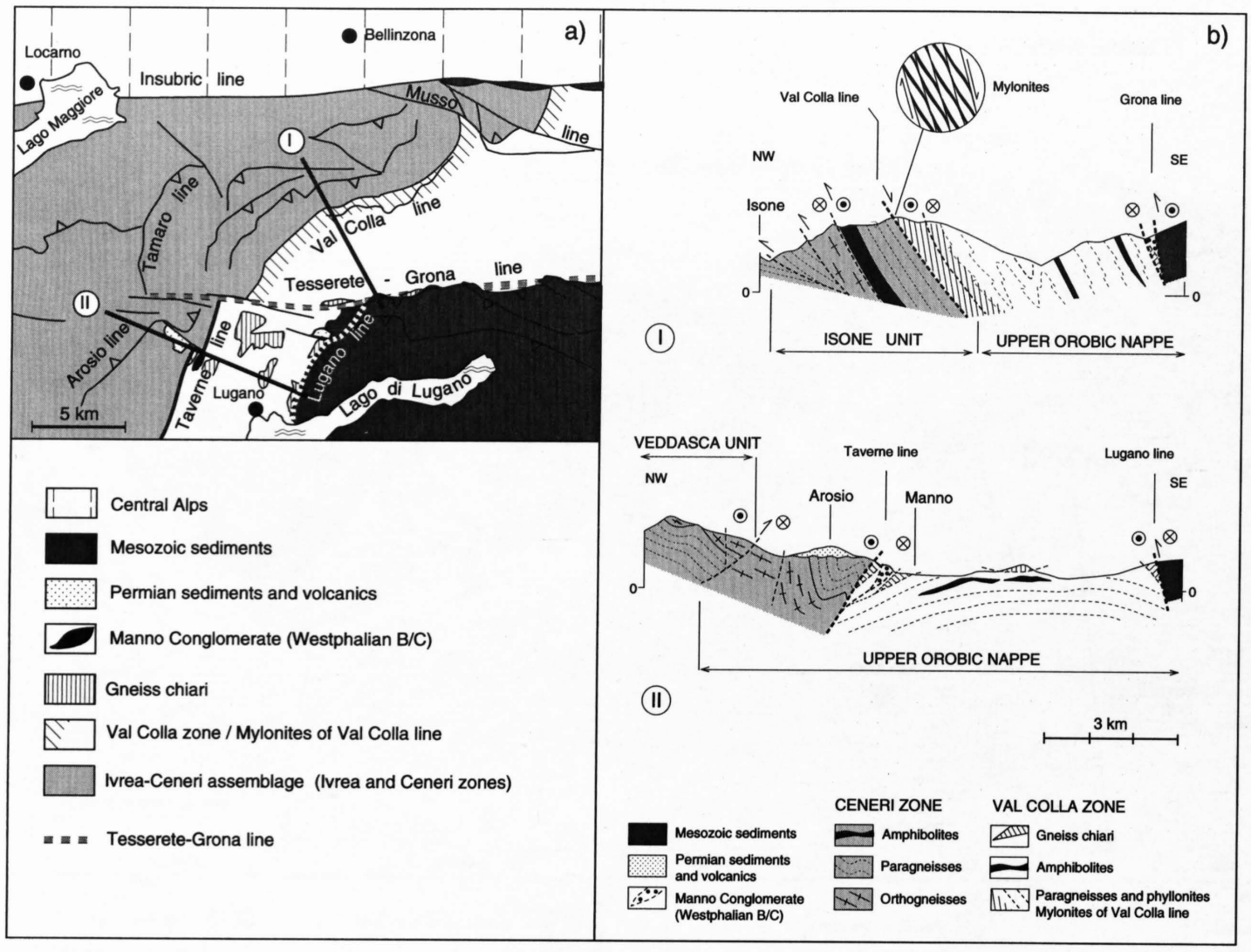

Figure 15-3
The boundary between the Val Colla and the Ceneri zones as a key horizon in the South-Alpine basement between Lago Maggiore and Lago di Como, indicating the importance of the Tesserete line and dextral movements along the Musso line (cf. Schumacher 1990).
a) Map view with location of profiles I and II.
b) Profiles across the basement area of the Val Colla/Ceneri zone boundary north (profile I) and south (profile II) of the Tesserete line, after Schumacher 1994a.

mation was post-Late Carboniferous. However, we do not think this argument to be cogent: many portions of granitic bodies in Alpine nappes have a deceptively undeformed aspect.

Another basement feature that has aroused considerable interest in the past is the up to one kilometer thick greenschist facies mylonite belt of the Val Colla line that locally separates the Val Colla zone from the Strona Ceneri zone to the northwest (Figures 15-2, 15-3; Reinhard 1953, 1964). It dips with up to 60° to the southeast, and sense-of-shear observations characterize it in its present position as an extensional, normal fault. In the Val Colla zone, a crude correlation of the metamorphic conditions indicated by the synkinematic mineral assemblages of the Val Colla fault zone with the radiometric ages from adjacent samples (K-Ar biotite ages of 314, 315, and 317 Ma! [McDowell, 1970], recalculated using the new constants given by Steiger and Jäger 1977) suggest a late Palaeozoic activity of this fault (Bernoulli et al. 1990b). According to scant fission track ages (Hunziker et al. 1992) it would appear to be pre-Alpine. Reinhard (1953) connected this mylonite belt with his Taverne-Caslano line (Figure 15-3). However, as the latter is characterized by brittle deformation and contains imbricates of the non-metamorphic Upper Carboniferous Manno Conglomerate, we consider the Taverne Line to be either a Permian or even an Alpine fault separating two Alpine basement units (Figure 15-3). Inasmuch as remainders of Permo-Triassic sediments on the two sides of the fault do not appear to be displaced much vertically, an Early Permian age seems most probable, although reactivation by important Alpine strike-slip motions would fit the regional frame.

In the **Strona-Ceneri zone** (2) most U-Pb zircon ages of orthogneisses are closely concordant or concordant and are between 440 and 460 Ma. Discordant U-Pb zircon ages show a lower intercept between 400–500 Ma (Pidgeon et al. 1970, Köppel & Grünenfelder 1971). A similar age is given by two Rb-Sr whole rock isochrons of 478 ± 20 Ma and 466 ± 5 Ma for paragneisses of the Ivrea zone (Hunziker & Zingg 1980) and orthogneisses of the Strona Ceneri Zone (Boriani et al. 1982/83), respectively. Based on the 478 Ma Rb-Sr isochron of Ivrea paragneisses and on a concordant U-Pb monazite age of 450 Ma from a paragneiss of the Strona-Ceneri zone (Köppel & Grünenfelder 1971), Hunziker & Zingg (1980) proposed an Ordovician age for the peak of the regional amphibolite-grade metamorphism, whereas Boriani et al. (1982/83, 1985) attribute the 400–500 Ma ages to Ordovician magmatic activity and associated contact metamorphism. However, the clustering of radiometric signatures between 400–500 Ma, concordant U-Pb zircon ages (455±5 Ma, Ragettli 1993) and the mentioned U-Pb monazite age which were not obliterated during later Variscan metamorphism argue for an important magmatic/metamorphic event around 450 Ma. K-Ar cooling ages of biotites are in part Carboniferous (McDowell 1970); in the deeper crustal layers they are significantly younger and related to cooling following Mesozoic extension and uplift (Handy & Zingg 1991).

The **Ivrea zone** (3) is predominantly composed of paragneisses and mafic rocks with minor ultramafics. It is generally interpreted as a section across the lower crust of the northwest corner of the Adriatic (Apulian) plate or subplate. A wealth of radiometric data (compiled by Zingg et al. 1990, see also Gebauer et al. 1992, Voshage et al. 1990) suggests a complex history of late Palaeozoic and possibly older high-grade metamorphic processes which during their latest, Permian, phases appear to have been connected with extension (Brodie & Rutter 1987, Brodie et al. 1989) and "magmatic underplating" by the mafic rocks (Voshage et al. 1990, Gebauer et al. 1992, Quick et al. 1994). K-Ar ages on biotite clustering around 180 Ma (Hunziker & Zingg 1980) suggest cooling during and following extension in early Mesozoic times (Handy 1987, Schmid et al. 1987, Handy & Zingg 1991). The very occurrence of part of these micas points to the ascent of mantle material in the Late Triassic to Early/Middle Jurassic rifting stage of Tethys opening. This is also suggested by concordant (204 ± 4 Ma) and slightly discordant (207± 5 Ma) U-Pb ages on zircon from a chromitite of the Finero phlogopite-peridotite (von Quadt et al. 1993). These ages are interpreted as crystallization ages during K-metasomatism and crystallization of phlogopite, zircon and chromite accompanying the generation of fluids and probably also partial melting during extension and uplift during the latest Triassic to Early Jurassic (von Quadt et al. 1993).

Variscan metamorphism in the Val Colla zone and its eastern continuation (cf. Gansser & Pantic 1988) obviously does not exclude older metamorphism in part of it or in the Ivrea and Strona-Ceneri zones. For the western Southern Alps, Schmid (1993) proposed a scenario which includes (1) pre-Ordovician, Late Proterozoic or Early Palaeozoic accretion and underplating of sediments and slivers of oceanic crust and lithosphere (mafics of oceanic origin, amphibolites with high-P relics, peridotite lenses) along an active margin; (2) High-T metamorphism, anatexis and the emplacement of Ordovician granites; (3) Variscan deformation at deeper crustal levels, inferred from the pervasive deformational overprint of the various unit assembled in pre-Ordovician times and from the deformation of the Ordovician granites, followed by uplift and cooling at 325–310 Ma. Uplift and erosion must predate the Permian magmatic and metamorphic events, as the Upper Carboniferous/lowermost Permian sediments directly overly amphibolite grade Variscan metamorphic rocks. The basement of the western Southern Alps, including the Val Colla zone, could therefore consist of (1) an older accretionary complex comprising Proterozoic metasediments (detrital zircons of 600 Ma, Grünenfelder et al. 1984) and oceanic metavolcanics (Buletti 1983), which underwent high temperature metamorphism and intrusion by granitic melts during the Ordovician and (2) younger, middle Palaeozoic sediments (occuring mainly to the east) that underwent Variscan metamorphism of greenschist to amphibolite grade. At the end of the Variscan orogeny, the crustal thickness appears to have reequilibrated to normal crustal thickness (Schmid 1993).

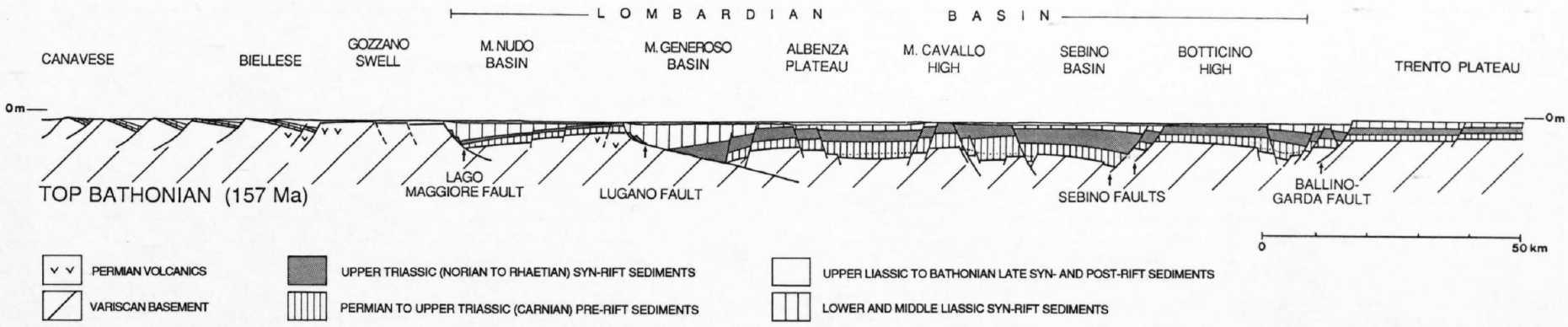

Figure 15-4
Palinspastic profile across the passive continental margin of the Southern Alps during Late Bathonian time, from Bertotti et al. (1993a). Horizontal scale = vertical scale.

15.2.2 Permo-Triassic extension

Amphibolite-grade metamorphic mineral assemblages in the Variscan basement of the Lago di Como transect document extremely low-p, high-T metamorphism as it is characteristic for extensional areas with a high heat flow (Lardeaux & Spalla 1991, Bertotti et al. 1993b). The onset and duration of this thermal anomaly cannot be determined precisely because of the large scatter of radiometric data obtained from the area, but K-Ar-muscovite ages clustering around 200 to 230 Ma (Mottana et al. 1985) suggest that cooling of middle crustal layers extended into the Early Mesozoic. However, these ages could equally well be associated with a Late Triassic to Early Jurassic rifting phase. In the lower crust and the crust/mantle transition, Permian extension is suggested by high temperature shear zones of possibly Permian age (Brodie & Rutter 1987, Brodie et al. 1989) and the syntectonic intrusion of gabbros accompanied by partial melting in the lower crust (Bürgi & Klötzli 1990, Gebauer et al. 1992, Quick et al. 1994). Coevally, in the Early Permian, granitic batholiths were emplaced in the middle to upper crust (see discussion in Sinigoi et al. 1994), contemporaneously with the extrusion of rhyolithic, dacitic and andesitic volcanic rocks at the surface (Lugano and Bolzano volcanic complexes). Early Permian graben formation and volcanicity is also documented from the Collio Formation of the Bergamasc Alps (Assereto & Casati 1965) where the Early Permian basin margins appear to strike predominantly WSW to ENE (Dozy 1935b).

The Permian magmatic activity and the thermal anomaly coupled with it have been interpreted in different ways. Several authors have associated them with initial phases of Tethyan rifting (Ferrara & Innocenti 1974, Lardeaux & Spalla 1991); also the Permian extensional basins of the Bergamasc Alps have been viewed in this context (Winterer & Bosellini 1981). In contrast, Stille & Buletti (1987) have interpreted the granitic intrusions and the accompanying volcanicity as related to the subduction of a Variscan ocean originally situated to the north. However, no such large-scale tectonic activity is evident for Permian times in western Europe, and the geochemical signature of the igneous rocks is more likely an inherited signal of older, Variscan subduction (Dixon & Robertson 1993). Finally, a more probable scenario for that time would appear to be that of large-scale dextral shear in western Europe, associated with major transtension and local transpression, as proposed by Arthaud & Matte (1977) and adopted specifically for the Southern Alps by various authors (Massari 1986, Handy & Zingg 1991, Schmid 1993). Such Late Palaeozoic transtension might indeed be the cause for the formation of the Collio troughs and for the volcanic rocks of the Luganese and, at a deeper level, the magmatic activity of the Ivrea and Strona zones. In the Dolomites area to the east, transpression and transtension, associated with volcanic activity, is again documented for the Ladinian-Early Carnian interval (Doglioni 1987). Gabbroic dikes intruded into deep crustal rocks of the Ivrea zone, contemporaneously or later deformed under amphibolite-facies conditions, also yielded a concordant zircon age of 238 Ma (Ladinian, Gebauer & Grünenfelder in Gebauer 1993). For this time, the sediments indicate strong subsidence, combined with local uplift, and the development of a very complex pattern of carbonate platforms and intervening deeper basins (e. g. Bosellini 1984, Brack & Rieber 1993). In the Carnian, a marked sea level fall associated with the input of siliciclastic and volcanic detritus caused the extinction of most of the platforms. The terrigenous and volcaniclastic material is derived from a volcanic and tectonic belt south of the present-day Southern Alps (Brusca et al. 1981). The Ladinian-Carnian event is interpreted by Stampfli et al. (1991) as related to rifting of the Hallstatt-Meliata ocean located east of the Adriatic plate.

15.2.3 Late Triassic-Early Jurassic rifting and continental margin evolution

Whatever the nature of the Permian and Middle Triassic events, they seem not to be directly related to the Late Triassic-Early Jurassic rifting events that preceded the opening of the Jurassic-Early Cretaceous Tethyan ocean; they must, however, have affected the crustal structure of the Southern Alps. Unfortunately, radiometric data are in general not accurate enough to distinguish between post-Variscan transtension and Late Triassic/Early Jurassic rift-related extension.

Whereas Middle Triassic tectonic movements in the western Southern Alps can only be surmised from changes in facies and formational thicknesses, elements of the geometry of Late Triassic-Early Jurassic rifting are observable in places (Bernoulli 1964, Bertotti 1991). During this time, the major provinces of the evolving South-Alpine continental margin (Figure 15-4), from E to W, Friuli platform, Belluno Basin, Trento Plateau, Lombardian Basin and the distal margin west of Lago Maggiore and in the Canavese zone, came into existence (Aubouin 1963, Bosellini 1973, Bernoulli et al. 1979, Winterer & Bosellini 1981). Figure 15-5 shows the palinspastic position of established or presumed Norian to Liassic faults in the Lombardian basin.

In the Norian, normal faulting affected the extensive Hauptdolomite platform covering the entire area of the Southern Alps (Jadoul 1985, Bertotti 1991). Extension was accommodated by numerous faults of different amount of displacement and orientation (Bertotti 1991). As a consequence of normal faulting, one to some ten kilometer wide morphological basins developed in which thick sequences of fault-related coarse resediments and fine-grained limestones and dolomites were deposited (Zorzino Formation). The shape and orientation of these basins (Figure 4 in Bertotti et al. 1993a) could suggest a left lateral component in their formation. During the Rhaetian, extension continued in the Lombardian Basin, however, because of the high sedimentation rate, the faults had no major morphological expression (Bertotti et al. 1993a).

In the Early Liassic, the number of active faults decreased and strain was gradually concentrated along a few major crustal faults defining tilted blocks some 30 to 50 km wide. This tectonic configuration remained more or less constant until the end of the Middle Liassic. In the west, the Monte Nudo basin was limited by the east-dipping Lago Maggiore fault (Figure 15-4). The eastward transition to the elevated part of the block (Arbostora high) is marked by a number of smaller intrabasinal faults. In the east, the Arbostora high was bounded by the Lugano fault which controlled the sedimentation in the adjacent Generoso basin (von Bistram 1903, Bernoulli 1964, Bertotti 1991). Near the Lugano fault, the sediments in the footwall were affected by intense synsedimentary tectonics which caused the development of a polyphase network of fractures and cross-cutting sediment-filled (neptunic) dikes and complex tectono-sedimentary breccias in the brittle Upper Triassic dolomites and limestones (Wiedenmayer 1963). During the Early to Middle Liassic, several kilometers of sediment were deposited in the strongly subsiding basins of M. Nudo and M. Generoso (Bernoulli 1964, Kälin & Trümpy 1977, Bernoulli et al. 1990a). The basinal sediments are hemipelagic spiculitic siliceous limestones which obviously were redeposited by currents, probably of contour or dilute turbidity type. Slumping is ubiquitous and basinal sediments are affected by synsedimentary listric growth faults. At least locally, fault scarps must have been exposed at the sea floor, as olistholiths and coarse lithic breccias occur adjacent to the Liassic faults.

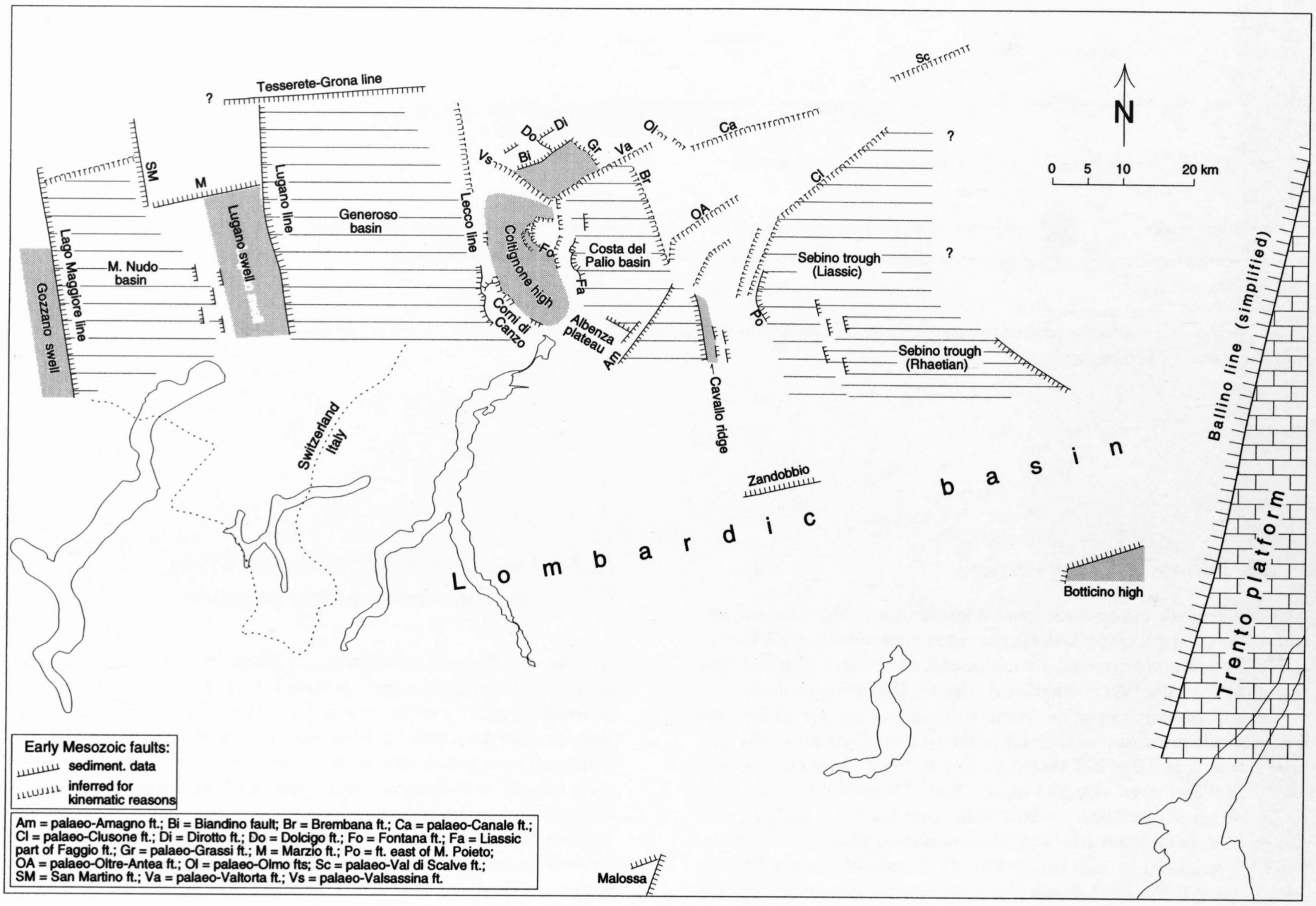

Figure 15-5
Tentative palinspastic map showing the original position of established or presumed Norian to Liassic faults in the Lombardian basin. Faults east of the Generoso basin from Schönborn (1992b), near Malossa after Errico et al. (1980).

As to the geometry of the N–S striking Lugano fault (Figures 15-5 and 15-6), an interesting controversy exists. Its apparent continuation, the E–W striking Monte Grona and Val Grande faults, today are at a right angle to the Lugano fault proper. This has been interpreted by Bertotti (1991) as due to Alpine rotation about the E–W striking axis of the San Marco basement ramp fold (Laubscher 1985) of an originally listric, shallow angle geometry of the Lugano fault (Figure 15-4). Apparent evidence for such an originally listric geometry of the Lugano-Val Grande fault is the depositional geometry of the basinal sediments and the rheology of the fault rocks: Along the shallow (today western) parts of the fault, only cataclasites occur, whereas in the deeper (today eastern) levels mylonites and cataclasites are found. The mylonites are restricted to the footwall in the vicinity of the fault. The overprint of the mylonites, formed under greenschist facies conditions, by cold cataclasites indicates that deformation went on under decreasing temperatures in the footwall (Bertotti 1991). At depth, the fault zone separates two zones of basement with a different Late Palaeozoic-Early Mesozoic cooling history, which means that the two zones have been juxtaposed only after the Triassic (Bertotti et al. 1993b).

This model, however, is not without difficulties when other aspects of the problem are considered. It is particularly the north limb of the postulated folded fault, that ought to be clarified. Assuming an originally flat-lying bottom of the listric Lugano fault at a depth of 10 km, the north limb of the folded fault ought to be found again at a corresponding position, not at the Musso line itself, as conjectured by Bertotti (1990). Possibly quantitative kinematic modeling will help to bring more light to the problem. As it is, consideration of an alternative hypothesis would comply with the postulate of multiple working hypotheses. Such an alternative hypothesis considers the Jurassic part (as separated from Alpine overprinting) of the Grona line as an originally E–W striking sinistral transfer fault zone of considerable importance. Its western continuation may have followed the Tesserete line. Approximately in its eastern continuation, even if not directly connected, are such features as the Valsassina and the Valtorta lines (Schönborn 1992b). The Lugano, the Lecco, the Fontana and other faults (Figure 15-5) end at the sinistral transfer system. In this view, the Tesserete-Grona-Val Grande line was an element of the tremendous sinistral transfer zone that in the Jurassic tore apart Gondwana (e. g. Dewey et al. 1973; Weissert & Bernoulli 1985).

Another geometrical element of the rifting phase may be the Pogallo line, a deep crustal fault zone in the Ivrea-Ceneri-body. The contrasting pre-Liassic cooling histories on both sides are arguments for an early Mesozoic low-angle extensional fault in the middle crust (Hodges & Fountain 1984, Handy 1987, Handy & Zingg 1991). Uplift of deep crustal and upper mantle rocks during the latest Triassic-Early Jurassic interval is also suggested by the crystallization of phlogopite, zircon and chromite from K-rich fluids and probably also from partial melts generated during the ascent of the mantle material mentioned above (von Quadt et al. 1993).

Similar geometries to those described are suggested for other Early Jurassic rift-basins along Tethyan margins. After the Middle Liassic, faulting in the Lombardian basin gradually ceased and the site of extension shifted westward towards the future site of crustal separation, i. e. to the distal margin west of Lago Maggiore and in the Canavese zone (Bernoulli et al. 1990a).

Based on the inferred depositional geometry of the synrift sediments, Bertotti et al. (1993a) estimated a stretching factor of 1.22 for the South-Alpine margin. This factor represents a conservative value; for the thinning of an originally 35 km thick Variscan crust to about 23 km (the thickness of the autochthonous South-Alpine crust near Chiasso; Bernoulli et al. 1990b, Schumacher, Chapter 10) a stretching factor of 1.5 would be required.

During the Middle Jurassic to Early Cretaceous, the area of the Southern Alps sank to a few kilometers water depth, as suggested by the encroachment of deep oceanic facies (radiolarites, Maiolica) onto the distal continental margin in the Lombardian zone. This gradual deepening of the sea reflects the exponential decay of post-rift thermal subsidence (Winterer & Bosellini 1981).

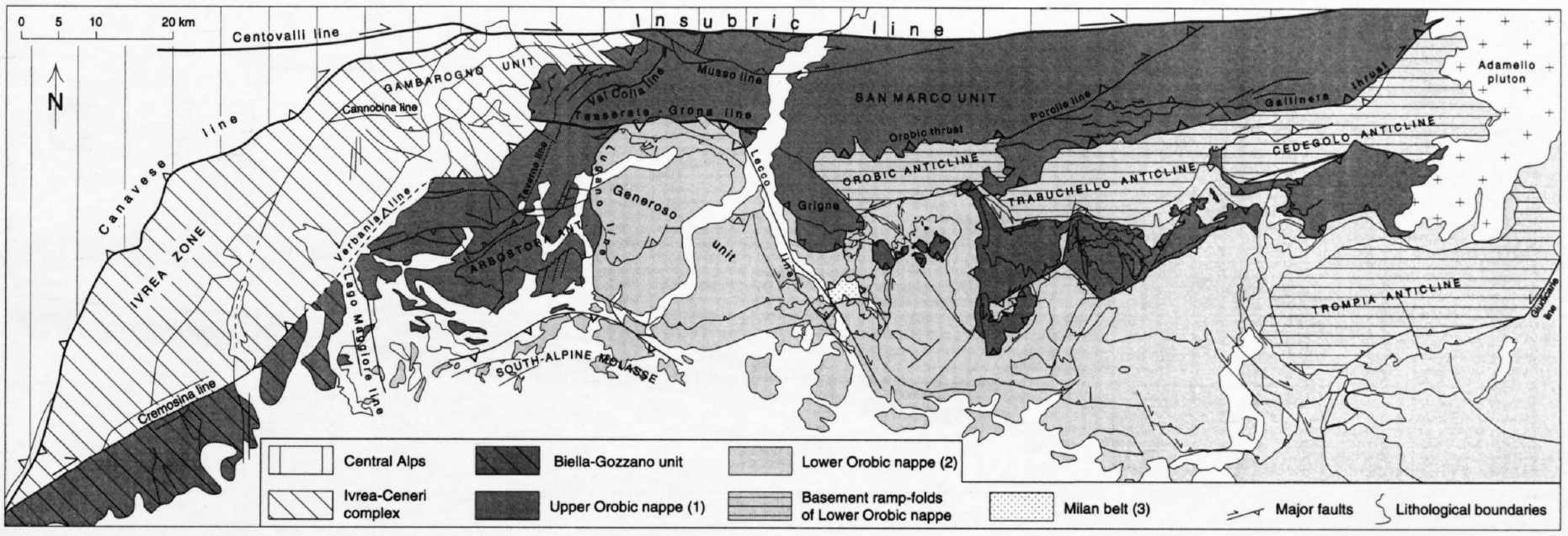

Figure 15-6
Tectonic sketch-map showing the areal distribution of the different thrust sheets and transpressive units of the western Southern Alps.

15.3 Alpine history

15.3.1 Main structural elements and timing in the western Southern Alps

The western Southern Alps between the Giudicarie and Ivrea may be roughly subdivided into 3 segments with different Alpine tectonic structures which comprise different levels of the crust (Figure 15-2): (1) the eastern segment between the Giudicarie and Lago di Como, dominated by Triassic thrust masses in front of ramp folds of pre-Mesozoic rocks; (2) an intermediate segment between Lago di Como and Lago Maggiore, where NE–SW and N–S trending, thick-skinned basement structures interfere with E–W directed thin-skinned ones; and (3) the segment west of Lago Maggiore, where the Southern Alps begin to curve into the arc of the Western Alps and lower crustal and even some upper mantle rocks of the Ivrea body emerge. We use the term "thin-skinned" nappes in the sense that they involve not only sediments but also a few km of the topmost basement, whereas "thick-skinned" units contain rocks of the entire crust. All segments may be further subdivided into domains and units for easier description. The segmentation mainly originates in the Norian to Liassic extensional fault systems (cf. section 15.2.3 and Figures 15-4 and 15-5) that were reactivated during Alpine compression as separating, north-south trending transverse zones (Giudicarie, Lecco, and Lago Maggiore lines in addition to a number of transverse lines, particularly the Lugano line, that compartmentalize the segments internally).

The NRP 20 seismic lines across the Southern Alps are located in the intermediate segment (2), where the structure is particularly difficult to interpret. The intermediate position of this segment in the hinge area between the roughly E–W striking eastern segment (1) and the NE–SW striking western segment (3) requires an approach from both sides. We start with a short description of the segment East of Lago di Como, because here the tectonic structures are better defined and a more precise estimate of shortening is possible than in the western segments. A tentative correlation of the thrust nappes (in the sense of McClay, 1981) of the western Southern Alps across the three segments is given in Figure 15-6.

Of particular importance is the timing problem, as Alpine history south of the Insubric line, according to current information, deviates in important points from that north of the line. In the western Southern Alps there is not much evidence for an important event in the Eocene, when north of the Insubric line the main emplacement of the central Penninic nappes took place. A similar discrepancy is documented for the Late Oligocene-Early Miocene, when north of the Insubric line a compressional uplift of 15–20 km is documented (Hurford 1986), together with the emplacement of the Helvetic nappes, while south of the Insubric line there is evidence for only moderate transpression in the neighborhood of some segments of the Insubric line. Movements farther south are suggested by recycling of synorogenic sediments within the Oligo-Miocene Gonfolite Lombarda Group s. l. (Bernoulli et al. 1989, Gelati et al. 1991). This circumstance makes an integration of the Southern Alps into the kinematics of the Central Alps difficult, and for this reason a special section on timing is added to the detailed discussion of the individual segments of the Southern Alps (see also Chapter 14). It summarizes and completes the information scattered in the discussion of the segments (cf. Figure 15-18). Three phases turned out to be of particular importance: the *Orobic phase* (Late Cretaceous to Early Eocene), the *Insubric phase* (Late Oligocene to Early Miocene) and the *Lombardic phase* (Middle Miocene to Late Miocene). The term phase is defined in this article as a relatively sharply bounded puls of orogenic activity.

15.3.2 The eastern segment (east of Lago di Como)

Overview

The Southern Alps between Lago di Como and Lago di Garda consist of a thrust belt comprising east-west trending zones of basement rocks in the north and zones of sedimentary rocks of increasingly younger age in the south (Figures 15-2, 15-6 and 15-7). Within the thick Triassic deposits, pronounced ramp-flat tectonics developed in function of the stratigraphy: flats in the Upper Scythian (Carniola di Bovegno Formation), Upper Carnian (San Giovanni Bianco Fm) and Lower Rhaetian (Riva di Solto Fm) detachment horizons and ramps in the 1000 to 1500 m thick carbonate layers in between. These carbonate bodies, consisting predominantly of platform carbonates (Ladinian Esino Fm and Norian Dolomia Principale) behaved rather competently during deformation. Thus ramp-folds developed in the Norian layer, the Middle Triassic layer and also in the upper part of the crystalline basement. In the Jurassic and Cretaceous strata, ramp-flat style is less developed, probably because the rheological contrast between the various strata is smaller. Folds are more common and tighter than in the Triassic beds.

Pre-existing Triassic-Jurassic normal faults were reactivated as transverse zones that dissect the thrust belt into compartments with different structure. In particular, those that trend roughly north-south were reactivated as transpressional or transtensional strike-slip zones (lateral ramps), whereas more obliquely trending faults initiated thrust ramps. Across the transverse zones, no direct correlation of individual tectonic structures is possible. However, balanced cross-sections have been constructed with the assistance of the Geosec-20™ software and help in establishing kinematic continuity throughout the various compartments (Figures 15-7 and 15-8, corresponding to sections D and E in Figure 15-2), preserving bedlength and thickness. This would seem reasonable as the thrust sheets did not suffer much internal deformation and folds are commonly of a flexural slip type. The cross-sections are laterally correlatable, retrodeformable for each step of thrusting (Figure 15-8), kinematically admissible (in the sense of Geiser, 1988) and as simple as possible. No thrusts have been drawn in the subsurface whose attendant deformations are not observed at the surface or on seismic sections. For details see Schönborn (1992b).

Two major thrust sheets – the Upper Orobic nappe (1) and Lower Orobic nappe (2) – are well exposed, both composed of a crystalline basement and a sedimentary part. A third sheet crops out in places (see below). It is part of the underlying Milan belt (Figure 15-7 and Schönborn 1992b).

The segment east of Lago di Como may be subdivided into a number of domains in order to facilitate description.

a)

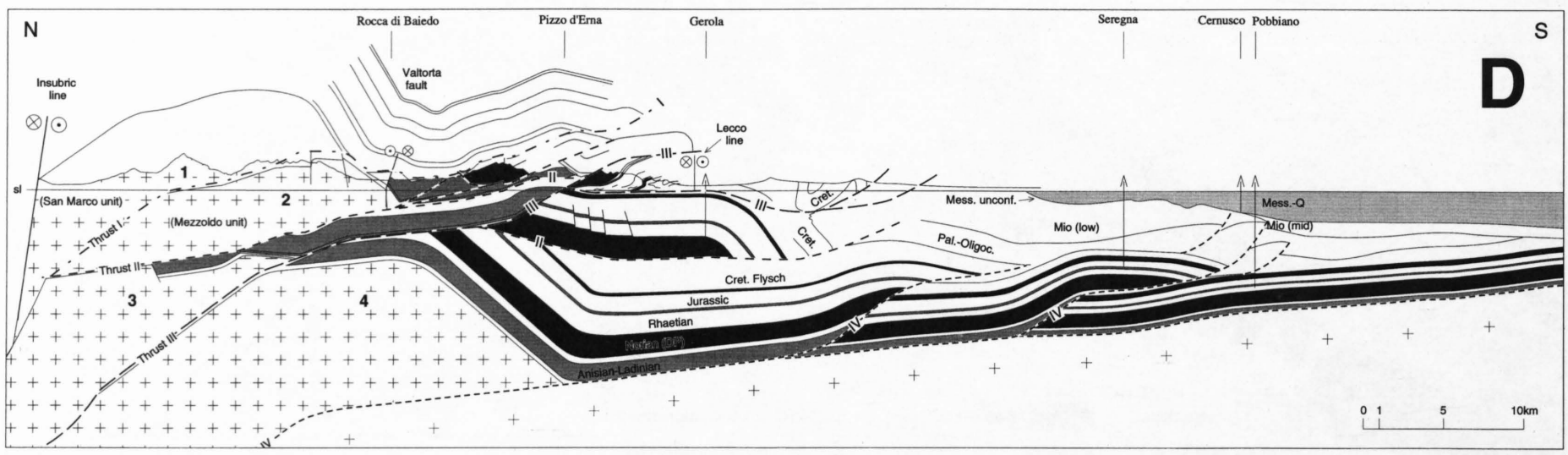

b)

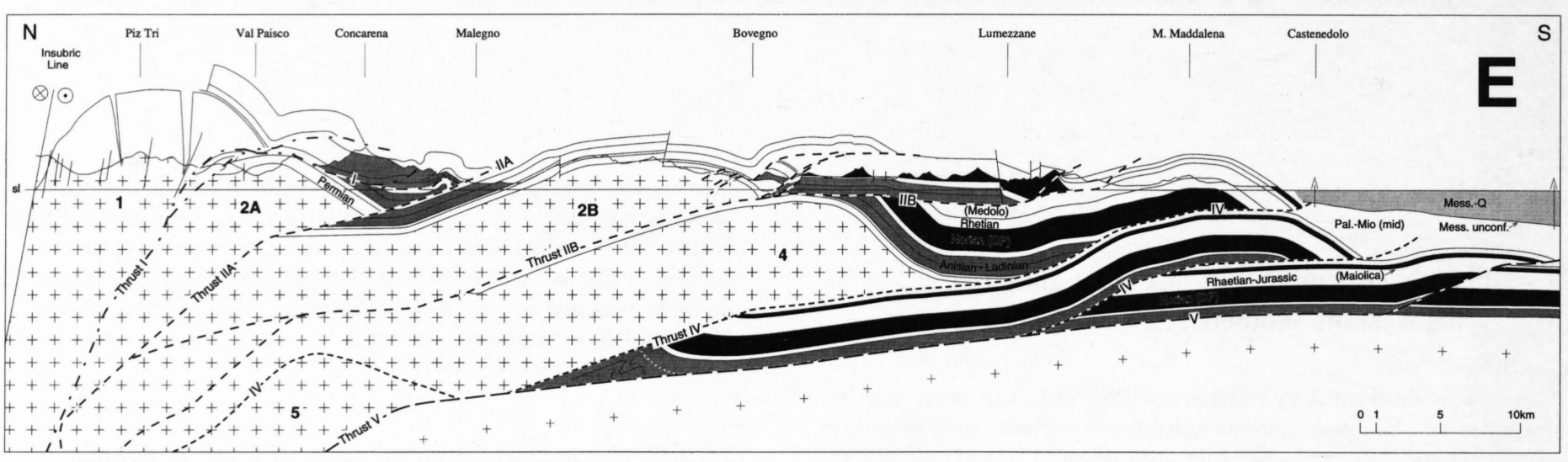

Figure 15-7
Balanced cross sections through the South-Alpine nappes after Schönborn 1992b (see Figure 15-2 for location).
a) section D east of Lago di Como. b) section E east of Lago d'Iseo.

The western domain (Grigne and Orobic mountains)

Of particular importance is the western domain immediately east of Lago di Como, comprising roughly the Orobic and Grigne mountains north of Lecco. It is here that the continuity of the basement and sedimentary parts of the Upper Orobic nappe (thrust sheet 1, Figure 15-7a) is observed, which serves as a key for unraveling the tectonics of the western Southern Alps (Laubscher 1985, Schönborn 1992b). It turns out that the Upper Orobic nappe is folded by the Orobic anticline, and this anticline in turn fits a ramp fold of the Lower Orobic nappe (thrust sheet 2). The thrust fault of the Lower Orobic nappe at the base of the Middle Triassic (Coltignone thrust) is exposed immediately north of Lecco. The basement part of both nappes is found to be quite thin – no more than 4–5 km –, meaning that only the uppermost part of the crust was involved in these nappes. For this reason we would like to speak of "thin-skinned tectonics" for both the sedimentary and basement parts.
Underneath the Coltignone thrust the Middle Triassic layer of an even deeper nappe system (3) is observed in a window (below Pizzo d'Erna in Figure 15-7a). Farther south the Lecco thrust (III) ends in a fault-propagation fold at the tip of a ramp through the Upper Triassic to Lower Cretaceous strata of the overlying Lower Orobic nappe (2). Consequently, thrust III is out-of-sequence, and the most external part of the Lower Orobic nappe is to be located in its footwall. The only known candidate for this external part is the Upper Triassic to Lower Cretaceous sequence of the Gerola well (Figure 15-7a). Near the cross-section of Figure 15-7a, a splay broke through the hinge of the fault-propagation fold and overturned its footwall (cf. Figure 10 of Schönborn 1992a). Between Como and Lago d'Iseo this fold constitutes the morphological boundary between the Southern Alps and the Po plain ("Flessura Frontale").
The top of the autochthonous basement in Figure 15-7a is placed according to early interpretations of the NRP 20 South lines (Bernoulli et al. 1990b; Holliger 1990). The space between the autochthon and the exposed nappes was filled with deeply buried Mesozoic duplexes of the Milan belt (see below), which were constructed in the simplest way possible and are expected to be more complex in nature. Newer interpretations of the NRP 20 reflections in southern Ticino (Schumacher, Chapter 10) assume a somewhat deeper level for the top of the autochthonous basement. The CROP Alpi-Centrali line extending from Bergamo to the north (Cernobori & Nicolich 1994), however, seems to support the level chosen in Figure 15-7a. An alternative deeper level of this horizon would call for small scale duplexes and imbrications and/or for a thicker stratigraphic sequence.

The Po basin domain

The industrial reflection seismic lines published by Pieri & Groppi (1981) revealed a belt of folded and thrust Mesozoic and Tertiary beds beneath the Po plain (Milan belt). The age of deformation is Middle to Late (pre-Messinian) Miocene. Although the structure of the Mesozoic strata is not well documented by these lines, it can be constructed in a simplified way with the help of the better constrained Tertiary beds. In the southern part of Figure 15-7a, the top of the autochthonous basement was adopted from Cassano et al. (1986). The northern end of the Milan belt was constructed using compatibility criteria (for details see Schönborn 1992b). Its basement part is shown as a single thick ramp fold, although a pile of thinner duplexes similar to those of the Aar massif in the northern part of the Alps (Laubscher 1992) may be more plausible and cannot be ruled out on available information.

The central domain between the Grigne and Lago d'Iseo (sedimentary décollement sheets)

Between cross-section D and Lago d'Iseo (Figure 15-2), the exposed structures change along transverse zones. These changes are triggered by Mesozoic normal faults which displaced vertically the décollement horizons and so led to the development of different thrust geometries on opposite sides (e. g. Schönborn 1994). In addition to these N–S trending zones, other features seem to be influenced by inherited structures also: N-vergent backthrusts developed frequently at the base of the rigid Upper Triassic layer. They thrust the Upper Triassic layer of the Lower Orobic nappe (2) back to the north onto the Middle Triassic of the Upper Orobic nappe (1) (Figures 15-2 and 15-6). In map view, these backthrusts trend somewhat obliquely (ENE) with regard to the general more E-directed strike of the two nappes (large-scale trends and numerous small-scale transport criteria). Most of these oblique structures end near N- to NNE-striking faults, whose Liassic

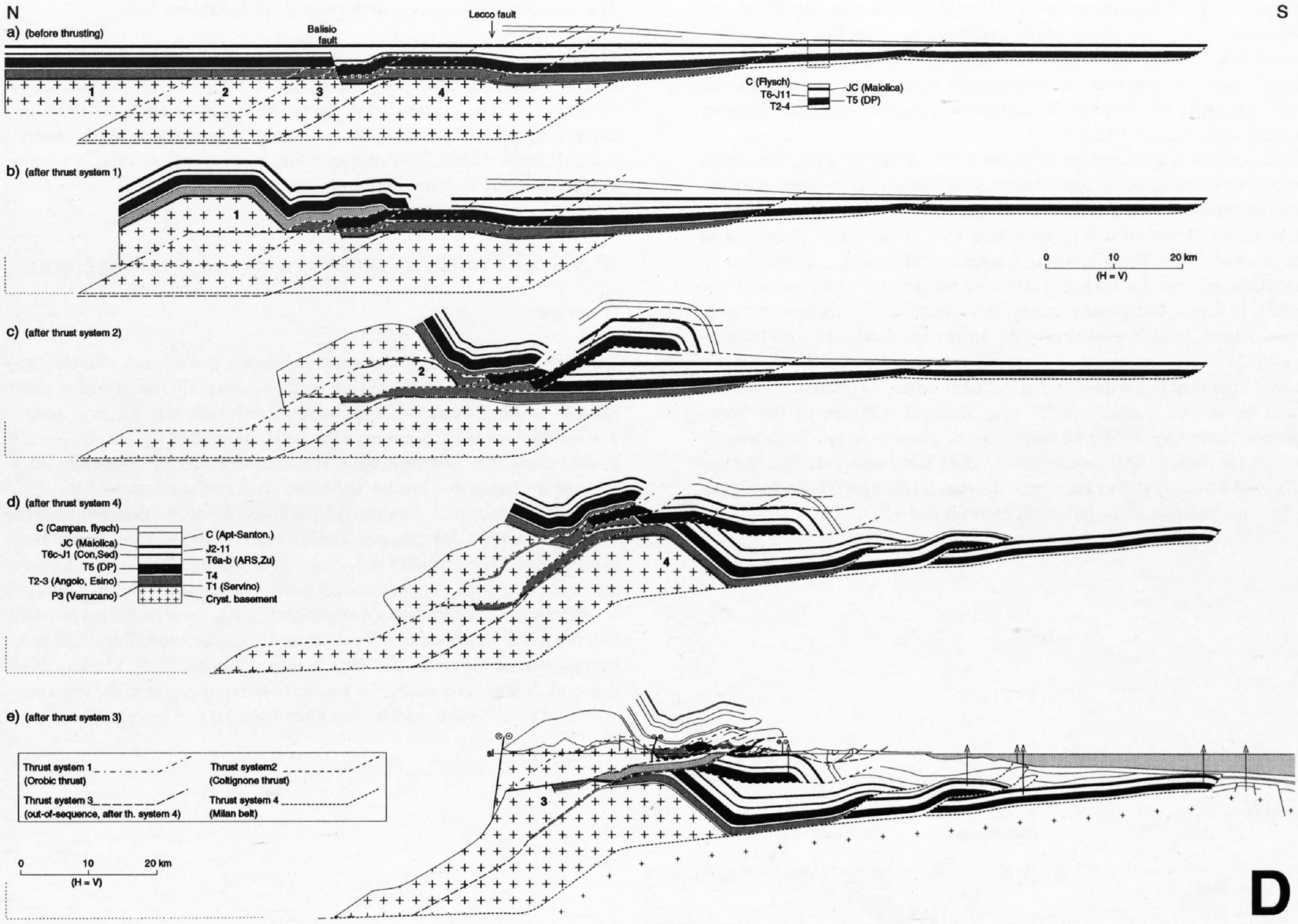

Figure 15-8
Kinematic model for the evolution of the Southern Alps along cross section D (Figure 15-7a), from Schönborn 1992b.

origin is documented by syntectonic sediments. Therefore a Liassic age is suggested also for the ENE-trending inherited structures, although no Liassic deposits are preserved along these. The ENE-trending sinistral structures are more pronounced than the NW-trending dextral ones. This might point to a predominance of ENE-trending Mesozoic faults (Figure 15-5). These oblique zones not only gave rise to backthrusts (triangle structures), they also preformed the ramp of thrust system 1 through the Upper Triassic layer and some Alpine strike-slip motions.

The central domain (pre-Mesozoic northern part)

Farther north a similar system of Alpine sinistral (ENE) and dextral (NW) faults follows the southern flanks of the basement anticlines (narrow horizontal ruling in Figure 15-2). Moreover, ramps of both the Upper Orobic nappe (1) (across the Middle Triassic layer) and the Lower Orobic nappe (2) (across the uppermost part of the crystalline basement), trend, closely parallel, to the ENE, i. e. obliquely to the average Alpine strike. Possibly this trend too may be due to inherited structures (predecessors of the Valsassina, Valtorta, Olmo, Canale and Scalve faults in Figure 15-5). ENE- and NW-trending elements apparently had been active already during Permian transtension: The distribution of thickness and facies of the Permian sediments point to ENE-trending basins, partly with NW trending borders in the E and the W (Dozy 1935b, Schönborn 1992b).
The right-stepping (dextral) arrangement of the basement anticlines north of Bergamo may thus be due to these inherited structures; on the other hand, they also suggest the possibility of some dextral transpression, particularly as indications of dextral strike-slip are abundant in the Upper Orobic nappe (e. g. Schönborn 1991, Siletto 1991). Both influences are plausible and are not mutually exclusive.

The eastern domain (between Lago d'Iseo and the Giudicarie)

The general tectonic elements of cross-section D (Figure 15-7a) can be extrapolated eastward as far as the transverse zone near Lago d'Iseo (Figure 15-2). Farther east, however, important changes take place. In the northern part, there are two basement anticlines (thrust systems I and IIA, Figure 15-7b), whereas in the southern part, which farther west is occupied by the sedimentary décollement sheets, a third basement ramp-anticline appears (Trompia high, thrust system IIB). It constitutes a southward-pointing indenter bounded by a large dextral transverse zone in the west (north of Lago d'Iseo) and the sinistral Giudicarie line in the east (Figure 15-2). Of particular importance is the relation of the three basement structures to the Adamello intrusion (Figure 15-18). The two northern ones are sealed by the intrusion, whereas the Giudicarie fault that bounds the Trompia high in the east cuts it. Numerous sedimentary thrust sheets emerge from the base of the Trompia basement ramp-fold. These thrusts, belonging to the post-Adamello Trompia-Giudicarie system, dip gently north and therefore must cut the Adamello pluton in the subsurface (Figure 15-2).
The Trompia indenter is kinematically linked to the basement anticlines of the western and central domains (Trabuchello and Orobic anticlines) through the transverse zone north of Lago d'Iseo. These basement anticlines are part of the Lower Orobic nappe (2) and split, in the eastern domain, into a pre- and a post-Adamello part (Cedegolo and Trompia anticlines, respectively). Apparently the pre-Adamello Lower Orobic thrust II was reactivated while the Trompia indenter formed. Near Lago di Garda, the shortening is transferred to the NNE by the large Giudicarie transpressive belt (Laubscher 1988, Castellarin et al. 1993).
Figure 15-7b depicts a balanced cross-section (E in Figure 15-2) through the Adamello-Trompia domain. Thrust system II is subdivided into system IIA (forming the Cedegolo anticline, pre-Adamello activity) and system IIB (forming the more southerly located Trompia high, post-Adamello activity), both with basement and Triassic units. Total shortening for the Lower Orobic nappe (2) was assumed equal to that farther west for lack of contrary information. In detail, there are a number of changes with respect to cross-section

D (Figure 15-7a). Thus, basement unit 4 is shown thrust onto parts of the sediment units of the same thrust sheet, deforming them as footwall imbrications. A new basement unit (5) is required to equal the shortening of the sediments. Thrust system V is in-sequence and replaces the out-of-sequence thrust system III of Figure 15-7a, which ends together with the "Flessura Frontale" east of Lago d'Iseo.

Of fundamental importance for the construction of the balanced sections is the location of the autochthonous basement. As no seismic data are available for cross-section E, the location shown in Figure 15-7b may be somewhat controversial. However, it is in agreement with cross-section D as well as with Roeder (1989, beam models), Cassano et al. (1986, gravimetric and magnetic data), and Laubscher (1990, area balance and extrapolation from the Lessini high). Additionally, section E is quantitatively coherent for each step with the kinematic evolution of the areas adjoining to the west (Schönborn 1992b).

Another argument is provided by the southern Adamello pluton situated just east of the section (within unit 2B, near Malegno in Figure 15-7b): Some 12 km of vertical uplift (3.5 kb emplacement pressure in the southernmost part, John & Blundy 1993) occurred not before Early Miocene. This late uplift is most plausibly due to important Miocene thrusting as shown in Figure 15-7b (superposition of the basement units 2B and 4).

The amount of shortening in the South-Alpine thrust belt

The total amount of shortening in the South-Alpine thrust system increases from approximately 80 km in cross-section D (Figure 15-7a) to some 110 km in cross-section E (Figure 15-7b). Some 25 km may be attributed uniformly to pre-Adamello deformation, the remaining 55 to 85 km to Miocene shortening (Schönborn 1992b). This may imply some dextral rotation in addition to approximately N–S translation (Laubscher, in press).

15.3.3 The western segment (west of Lago Maggiore)

Overview

The northwestern corner of the Adriatic indenter, in a schematic model, may be represented by an E–W striking northern, dextrally transpressive, and a NE–SW striking western, compressive to sinistrally transpressive margin. The western end of the Southern Alps, between Lago Maggiore and Ivrea, is located along the western margin. It is characterized by apparently thick-skinned structures that involve the entire crust and even parts of the upper mantle. Moreover it is dominated by the geophysically determined **Ivrea body** (Giese 1968, Berckhemer 1968), which at the surface, in the **Ivrea zone** (Figure 15-2; Schmid 1967, Zingg 1983, Zingg 1990), shows Late Palaeozoic lower crust to upper mantle mafic to ultramafic igneous rocks and amphibolite to granulite facies metasediments. It is these rocks that plausibly give rise to the very pronounced gravity and magnetic anomalies all along the internal side of the arc of the Western Alps (Vecchia 1968, Kissling 1980, Rey et al. 1990). Seismically, the bottom of the central part of the Ivrea body is marked by a P-wave velocity inversion from 7.4 to 5 km/s at about 20 km

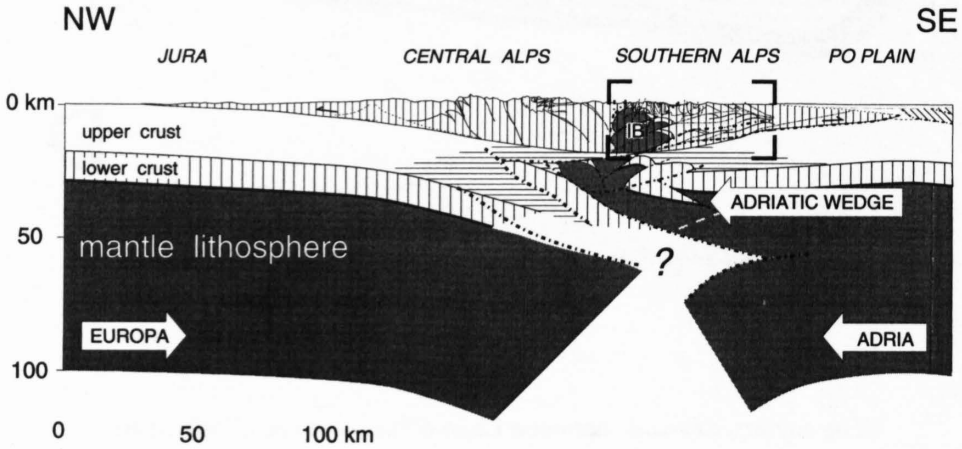

a)

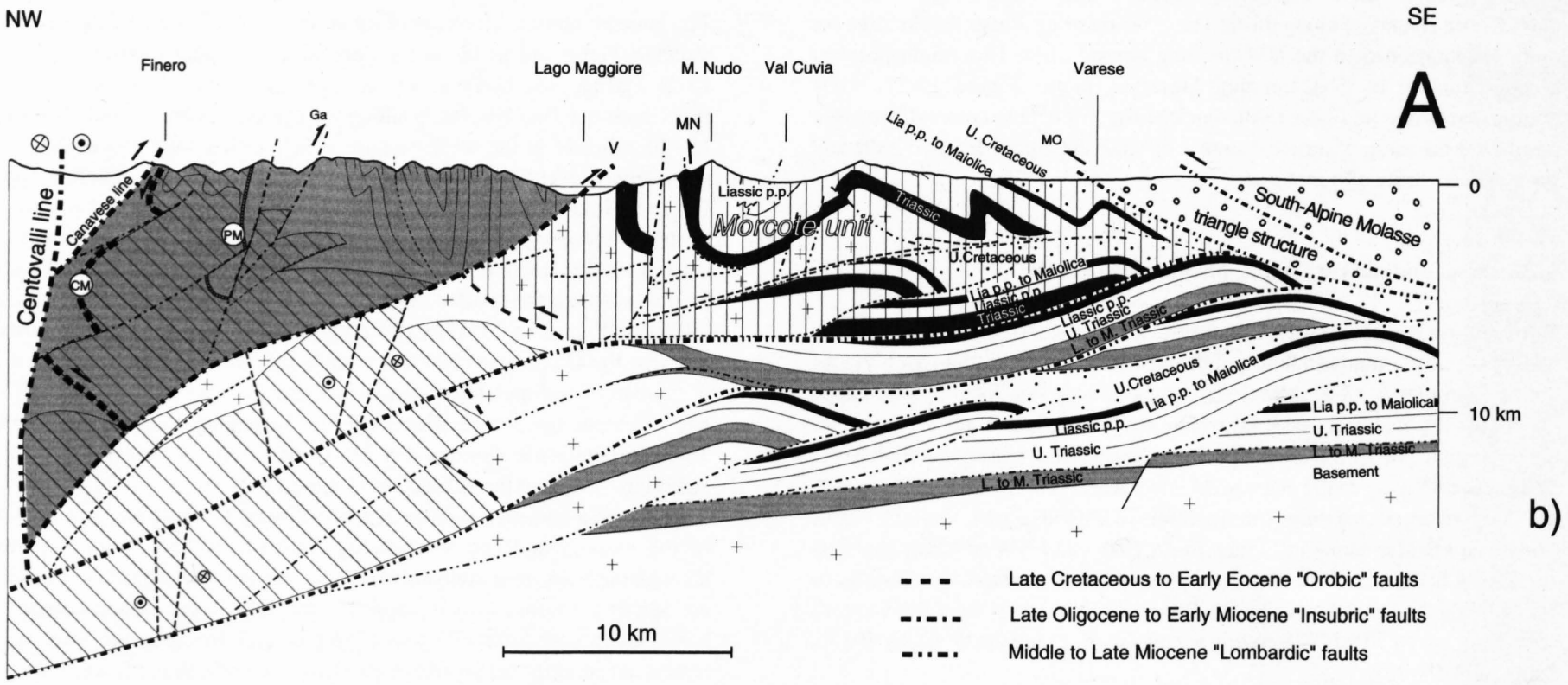

Figure 15-9
The interference between the thick-skinned Ivrea-Ceneri system and the thin-skinned South Alpine nappes.
a) Lithospheric section showing the location of Figure 15-9b within the Alpine collision zone. The Ivrea body (IB) forms part of the Neogene orogenic lid (cf. Laubscher 1990).
b) Cross section A through the thick-skinned, transpressive Ivrea-Ceneri system northwest and the steeply tilted sediments of the Mesozoic Monte Nudo basin (Upper Orobic nappe) southeast of Lago Maggiore (see Figure 15-2 for location). The Ivrea-Ceneri complex (grey) forms the cut-off upper part (including middle and upper crustal rocks of the Ceneri zone) of the early Alpine, sinistrally transpressive Ivrea-Ceneri system. Lower crustal and upper mantle rocks are indicated by oblique ruling. The whole Ivrea system is again cut-off from its roots by the late Alpine Lombardic thrust system. The Orobic nappe system is indicated by vertical ruling. Notice that for most of the tectonic units in this profile the transport direction is out of section. CM: early Alpine Canavese mylonites; Ga: Gambarogno line; MN: Monte Nudo backthrust; MO: Monteolimpino backthrust; PM: pre-Alpine Pogallo mylonites; V: Verbania line.

depth (Giese 1968, Ansorge 1968, Ansorge et al. 1979). The **Ivrea zone** passes without a clear cut Alpine boundary into the **Strona-Ceneri zone,** which consists of highly metamorphic, mostly silicic rocks that are devoid of the upper mantle to basal crustal rocks of the Ivrea zone. They have been largely involved in thick-skinned tectonics during the Orobic (Ivrea-Ceneri system) and the Insubric phase (Ivrea-Ceneri complex). The categories of Alpine tectonic units are schematically outlined in Table 15-1.

The structural evolution of the western segment is still a matter of debate, and many questions remain unanswered. However, it is generally accepted that the Ivrea zone and the adjacent South-Alpine basement together offer an unique exposure of a section through the entire continental crust. Early interpretations of the seismic sections proposed a simple bending of the western margin of the Adriatic indenter (e. g. Berckhemer 1968), and this view was adopted by Laubscher (1971). It is still widely held (e. g. Handy 1987, Schmid et al. 1989, Zingg et al. 1990) and helps explain the present sequence of outcrops (Figure 15-2) with the Late Palaeozoic intrusions of mafic mate-

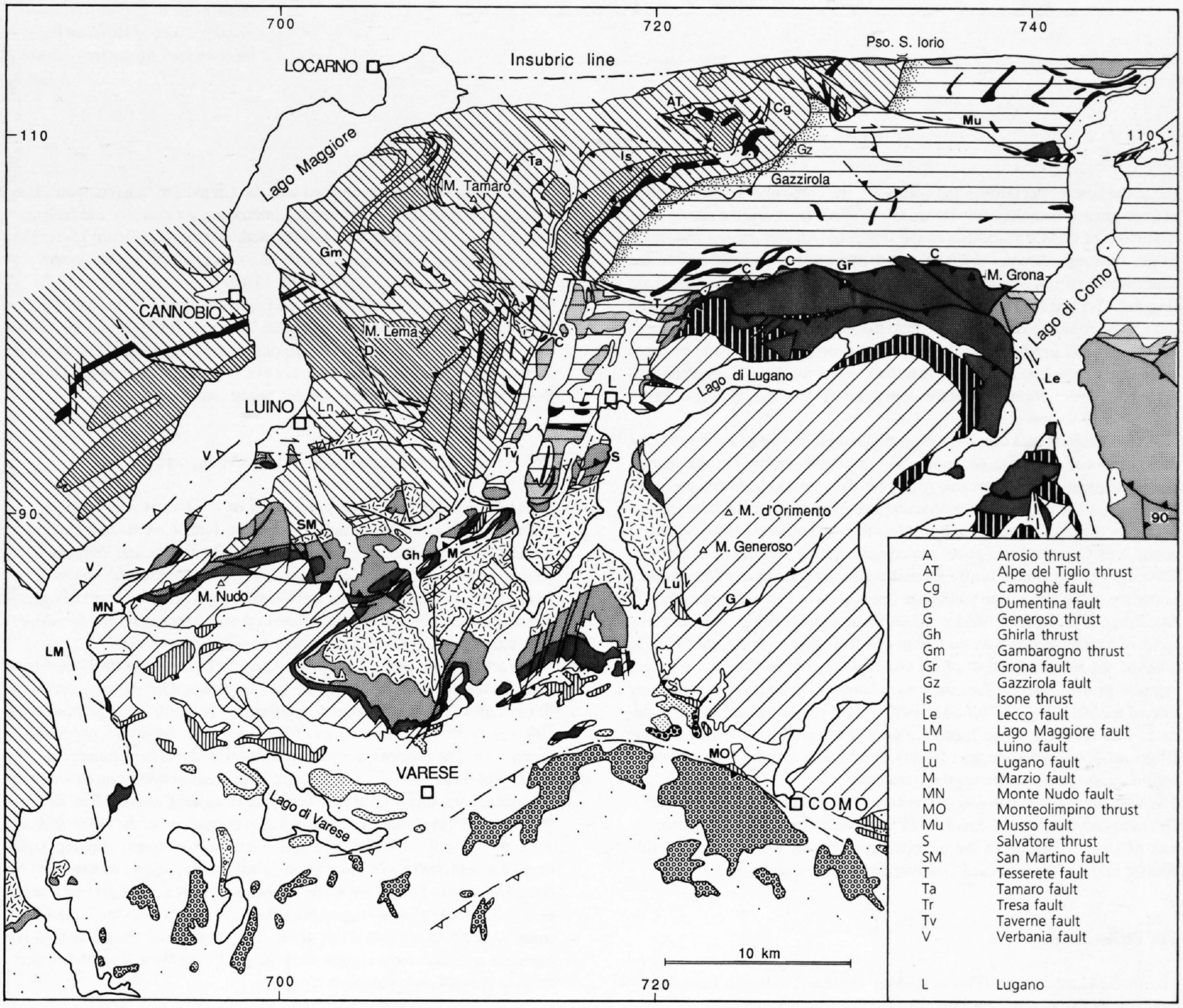

Figure 15-10
Geologic map of the Southern Alps between Lago Maggiore and Lago di Como based on published maps and on recent data by Schumacher.

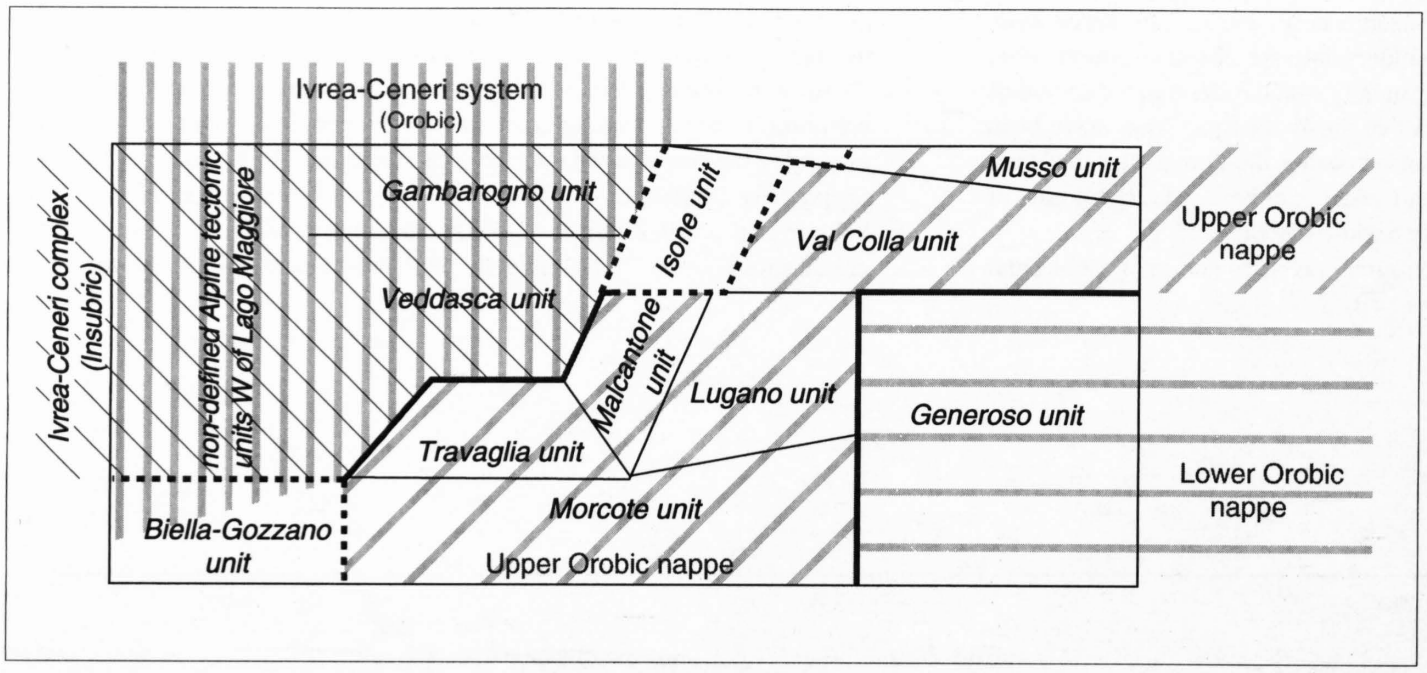

Table 15-1
Overview of the Alpine tectonic units defined in this paper to describe the junction of the Ivrea-Ceneri system and the Orobic nappe system. Allocation of the Biella-Gozzano unit to the Orobic nappe system is arbitrary. It could be part of the Ivrea-Ceneri system. Ivrea, Strona-Ceneri and Val Colla zones do not appear in this scheme as they describe petrographic zones of Variscan basement and not Alpine tectonic units.

rial at the base of the crust in the northwest, the contemporaneous insertion of large granitic batholiths into the middle to upper crust, and the coeval manifestations of surface volcanism in the southeast. All this implies post-magmatic, obviously Alpine, uplift of the northwestern part relatively to the southeastern part of this area. However, the internal front of the Alpine arc (Figures 15-1 and 15-2), buried below the Plio-Quaternary deposits of the Po plain, is backthrust towards S and E onto the Adriatic indenter (Cassano et al. 1986), and this implies truncation of the pre-existing Ivrea body at depth (compare Laubscher 1990). We therefore argue for a now allochthonous Ivrea body which forms part of the upper crustal orogenic lid as it is shown in Figures 15-9a and b.

Geochronological data demand a polyphase emplacement of the Ivrea body. Its exceptional structural situation was pre-determined by late Palaeozoic and subsequently early Mesozoic rifting (cf. Schmid 1993). In this presumably distal part of the Adriatic continental margin, due to crustal thinning, the bottom of the crust reached a depth of less than 10 km (pre-Alpine cooling to about 300° C in the Ivrea zone, see compilation by Hunziker et al. 1992). K/Ar ages of synkinematically formed white mica along the northwestern boundary of the Ivrea zone yield Late Cretaceous to Paleocene ages (60–76 Ma, Zingg & Hunziker 1990) for the southern segment of the Canavese line, south of its intersection with the Cremosina line (Boriani & Sacchi 1973). In contrast, the white mica ages of the Canavese mylonites along the northern segment of the Canavese line show ages between 43 and 19 Ma, younging toward the NE (Zingg & Hunziker 1990). The Cremosina line, in turn, connects with splinters of the Insubric line and therefore is probably of Late Oligocene-Early Miocene age. Finally, the Middle to Late Miocene Lombardic thrust system undercuts the Ivrea body.

The western segment consists of the Ivrea-Ceneri complex and the Biella-Gozzano unit (Figures 15-2 and 15-6). The Ivrea-Ceneri complex continues east of Lago Maggiore in the intermediate segment where it can be subdivided into the Veddasca and Gambarogno units (cf. section 15.3.4).

The Biella-Gozzano unit

The Biella-Gozzano unit (Figure 15-6) is separated from the Ivrea-Ceneri complex by the **Cremosina line.** The basement is covered by mainly flat-lying Permian volcanics and locally Mesozoic sediments. This configuration may be seen as related to both the now eroded top of the Ivrea system or the Upper Orobic nappe east of Lago Maggiore (Morcote unit, Figure 15-9b and section 15.3.4). During the Orobic phase it may have been part of the western margin of the Adriatic indenter and a rather thin-skinned lateral sliver of an inferred Ivrea flower structure (Ivrea-Ceneri system). Another possibility is that it was part of the Upper Orobic nappe that was subsequently deflected into the western margin of the Adriatic indenter and tucked under the Ivrea body. The present northwestern boundary of the unit, the Cremosina line, is considered a younger feature connected with the Insubric line (see above). It comprises a system of WSW–ENE trending, subvertical faults (Boriani & Sacchi 1973), along which several slices of strongly tectonized Mesozoic sedimentary rocks are found. They suggest late Alpine strike-slip tectonics, and the array of Permian intrusions as well as the pre-Alpine mylonites separating the Ivrea and Strona-Ceneri zones (Figure 15-2) seem to be dextrally offset in the order of 15 km (Boriani & Sacchi 1973). However, there is also a compressive component evident along the **Verbania line** (Figure 15-6 and section 15.3.4) which is connected with the Cremosina line (compare cross-section A, Figure 15-9b). Structurally interesting are also sinistral faults cutting across the Cremosina line near its southwestern end (Figure 15-2). They may indicate some late Alpine clockwise rotations of the whole western segment around a vertical axis (cf. Figure 15-17).

The eastern boundary of the unit is the Lago Maggiore line, probably a reactivated Mesozoic normal fault (compare Bernoulli 1964). It may be viewed as a sinistral Alpine transfer zone, similar to the Lugano line, that separates the two Orobic nappes, or alternatively as a boundary fault between the Ivrea flower structure and the Upper Orobic nappe (see above).

The Ivrea-Ceneri complex (west of Lago Maggiore)

West of Lago Maggiore, the subdivision of the Ivrea-Ceneri complex remains open. The bounding fault zones of the Ivrea-Ceneri complex both in the northwest (Canavese line) and southeast (Cremosina and Verbania lines) seem to be parts of the Late Oligocene-Early Miocene Insubric system. However, it remains unclear whether and to what extent brittle and possibly greenschist facies Alpine movements followed and overprinted the pre-Alpine high-temperature mylonites separating possible internal units.

Not much is known about the internal Alpine deformation of the Ivrea-Ceneri complex and the contribution of the various phases. One Alpine element are flexural slip folds (e. g. Proman antiform of Schmid 1967, Schmid et al. 1987) in the lower crustal rocks of the Ivrea zone, along the northern Canavese line. They suggest a relatively shallow, internal detachment (see Figure 15-9b). Schmid et al. (1987) regard these folds as synchronous with Late Oligocene back-thrusting of the Sesia zone along the Canavese line, although the lack of direct chronological data would permit any of the other phases as well. We believe, however, that upthrusting along steeply dipping faults, combined with strike-slip movements, would be a plausible way to bring the Ivrea rocks up to the surface in the Orobic phase. As to younger movements, fission track data of apatites (see Hunziker et al. 1992) from the Ivrea-Ceneri complex seem to confirm a late uplift. They apparently cluster around late Miocene ages and seem significantly younger than those from the adjacent areas to the east and southwest.

15.3.4 The central segment between Lago Maggiore and Lago di Como

The problem and an overview of the tectonic assemblage

The most important problem of the Southern Alps between Lago Maggiore and Lago di Como (Figure 15-10) is the junction of the two completely different tectonic systems, the **Orobic nappes** in the east and the deeply rooted **Ivrea system** in the southwest. While the Orobic nappes are thin-skinned in the sense, that their basement part involves only few kilometers of the topmost crust, the Ivrea system is exceptionally thick-skinned as it contains rocks of the entire crust, including its transition to the mantle. As no sediments separate these two fundamentally different Alpine basement structures, other criteria for determining the boundary must be found, such as low-T, mostly brittle dislocation zones. They will arguably help in

separating pre-Alpine, for the most part high-T deformations from Alpine, essentially low-T (in the Southern Alps) features.
North of a roughly E-W trending boundary formed by the **Tesserete-Grona line** in the east and the **Arosio** and **Luino lines** in the west (Figures 15-10 and 15-11), the San Marco basement unit of the Upper Orobic nappe appears to continue westward across the Lago di Como as far as the Gazzirola line or Val Colla line (see below).
South of this boundary both sedimentary and (subordinately) basement parts of the Upper Orobic nappe may be followed as far west as Lago Maggiore; however, correlation is made difficult because of segmentation by important transverse and oblique fault zones, see Figure 15-11 (from E to W: Lecco line, Lugano line, Valcuvia-Salvatore belt, Taverne line, Lago Maggiore line). Most of these lines had originally been Permian and/or Mesozoic normal or transfer faults, for which there is compelling stratigraphic evidence (see section 15.2). In this southern domain, the boundary between the thick-skinned Ivrea system and the thin-skinned Orobic nappe system follows the Arosio, Luino and Verbania lines (Figure 15-11).
Both the northern and southern domains have been subdivided into an assemblage of tectonic entities we chose to call "units", as identified in Figure 15-11 and Table 15-1. Tectonic boundaries are indicated as lines on Figure 15-11, and are more specially termed on Figure 15-10 and in the text. The description of the units generally proceeds from east to west, as the tectonics east of Lago di Como is easier to understand and less controversial.

The units of the northern domain

a) The San Marco and Val Colla units
The sedimentary cover of the frontal limb of the San Marco unit on the eastern shore of Lago di Como correlates without difficulty with the cover of the Val Colla unit on the western shore (Laubscher 1985, Schönborn 1992b). Moreover, pre-Alpine metamorphic isogrades and the internal structures of the San Marco unit continue into the Val Colla unit (Bocchio et al. 1980). This is in contrast to the sedimentary décollement parts of the southern domain, where the Lecco line separates south-vergent thrusts in the east from north-vergent ones in the west.
The northern boundary of the Val Colla unit is the **Musso line** (Figure 15-12). This important, ESE-trending, subvertical to north-dipping brittle fault system splays off the Insubric line and dislocates characteristic lithologies dextrally by at least 5 km (Schumacher 1994). The northwestern boundary is the **Val Colla line**. This is a greenschist facies mylonite belt (VM in Figure 15-11) that is at least 1 km thick. Its metamorphic facies suggests that it is pre-Alpine in age (p. 000), although reactivation during the early Alpine phases cannot be excluded. The brittle, apparently sinistral **Gazzirola fault** (Gz in Figure 15-10, Schumacher 1990) follows this mylonite belt. The Val Colla line certainly is pre-Musso line and, accepting this to be a splay of the Insubric line, pre-Insubric phase. Its present somewhat sinusoidal shape may be attributed to deformation by distributed dextral shear during the Insubric phase (cf. Figure 15-17). If this view is accepted, it follows that some Insubric shear extended as far south as the Tesserete-Grona line.

b) The Musso unit
In this unit between the **Musso line** and the **Insubric line** there are several brittle splays of the Insubric line, similar to those mapped by Fumasoli (1974) north of the Insubric line. These faults displace dextrally both the Val Colla mylonites and lithologies of the Ceneri zone north of it (Figures 15-10 and 15-11). Their relation to the Insubric line is that of synthetic Riedel shears, and this implies that Insubric dextral shear extended at least as far south as the Musso line (Figures 15-11 and 15-12, Schumacher 1990).

c) The Isone unit
Northwest of the Val Colla line follows a zone of brittle, northwest-vergent imbrications that already contains lithologies of the Ceneri zone, which typically occur in the Alpine Ivrea-Ceneri system. The northwestern boundary of the unit is the **Tamaro brittle fault zone** (Ta in Figure 15-10), where structural elements of oblique, sinistral transpression are found (Schumacher 1990). Together with the equally sinistral **Gazzirola fault** it presents evidence for a sinistrally transpressive relationship between the Orobic and the Ivrea(-Ceneri) systems, the former overriding the latter. For possible explanations of this peculiar relation see below.

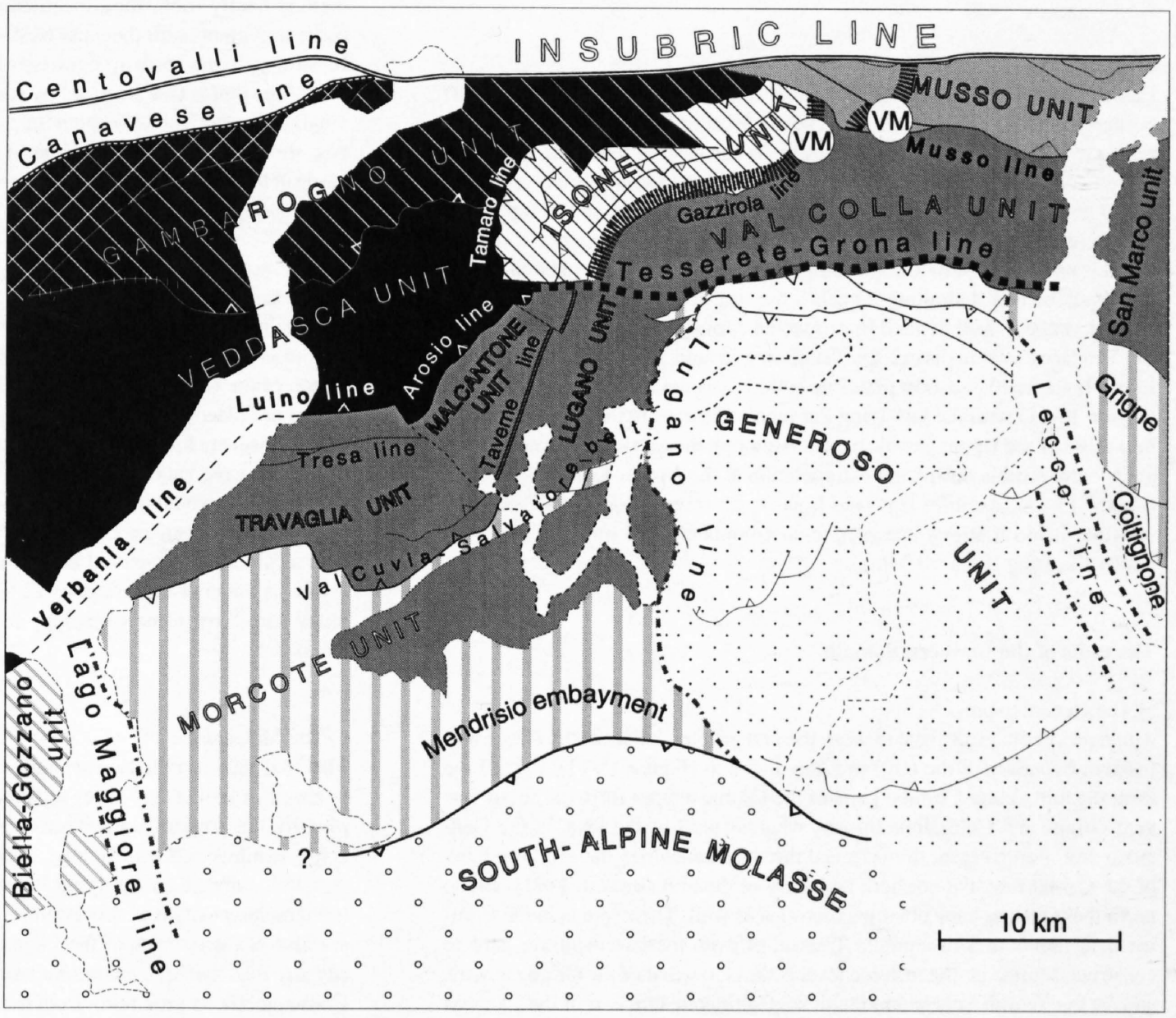

Figure 15-11
Map view of the principal tectonic units and the separating lines in the area of interference between the Ivrea-Ceneri complex (black background) and the Upper Orobic nappe (grey: basement; vertically hatched: sediments). The Val Colla mylonites (VM) show a dextral offset along the Musso fault system. North of the Tesserete line a wide zone of northwest-vergent imbrication (Isone unit) forms the boundary between the Ivrea-Ceneri complex and the Upper Orobic nappe whereas south of it the southeast-vergent Veddasca unit of the Ivrea-Ceneri complex overrides the Upper Orobic nappe. The change of vergence takes place at the Tesserete line (compare Figure 15-14)

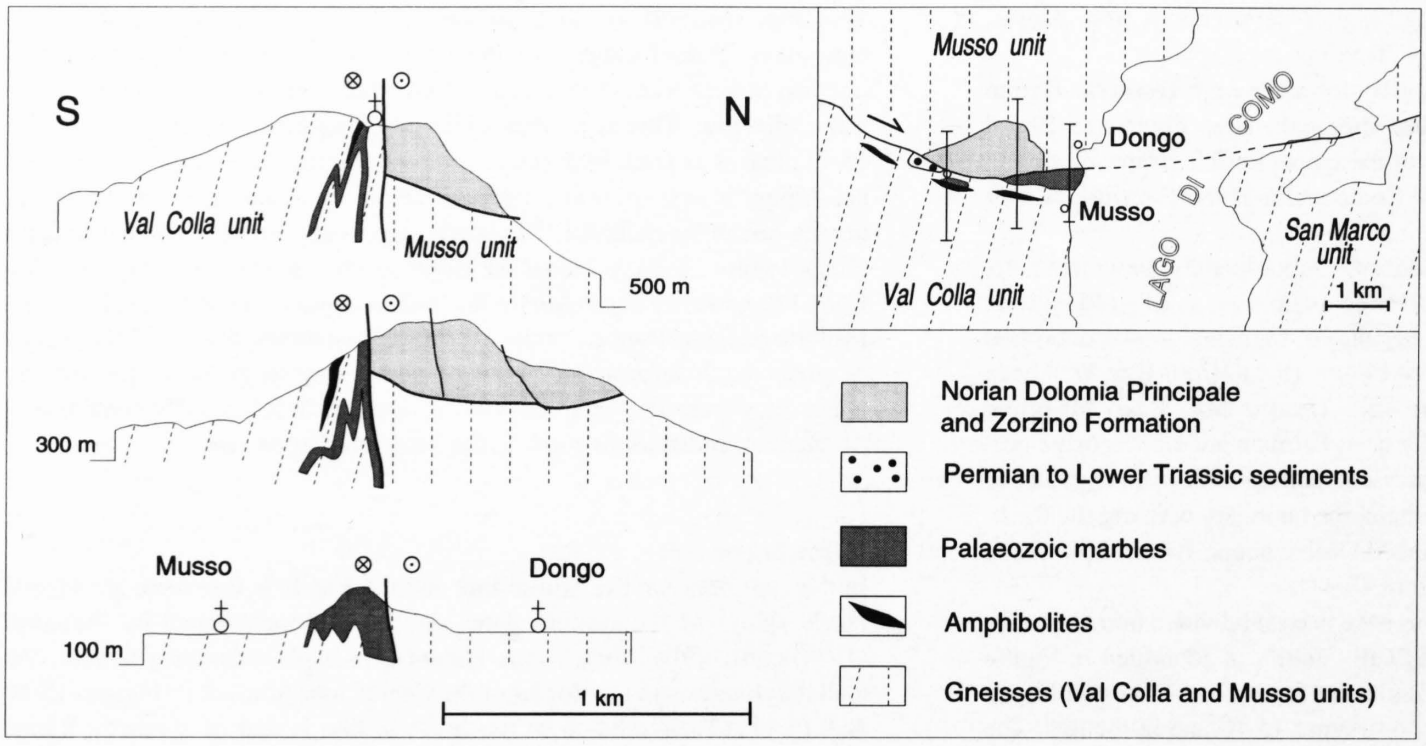

Figure 15-12
Profiles across the Musso line west of Lago di Como. Together with other remnants of Triassic sediments on top of the basement between the Insubric and the Musso lines the relict of Norian Dolomia Principale near Musso (Repossi 1904) documents downfaulting of this area. The vertical Musso fault cuts an apparently older fault at the base of the Norian dolomite. The dextral Musso line shows the orientation of synthetic Insubric Riedel shear (Figure 15-10) and may have acted as a releasing bend giving rise to a pull-apart (Schumacher 1990).

d) The Gambarogno unit

Located between the Isone unit and the Insubric line, the Gambarogno unit of the Ivrea-Ceneri complex is characterized by a Palaeozoic Schlingen-structure with a steeply southeast-dipping axial surface (Bächlin 1937). This structure can be traced to the west of Lago Maggiore in the Ceneri Gneisses north of Cannobio (Boriani 1977, R. Zurbriggen pers. comm. 1994). The Gambarogno unit seems to have moved along the **Gambarogno thrust** (Gm in Figure 15-10, Bächlin 1937) towards the south or southeast onto the Veddasca unit. An important displacement along the Gambarogno thrust has to be supposed because there is no continuation of the Schlingen-structure in the footwall. To the east the corresponding shortening was transferred to the north by the sinistrally transpressive **Tamaro fault zone**. Inasmuch as the Gambarogno thrust is southeast-vergent, whereas the Isone thrusts are northwest vergent, the Tamaro fault separates systems of opposite vergences.

e) The Veddasca unit

East of Lago Maggiore, the Veddasca unit (part of the Ivrea-Ceneri complex) borders the Gambarogno unit to the south. West of Lago Maggiore the relations are less clear. The mountain range on the eastern border of the Ivrea-Ceneri complex with the peaks of Monte Lema and Monte Tamaro (Figures 15-10 and 15-11) rises to altitudes more than 1000 m above the top of the basement in the Malcantone. By virtue of this characteristic alone it reveals that it is part of the Ivrea-Ceneri complex. However, the western boundary of the Veddasca unit delimiting it against the rest of the Ivrea-Ceneri complex has not yet been well defined by suspected Alpine dislocations. In the north the Veddasca unit underlies the Gambarogno unit along the Gambarogno thrust. In the south the most plausible boundary is the conjectured **Luino line** (Figure 15-11) with the low-lying Permian sediments in the footwall that fit into those of the Upper Orobic nappe. Although the exposures do not permit an incontrovertible downward extrapolation of the **Arosio-Luino** dislocation (Figure 15-11), we infer from the high structural position of the Veddasca unit that it has a strong compressional component and most probably involves thrusting (Figure 15-9b).

The units of the southern domain

a) The Generoso unit

Again proceeding from east to west, the first problem arises at the **Lecco line** (eastern boundary of the unit) in Lago di Como (Figure 15-11). East of the lake, the thin-skinned frontal parts of the Orobic nappes form the south-vergent Grigne and Coltignone thrusts, whereas west of the lake, in the Generoso unit, northvergent thin-skinned thrusts characterize the southern flank of the **Grona line**, the northern boundary of the unit (Bertotti 1991). To the north these thrusts have other peculiarities as well. Their sole is in the Carnian, and ramps into the middle Triassic or even the basement are hard to construct. Moreover, the tectonic level is far below that of the Grigne thrusts, and for that reason a correlation with the Coltignone unit east of the lake was proposed by Laubscher (1985). He found, that ramping into basement, which should produce a pronounced basement ramp fold, would have to be placed under the basement high north of the Grona line, below the Val Colla unit (Figure 15-13), in a position equivalent to that of the Mezzoldo basement unit below the San Marco unit in the Orobic mountains (Figure 15-7a). This, in turn, would demand underthrusting and triangle structures along the Grona line.

Another difficult problem arises at the **Lugano line**, the western boundary of the unit. At this line, a very large Mesozoic normal fault was reactivated during Alpine compression as a sinistral transfer zone, as the frontal ramp fold of the basement part of the Upper Orobic nappe (Val Colla unit in the northern domain) apparently was transferred as far south as the Arbostora anticline west of the line (see discussion of the Lugano unit). This situation has consequences for the deep structure, compare cross-sections B and C (Figures 15-13 and 15-15): Whereas under the Generoso unit east of the Lugano line there is hardly room for allochthonous basement masses, such masses become important in all the units west of the Lugano line.

In contrast to the northern border with its north-vergent thrusts, the southern half of the unit is characterized by south-vergent thrusts and folds (Bernoulli 1964). However, the very southern boundary of the unit is again a north-vergent thrust, albeit a Miocene one: it carried the Oligocene Gonfolite Lombarda in the passive roof of a triangle zone on top of the Mesozoic of the Generoso unit (Bernoulli et al. 1989).

b) The Lugano unit

This unit consists essentially of basement outcrops. Its main characteristic feature is the widespread occurrence of essentially flat-lying Gneiss Chiari on top of the basement (Figures 15-3, 15-10 and 15-14), below small relics of Upper Palaeozoic-Triassic sediments west of the **Lugano line** and south of the **Tesserete line**. This association is typical for the top of the Upper Orobic nappe in the Val Colla unit north of the Tesserete line and its continuation farther east. It would imply that the Lugano unit too is part of the Upper Orobic nappe. The southern boundary of the unit is the San Salvatore-Val Cuvia belt, a complexly structured zone of sedimentary rocks. The western boundary is the **Taverne fault**, a mostly pre-Alpine dislocation zone that separates rocks with Ivrea-Ceneri lithology from those of Orobic affinity (Val Colla zone).

c) The Malcantone unit

The Malcantone unit is essentially a basement complex characterized by gneisses of the Ceneri zone, separated from the Alpine Ivrea-Ceneri complex by the **Arosio line** (Figure 15-11). The top of the gneisses (Ceneri zone) exhibits a deep-reaching, reddish-tinted weathered layer, which at Arosio is covered by flat-lying Permian sediments and volcanics. Both the topographic position of this Permian relic and its essentially flat-lying strata are also characteristics of the Lugano unit of the Upper Orobic nappe and suggest that the Malcantone unit too is part of the Upper Orobic nappe. Consequently its separation from the Lugano unit by the **Taverne line** is as-

sumed to be pre-Alpine – a conclusion already arrived at by previous authors (Graeter 1951, Reinhard 1953,1964). We conclude, that in the late Palaeozoic that part of the Ivrea-Ceneri assemblage now forming the Malcantone unit was welded to the Lugano unit along the Taverne fault, and that in early Alpine times the Malcantone unit was separated from the thick-skinned Ivrea(-Ceneri) system and incorporated into the Upper Orobic nappe. The present western boundary, the cataclastic Arosio line, continues to the north into the cataclastic zones of the Isone unit. As the latter are fed by splays of the Insubric line, it may be inferred that the Arosio line too was, at least partly, an important dislocation feature of the Insubric phase (compare Figures 15-3, 15-11 and 15-17).

d) The Morcote unit and the Salvatore-Val Cuvia belt

The Morcote unit contains a basement part (Arbostora unit of Schumacher, this volume) west of the Lugano line which is separated from that of the Lugano unit by the San Salvatore-Val Cuvia belt of sediments (Figure 15-11). The complex structure of this belt involves sinistral strike-slip faults as well as thrusts (Leuzinger 1926, Bernoulli et al. 1976). It appears to be, however, an internal and subordinate structure of the Upper Orobic nappe rather than a nappe boundary (compare Figures 15-9 and 15-15). The basement of the Morcote unit, with its extended cover of Permian volcanic rocks forms the core of an asymmetric anticline (**Arbostora anticline**), which plunges axially to the west (Figure 15-10).

e) The Travaglia unit

North of the western part of the Salvatore-Val Cuvia belt the basement, with Ceneri zone lithology and remnants of the Permo-Triassic cover, rises again to the surface in the Travaglia unit (Figure 15-11). The northeastern boundary separating it from the Malcantone unit is purely conjectural; if a fault that passes through Lago di Lugano, joining the Salvatore-Val Cuvia belt, is present, it needs not to be of great importance. Both the Malcantone and Travaglia units, according to the foregoing discussion, are parts of the Upper Orobic nappe. To the west, the sedimentary section becomes more complete (Pizzoni di Laveno, Rocca di Calde). Their structure points to a complicated Alpine deformation history along both the western and southern boundaries of the unit. Along the western boundary the vertical to overturned sediments point to a compressive component along the **Verbania line** (Figures 15-2, 15-10 and 15-11). At the southern boundary the sediments of the Monte Nudo basin were first thrust to the north on a moderately inclined **Monte Nudo thrust.** A subsequent transpressional phase produced a fold and rotated the thrust into a subvertical or even overturned position (Val Cuvia syncline, Figure 15-9b).

A synopsis of kinematics in the Lago Maggiore-Lago di Como segment

In the foregoing discussion of the units, an assessment was made on local data as to their position in the larger-scale Alpine entities (thick-skinned Ivrea system versus thin-skinned Orobic nappes). In conclusion an attempt is made to sketch the kinematics of the emplacement of the Orobic nappes and the underlying Lombardic thrust sheets, and to check its viability by means of a balanced section construction.

Beginning in the north and east with the basement part of the Upper Orobic nappe, it has been found, that it continues into all the units west of the Lugano line, but is separated from the Ivrea-Ceneri complex by a fault zone that in the northeast splays off the Insubric line (Gazzirola fault) and may be traced to the southwest along several intermediate faults into the Cremosina line.

South of the Tesserete-Grona line several complications are found. Beginning in the east at the Lecco line, a radical change in the structure of the sedimentary décollement sheets is observed (Figure 15-6). Instead of the south-vergent Grigne thrust sheets, north-vergent backthrusts at the Grona line characterize the northern margin of the Generoso basin, whose sediments, moreover, are at considerably lower altitude than those of the Grigne. The thrust sheets are detached in the Carnian, and no ramping into deeper levels may be inferred from either surface or seismic data (Schumacher 1994b). Consequently, these backthrusts document a triangle structure, with the basement ramp fold of the Upper Orobic nappe wedged southward into the Carnian interval of the sedimentary pile in front (compare Laubscher 1985). However the surface data are much less constraining than east of Lago di Como, and there is scope for other solutions.

It is particularly the deeper levels that require constraining seismic information. In section C (Figure 15-13; see Figure 15-2 for location) the seismic data in Schumacher (Chapter 10) are combined with the surface data from several authors (Lehner 1952, Vonderschmitt 1940, Bernoulli 1964, Bernoulli et al. 1989, Schumacher 1990, Bertotti 1991 and unpubl. data by Schumacher). They show clear evidence for additional sedimentary décollement units between the Generoso décollement sheets (representing the Orobic nappes) and the top of the autochthonous basement at about 14 to 15 km depth, which continue to the south into the Lombardic (Middle to Late Miocene) frontal thrust sheets of the Milan belt (Pieri & Groppi 1981, Cassano et al. 1986).

A correlation of the individual thrusts in the Generoso area (profile C) with those east of Lago di Como (profile D, Figure 15-7a) remains somewhat arbitrary, although the following quantitative considerations provide some suggestions. The backthrusts at the Grona line produced a shortening of about 15 km, of roughly the same magnitude as that of the Upper Orobic nappe and probably coeval with it (b in Figure 15-8). Subsequently – if thrusting pro-

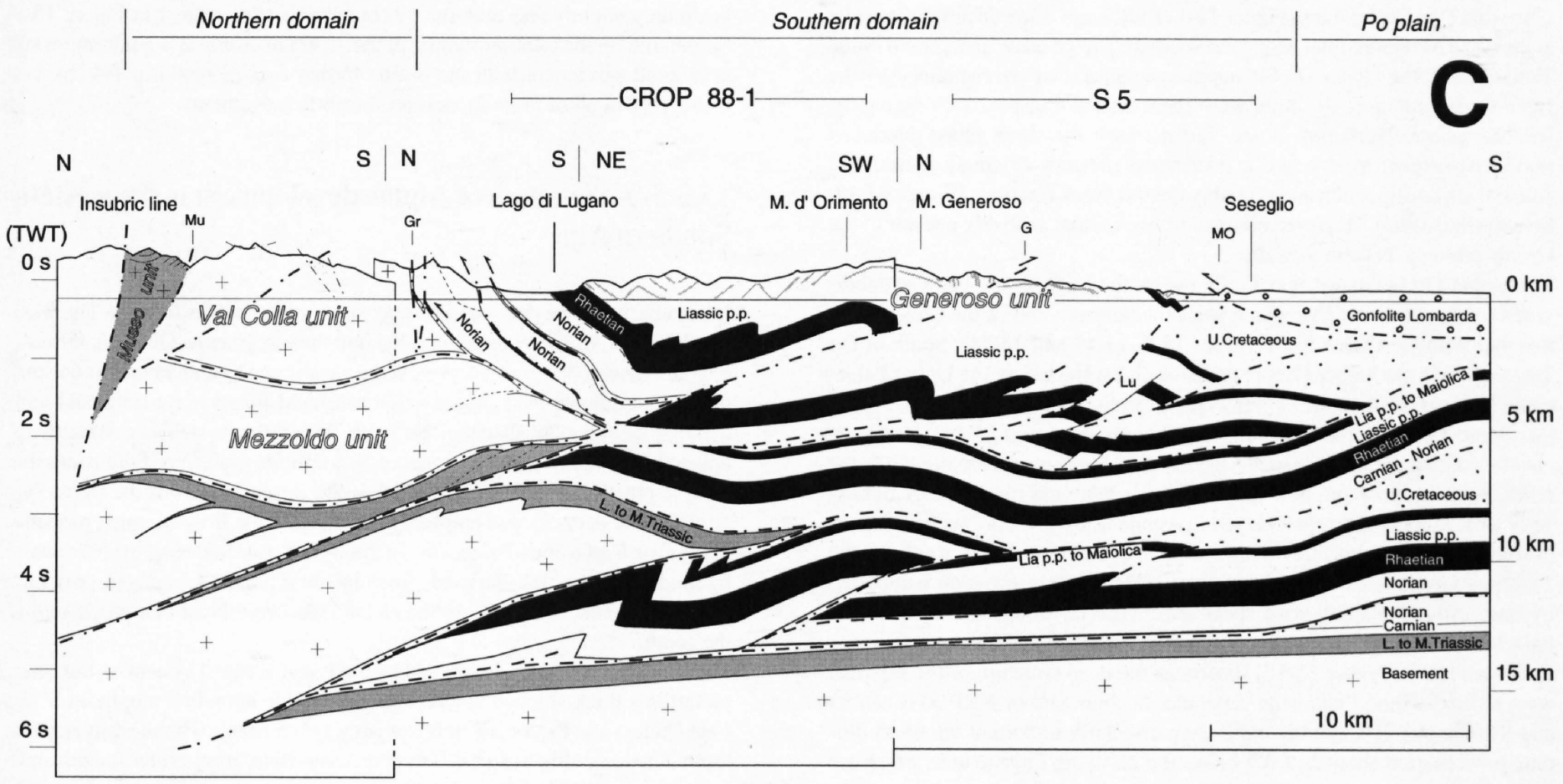

Figure 15-13
Cross section C through the Southern Alps between Lago di Lugano and Lago di Como following the NRP 20 and CROP seismic lines across the Generoso area (see Figure 15-2 for location). G: Generoso thrust; Gr: Grona fault; Lu: Lugano fault system; MO: Monteolimpino backthrust; Mu: Musso fault.

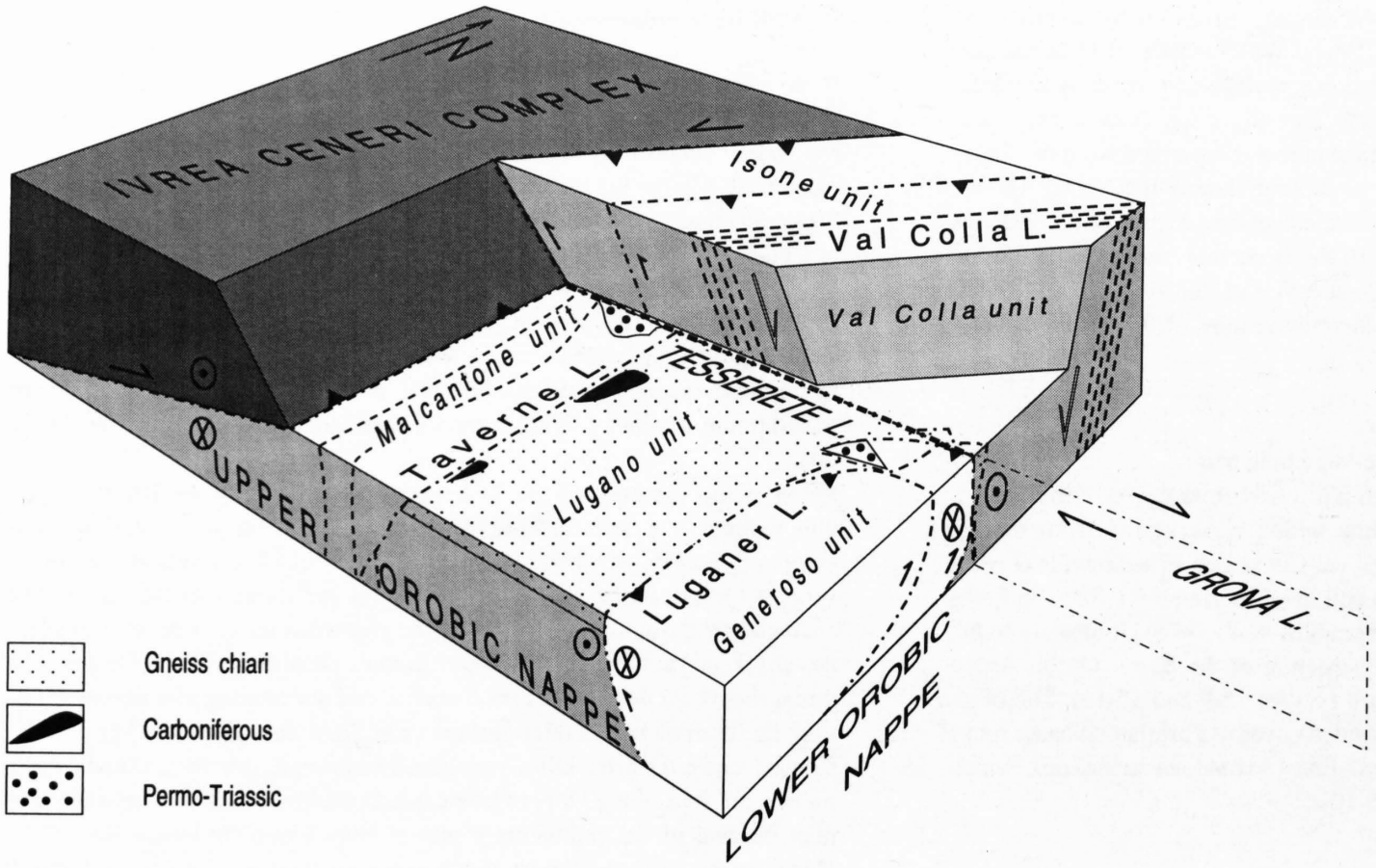

Figure 15-14
Schematic block diagram of the Tesserete area. North of the Tesserete line the Ivrea-Ceneri complex was wedged below or into the Upper Orobic nappe, south of the Tesserete line the Ivrea-Ceneri complex was thrust over the Upper Orobic nappe.

ceeded in sequence – décollement of the Generoso basin was completed with south-vergent frontal structures, contemporaneously with the motions of the Lower Orobic nappe east of Lago di Como (c in Figure 15-8). Finally backthrusting of the Oligo-Miocene Gonfolite Lombarda along the Monteolimpino fault (MO in Figure 15-10; Bernoulli et al. 1989) documents frontal wedging (a triangle structure) in the Lombardic phase. No attempt is made to correlate this and the deeper, seismically documented parts of the Lombardic system of the central segment with those of the eastern segment.

At the Lugano line the structure again changes appreciably. This Mesozoic fault zone was reactivated in various ways. On the eastern side, décollement and backthrusting of the Generoso basin sediments end, which requires a sinistral transfer in the sediments. On the western side the basement of the Upper Orobic nappe and frontal décollement are sinistrally transferred about 20 kilometers to the south. New internal structures of the nappe such as the Arbostora anticline and the San Salvatore-Valcuvia sedimentary belt further testify to an independent development of the western flank. This part of the Upper Orobic nappe, with some variations in internal structure, may be followed to the west as far as the Cremosina-Verbania-Luino-Arosio-Tamaro-Gazzirola (Val Colla) lines (Figure 15-11), although some uncertainties exist at the Lago Maggiore line. Along the southern part of these lines, south of the Tamaro fault, the Upper Orobic nappe was apparently overwhelmed by the Ivrea-Ceneri complex by southeast-vergent dextral transpresssion during the Insubric phase. Northeast of the Tamaro fault the same phase produced northwest-vergent thrusts and a distributed network of small dextral and sinistral strike-slip faults and probably dextral block rotations (Figure 15-17, Schumacher 1995). However, sinistral transpression, probably a result of the Orobic phase, is present as well.

The Upper Orobic nappe is not only cut by the Lugano line but also subdivided by the Tesserete line which joins the northern end of the Lugano line together with the Grona line (Figures 15-6, 15-11 and 15-14). South of the Tesserete line, the Upper Orobic nappe is characterized by the Upper Palaeozoic Gneiss Chiari nappe, which is not present north of the line, except for the topmost parts of the Val Colla unit (Figures 15-3 and 15-14). It may be concluded, that the line represents a considerable basement flexure, up to the north, but it is uncertain, how much of this is inherited (pre-Alpine) and exactly what kinematical role it played in Alpine tectonics. Inasmuch as dextral movements in the Insubric phase seem to penetrate as far south as the Tesserete-Grona lines, a certain amount of dextral transpression (supported by observations of small-scale shear sense criteria) would not seem to be a far-fetched conjecture.

Cross-section B (Figure 15-15) illustrates the deep structure of the segment west of the Lugano line, using seismic reflection data of NRP 20 (lines S3 and S7, Chapter 10). Among them are particularly important the north-dipping reflections at about 2s TWT below the flat-lying Lugano unit, which are discordant to the horizontal reflections immediately below, and the south-dipping reflections between 0.5 and 1s TWT below the southern limb of the Arbostora anticline, which suggest an additional, deeper ramp-fold (Lower Orobic nappe).

Geometry and kinematic viability of profile B were tested by forward modeling of the balanced cross-section (Figure 15-16). For balancing, bed length and thickness were generally preserved, and shear was assumed parallel to bedding. However, where ramp-folds are moved over more than one ramp additional simple shear-systems had to be used (area balance). Such shear-systems would appear also reasonable in view of the fact that basement units with pre-existing, generally not horizontal layering and foliation were deformed.

The model shows 14 km of shortening for the Upper Orobic nappe, which is of the same order as that in the profiles farther east (Figure 15-8, Schönborn 1992b). For the Lower Orobic nappe 41 km of shortening were used, assuming that a larger portion of Lombardic shortening than farther east followed this thrust system. The sum of shortening for stages 2 and 3 in profile D (Figures 15-7b, 15-8), however, is of the same order (44 km in profile D, Schönborn 1992b). Finally, a very simplified solution was chosen for the detachment of the Milan belt, constrained mainly by the deep-seated ramp-fold suggested by reflection data at about 3s TWT (Schumacher, Chapter 10, compare also Figure 15-8). The 17 km shortening postulated for this stage are again only slightly less than the 19 km proposed for stage 4 in Figure 15-8. Summarizing, the total shortening of the 72 km in profile B is a minimum and is in good agreement with the results farther east (Schönborn 1992b). Not considered in all of these models are Insubric movements.

15.3.5 A summary of Alpine development in the western Southern Alps

In summary, Alpine development may be characterized as follows. The western Southern Alps may be subdivided into three segments. Of these, the eastern one, though complex enough, is the easiest one to understand. It consists of a pile of thin-skinned nappes – thin basement slivers in the north and sedimentary décollement sheets in the south. This thrust system is compartmentalized by a number of approximately N–S striking transverse fault zones that involve reactivated Mesozoic normal faults. An older part of the thrust system (Orobic nappes) was emplaced before the Late Eocene, most probably in the Late Cretaceous-Paleocene. In the west it was deformed to some extent by the Late Oligocene-Early Miocene Insubric phase. A younger, post-Late Oligocene, most probably Middle to Late Miocene thrust belt was added in the south.

The western segment is dominated by the Ivrea(-Ceneri) system, in our interpretation a thick-skinned assemblage of tectonic units first emplaced in the Late Cretaceous-Paleocene. It is probably synchronous with the thin-skinned Orobic nappes, although of different tectonic style. It was subsequently subjected to a series of additional deformations, particularly during the Late Oligocene-Early Miocene Insubric-Helvetic phase (Insubric Ivrea-Ceneri complex). The exact pre-Miocene shape of the assemblage is difficult to establish in detail, but its containing a narrow belt of lower crust to upper mantle rocks

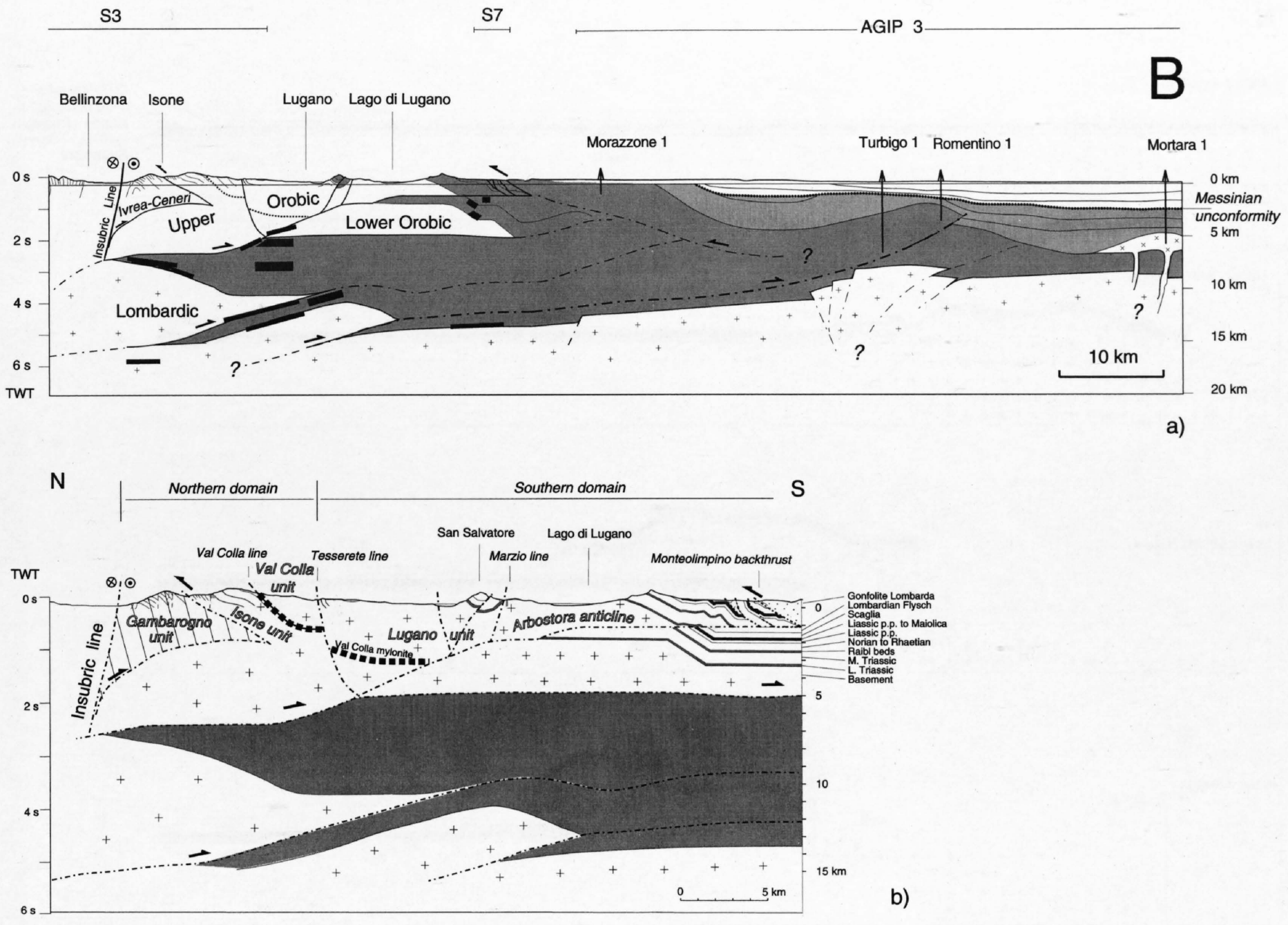

Figure 15-15
Cross section B through the Southern Alps between Lago Maggiore and Lago di Lugano along the NRP 20 seismic lines S3 and S7 and the AGIP seismic line 3 (Pieri & Groppi 1981) (see Figure 15-2 for location).
a) The overall section with the main seismic reflections from the upper crust (dark bands; Schumacher, Chapter 10). The pre-Messinian sediments are shown in grey.
b) The northern part of the section. Deep-seated, undistinguished sediments below the Orobic basement nappes are shown in grey. Compare kinematic model of Figure 15-16.

suggests some sort of flower structure. In subsequent stages it was cut off from its underpinnings and is now an allochthonous part of the Late Miocene orogenic lid of the Alps (Figure 15-9a).
The central or intermediate segment is the most difficult one to unravel as the thin-skinned eastern nappes and the thick-skinned Ivrea-Ceneri system meet and interfere. The original, Late Cretaceous-Paleocene interference pattern was superseded by the Late Oligocene-Early Miocene splinters of the Insubric line which introduced SW-trending, SE-vergent thrusting in addition to transpression and probable rotations at the boundary with the western segment. The basement structures between Lago di Como and Lago Maggiore may be attributed to the Upper Orobic nappe, sinistrally transferred to the south along the Lugano line. The Mesozoic sediments in the south correspond mostly to the sedimentary décollement parts of the Orobic nappes, although some of the original cover sediments of the Upper Orobic nappe are preserved, particularly in the San Salvatore-Val Cuvia zone and the Arbostora anticline.

15.3.6 Timing of Alpine events

In the Southern Alps, direct dating of orogenic movements by postorogenic sediments and structural unconformities (Figure 15-18) is only possible in the border regions of the thrust-and-fold belt to the south where Upper Miocene deposits seal the frontal thrusts of the Milano belt (Pieri & Groppi 1981). However, "middle" Cretaceous to Upper Eocene terrigenous flysch and other deep-water mass flow deposits document ongoing deformation to the north, in the Austroalpine area and also in the Orobic zone (Figure 15-18, Castellarin 1976, Bersezio & Fornaciari 1988, Bernoulli & Winkler 1990). Synorogenic sediments of the Oligo-Miocene foreland basin (Gonfolite Lombarda, Gunzenhauser 1985, Gelati et al. 1988) reflect uplift of the Central Alps during the Insubric phase and movements in the Southern Alps.

Lombardian Flysch

Unconformities and chaotic deposits in the Upper Cretaceous flysch sequences of the Bergamasc Alps point to large-scale submarine erosion and mass wasting. According to Bersezio & Fornaciari (1988), these deposits are related to growing structures within the Lombardian flysch basin which was part of the southern foreland of the Cretaceous orogeny in the Southern Alps. However, in the western Southern Alps, the distinction between Late Cretaceous/ Early Tertiary and Late Tertiary structures heavily relies on circumstantial evidence and correlation with the Adamello-Giudicarie area where stratigraphical relationships are clearer.

Orobic phase

Dating of the Orobic thrust systems of the Bergamasc Alps (Thrust systems I, IIA and IIB, Schönborn 1992b) is possible to some extent in the area of the Adamello intrusion but has to be extrapolated to the west. The Adamello intrusions are dated 43 Ma (Middle to Late Eocene) to 30 Ma (Middle Oligocene) with a general younging of the intrusions from S to N (Del Moro et al. 1983). Two periods of major deformation are separated by the intrusions. Thrust system I (Gallinera, Porcile, Orobic and associated thrusts) is older than the Adamello intrusions, since these have cut the associated structures. Folding and schistosity along the Gallinera thrust are overprinted by contact metamorphism (Cornelius & Cornelius-Furlani 1930, Cassinis & Castellarin 1988), and folds in the Middle Triassic of thrust sheet 1 are cut and deformed by the intrusions (Brack, 1981, 1984). Andesitic dikes cutting the basal thrust and the Middle Triassic of thrust sheet 1 near the Presolana mountains are dated 64 Ma (K/Ar on groundmass and amphibole, Zanchi et al. 1990). Lardelli (1981) obtained still older ages of 80 and 96 Ma (K/Ar on amphibole) on dikes near the Insubric line. Dikes of the same type cut the Porcile

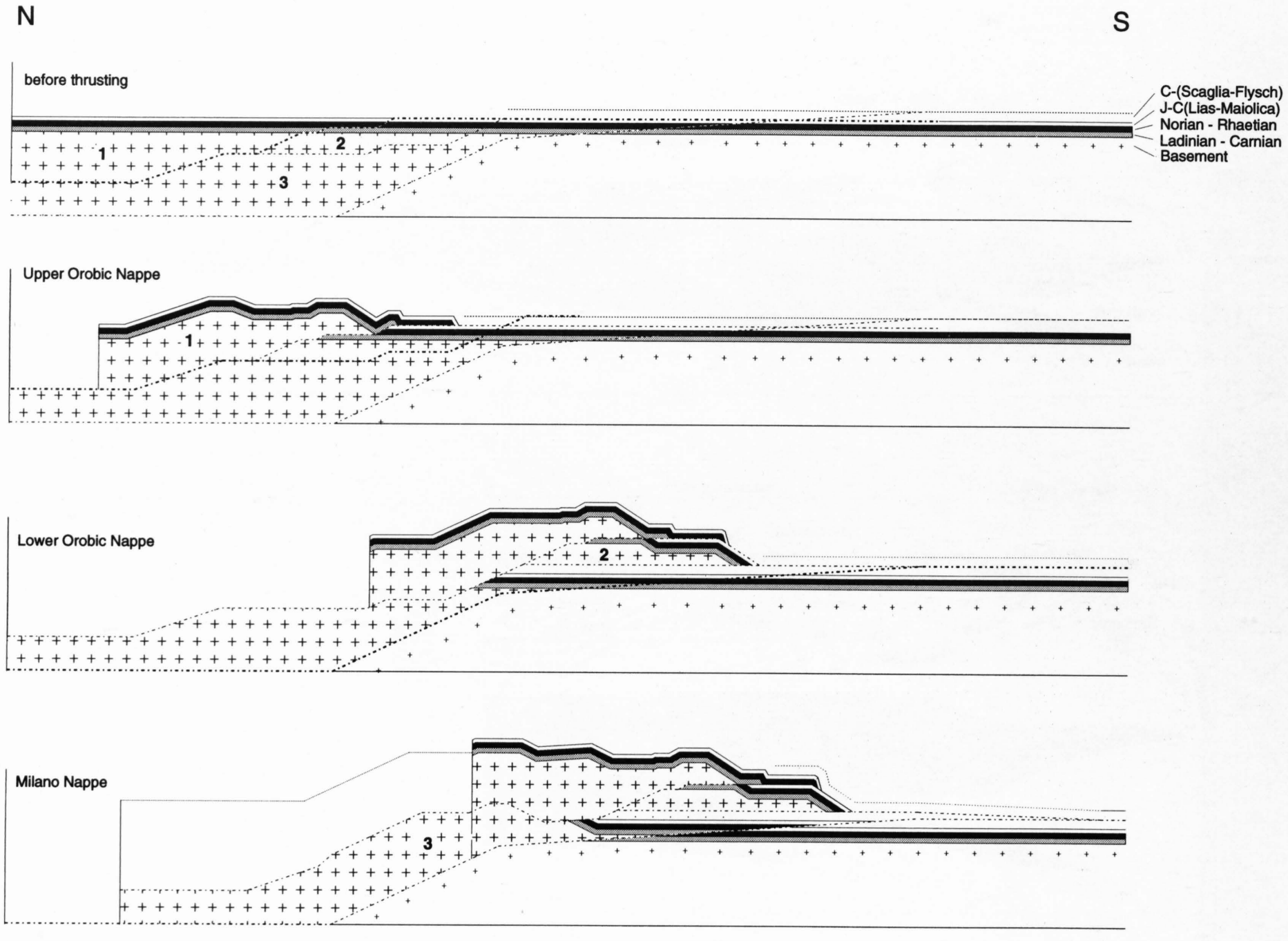

Figure 15-16
Kinematic model for the evolution of the Southern Alps along cross section B (Figure 15-15).

line (thrust system I) nearby. Similar but not yet dated dikes cut various system 1-thrusts and folds in the Permian and the basement, e. g. near Passo Cigola (Dozy 1935a). Therefore, thrust system I was presumably active during the Late Cretaceous.

Following the arguments in the previous paragraphs, the Upper Orobic nappe extends westward to the Val Colla, Lugano, Malcantone-Travaglia and Morcote units. According to our model, obduction of the Ivrea zone occurred in a sinistrally transpressive flower structure that was largely contemporaneous with Orobic thrusting (Laubscher 1991).

The Cedegolo anticline (of thrust system IIA, cf. Figure 15-2) deformed thrust system I and consequently is younger. This younger thrust system IIA was also active before the intrusion of the Adamello since the Cedegolo anticline is cut by the pluton. Therefore, its activity must fall into the Late Cretaceous to Middle Eocene interval. During this interval, from Maastrichtian to Late Eocene times, small submarine fans developed in the area of the southern part of the Lower Orobic nappe (Piano di Brenno and Tabiago Formations, Kleboth 1982). First-cycle terrigenous clastics are conspicuously rare. We therefore may speculate that the growth of thrust system IIA mainly occurred contemporaneous with the deposition of the (upper part of) Upper Cretaceous Lombardian Flysch but may have extended into the Maastrichtian to Middle Eocene interval.

Dating the emplacement of the Upper Orobic nappe in the west (cross sections A and B) meets with considerable difficulties. In the Morcote unit, thrusting appears to be younger than Turonian, the age of the flysch overlying the middle Cretaceous pelagic sequence without an apparent unconformity (e. g. S. Pietro di Stabio, Gropello; Bichsel & Häring 1981). Scattered, isolated outcrops south of Mendrisio (Prella) and Lago di Varese document deep-water deposits of Late Cretaceous age as young as Campanian (Bernoulli et al. 1987, Barnaba 1989). The tectonic relationship of these outcrops to the Upper Orobic nappe are not clear, nor are those of the Upper Eocene Ternate Formation in the same areas (Bernoulli et al. 1987, 1988). This latter formation, a bioclastic submarine fan deposit, is dominated by shallow-water bioclastic material and by clasts from older deep-water sediments (as young as Middle Eocene) exposed along a northern basin slope or in submarine valleys (Bernoulli et al. 1988). These Upper Cretaceous to Upper Eocene sediments, together with the Oligo-Miocene deposits of the Gonfolite Lombarda, are involved in later thrusting and folding (most obviously in the Lisanza well north of Sesto Calende near the southern end of Lago Maggiore). Whether the late Upper Cretaceous to Upper Eocene deposits are unconformable, syntectonic deeper marine deposits overlying the Upper Orobic nappe or whether they belong, together with the Gonfolite Lombarda, to the external thrust sheet 2B of the Lower Orobic nappe system remains unclear (cf. Figure 15-11).

Insubric phase

The outcrops of the Gonfolite Lombarda (Gunzenhauser 1985, Gelati et al. 1988) near Como are one of the key areas for dating the tectonics (Bernoulli et al. 1989). Middle Oligocene hemipelagic marls and fine grained turbidites with sparse deep-water conglomerates (Chiasso Formation) are unconformably overlain by Chattian to Aquitanian deep-water conglomerates (Como Formation) containing pebbles derived from the Central Alps and the Bregaglia intrusion (Giger & Hurford 1989, Giger 1991). Pebbles of lithified Upper Eocene sediments (Ternate Formation) in the Oligocene conglomerates (Villa Olmo Conglomerate and Como Formation) suggest more or less continuous growth of thrusts through the Oligocene-Early Miocene interval. The clastic content of the Como Formation also documents rapid uplift of the Central Alps contemporaneous with dextral strike-slip along the Insubric line (e. g. Schmid et al. 1987, 1989, Laubscher 1990, Giger 1991). Younger, Middle to Late Burdigalian coarse grained deposits (Lucino Formation, Gelati et al. 1988) overlie the Como Formation with an progressive unconformity (Ge-

lati et al. 1991), they contain also South-Alpine basement clasts (Giger 1991) and reworked material from the Lower Oligocene Chiasso Formation (Bernoulli et al. 1989) and record contemporaneous thrusting in the South Alpine area, not only along the Insubric line.
Movements, contemporaneous with and linked to those along the Insubric line, include the pull-apart along the Musso line (Musso unit in Figure 15-11) and the E- to SE-vergent emplacement of the Ivrea-Ceneri complex (Figure 15-17, Schumacher 1995). The latter may be quantified approximately with the 15 km of dextral displacement along its southern boundary, the Cremosina line. Farther NE, the thrust front follows the Verbania line (Figure 15-11), and SE-vergent thrusts between Lago Maggiore and the Tesserete line (Figure 15-11). To the N, these are replaced by NW-vergent thrust faults that join the pull-aparts along the Insubric line. East of Lago di Como, the deformations of the Insubric phase seem to be concentrated mainly along the Insubric line itself and nearby steep faults (e. g., along cross-section E, Figure 15-7b).

Lombardic phase

Thrust system IIB, the thrusting and folding of the Trompia high (Figure 15-7b), is closely linked to the Giudicarie line cutting and deforming the northern part of the Adamello intrusive complex. In addition, the external thrusts of this system deformed Paleocene and Eocene deposits in the western Bergamasc Alps and in the Brianza area and along the Giudicarie line (M. Sabbion area, Castellarin et al. 1993). In the lower Val Seriana, thrusts belonging to system IIB appear to deform dikes emplaced during the Eocene (50 Ma Zanchi et al. 1990, cf. Berra et al. 1991). Adjacent to the Giudicarie line, near Lago di Garda and farther north, hemipelagic marly limestones and marls and bioclastic turbidites of Paleocene to Oligocene age appear not to be influenced by contemporaneous thrusting (e. g. Oligocene Argille marnose di Ponte Arche, Castellarin 1972). At M. Brione (Luciani 1989) and near Peschiera (Zinoni 1951, Cita 1955) marine deposition lasted up to the Early Miocene. Both localities are within thrust sheets 2B and 4. Middle Miocene sediments commonly are lacking, probably due to Messinian erosion, but where they are preserved (e. g. M. Orfano Bresciano, Cita 1954) they consist mainly of conglomerates. The sedimentary record of the Giudicarie area therefore suggests that most of the post-Adamello tectonics is not older than Miocene. Tectonic arguments favour (a Middle to Late) Miocene activity, because the Giudicarie line cuts the Oligocene-Early Miocene Insubric line and presumably stopped its activity.

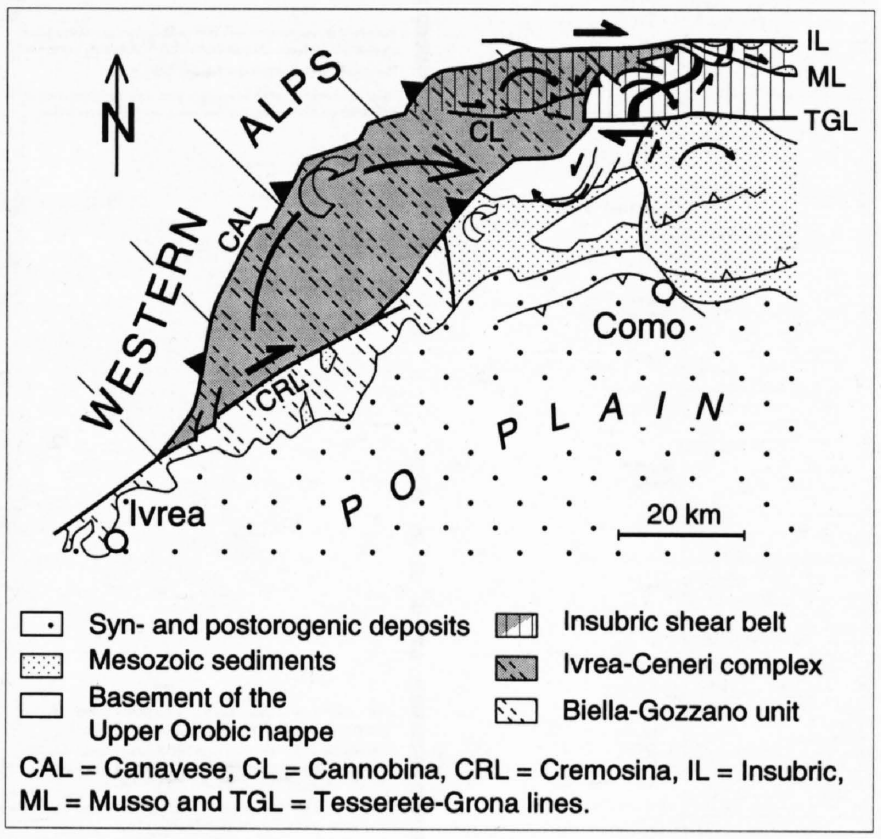

Figure 15-17
Sketch-map of the northwestern corner of the Southern Alps showing the kinematics (arrows) attributed to the Insubric phase (modified after Schumacher 1995). The Ivrea-Ceneri complex was pushed between sinistral and dextral transfers toward SE and rotated around horizontal and vertical axes. To the N it was incorporated into the dextral, brittle Insubric shear belt. The latter apparently developed between pre-existing boundary faults (CL, TGL and IL) and accommodated dextral simple-shear and pure-shear by synthetic Riedel shears, clockwise block rotations and transpressive wedging along antithetic Riedels.

In the west, the outcrops of the Gonfolite Lombarda Group are part of the external thrust sheet 2B, i. e. part of a western analogue of the Gerola unit (Figure 15-7a) deformed subsequently by thrust system III (Schönborn 1992b). Growth of this thrust system may therefore fall into the Middle to Late Miocene interval.
Thrust system IV, forming the Milano belt, is Middle to Late Miocene in age. This is well documented by reflection seismics and boreholes in the Po basin (Cassano et al. 1986, Pieri & Groppi 1981, Pieri 1983). Folded and thrust Middle Miocene and older deposits are unconformably overlain by Messinian and Pliocene strata (Messinian unconformity). Other Miocene unconformities are not easy to localize exactly in the stratigraphic column, because commonly no cores have been taken in the AGIP-wells. It may be noted that the seismically conspicuous Aquitanian deposits outcropping along the northern margin of the Po plain are buried up to more than 6 km below sea level inside the basin (Pieri & Groppi 1981). This relief has to be explained by post-Early Miocene tectonics. In the French-Italian ECORS-CROP deep seismic profile Roure et al. (1990) postulated a Burdigalian unconformity above folded and thrust Aquitanian. However, this location is in the foredeep of the Apennines, where a Burdigalian unconformity is well-known (Gelati & Gnaccolini 1982, Schumacher & Laubscher 1996).
Thrust system III, the out-of-sequence thrust system folding the Flessura Frontale between Lago d'Iseo and the Lugano fault also is older than the Messinian but could be younger than thrust system IV. A relatively young age is also suggested by the youthful morphology of the Flessura Frontale. The conglomerate fill of presumably Messinian canyons (Bini et al. 1978) cuts across the folds related to thrust system III near Morbio in the southern Ticino (Vonderschmitt 1940). In the same area the western continuation of the Flessura Frontale (a system III-structure) is wedged beneath the Oligo-Miocene Gonfolite Lombarda (Bernoulli et al. 1989). Burdigalian to late Tortonian therefore is the time bracket for the activity of this thrust system. Pliocene marine marls occurring at approximately 300 m altitude in some of the South-Alpine valleys indicate that the Southern Alps were uplifted since then. This may be explained as the expression of a peripheral bulge of the Northern Apennines or as due to the isostatic uplift of the Alps continuing to this day.
Summarizing, three not everywhere sharply separated periods or phases of compressional activity can be recognized. The first (Orobic) is pre-Adamello (pre-middle Eocene), presumably starting in the Late Cretaceous, and comprises the thrust systems I and IIA. The Oligocene to Early Miocene Insubric deformation plays an important role in a belt along the Insubric line (Schumacher 1990, 1995). The third (Lombardic) is post-Adamello (post-middle Oligocene), presumably mainly Middle to Late Miocene. It consists of the thrust systems IIB, III and IV, which all merge in the Giudicarie belt. The Late Eocene "phase" of the Central Alps cannot be correlated with major compressional features in the central and eastern Lombardic Alps on the base of the data available at present.

15.4 Summary and conclusions

With the data now available it is possible, for the first time, to sketch what we think is a coherent and plausible picture of the development of the Southern Alps between the Giudicarie in the east and Ivrea in the west (western Southern Alps). The data do not yet permit, however, construction of a definite model.
The Variscan metamorphic basement of the Southern Alps was affected by Late Palaeozoic transtensional tectonics accompanied by magmatism at different crustal levels. In Triassic time large carbonate platforms established with the proceeding transgression from the evolving Hallstatt-Meliata-Vardar ocean. Extension during Norian to Liassic rifting, preceding opening of the Jurassic-Cretaceous Tethys ocean, formed the overall N–S trending basins of the South-Alpine continental margin and reactivated partly the Late Palaeozoic E- and ENE-trending troughs as transfer zones. During the Middle Jurassic to Early Cretaceous deep pelagic sediments reflect gradual deepening of the sea by post-rift thermal subsidence.
In Late Cretaceous to Tertiary time the South-Alpine continental margin was converted into the fold-and-thrust belt of the Southern Alps. Along the northern edge of the Adriatic indenter the dextrally transpressive, thin-skinned Orobic nappes developed, whereas along the western edge sinistral transpression may have caused formation of the thick-skinned Ivrea system with obduction of lower crustal and upper mantle rocks. The two different structural edifices interfere at the northwestern corner of the Southern Alps where the reflection seismic profiles of NRP 20 are situated. In the Lombardian segment of the Southern Alps a total shortening in N–S direction of the order of 100 km was accommodated from Late Cretaceous until Late Miocene time. Mid-Eocene to Early Oligocene magmatism allows to distinguish between a pre- and a post-magmatic nappe transport. Growth of the fold-and-thrust belt

is reflected by the southward shift of the depocenter of the Upper Cretaceous to Middle (?Late) Miocene syn-orogenic sediments.

Alpine deformation in the Southern Alps was largely influenced by older, pre-existing tectonic elements, namely Permian and Late Triassic-Liassic extensional and transtensional faults. The east-northeast trending Permian faults appear to have been, at least partially, reactivated as sinistral transfer faults during the Late Triassic-Liassic. They also have become the site of Alpine thrusting. The Late Triassic-Liassic normal faults originated during rifting preceding opening of the Jurassic-Cretaceous Tethys ocean to the north and west; they trend approximately north-south (except for an important population of E to NE and less frequent NW striking faults) and were reactivated during Alpine compression as transverse zones and lateral ramps.

In the western Southern Alps, Variscan basement rocks and Mesozoic-Tertiary sediments are involved in large-scale Alpine thrusting and folding. East of Lago di Como, surface geology and resulting kinematic analysis allow the reconstruction of four thrust systems that generally prograded from the interior of the chain (thrust systems I, II and IV) but also include out-of-sequence thrusting (thrust-system III). West of Lago Maggiore, the surface geology is dominated by the thick-skinned Ivrea-Ceneri system that underwent a complex history which began with obduction in the Late Cretaceous and continued into the Late Oligocene to Early Miocene with transpression along the Insubric line. Between these two segments where the reflection seismic profiles of NRP 20 are situated, NE–SW-trending basement-rooted structures interfere with E–W-trending ones. Basement outcrops southeast of the thick-skinned Ivrea-Ceneri system are found to belong to the thin-skinned Upper Orobic nappe.

Early Alpine thrusting in the Southern Alps (Orobic phase, thrust systems I and IIA in the eastern segment) predates the Late Eocene-Oligocene Adamello intrusion and probably was contemporaneous with the deposition of Upper Cretaceous flysch and Paleocene-Eocene minor resediments. Late Oligocene to Early Miocene uplift of the Central Alps and the western Southern Alps during transpressional movements along the Insubric line (Insubric phase) and southward progradation of the thrust belt during the Miocene (Milano belt, Lombardic phase) are reflected by the growth and southward progradation of the deep sea fans of the Gonfolite Lombarda Group. A Messinian unconformity constrains the age of the youngest movements.

Acknowledgments

We thank M. Grünenfelder and V. Köppel for reading early versions of this manuscript, A. Bernasconi, G. Bertotti, P. Casati, R. Fantoni, and A. Valdisturlo for fruitful discussions and A. Castellarin and S.M. Schmid for critical review of this paper. M.E.S. appreciated several field trips together with A. Boriani, L. Burlini and M. Handy in the area west of Lago Maggiore. Financial support from the Swiss National Science Foundation (grant numbers 20-4798.85 and 4.903-0.85.20) is gratefully acknowledged.

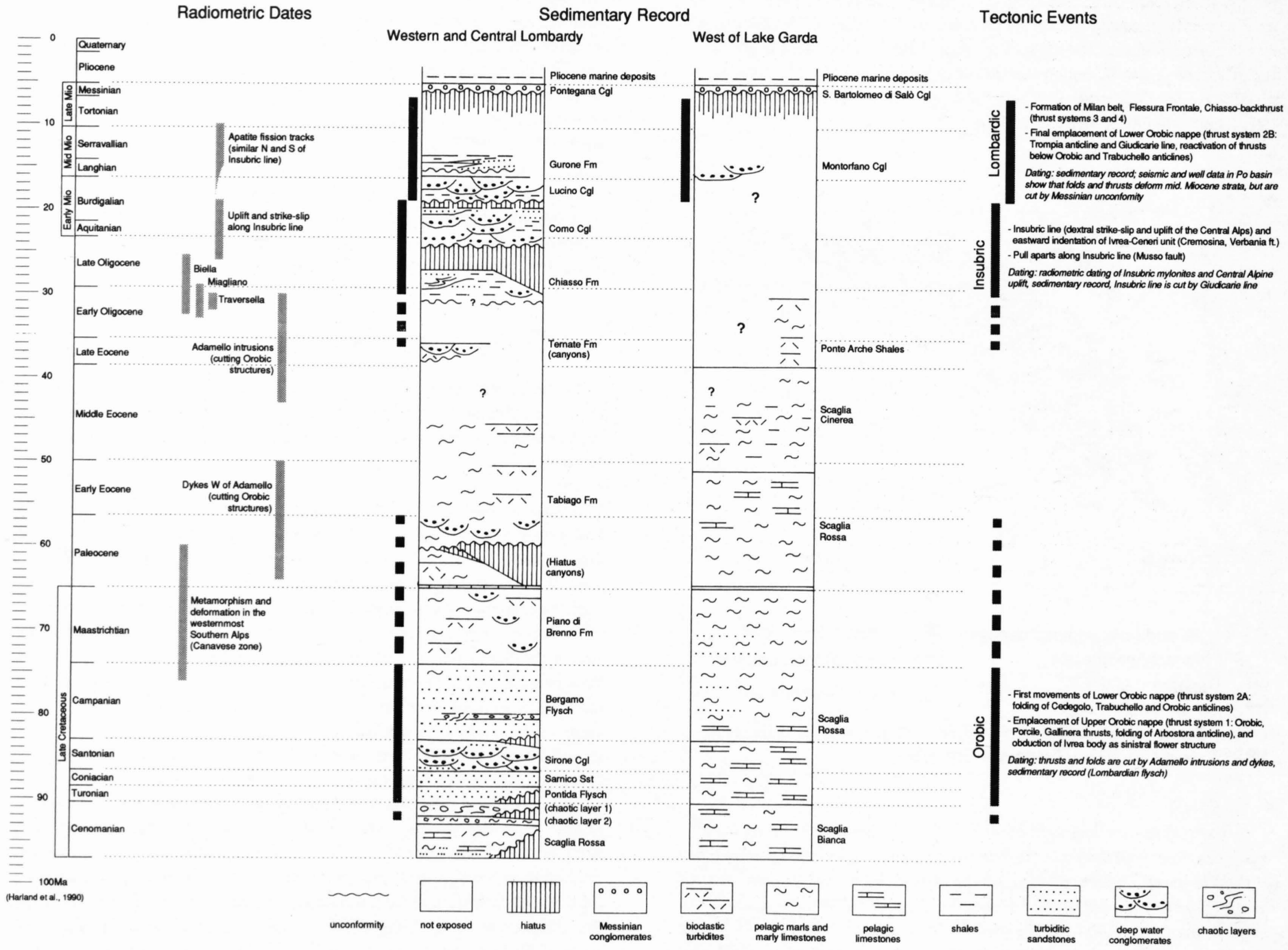

Figure 15-18
The sedimentary record, radiometric data and tectonic events in the Lombardic Alps. Data from various sources mentioned in the text. The radiometric time-scale used is from Harland et al. (1990).

16 Geologic framework and structural evolution of the western Swiss-Italian Alps

A. Escher, J.-C. Hunziker, M. Marthaler, H. Masson, M. Sartori & A. Steck

Contents

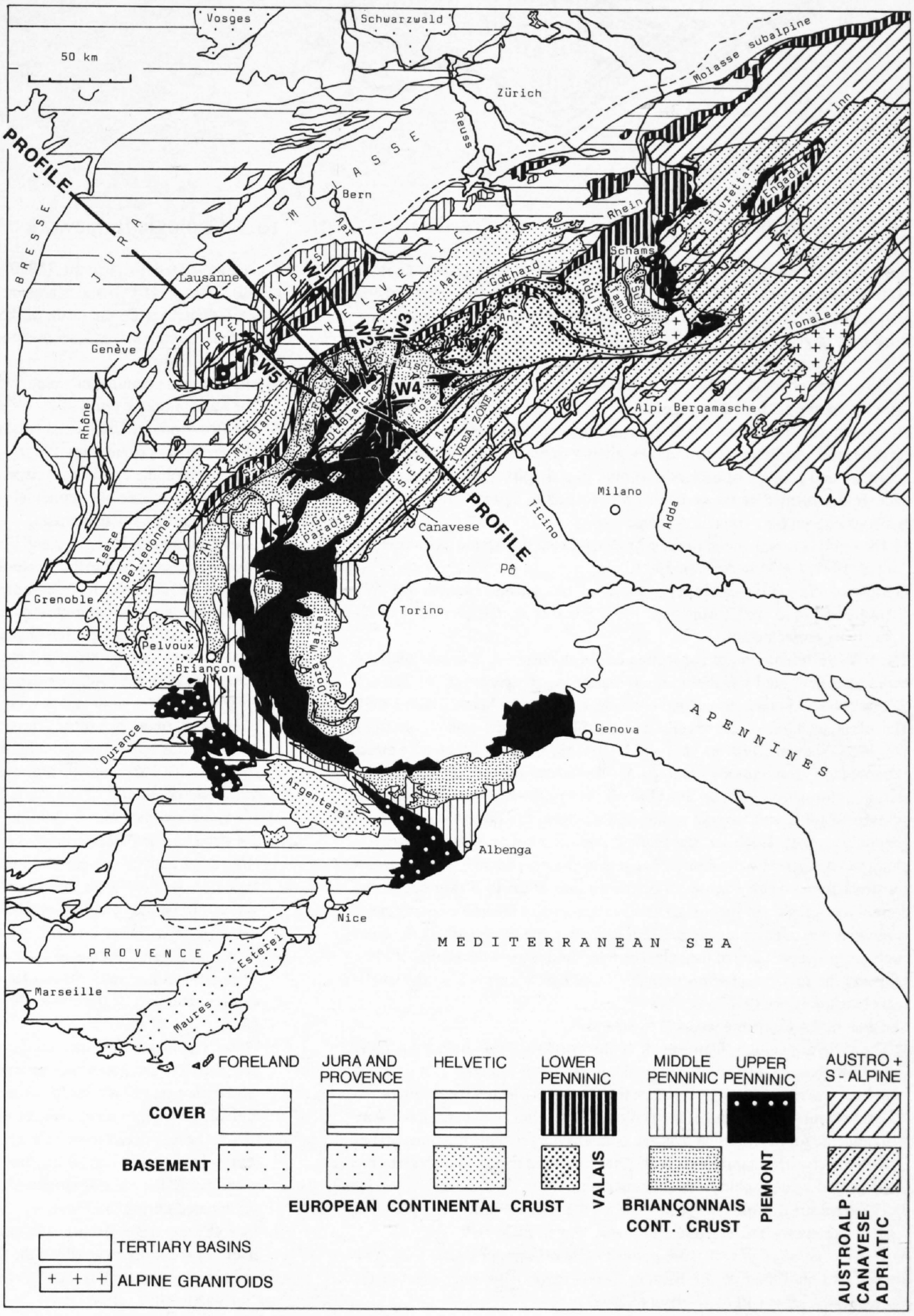

Figure 16-1
Simplified structural map of the Western Alps with location of the geologic profile on plate 16-1 and the seismic profiles W1–W5. An attempt is made to underline the two major units of oceanic origin (Valais and Piemont).

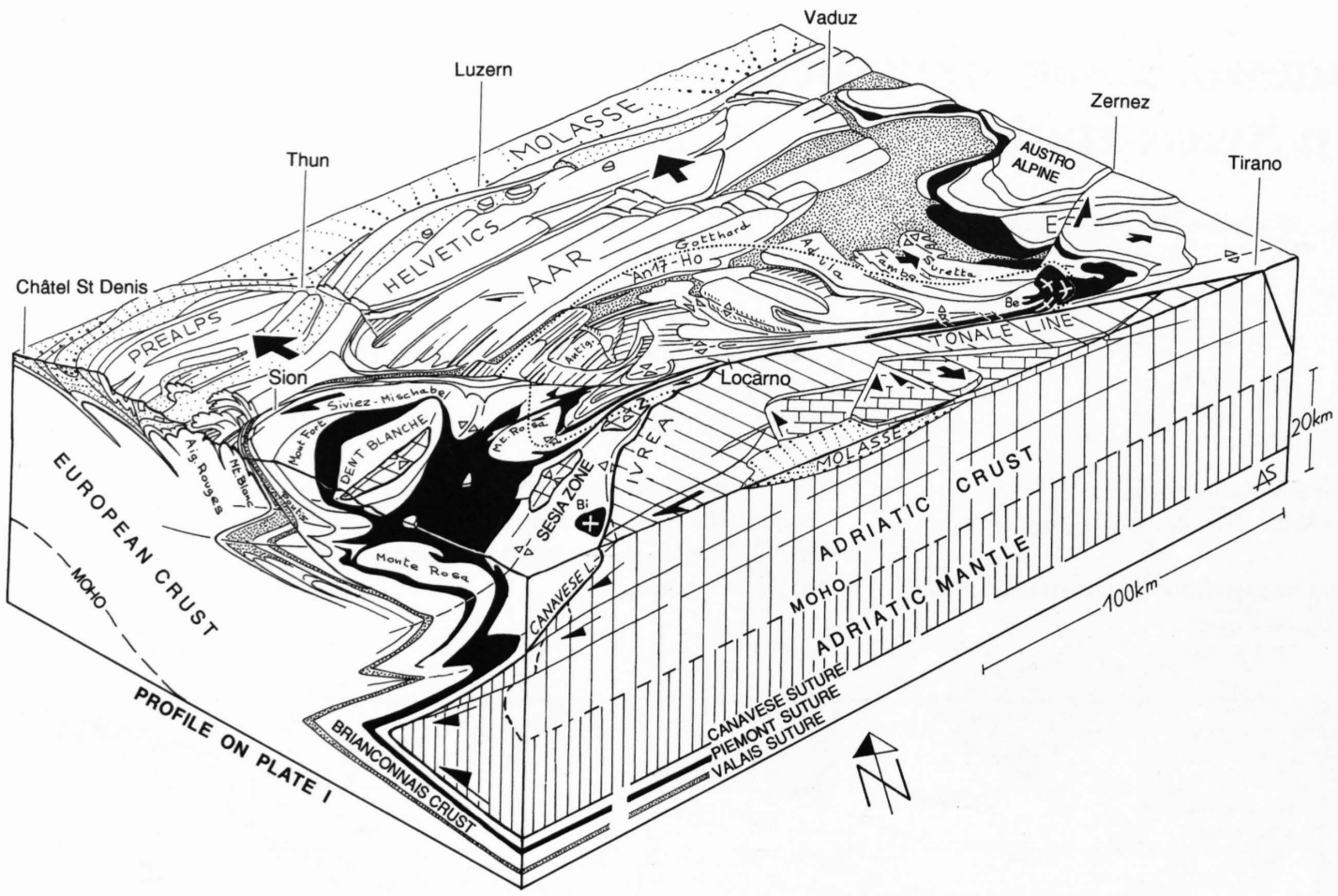

Figure 16-2
Block diagram showing the main geologic units in the Western Swiss-Italian Alps and their relations to the major structures in the east (modified after Steck & Hunziker 1994).

16.1 Introduction

Since the early revolutionary investigations by famous geologists as Gerlach (1869), Schardt (1907), Heim (1921–1922), Argand (1911, 1916) and Lugeon (1914), the knowledge of the Western Swiss-Italian Alps has been steadily refined by a large number of field geologists. The deep seismic survey of the NRP 20 program is the first reflection seismic study that has been undertaken in this region of the Alps. For the first time it is now possible to control to some extent the geometric extrapolations and reconstructions of the deep Alpine structures. The actual result, though fundamentally not much different from Argand's brilliant reconstruction, gives a better knowledge of the exact geometry and geology of each Alpine unit. In a simplified way part of these data are represented on the geologic cross section of Plate 16-1. Its location has been chosen for two main reasons:

1) The profile crosses one of the best known parts of the Alpine chain (Escher et al. 1987, 1993, Steck et al. 1989).
2) Most of the geological interpretations of the seismic profiles W1–W5 (Marchant et al. 1993, Marchant 1993, Steck et al., Chapter 12) can directly be projected onto it.

The NW–SE orientation of the section has been chosen to coincide with the major stretching and translation direction during the paroxysm of Tertiary deformation (D I phase according to the classification by Steck, 1984, 1990). The exact location of the profile and its relation to the seismic sections W1–W5 is shown in Figures 16-1 and 16-3. It has been constructed by direct extrapolation from surface outcrops and by lateral projection of field and seismic information from up to 25 km off the profile. Because of often non-cylindrical folds and varying trends and plunges, the projection paths are generally curved. However, the marked Alpine relief and the strong axial plunges, together with the remarkable seismic results, made it possible to reconstruct the geometry up to 10 km above and down to 50 km below the present topography. In spite of all these exceptionally favorable conditions it is obvious that many parts of the profile remain highly hypothetical, especially in the deeper parts of the belt. The relations between the profile of Plate 16-1 and the major geologic structures to the East are shown on the small-scale block diagram on Figure 16-2 .

The goal of the following pages is to present :

1) The general **geologic framework** of the Western Swiss-Italian Alps, essentially based on the synthetic geologic profile of Plate 16-1. It includes a short description of the geometry, the tectonic style and the origin of the various units. The legend of the geologic profile has been chosen in a way to indicate for the different tectonic domains the probable relationship between each cover nappe and its original basement nappe. It also gives the simplified stratigraphic content of each unit.
2) The **structural evolution** of this part of the Alps, in order to explain the actual geometry, presented in a synthetic way in Plate 16-1.

As it is not possible in this short paper to cite all the geologists who have worked and published on the Western Swiss-Italian Alps, only some of the representative ones will be referred to.

16.2 Geologic framework

As demonstrated by Trümpy (1980, 1988, 1992), Stampfli & Marthaler (1990), Stampfli (1993) and Marchant & Stampfli (Chapter 24), the Western Swiss-Italian Alps are the result of the collision between seven main paleogeographic continental and oceanic domains, from the NW or external to the SE or internal part :

1) The European continental crust.
2) The Valais oceanic crust.
3) The Briançonnais continental crust (possibly attached to the Iberic plate).
4) The Piemont oceanic crust.
5) The Austroalpine continental crust.
6) The Canavese zone of continental and possibly oceanic crust.
7) The Adriatic continental crust.

As shown in Figures 16-1, 16-2 and Plate 16-1, remnants of each of these domains can be recognized in the Western Swiss-Italian Alps. The continent-derived units are mostly well preserved as basement and cover nappes, while of the oceanic crusts only ophiolite sutures and associated sediments remain. As can be expected, the latter often display accretionary prism characteristics.

Two definitions can be proposed for the *interface separating cover from basement* rocks in the continent-derived parts:

a) *A stratigraphic limit* underlying the first post-Variscan sediments (= Upper Permian or Lower Triassic).
b) *A tectonic boundary* corresponding to a major ductile layer within the Mesozoic deposits. This is mostly represented by Middle or Upper Triassic evaporites and cornieules or dolomitic breccias (Masson 1972, Jeanbourquin 1988), or in some cases by Middle Jurassic shales. These horizons permit the detachment ("décollement") of cover nappes leaving behind them "basement nappes" which often include a remnant of Triassic or Lower Jurassic cover rocks. In the following pages, it is this second definition which will be only used when talking of cover and basement nappes.

Flysch type deposits can be roughly separated in two main groups:

a) Flysch sediments deposited on top of little- or un-deformed sequences. They possess generally a distal facies and are incorporated into the upper stratigraphic part of the cover sequences (see legend of section on Plate 16-1).
b) Flysch sediments deposited above tectonically active zones (moving nappes, active thrust zones, accretionary prisms). They are often associated with mélanges and are mostly proximal and coarse grained, and may contain slices of other formations or tectonic slivers. It is not possible to attribute these deposits to specific pre-orogenic domains. Therefore they are represented on the legend of Plate 16-1 as loose "blocks" overlying approximately the various structural units over which they may have been sedimented during deformation.

In the following pages a short structural description of each major Alpine unit is given. In order not to lengthen the text unnecessarily, stratigraphic details will not been given; for this the reader is referred to the legend of the geologic section and to cited references.

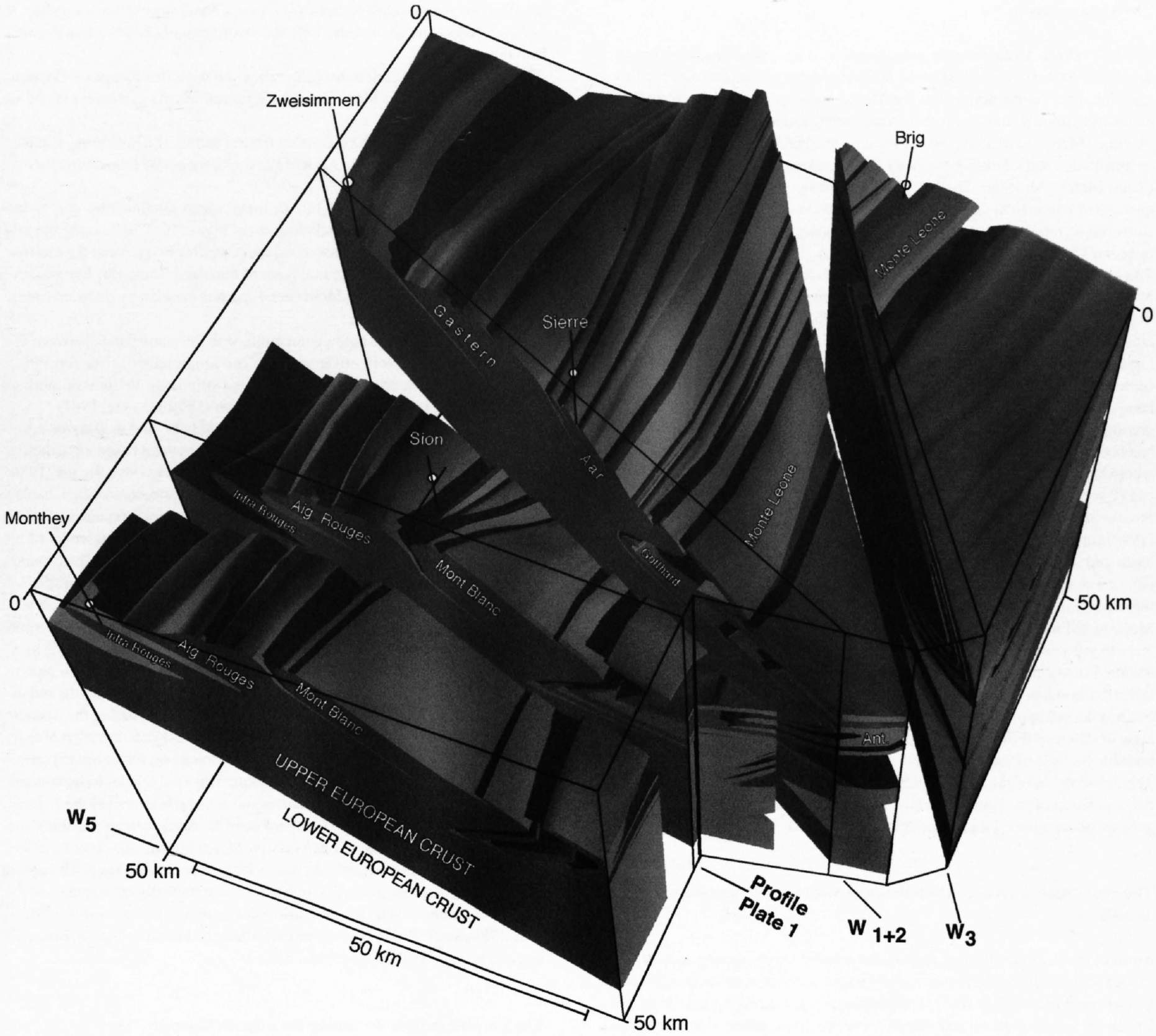

Figure 16-3
Block diagram showing the European basement / cover interface from the external massifs in the NW to the lower Penninic nappes in the SE. The lower surface corresponds to the limit between the upper and lower continental crusts. The block diagram has been constructed by 3D computer methods using directly the geologic interpretations of the seismic profiles W1 to W5 (3-D computer construction by Marc Escher).

16.2.1 Tectonic units derived from the European domain

The European crust is well represented in the external (NW) part of the belt. It forms the major component, in volume and surface, of the Swiss Alpine chain. The intensity of deformation clearly increases towards the SE, from thin-skinned thrust nappes in the cover passing progressively to more ductile basement and cover fold nappes. All structures show an initial NW vergence, while the effects of later backfolding (S-vergence) are only recognizable SE of the Aiguilles Rouges massif. The following tectonic units derived from the European crust have been defined (from NW to SE):

The Jura fold and thrust belt:

The Jura belt (Buxtorf 1907, Laubscher 1961, 1965, 1980, Bergerat 1987, Burkhard 1990, Wildi & Huggenberger 1993) represents the most external part of the Alpine chain. It is characterized by a typical thin-skinned tectonic style controlled by the presence of a basal decollement horizon within Triassic evaporites (Jordan 1988, Jordan & Nüesch 1989). Two main structural zones can be distinguished: 1) The external plateau Jura, which has been passively translated towards the NW and overthrusted the Bresse graben during the Pliocene. 2) The internal folded Jura where fault-propagation folds and fault-bend folds are common (Suppe & Medwedeff 1990).

Displacement of the cover towards the NW in relation to the underlying basement varies from 10 km at the Bresse graben to more than 30 km near the Molasse basin. The internal shortening attains thus approximatively 20 km. The underlying basement rocks are only affected by a brittle strike-slip faults system in which sinistral horizontal displacement dominates. These basement deformations can not by far compensate the shortening and translation of the overlying sedimentary cover. Moreover this strike-slip-fault system is probably connected to the evolution of the Rhine and Bresse grabens and thus to an Eocene-Oligocene event which pre-dates the main deformation of the Jura cover. For all these reasons, the compensation for the shortening and translation of the Jura cover sequences must be found somewhere in the more internal and deep parts of the basement as was proposed by Buxtorf (1907) and Laubscher (1961) as the "Fernschubhypothese". In fact, the two anticlinal structures affecting the basement NW of the Aiguilles Rouges massif (Plate 16-1), may well be responsible for the folding and translation of the Jura. They could or not be associated with basement thrusts. Anyway a NW translation of the cover in relation to the basement would occur (Escher et al. 1993, Epard & Escher 1996).
The Jura deformation started 11 Ma ago, during the Late Miocene and probably continued at least until the Pliocene around 3 Ma ago (Naef et al. 1985, Laubscher 1987).

The Molasse basin:

The NW-Alpine Molasse basin corresponds to a peripheral foredeep which developed by flexural bending of the lithosphere during the last stages of European crustal subduction below the Alpine nappe pile. It has been studied extensively, though mostly from a stratigraphic and sedimentological point of view (Matter et al.1980, Homewood 1986, Weidmann 1988). Molasse sedimentation started during the Early Oligocene and continued until the end of the Middle Miocene. Shallow marine deposits alternate with thick sequences of continental detrital and often coarse sediments. Four major divisions can be recognised: a Lower Marine Molasse, a Lower Freshwater Molasse, an Upper Marine Molasse and finally an Upper Freshwater Molasse. The axis of the basins of these successive deposits was displaced toward the NW due to the simultaneous advance in the same direction of the Alpine active front and the European plate flexuration. The most important NW translation took place between the Lower Freshwater and the Upper Marine Molasse. It corresponds to the major last advance of the Prealpine nappes (around 22 Ma) over parts of the already deposited Lower Freshwater Molasse and was directly followed by the Early Miocene "Burdigalian" transgression of the Upper Marine Molasse. The upper Prealpine Simme nappe has been a major source for the detritus of the Lower Freshwater Molasse, where large conglomerate fans, composed of pebbles from the Simme nappe, can be reconstructed (Trümpy & Bersier 1954).
Structural work carried out by Pfiffner (1986), Burkhard (1990) and Jordan (1992) suggests that internal deformation and shortening within the Molasse basin and its underlying Mesozoic cover, is relatively weak. Only the internal, or Subalpine Molasse has seriously been affected by thrusting and folding, mainly during the Miocene. It is therefore reasonable to suggest that the Molasse sediments transmitted part of the Alpine push to the Jura belt and were thereby translated towards the NW, together with the underlying post Middle Triassic cover. Both units probably used the Triassic evaporites as detachment horizon in respect to the basement. In the SE part of the Molasse basin, a deviation of the decollement surface upwards to the base of the Molasse or downwards to Permo-Carboniferous ductile layers (Jordan 1992), is possible because of the absence of Triassic evaporites.
The deformation of the Molasse deposits started already during or just after the deposition of the Lower Marine Molasse, at around 32 Ma (Middle Oligocene) and continued thereafter at least until 10 Ma ago (Late Miocene).

The area situated between the Subalpine Molasse and the external massifs:

North of the Aiguilles Rouges massif, the seismic survey clearly reveals the existence at depth of at least two major wedges of cover-sediments separated by basement units (Plate 16-1). These structures are probably similar to the Chamonix zone and to the Aar massif cover synclines, observable at the surface. They are therefore interpreted as synclinal structures on the profile of Plate 16-1. Although these synclines appear to be slightly less deformed, they still document that the external Alpine basement, below the Prealpine and Helvetic cover nappes was drastically shortened by folding and thrusting. This was previously suspected but never could be proven without seismic profiles (W5, Steck at al., Chapter 12). As mentioned above, this basement shortening may be partly responsible for the translation and deformation of the Molasse and Jura cover sequences. One of the synclinal zones, revealed by the W5 seismic section, is situated just NW of the Infra Rouges basement. Its existence was postulated already by Badoux (1962). Extrapolated to the present erosion surface it coincides with a major thrust separating the external from the internal part of the Prealpine nappes. This important tectonic feature now explains why in the Prealps, the more external Gets nappe locally overthrusts the more internal Simme nappe (Caron, 1972).

The external basement "massifs":

The NW part of the Western Swiss Alps contains several longitudinally elongated basement outcrops referred to as external "massifs". They all consist more or less of the same pre-Alpine basement rocks: pre- Late Carboniferous amphibolite facies gneisses, Permo-Carboniferous clastic sediments and Upper Carboniferous or Lower Permian granitoids (Bellière 1951, 1980, Von Raumer 1971, 1984, Bussy 1990, Hunziker et al. 1992). The Late Precambrian and Paleozoic evolution of these basement rocks has been reconstructed by Von Raumer (1984) and Von Raumer & Neubauer (1993). They show the existence of a complex Variscan orogen between 500 and 320 Ma, including the subduction of an oceanic crust and the collision between continental crusts. Most parts of the external massifs have been affected later by an Alpine heterogeneous ductile deformation under low to intermediate greenschist facies conditions. The Gotthard massif recorded even an Alpine ductile deformation under amphibolite facies conditions (Marquer 1990). It is during these events that the Late Paleozoic granitoïds were transformed into orthogneisses.
The actual structural relationship between the Aiguilles Rouges – Gastern, Mont Blanc – Aar and Mont Chétif – Gotthard massifs can be explained in two ways:

1) They are arranged in an en-échelon dextral pattern (Pfiffner et al., Chapter 13.1, Steck et al., Chapter 12) and can therefore not be linked directly one to the other.
2) They are arranged more or less in longitudinal continuation one to the other as illustrated in the block diagram of Figure 16-3. In this case the following direct links exist between a) the Aiguilles Rouges and the Gastern frontal structure, b) the external parts of the Mont Blanc and Aar massifs, c) the internal parts of the Mont Blanc and Aar massifs, c) the Mont Chetif and the Gotthard massifs.

The second possibility is better compatible with the equivalence between the Morcles and Doldenhorn cover nappes. The longitudinal limits separating the various massifs are likely to correspond originally to Jurassic normal faults, reactivated during Tertiary compression (Lemoine et al. 1981).
Many geologists having mapped the external "massifs" and their cover, agree that each massif is formed of one or more large recumbent basement anticline or fold nappe (Heim 1921–1922, Ayrton 1980, Steck 1984, Epard, 1986, 1990, Thelin 1987, Escher et al. 1993). These Alpine structures often display well developed overturned flanks with an inverted stratigraphic sequence. This is particularly obvious in the overturned flank of the external Mont Blanc massif and its cover sequence, visible in good outcrops in the Chamonix zone. The outcrop shape of the external "massifs" is mainly controlled by the interference between an early tectonic phase, responsible for the NW vergent overturned basement fold nappes, and a late transversal weak deformation which causes the plunges of the early fold axes. Backfolding starts to be clearly visible S of the Aiguilles Rouges and Gastern massifs. From here to the SE, the action of large scale backfolding increased dramatically and affected the whole pile of earlier formed Alpine nappes, including the Adriatic crust of the Southern Alps (Figure 16-3 and Plate 16-1). In the external massifs, the first well developed backfold can be traced on the seismic profiles with a hinge zone at a depth of 10 to 15 km. This fold affects basement and cover rocks of the internal Mont Blanc and Aar massifs as well as the X-basement, the Mont Chétif and the Gotthard massifs. Surface outcrops along and on both sides of the various seismic profiles, confirm this interpretation. Therefore little doubt remains about this large-scale backfolding. Moreover, as shown on the geologic section of Plate 16-1, it logically corresponds to the Evèque-Balmahorn antiform and, lower down, to the Berisal synform (Steck et al. 1989, Steck 1990). Both structures affect the Penninic domain to the SE and can be very well observed in outcrops.

The Helvetic nappes (including the Morcles nappe):

The Helvetic cover nappes (Figure 16-4) constitute probably the best known part of the Swiss Alps. Their Western Swiss part has been studied by Lugeon 1914, 1918, Trümpy 1963, Badoux 1971, 1972, Ayrton 1972, 1980, Masson et al. 1980, Ramsay 1981, Steck 1984, Burkhard 1988, Dietrich 1989, Dietrich & Casey 1989, Epard 1990 and Badoux, Gabus & Mercanton 1990. This list of authors is by far not complete, it just refers to some of the more relevant ones, dealing with stratigraphy as well as tectonics.
The cover of the Aiguilles Rouges massif is not included in the Helvetic realm. It is in fact mainly autochthonous with respect to its basement, with local internal thrusting as shown by Badoux (1972). Therefore the Helvetic structural domain s.l. starts with the Morcles – Doldenhorn nappes in the NW and ends to the SE with the Sublage – Wildhorn nappes.
As shown in Figure 16-4 and Plate 16-1, there exists a definite relationship between each Helvetic nappe and its original basement. The following links have more or less well been established along the Plate 16-1 cross-section:

1) Morcles nappe – external Mont Blanc massif.
2) Ardon nappe – internal Mont Blanc massif.
3) Diablerets nappe – X-basement
4) Mt. Gond and Sublage nappes (=Wildhorn nappe) – Mont Chétif. Similar links exist more to the east between the Aar-Tavetsch-Gotthard massifs and their Helvetic nappes (Masson et al. 1980, Escher et al. 1987).

The Morcles nappe consists of a thick pile of dolomites, limestones, marls and shales deposited almost continuously from the Triassic to the Cretaceous. It is unconformably overlain by a Lower Oligocene flysch. The geometry of the nappe corresponds to a large overturned isoclinal anticline, with a NW vergence. Its core corresponds to the **external Mont Blanc massif.** The inverted limb is clearly much more tectonically thinned than the normal flank. To the E, the Morcles nappe corresponds to the Doldenhorn nappe.
The Ardon nappe is formed by a reduced sedimentary sequence in which large parts of the Lower and Middle Jurassic are missing. Its frontal part is

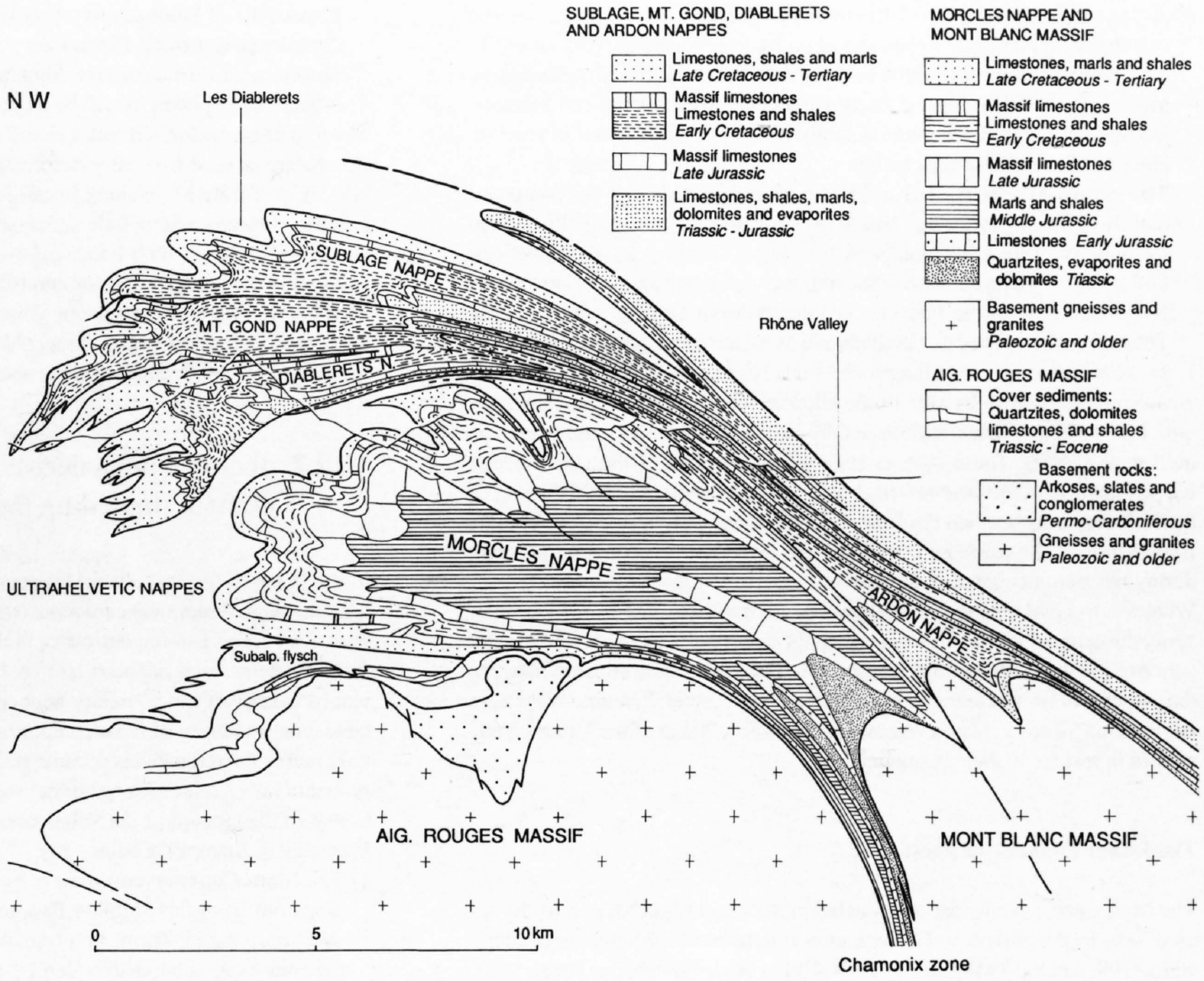

Figure 16-4
Geologic cross-section through the Helvetic basement and cover nappes in the Diablerets–Rhone region (Modified and completed after Escher et al. 1993).

mainly composed of Cretaceous to Lower Oligocene limestones, marls and shales. The corresponding lower part of the stratigraphic sequence, consisting of Triassic to Upper Jurassic quartzites, dolomites, limestones and shales, can be found in local relicts on the **internal Mont Blanc massif.** Geometrically the Ardon nappe is a thrust nappe with a frontal anticline. There is no discrete basal thrust: movements took place along two relatively wide ductile shear zones composed of Middle Jurassic and Lower Cretaceous shales.
Eastern equivalents of the Ardon nappe are the Jägerchrüz and Plammis nappes.
The Diablerets, Mont Gond and Sublage nappes can best be considered as belonging all three to the **Wildhorn "super nappe"**. Their stratigraphic succession is more or less the same; it consists of a complete sequence of Triassic to Cretaceous dolomites, limestones, marls and shales, unconformably overlain by Lower Oligocene flysch. An important basal thrust separates the Sublage from the Mont Gond nappe (Figure 16-4), while the latter is linked to the Diablerets nappe by an isoclinal recumbent syncline. An important thrust surface occurs at the base of the Diablerets nappe, it was active between 34 and 15 Ma ago (Crespo et al. 1995).
It is evident that the *variations in volume* from one Helvetic nappe to the other, is controlled by the original stratigraphy (Lemoine & Trümpy 1987, Masson et al. 1980). Large nappes like the Morcles and Wildhorn nappes correspond to original Tethyan graben or half-graben structures in which a thick pile of sediments was deposited. In contrast, the Ardon nappe with its stratigraphically reduced sediments, is certainly derived from a sub-marine structural high.
Except for the Morcles nappe, which displays a clear fold-nappe geometry, the Helvetic cover nappes are essentially thrust nappes, often with a frontal fold geometry. While discrete thrust planes may locally have played a certain role (Pfiffner 1985), *deformation essentially took place by simple shear*, in the Morcles nappe of the entire inverted limb, and for the other Helvetic nappes within selected ductile stratigraphic layers, such as the Triassic evaporites, the Middle Jurassic and the Lower Cretaceous shales. These layers acted often simultaneously and resulted in the splitting of each Helvetic "thrust nappe" into successive but connected parts: a frontal part composed essentially of Cretaceous rocks, an intermediate mostly Upper Jurassic part and an internal section composed only of Triassic and Lower Jurassic rocks, separated from their basement by a basal Triassic shear zone. The final result is of course that the younger stratigraphic parts traveled farther to the NW than the older ones. This is particularly evident in the Diablerets, Mt. Gond and Sublage nappes where the main part of the nappes s.s. is made of Cretaceous and Tertiary rocks, the older ones beeing found in the more internal parts. Translation distances vary between 12 km for the Morcles nappe to 40 km for the Sublage nappe. The proposed mechanism by *selective simple shear* probably represents the main way in which deformation and translation takes place in sedimentary cover nappes. Tricart (1986) proposed a similar mechanism for the differential translation of the Briançonnais nappes in the French Alps.
In addition to this important ductile translation by *selective simple shear*, most Helvetic nappes display an internal ductile strain which increases considerably together with the metamorphic grade from their front towards the root zone (Dietrich 1989, Groshong et al. 1984). As shown by Dietrich & Casey (1989), this observed thinning of the Helvetic nappes towards the root zone can be explained by the superposition of pure shear deformation on simple shear. The amount of the pure shear component increasing towards the internal part of the nappes.
Several early deformation phases can be recognized in the Helvetic nappes. They are accompanied by a NW–SE stretching lineation. Like the external massifs, backfolding also affects the Helvetic nappes in their internal part (Figure 16-3, Plate 16-1). Finally it is important to mention that most basement nappes corresponding to Helvetic thrust nappes display the geometry and stratigraphy of ductile fold nappes. A mechanism should therefore exist, that explains the simultaneous formation of a basement fold nappe and of the corresponding cover thrust nappe (Escher et al. 1993, Epard & Escher 1996).

The Ultrahelvetic nappes:

The Ultrahelvetic units show a very complex tectonic and sedimentary setting. They are composed of relatively small nappes (diverticules), slices and blocks in a variable, more or less abundant flysch matrix of Eocene to Early Oligocene age. The age of the rocks making up the diverticules and slices, spans from Triassic to Late Cretaceous. According to Badoux (1945, 1946, 1963) the stratigraphic content of each of the small nappe-diverticules fit into an original depositional basin-sequence which must have existed in a SE continuity with the Wildhorn basin. During the Early Oligocene, the basin was uplifted in its SE part and the diverticules glided by gravity towards the NW on top of the Helvetic nappes, probably at an early stage of formation of the latter. This took place most likely in a submarine environment and was directly preceded by the deposition of an unconformable turbidite wedge (Homewood 1976, 1977). The mechanism thus described is called "diverticulation" (Lugeon 1943). Its final result is an inversion of the vertical succession within the pile of small nappes, while the internal stratigraphy of each unit remains normal. It is important to note that such complex structures are commonly found in accretionary prisms and that gravity may not have played such an important role during the "diverticulation". Two main Ultrahelvetic subdivisions can be made:

1) A lower **supra-Morcles Ultrahelvetic** (UH-M, Plate 16-1), formed mainly by the Anzeinde nappe and a chaotic flysch mélange (Gabus 1958). This unit was deformed and translated, together with the Morcles nappe, towards the NW, during the Early Oligocene. Remnants of the Morcles-Ultrahelvetic flysch are found actually below and at the front of the Prealpes Medianes Plastiques nappe.
2) **The supra-Wildhorn Ultrahelvetic** (UH-W, Plate 16-1), composed mainly of the Sex mort, Bex and Arveyes diverticules as originally defined by Badoux (1963), accompanied by various Tertiary flysch sequences. Following the diverticulation, this unit was deformed and translated to the NW together with the Helvetic Diablerets-Mont Gond-Sublage nappes. The originally defined as Ultrahelvetic Meilleret and Chamossaire nappes are now considered to belong to the Infra Niesen complex.

An even more refined division of the Ultrahelvetic is proposed by Jeanbourquin (1991, 1992), Jeanbourquin & Goy-Eggenberger (1991) and Jeanbourquin et al. (1992). These authors suggest an assembly of the Ultrahelvetic nappes mainly by tectonic mélange formation, during the underthrusting of the Helvetic units beneath the Lower Penninic ones, along a major Penninic frontal thrust. The same authors show the important role of fluid pressure during the tectonic mélange formation.

Whatever the real mechanism responsible for the formation of the Ultrahelvetic, the original basement from which the cover units were derived has not yet been identified. It could correspond to a basement area situated between the Mont Chetif–Gotthard basements and the Lower Penninic Verampio nappe. This means a relative translation of at least 90 km of the Ultrahelvetic nappes in respect to their basement.

The Lower Penninic nappes:

The Lower Penninic nappes are situated in the deepest visible part of the Alpine belt, in the Simplon–Ticino region (Gerlach 1869, Schmidt & Preiswerk 1908, Argand 1916, Milnes 1974, Huber et al. 1980, Milnes et al. 1981, Steck 1984, 1990). This area was uplifted during the last important phase of Alpine deformation. The uplift affected the whole of the Aar–Toce culmination.

The Lower Penninic nappes form the logical continuation to the SE and at depth of the external massifs and their Helvetic cover nappes and represent the continuation of the European continental crust (Marchant & Stampfli, Chapter 24). Their existence at depth, in the Western part of the Swiss Alps, below the Middle and Upper Penninic nappes, was suspected before, but has been proven for the first time with the recent reflection seismic records (Marchant et al. 1993, Steck et al., Chapter 12). Traditionally, the Lower Penninic nappes were attributed to the Valais paleogeographic domain. Its seems more logical, however, to restrict this denomination of Valais to the oceanic crust and associated sediments and accretionary prism formations which separates the European from the Briançonnais continental crusts (Stampfli & Marechant, Chapter 17).

From the NW to the SE, the following Lower Penninic units can be distinguished (Plate 16-1, Figure 16-3):

1) **The Verampio nappe**, of wich only the upper part outcrops as a dome in the Simplon region. The seismic profiles suggest however a basement fold nappe geometry for this unit.
2) **The Antigorio nappe** displays all the characteristic features of a true ductile fold nappe, with a normal flank, a frontal part and an inverted limb (Spring et al. 1992).

Both the Verampio and Antigorio nappes have an envelope of metasedimentary rocks of Late Paleozoic to Jurassic age. It is probable that this cover is incomplete and that there existed originally a younger sequence of Cretaceous and Tertiary rocks. This very ductile part of cover rocks may have been displaced towards the NW, to the Prealps. A possible equivalent may be found in the Infra-Niesen nappe as suggested on the profile of Plate 16-1.

3) **The Lebendun nappe** (Steck 1987, Spring et al. 1992) is formed by a Paleozoic paragneissic core (Valgrande gneiss) and a Mesozoic sedimentary cover in an overturned position. The cover sequence documents continuous clastic sedimentation with conglomerates and schists. The Lebendun nappe probably comes from an area originally situated between the Monte Leone and the Antigorio nappes. It has been strongly refolded around the frontal parts of the Antigorio and Verampio nappes, probably during an early second phase of deformation (Steck 1987).
4) **The Monte Leone nappe** forms the most internal outcropping unit of European crust, situated originally directly NW of the Valaisan oceanic trough. It presents an elongated ductile recumbent fold of crystalline basement with a thin Triassic cover of quartzites and dolomites, well preserved on the overturned limb. Its total amplitude may well attain over 40 km. According to Leu (1986), the post-Triassic cover of the Monte Leone nappe is represented by the Fäldbach zone, made of chaotic sediments and the Rosswald detrital series. It seems however more reasonable to attribute the Rosswald and Fäldbach flysch-type sediments to the relicts of an Upper Cretaceous to Lower Tertiary accretionary prism developed between the European and Briançonnais domains during the subduction of the Valais oceanic lithosphere, as will be explained in the next section.

The four above described tectonic units were probably shaped as ductile nappes during at least two early deformation phases accompanied by a strong NW-SE penetrative stretching lineation under *amphibolite facies* conditions. Later tectonic phases include successively a ductile SW oriented shear and strong backfolding, both under *greenschist facies* retromorphic conditions, and finally the partly brittle Simplon-Rhône fault zone. The latter affects essentially the Monte Leone nappe (Plate 16-1). The most conspicuous backfold is the well developed S vergent Vanzone antiform which affects the entire pile of Lower Penninic nappes and their covers.

16.2.2 Tectonic units derived from the Valais oceanic domain (including the Niesen nappe)

In the Western Swiss-Italian Alps remnants of the Valais oceanic crust and their associated sediments are represented in the Sion-Courmayeur zone, the Rosswald series and the narrow ophiolite zone separating the Monte Leone from the Moncucco nappe (Plate 16-1). These three structural units are all placed exactly at the boundary between the nappes derived from the European crust and those of Briançonnais origin. They must therefore contain the only remnants of the Valais oceanic realm. This is moreover suggested by the probable Late Cretaceous age of the sediments, which could well correspond to that of the closure of the Valais ocean (Polino et al. 1990, Stampfli 1993, Marchant & Stampfli, Chapter 24).

1) **The Sion–Courmayeur zone** is by far the most important Valais unit. It crops out from the Simplon Pass to Moutiers parallel to the Alpine belt over more than 200 km. In a transverse section, from the NW to the SE, the following subdivisions can be recognized: a) The Ferret calcareous and siliciclastic flysch. b) The flysch trilogy nappe composed of the Aroley, Marmontains and St. Christophe sub-units. c) The Versoyen and Pierre Avoi chaotic complex, made up of a mélange of black schists with blocks and slivers of metagabbro, metabasalt and serpentinite, locally with large slices of gneiss, Triassic quartzites, dolomites and marbles, and of Mesozoic breccias. This last unit corresponds to the most internal part of the Sion–Courmayeur zone, and does not necessarily represent its stratigraphic base as proposed by many authors. Locally it includes rock slices of external Briançonnais origin.

These divisions were defined by Trümpy (1952, 1955) in the Western Swiss Alps and by Antoine (1971, 1972) in the French part of the Sion–Courmayeur zone. Later work by Burri (1967, 1979), Ackermann et al. (1991) and Jeanbourquin & Burri (1989, 1991) suggested that the basal Versoyen – Pierre Avoi unit is a remnant of a Cretaceous accretionary prism developed between the European and Briançonnais domains, during the subduction of the Valais oceanic crust. The overlying flysch sequences probably were deposited during subduction, in the upper part of the accretionary prism, and were subsequently underthrusted and associated with the tectonic mélange.

2) **The Rosswald and Fäldbach** units represent, according to Leu (1986), the post-Triassic cover of the Monte Leone nappe. They are made up of monotonous calcareous and siliciclastic turbidites, with at their base a chaotic flysch unit containing blocks and slices of metagabbros and rhyolites. In fact they resemble very much the Sion–Courmayeur flysch sequence which contains an identical internal mélange unit. It seems therefore reasonable to attribute part of these sediments as well to the remains of an Upper Cretaceous accretionary prism developing between the European and Briançonnais domains, during the subduction of the Valais oceanic crust. They could in fact be the external and Eastern equivalents of the Sion–Courmayeur zone and have probably no original relation to the Monte Leone nappe. This interpretation was proposed by Ackermann et al. (1991) and Jeanbourquin and Burri (1991), and was later adopted by Stampfli (1993) and Marchant & Stampfli (Chapter 24).
3) **The Infra-Moncucco ophiolite zone** is essentially composed of serpentinites and metagabbros. Its structural position makes it an internal equivalent of the above mentioned units; most likely it represents an ophiolitic remnant of the Valais oceanic crust. Its probable Cretaceous age has not been proved.
4) **The Niesen nappe** is composed of a thick pile of flysch-type turbidites onlapping locally onto a thin wedge of Triassic and Jurassic layers which include at one place a slice of gneissic basement. The main age of the flysch is Late Cretaceous to Eocene. The turbidites are locally very coarse grained and include boulders, conglomerates and coarse sandstones. Hemipelagic intervals are common and suggest relatively deep water depositional conditions. Most authors have suggested that the Niesen nappe was derived from the N part of the Valais trough, from above the older

sediments covering the original Antigorio or Monte Leone basements (Trümpy 1960, Lombard 1971, Homewood 1974, Leu 1986). According to Homewood (1977) the immaturity of the sediments and variety of the clasts of the Niesen flysch indicate rapid accumulation of material from a freshly eroded subaerial to shallow marine source area, suggesting simultaneous tectonic activity. These important observations, together with the new interpretation of the Sion–Courmayeur and Rosswald–Fäldbach sequences, makes it clear that it is not possible to attribute a specific "basement" to the Niesen flysch. As suggested by Marchant & Stampfli (this volume) it was most likely deposited directly NW of the Valais accretionary prism, during the last phases of its activity, probably on top of a pile of early shaped Lower Penninic nappes. The basal wedge of eroded Jurassic rocks could well belong to the top of one of these juvenile nappes.

From a structural point of view it is important to note that all the units described in this chapter are extremely ductile and thus form a weak link between the European and Briançonnais nappe piles. This property has extensively been used to accomodate the various Alpine compressive and transpressive stress directions, and resulted in the formation of the following successive ductile or brittle movements, mostly contained within the Sion–Courmayeur and Rosswald–Fäldbach nappes:

1) The underthrusting of the Helvetic and Lower Penninic units underneath the Middle Penninic nappes, and the simultaneous expulsion towards the NW of the Niesen and Infra-Niesen Prealpine nappes.
2) An important ductile dextral strike-slip movement of at least 40 km along the Simplon Shear Zone (Steck 1980, 1987, Steck & Hunziker in press).
3) A late, partly brittle dextral and normal movement along the Rhône–Simplon fault (Steck 1981, Manktelow 1985).

16.2.3 Tectonic units derived from the Briançonnais domain (middle Penninic nappes), and associated flysch nappes

The Briançonnais paleogeographic domain is characterized by the existence during most of the Jurassic of a central platform area and an external or Sub-Briançonnais basin.

The basement nappes derived from the Briançonnais continental crust form a well individualized central unit in the Western Swiss-Italian Alps. It is limited to the NW by the Valais derived flysch sequences and to the SE by the Piemontais ophiolite nappes. Most of the Briançonnais Mesozoic and Tertiary sedimentary cover was separated from its original basement during early Alpine deformation, and translated to the NW . It actually forms the bulk part of the Prealpine nappes (Plate 16-1). A short description will follow, of each basement nappe and corresponding cover unit, from NW to SE :

The Zone Houillère:

The zone Houillère can be traced from Italy through France into Switzerland in the Brigue region where it corresponds to the Lower Stalden and Visperterminen zones (Bearth 1963, Escher 1988). It comprises an external and an internal part separated by thin slices of Triassic cover (Gerlach 1871, Oulianoff & Trümpy 1958).

The external Zone Houillère displays an imbricated structure of Carboniferous shales and sandstones, Permian conglomerates and quartzites, as well as Triassic quartzites and dolomitic marbles (Burri & Jemelin 1983). It represents evidently the most external part of the Briançonnais domain, and was strongly deformed during the subduction of the Valais and Lower Penninic nappes. It may in fact even form the continuation of the Pierre Avoi accretional prism mélange.

The internal Zone Houillère reveals a more regular structure. It is composed of Carboniferous and Lower Permian metagraywackes, shales, schists, quartzites and conglomerates containing locally coal-bearing layers. It shows a normal stratigraphic sequence.

Important to note is that originally the Permo-Carboniferous series were deposited in a late Variscan SW–NE trending graben structure, extending over at least 140 km along strike, and which probably controlled the geometry of later Alpine nappes (Escher 1988).

Structurally, the Zone Houillère was sheared off its older Pre-Carboniferous basement which may have corresponded to the Moncucco unit (Plate 16-1), while its Mesozoic and Tertiary cover probably traveled even further to the NW, to the Préalpes Médianes Plastiques, as proposed by Baud & Septfontaine 1980. However, the absence of well preserved Triassic sequences on top of the internal Zone Houillère makes this correlation difficult.

The Alpine metamorphic grade of the Zone Houillère is low greenschist facies.

The Pontis basement nappe and the Préalpes Médianes Plastiques cover nappe:

The Pontis nappe is formed of a polymetamorphic basement gneiss core, overlain by Permo-Carboniferous clastic sediments and a relatively thick cover of Lower and Middle Triassic quartzites, dolomites and marbles. It occurs south of the Rhone Valley, mainly in the Sierre and Sion regions. The Berisal and Upper Stalden units to the NE and the Ruitor zone to the SW, form probably the continuation of the Pontis basement.

It is essentially a thrust nappe with only at the front a thin overturned limb. A huge synclinal zone of at least 30 km amplitude, links the Pontis nappe to the overlying Siviez-Mischabel nappe. The missing complementary sedimentary cover was sheared off along a basal Late Triassic evaporite layer towards the NW, during the Tertiary Alpine deformations and forms now the Préalpes Médianes Plastiques nappe (Baud & Septfontaine 1980, Sartori 1988). According to Jaboyedoff (PhD thesis in prep.), the marbles of the Pontis nappe underwent an epizonal metamorphism, which corresponds according to Frey (1988) to a temperature of 300° or slightly more.

The Préalpes Médianes Plastiques cover nappe, occurs in the external part of the Prealps where it was extensively studied by Badoux (1960, 1962, 1965) and Baud (1972). It forms the major body of the Prealps and has a stratigraphic sequence which ranges from Upper Triassic to Middle Eocene. This sequence is stratigraphically continuous in the NW where shales and marls are common, and passes southwards to a much thinner sequence where stratigraphic gaps replace most of the ductile layers. Paleogeographically, this facies change corresponds to the passage, particularly striking during the Middle Jurassic, from the external or Subriançonnais basin to the partly eroded Briançonnais platform. Detailed structural analyses by Plancherel (1976, 1979) and Mosar (1988,1991) show that parts of the Médianes Plastiques display an early thin-skinned structural style and are affected by late N–S oriented strike-slip faults similar to those observed in the Jura. The entire Médianes Plastiques underwent only deep burial diagenesis, in contrast to the Rigides where anchi- to epizonal metamorphism was observed (Mosar 1988).

The Siviez-Mischabel basement nappe and the Préalpes Médianes Rigides cover nappe:

The Siviez-Mischabel nappe forms south of the Rhone Valley in Valais, a huge structure representing the central unit of the Grand Saint-Bernard super-nappe (Escher 1988). During the past 20 years this unit has been mapped and investigated in detail from the Zermatt region to the Val de Bagnes (Bearth 1980, Burri 1983, Marthaler 1984, Thélin 1987, 1989, Sartori 1987, 1990, Sartori & Thélin 1987, Thélin et al. 1993). The result of these investigations can be summarised as follows:

The Siviez-Mischabel nappe has the geometry of a very large recumbent fold with an amplitude of more than 35 km. After its formation and emplacement it was backfolded in its internal part which resulted in the spectacular Mischabel backfold, analysed by Milnes *et al.* (1981) and Müller (1983).

The core of the nappe is made of polymetamorphic paragneisses and micaschists of pre Late-Carboniferous age, containing a wide variety of metamagmatites (calc.alkaline granitoids, gabbros, pyroxenites and volcanites). Eclogites and retroeclogites are locally present, usually associated with banded amphibolites. They show HP mineral assemblages which are overprinted by an amphibolite facies event of probable Variscan age (Thélin et al. 1990).

Surrounding the Siviez-Mischabel basement core, a metasedimentary cover can be followed from the normal flank throughout the front of the nappe to its inverted limb (Figure 16-5). This cover is made in most parts of Late Carboniferous, Permian and Early Triassic schists, conglomerates, quartzites and evaporites. Only in its eastern and internal part, in the **Barrhorn zone**, the normal flank displays a complete Briançonnais-type cover sequence up to the Eocene (Ellenberger 1953, Bearth 1980, Sartori 1990). It consists of quartzites, dolomites, marbles and meta flysch. There is in most places a stratigraphic continuity between basement and cover rocks and nowhere a trace of early thrust planes.

Most rocks of the Siviez-Mischabel nappe display an early penetrative axial-surface schistosity formed under upper greenschist facies. A SE–NW early stretching lineation can be observed in many places. The only brittle deformation is represented by frontal dextral transcurrent faults (D IV transpressional phase according to Steck 1990), and late normal faults. The part of the cover rocks (Middle Triassic to Eocene) missing in most parts of the normal and inverted limbs, was stripped from its basement before or at the same time as the nappe was formed, and was tectonically translated towards the NW. This separation was made possible by the presence of a extensive Middle Triassic evaporite layer, which is missing in the Barrhorn area.

The Préalpes Médianes Rigides nappe (Plate 16-1, Baud & Masson 1975, Baud & Septfontaine 1980, Sartori 1990) consists of large blocks or slices of

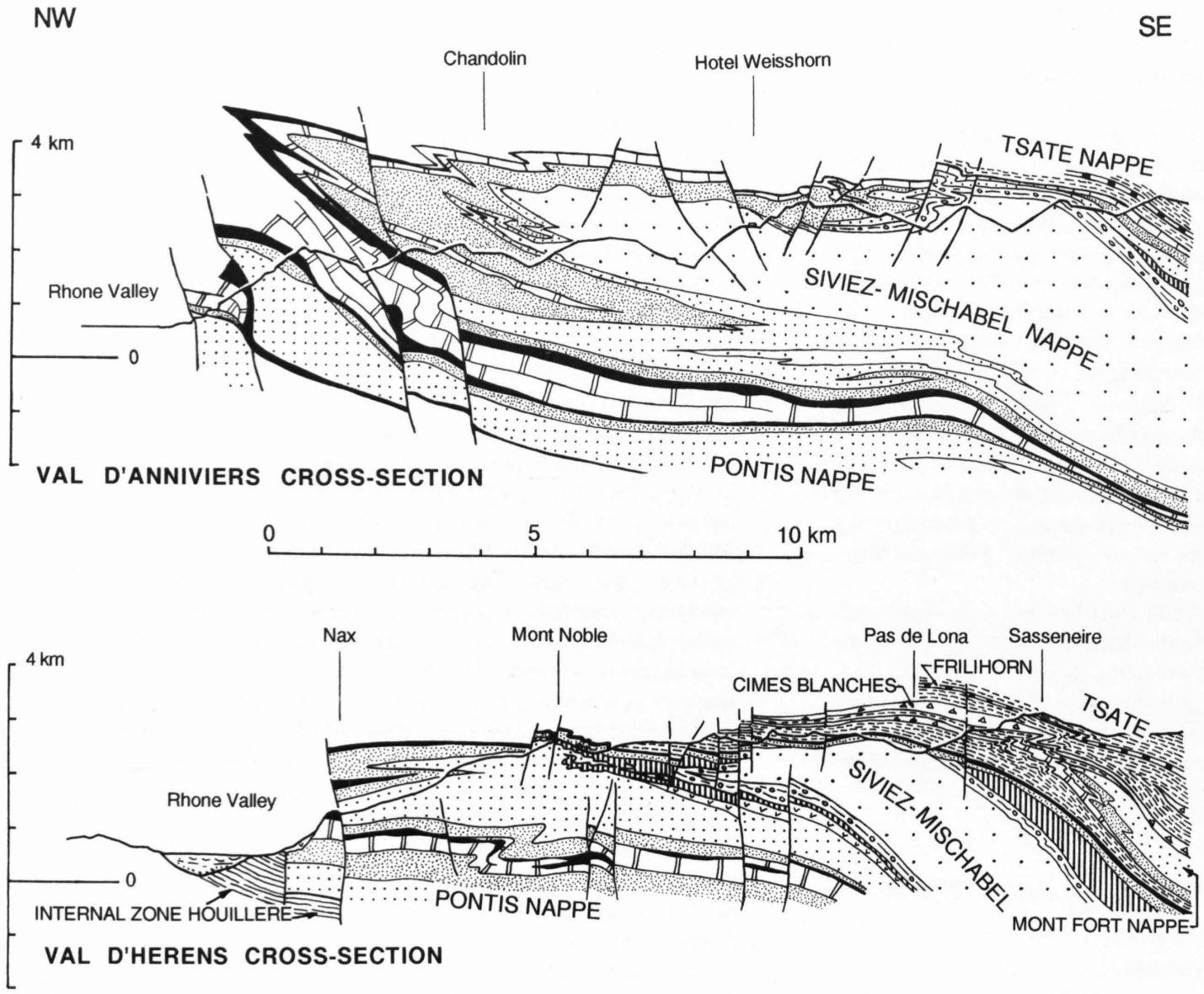

Figure 16-5
Geologic profiles through the Zone Houillère, Pontis, Siviez–Mischabel, Mont Fort and Tsate nappes in the Val d'Anniviers and Val d'Hérens regions, Valais.

kilometer size. It is the unit corresponding most likely to the stripped-off cover of the Siviez-Mischabel basement nappe. Its stratigraphy is identical to that of the Barrhorn zone and moreover it forms the exact complement to the thin Lower Triassic remnants found mostly on the latter. A major stratigraphic gap exists in the Médianes Rigides between the Upper Triassic and the Upper Dogger. This was caused by the uplift of the Briançonnais rift shoulder platform in Middle Jurassic time and its emersion and subsequent erosion (Stampfli 1993). The brittle style of deformation of this unit is due to the absence of the Lower and Middle Jurassic shales. The Médianes Rigides display thrust nappe characteristics (Escher et al. 1993). According to Baud & Masson (1976), Huon et al. (1988) and Mosar (1988) the Rigides rocks underwent at their base an epizonal metamorphism, whereas the majority of the nappe has been only slightly metamorphosed to anchizonal conditions. At the base of one of the Rigides blocks, the Gummfluh klippe, an important thrust plane has been dated by 40Ar/39Ar method as Late Cretaceous by Cosca et al. (1992). It may well represent a late Eoalpine event that developed at a depth of 800 m during marine sedimentation at the surface, and which was facilitated by the presence of warm fluids along the tectonic discontinuity.
An internal equivalent of both the Siviez – Mischabel and the Pontis nappes is probably the **Camughera gneiss unit**, found underneath the Monte Rosa and Antrona nappes.

The Mont Fort basement nappe and the Brèche cover nappe:

The Mont Fort and Brèche nappes are not necessarily directly related to each other, they both contain however Mesozoic breccias and are structurally situated at the same level in the Alpine nappe-pile, at the contact with the overlying Tsate and Gets ophiolite nappes. They may therefore represent an internal part of the original Briançonnais domain, characterized in Jurassic time by submarine fault breccia deposits.
The Mont Fort nappe forms, together with the Monte Rosa unit, the most internal of the Penninic nappes. It is made of a core of Permo-Carboniferous paragneisses and micaschists, containing locally metagabbros and metabasalts. Pillow lavas occur in some places in the Lower Permian. These basement rocks were studied by Schaer (1959), Bearth (1963), Caby (1968), Thélin & Ayrton (1983) Marthaler (1984) and Gouffon (1991). Surrounding this Upper Paleozoic core, Upper Permian meta-arkoses and conglomerates form a large, NW to NE vergent fold nappe structure which is entirely truncated at its base and separated from its original older basement. Triassic and Jurassic rocks containing Liassic(?) breccias are, according to recent investigations only found as isoclinal synclinal structures. These appear to be truncated by a thrust and tectonically overlain by rock sequences belonging to the Cimes Blanches nappe (see section 16.2.4). The significance of this probably Upper Cretaceous discordance is not yet really understood, it may correspond to an Eoalpine underthrusting event during the subduction of the Piemontais and internal Briançonnais crusts. The Mesozoic cover was studied mainly by Wegmann (1922), Moix & Stampfli (1981) and Allimann (1987, 1989).
The Mont Fort nappe (Plate 16-1 & Figure 16-5) is a typical example of an intermediate placed nappe: its original Pre-Carboniferous basement corresponds probably to the internal part of the Siviez-Mischabel or the Monte Rosa nappe, while its younger cover rocks are probably found further to the NW, in the Prealpine Brèche nappe. A possible remnant of the Mont Fort rocks, left behind during its translation towards the NW is the Stockhorn zone near Zermatt. Towards the E the Mont Fort nappe disappears completely with an E-vergent anticlinal closure, while to the W it increases considerably in volume (Escher 1988).
The metamorphic imprint of the Mont Fort rocks corresponds to the high-grade blueschist facies (Schaer 1959, Bocquet et al. 1974, Wüst & Baehni 1986), which may have been attained during Late Cretaceous or Early Tertiary metamorphism. It is of slightly higher-pressure than that of the underlying nappes, which indicates transported metamorphism. The later retrograde metamorphic history took place under greenschist facies conditions and affected the entire nappe pile during the Tertiary.

The Brèche nappe is situated in the internal part of the Prealps, where it directly overlies the Médianes rigides slices and their associated flysch with lenses of Couches Rouges. Its stratigraphic sequence ranges from Upper Triassic dolomite to Paleocene marly limestones (Couches Rouges), capped by a wildflysch which may well belong to another higher tectonic unit (Caron 1965, Caron & Weidmann 1967, Weidmann 1972). The Brèche nappe contains two thick formations of breccias of Middle and Late Jurassic age, hence its name. The basal thrust plane follows mostly an Upper Triassic evaporites and cornieule horizon. It is generally agreed that the Brèche nappe may come from a basin located on the SE margin of the Briançonnais platform. This assumption is based on the tectonic position (equal to the Mont Fort nappe), on the interpretation of its stratigraphic sequence, and on a comparison with the Prepiemontais Gondran series of the Franco-Italian Alps (Trümpy 1955, Lemoine 1961, 1988, Steffen et al. 1993). The original basement of the Brèche cover nappe is not known, it may well correspond to a basement unit equivalent to the Mont Fort nappe or to the internal parts of the Monte Rosa basement, but probably situated now more to the SW because of the late dextral horizontal movements.

The Monte Rosa basement nappe:

As shown on the section of Plate 16-1, the anticlinal root zone of the Monte Rosa nappe is most likely refolded by two major S-vergent backfolds: the Vanzone and the Boggioletto antiforms. The latter has been observed at the surface in the Sesia zone and most likely can be traced to the same antiform which refolds the Lanzo and Dora Maira units in the French-Italian Alps. This tentative correlation makes the Dora Maira nappe the internal and eastern equivalent of the Monte Rosa nappe, and in its lower part even maybe the equivalent of the internal Siviez-Mischabel – Camughera units. In the following text, only the Monte Rosa nappe will be briefly described, the other units not appearing at the surface in the Western Swiss-Italian Alps.

The Monte Rosa nappe has been studied, mostly from a petrographic-metamorphic point of view by a multitude of experts. Some of the most representatives are: Bearth (1952), Dal Piaz (1964,1966, 1971), Dal Piaz & Lombardo (1986) , Hunziker (1970, 1974), Frey et al. (1976), Wetzel (1972) and Chopin & Monié (1984). The geometry of the Monte Rosa nappe is that of a huge isoclinal and recumbent basement anticline with an approximately NW vergence. It was strongly refolded by later, Oligocene S-vergent backfolds. The core of the nappe is composed of Pre-Carboniferous high-grade paragneisses with rare intercalations of basic rocks, intruded during the Carboniferous and Permian by large bodies of porphyritic granitoids. The envelope, following more or less continuously the anticlinal shape of the nappe, is formed by the same high-grade gneisses, locally associated with scarce Permo-Carboniferous schists and conglomerates. All these rocks have been more or less strongly overprinted by polyphase Alpine deformation and metamophism, transforming the granitoids into augen-gneisses. This started with a very HP metamorphism of Cretaceous age, followed by a pervasive medium grade greenschist to amphibolite facies metamorphism of Tertiary age.

Mesozoic cover rocks belonging to the Monte Rosa nappe were found only in its frontal part (Jaboyedoff in prep.) and form the Furgg zone s.s. They are composed of Triassic and Early Jurassic(?) dolomites, marbles and calcschists, cut by metadolerites. A meta-flysch sequence containing blocks and slices of meta-basalt overlies the sequence. This part of the basement and cover is thought to represent originally the internal part of the Briançonnais shoulder (Stampfli & Marthaler 1990), uplifted during the Early Jurassic and cut by dolerite dykes.

The Sub-Médianes zone and the Gurnigel-Sarine nappe:

Both flysch units were probably deposited on top of early formed nappes of internal Briançonnais origin, after the closure of the Piemont oceanic domain, and resulted from the erosion of advancing south-Penninic or more internal nappes.

The Sub-Médiane zone is represented by a wildflysch mélange formed during Late Cretaceous to Eocene times. It was for a long time considered as a tectonic window of Ultra-Helvetic flysch, an interpretation rejected since the work of Weidmann et al. (1976). Its internal structure is extremely chaotic. Blocks and slices of Triassic and Late Jurassic rocks are common, they include quartzites, dolomitic and pelagic limestones, gypsum and locally radiolarites. This mélange also contains elements of Late Cretaceous and Tertiary Couches Rouges and slices of Médianes Rigides. It is even possible that most of the very large elements which make up the Préalpes Médianes Rigides nappe are in fact just blocks inside the Sub-Médiane zone. This interpretation appears very likely, many of the large Rigides-elements being often partly or entirely surrounded by a Sub-Médiane flysch matrix. The Flysch with lenses of Couches Rouges (Badoux 1962), is here included in the Sub-Médiane mélange. It might just represent a particular facies of the latter.

The genesis of the Sub-Médiane zone is very complex, and one must imagine a succession of sedimentary (olistostromes) and tectonic processes that have incorporated and mixed elements from several paleogeographical domains of which the Briançonnais probably was the dominant one.

The Gurnigel-Sarine nappe consists of a thick flysch sequence of terminal Cretaceous (Maastrichtian) to Middle Eocene age (Van Stuijvenberg 1979, Weidmann et al. 1976, Morel 1980). It is mainly exposed in the External Prealps, where it forms a set of large imbricated slices below the frontal thrust plane of the Médianes Plastiques nappe. Remnants also occur on top of the Médianes Plastiques, where its name is restricted to Sarine nappe (Caron et al. 1980). The basal thrust of the Sarine nappe is folded in the synformal cores of the Plastiques folds: this geometric relation as well as the frontal position of the Gurnigel outcrops indicate an early emplacement of this nappe over and beyond the Médianes Plastiques before the translation and folding of the latter. During this first (Late Eocene) phase, the Gurnigel-Sarine nappe probably advanced on a wildflysch sole whose elements were taken from various sources, like the Médianes Plastiques. Like in most of the other Upper Prealpine nappes, the Gurnigel rocks only show the effects of diagenesis with no metamorphism.

16.2.4 Ophiolite nappes of Piemont origin and associated cover and flysch nappes

Remnants of the Piemont oceanic domain are relatively well represented in the Western Swiss-Italian Alps: the internal Zermatt-Saas Fee and Antrona zones are probably both remnants of the NW part of the Tethyan oceanic lithosphere, thrusted during the Cretaceous on top of the Monte Rosa and Grand Paradis (Briançonnais) continental crust. Only few differences exist between the two ophiolite zones (Pfeiffer et al. 1989), their actual separation is probably the result of late boudinage during Oligocene backfolding. The Antrona zone forms the main filling of the synclinal core which separates the Monte Rosa from the Siviez–Mischabel nappe. The SE continuation in depth of the Zermatt–Saas Fee ophiolites could well link up with an equivalent of the Lanzo ophiolites and represent here the deepest visible part of the Piemont suture (Plate 16-1).

The Tsate nappe is probably the remnant of an accretionary prism formed during the Early to Middle Cretaceous subduction and closure of the Piemont oceanic domain (Marthaler & Stampfli 1989, Stampfli & Marthaler 1990). Near its base it contains a thin but continuous unit of Permian to Cretaceous rocks, the Frilihorn nappe. Separating the Zermatt–Saas Fee zone from the Tsate nappe over a long distance, another similar sedimentary unit occurs, the Cimes Blanches nappe. To the NW, the latter also follows the interface between the Mt. Fort and Tsate nappes (Figure 16-6 and Plate 16-1). The Cimes Blanches nappe overlies directly and continuously an important fault surface: *the Combin fault* which separates the very high pressure metamorphic units (Monte Rosa, Zermatt–Saas Fee, Antrona) from overlying medium pressure ones. According to Ballèvre & Merle (1993) this fault corresponds to an original eo-Alpine thrust, inverted during the Late Cretaceous to Early Tertiary as a detachment fault, and finally reactivated as a meso-Alpine thrust.

During the Middle to Late Cretaceous, two main flysch units, the Gets and Dranses nappes were probably deposited in front of the active accretionary Tsate prism. A short description of each unit and its possible significance will be given in the following text:

The ophiolite nappes:

The Zermatt–Saas Fee and Antrona zones consist mainly of metaperidotites, metagabbros and metabasalts (Bearth 1967, Dal Piaz 1965, Colombi 1989). Chemical studies reveal a tholeitic composition for the mafic rocks and a close similarity with transitional to normal MORB (Beccaluva et al. 1984, Pfeiffer et al. 1989). The metaperidotites are relatively undepleted lherzolites, quite similar to those of the Lanzo zone. Some oceanic metasediments are found, mainly associated with the Zermatt–Saas Fee ophiolites. They consist mostly of siliceous marbles, garnet and Mn-bearing quartzites (metaradiolarites) and calcschists (Vannay & Allemann 1990).

All these observations indicate that both units were part of an oceanic lithosphere formed in a slow-spreading environment (Lagabrielle & Cannat 1990). The presence of relics of eclogite facies parageneses shows that they underwent a HP metamorphism, probably during the Cretaceous Eoalpine subduction (Hunziker 1974). A later, Tertiary greenschist (Zermatt–Saas Fee) and amphibolite facies (Antrona) overprint is well documented (Laduron 1976, Colombi & Pfeiffer 1986, Ganguin 1988).

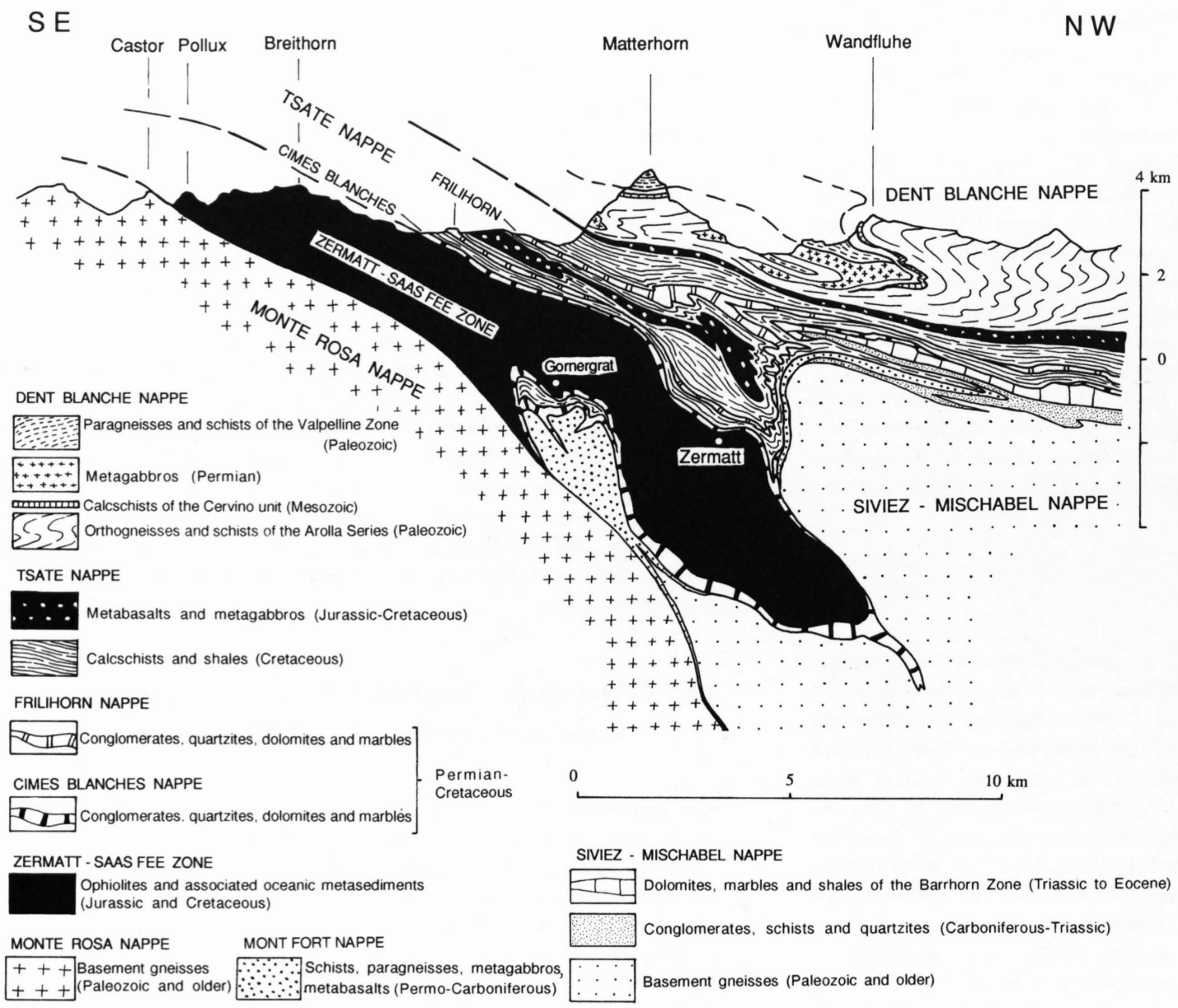

Figure 16-6
Simplified geologic section showing the relation between the Monte Rosa, Siviez–Mischabel, Zermatt–Saas Fee, Tsate and Dent Blanche nappes in the Zermatt region.

The Lanzo zone crops out in the Italian Alps. It consists of a huge peridotite of lherzolitic composition, associated with serpentinites, a few metagabbros and metabasalts, and remnants of metasediments and manganiferous quartzites (Nicolas 1966, Pognante et al. 1985). In our reconstruction it has been interpreted as the internal and SW continuation of the Zermatt–Saas Fee ophiolites as proposed by Dal Piaz (1974), Blake et al. (1980) and Lagabrielle et al (1989).

The Tsate nappe forms a large unit, corresponding to the oceanic part of the Combin zone s.s. as defined by Dal Piaz (1965) and Bearth (1967). It consists of a thick pile of imbricated metasediments and ophiolites. Metasediments consist mostly of Cretaceous calcschists and black shales, with locally Jurassic quartzites (meta-radiolarites ?) and Lower Cretaceous siliceous marbles and dolomitic breccias. The ophiolitic rocks are represented by metabasalts, meta-gabbros and meta-peridotites. Two types of basaltic rocks can be recognized, pillow lavas of probable Jurassic age and basaltic sands metamorphosed into prasinites. The latter are probably of Cretaceous age and occur as stratigraphic layers within the calcschists. The intense tectonic imbrication took place during Eoalpine subduction and corresponds logically to the internal structure of an accretionary prism (Sartori 1987, Marthaler & Stampfli 1989). The metamorphic history of the Tsate nappe is characterized by an early, relatively high pressure event resulting in the formation of greenschist-blueschist metamorphic assemblages (Dal Piaz 1976, Caby 1981, Ayrton et al. 1982, Pfeiffer et al. 1991). It was followed by a strong pervasive greenschist facies episode.

The cover nappes of unknown continental crust origin:

The Frilihorn and Cimes Blanches nappes correspond to the lower Combin zone of Dal Piaz (1965) and Bearth (1967). Though **the Frilihorn nappe** is entirely included in the lower structural part of the Tsate nappe, it diplays all the characteristics of an independent tectonic unit, with its own stratigraphy (Figures 16-6 and 16-7). The latter consists of the following rock sequence from base to top: Permo-Triassic conglomerates and quartzites, Triassic and Jurassic dolomites, marbles and breccias, Cretaceous calcschists (Dal Piaz & Ernst 1978, Marthaler 1984, Sartori 1987). In many places it overlies tectonically the basal part of the Tsate nappe, locally formed of massice siliceous marbles and calcschists (Série Rousse). The Frilihorn nappe often displays multiple repetitions due to intricate isoclinal folding, together with the Tsate calcschists. Although it locally also is isoclinally folded on itself, it generally shows the structure of a thrust nappe, entirely separated from its original basement. The basal Permo-Triassic quartzites indicate that it was deposited on a continental crust. The exact location of this original basement is not known but may have belonged to the internal Briançonnais crustal domain. The mechanism of early detachment and tectonic mixing with the Tsate nappe is still far from understood.

The Cimes Blanches nappe can be followed all along the base of the Tsate nappe, from Etroubles to Breuil (Plate 16-1 & Figures 16-6, 16-7). It has approximately the same stratigraphic content as the Frilihorn unit (Sartori 1987, Dal Piaz 1988, Vannay & Allemann 1990). The presence of Jurassic breccias indicates here also a probable internal Briançonnais origin, though no clues exist to the exact location of the original basement. Both the Frilihorn and Cimes Blanches cover nappes could in fact have had a SE origin, from an Austroalpine continental crust. Recent observations in the Mont Fort nappe region show that also there the Cimes Blanches cover nappe is tectonically discordant on the underlying Mont Fort basement.

The Flysch nappes:

The Gets nappe is the top unit of the internal Prealps, and overlies directly the Brèche nappe. The recent discovery on seismic profiles of a possible thrust between the external and internal Prealpine nappes could explain why the Gets nappe overrides the Simme unit which is of more internal origin. The Gets rocks consist of a complex sequence of Cretaceous flysch with abundant blocks and lenses of granite, ophiolites and various sedimentary rocks of Jurassic and Cretaceous age (Caron & Weidmann 1967). K/Ar radiometric age determinations of ophiolitic material from these lenses indicate a Lower to Middle Jurassic age for some of the gabbros associated with serpentinites, and a Late Cretaceous age for the emplacement of diabase lenses (Bertrand & Delaloye 1976). The latter would suggest that submarine basaltic eruptions occured at about the same time as the flysch sedimentation (Fontignie et al. 1982). The Gets nappe has been affected by anchizonal metamorphism which sharply contrasts with the much weaker metamorphic grade of the other Upper Prealpine nappes (Simme, Dranses, Gurnigel-Sarine). It is important to note that clasts of basic volcanics derived from the Gets nappe are found in sandstones in the north-Helvetic Subalpine Flysch (Sawatzki 1975). It seems logical to imagine the original depositional basin of the Gets nappe to be situated near the Piemontais accretionary prism. Therefore it can be considered as an external and superficial equivalent of the Tsate nappe, in a similar way as the Arosa zone in the Eastern Swiss Alps (Winkler 1988).

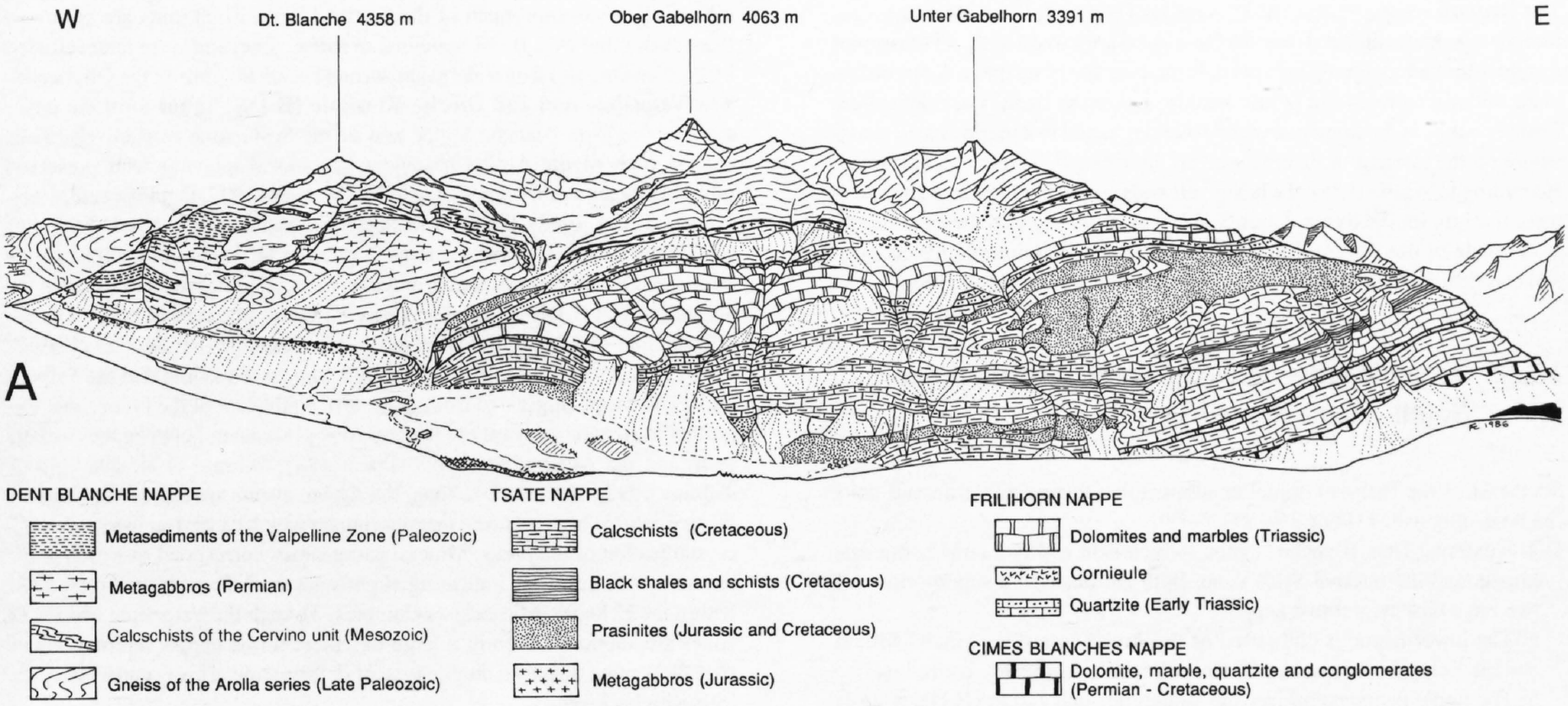

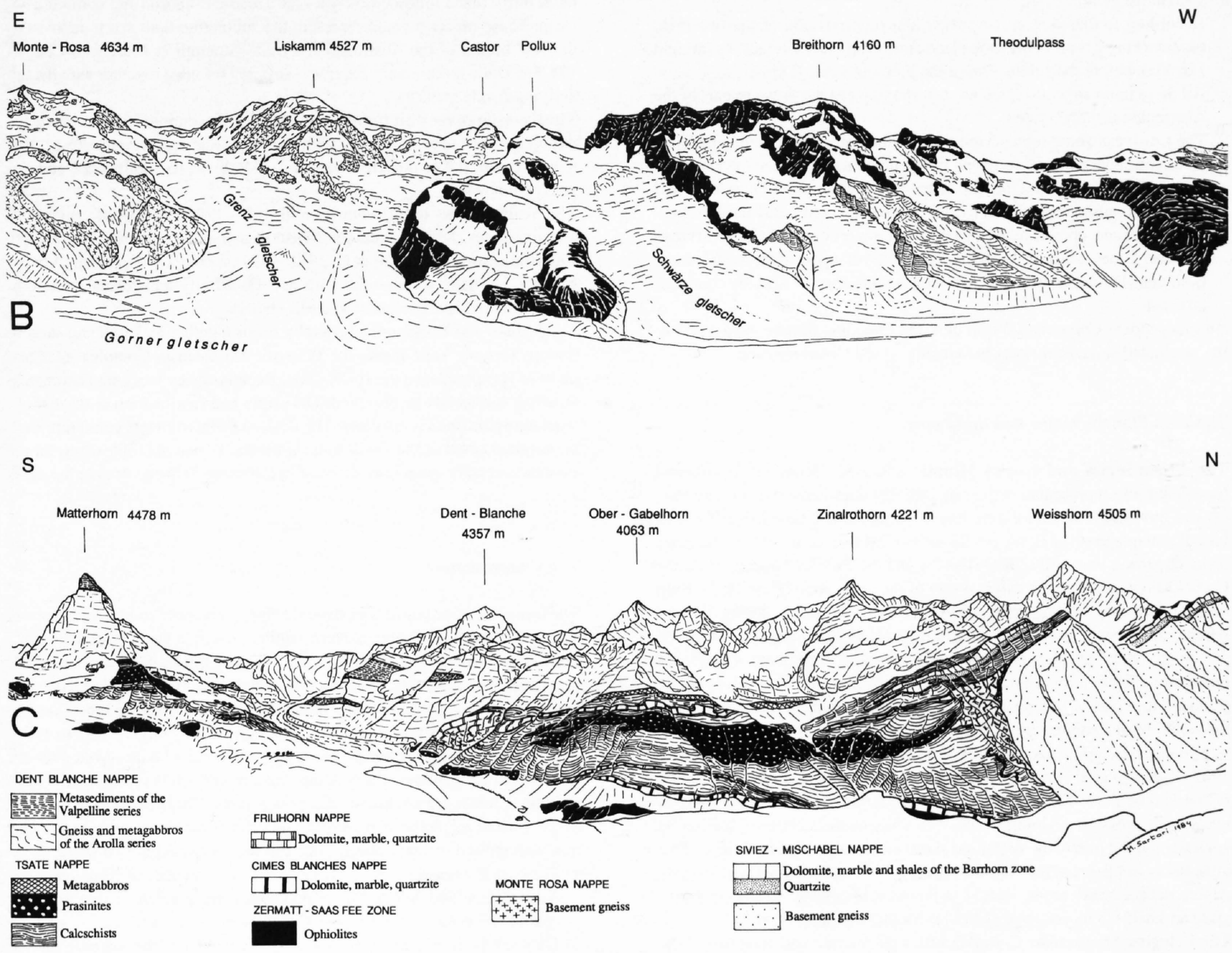

Figure 16-7
Panoramic views:
A) From the Schwarzsee above Zermatt towards the N, of the Piemont ophiolite zones and the overlying Dent Blanche nappe.
B & C) From the Gornergrat, above Zermatt, towards the S and W, on the Penninic and Dent Blanche nappes.

The Dranses nappe (Caron 1972), is made of Helmintoid flysch of Late Cretaceous age. It was thrusted over the Gurnigel-Sarine and Médianes Plastiques nappes after their common internal deformation: the basal thrust is discordant to the underlying folds and is only weakly affected by them. The origin of the Dranses nappe is not known, it could have originated in a marine basin somewhere on the internal or external part of the closing Piemont oceanic crust. According to Wildi (1985), the heavy minerals content indicates an European margin origin for the flysch deposits. Anyway, there seems to be an obliquity at the scale of the whole Alpine belt between the Helminthoid flysch basin and classical Jurassic paleogeographical domains (Caron et al. 1981).

16.2.5 Tectonic units derived from the Austroalpine and South-Alpine domains

Southeast of the Piemont ophiolite suture zone, three main structural units can be distinguished (Plate 16-1):

1) The external Dent Blanche "nappe" which is in reality a large composite klippe, and the internal Sesia zone. Both are made of a superposition of two huge basement thrust nappes:
   a) The lower nappe is composed of the Arolla series, the Gneiss Minuti and the Eclogitic Micaschist Complex which are probably equivalent.
   b) The upper nappe comprises the Valpelline zone and the II-DK zone or "Seconda Zona Diorito-Kinzingitica".
   Not far from their contact, a discontinuous, thin and refolded metasedimentary zone with ophiolitic relicts can be observed (the Cervino, Scalaro and Bonze units).
   According to Cosca et al. (in press), the superposition of the two main basement nappes probably took place during the Early Cretaceous (around 120 Ma), before the subduction of the Piemont oceanic crust.
   All these units are considered as corresponding to the Western part of the Austroalpine nappe system.
2) The Canavese zone, represented by a tectonically thinned zone of basement and cover rocks. It forms an independent unit between the exhumed Austroalpine system and the Ivrea zone. Rare serpentinised peridotite and metabasalt lenses suggest that a Canavese oceanic crust may have existed.
3) The Ivrea zone, consisting of well exposed lower continental crust (Ivrea–Verbano zone) overlain by basement rocks of upper continental crust. Both units belong to the South Alpine system formed of Adriatic continental crust.

An independent Cretaceous flysch unit, the Prealpine Simme nappe, probably originated somewhere near the already closed Canavese zone.

The Dent Blanche klippe and Sesia zone:

The Arolla series and Gneiss Minuti consist of pre-Alpine continental basement rocks represented mainly by orthogneisses derived from Late Hercynian granitoids and minor amounts of paragneisses. Layered gabbros of Late Permian age occur in the Arolla series (Dal Piaz et al. 1977). The latter forms the lower part of the Dent Blanche and the Pillonet klippes, while the Gneiss Minuti occur in the external part of the Sesia zone (Plate 16-1). Both units underwent extensive greenschist facies crystallisation during Tertiary Alpine metamorphism (Hunziker 1974, Lattard 1974, Mazurek 1986). Well preserved relics of high-pressure parageneses of presumed Cretaceous (eoalpine) age are only present in the Gneiss Minuti. It can however not be excluded that part of the greenschist facies metamorphism in the Arolla series could be of Eoalpine age as the Dent Blanche klippe represents the frontal part of the Eoalpine main nappe (Ayrton et al. 1982, Oberhänsli & Bucher 1987, Pognante et al. 1988, Pognante 1989, Canepa et al. 1990). According to Dal Piaz et al. (1972), Lardeaux et al. (1982) and Vuichard (1989), a relatively high pressure mylonitic zone forms the contact between the Arolla gneisses and the overlying Valpelline series in the Dent Blanche klippe. This most likely implies that the tectonic superposition of both units was an early Alpine (Cretaceous) event. Recent radiometric dating by Cosca (in prep.) gives an Early Cretaceous age (120 Ma) for this mylonite contact.

The Eclogitic Micaschists Complex forms the internal and main part of the Sesia zone. It consists of pre-Alpine basement, made of paragneisses and schists with relics of intermediate to low pressure granulite facies metamorphism (Dal Piaz et al. 1971, Lardeaux & Spalla 1991). This basement was later intruded by granitoids of Permian age (Paquette et al. 1989). The Alpine events started with an early (Cretaceous) pervasive *eclogite facies metamorphism,* followed by a Tertiary greenschist facies retrogression, localised in narrow ductile shear zones (Compagnoni et al. 1977, Pognante et al. 1980, Dal Piaz et al. 1983, Pognante 1989). It is possible that the Eclogitic Micaschist Complex represents the internal equivalent of the Gneiss Minuti, the essential difference between the two beeing the much more intensive greenschist facies retromorphism of the Gneiss Minuti. Both units are separated from each other by a II DK synclinal or thrust zone, and were later refolded by the Vanzone and Boggioletto antiformal backfolds, during the Oligocene.

The Valpelline and 2nd Diorite-Kinzigite (II DK) zones form the upper parts of the Dent Blanche klippe and of the Sesia zone respectively. They consist both of pre-Alpine basement gneisses displaying well preserved granulite facies assemblages (Argand 1934, Nicot 1977, Dal Piaz et al. 1971, Pognante et al. 1988). Slices of metagabbros and mantle derived peridotites are locally included in the gneisses (Cesare et al. 1989). In contrast to the Arolla and lower Sesia gneisses, no large Variscan granitoids are found in the Valpelline and II DK zones. The granulite facies gneisses of both units are quite similar to those of the Ivrea lower Adriatic crust (Rivalenti et al. 1984, Zingg et al. 1990, Rutter et al. 1993). It is logical to assume that the Valpelline-II DK nappe originated from an eastern equivalent of the Ivrea zone. Important horizontal sinistral movements took place later, between the Adriatic plate and the Austroalpine units (Frank 1987, Schmid et al. 1987, 1989, Trümpy 1992). In the II DK zone, the Alpine events are represented mainly by an Eoalpine high pressure metamorphism which caused an incomplete recrystallisation of the rocks. Mineral parageneses correspond to a high grade blueschists facies, thus indicating slightly lower P-T conditions than those within the Eclogitic Micaschists Complex. Though the Valpelline and II DK zones are supposed to form a large basement thrust nappe, internal Alpine structures often display a ductile type of deformation. This is particularly the case with backfolds.

The Dolin unit forms an isolated outcrop inside the Arolla series, in the NW part of the Dent Blanche klippe (Ayrton et al. 1982). It consists of Late Triassic dolomitic marbles, overlain by a thick sequence of Jurassic breccias. A basal thrust plane follows mostly a Late Triassic evaporite and cornieule horizon. These breccias could represent the submarine fault scarp deposits of the NW border of the Austroalpine terrain (Stampfli & Marchant, Chapter 17). The Dolin sedimentary cover was strongly refolded together with the underlying Arolla gneisses.

The Cervino cover unit forms a very thin and discontinuous layer inside the Arolla gneisses near its contact with the Valpelline zone (Figure 16-6). It is mostly composed of presumed Jurassic calcschists. Its significance and origin is unknown.

The Scalaro cover unit (Venturini et al. 1991, 1994) consists of conglomerates, quartzites, dolomites and calcschists of probable Permian to Jurassic age.

The Bonze unit (Venturini et al. 1991, 1994) is composed of sheared metagabbros, eclogitic metabasalts with MORB affinity and related metasediments (micaschists, quartzites and Mn-cherts).

The Scalaro and Bonze units generally occur together as a thin and discontinuous tectonic zone inside the Eclogitic Micaschists Complex near and more or less parallel to the II DK zone. Repetitions by isoclinal folding and thrusting can locally be observed. The origin and signification of these monometamorphic units is not clear: The Scalaro metasediments could represent the original cover of the Sesia zone, while the Bonze ophiolites suggest the existence of an original oceanic crust (= Canavese ?) inside or near the Sesia zone.

The Canavese zone:

The Canavese zone consists of strongly elongated cover and basement slices situated between the exhumed Austroalpine system to the NW, and the Ivrea Zone. The cover rocks consist of Permo-Triassic to Lower Cretaceous arkoses, quartzites, dolomites marbles and radiolarites. Tertiary conglomerates and andesite dykes occur locally along the internal Canavese limit *(the Canavese line).* Pre-Alpine basement rocks are mainly high-grade to retrogressed paragneisses containing elongated orthogneiss bodies. Mylonites are common in the gneisses. Early Alpine metamorphism is represented by anchizone to lower greenschists facies parageneses (Zingg et al. 1976).

Serpentinized peridotite slices are in some places present, mostly in association with the sedimentary cover. They can be interpreted in two ways:

1) They are the remnants of a Mesozoic oceanic mantle, in which case the Austroalpine and South Alpine domains corresponded to two different continental crusts separated by a Canavese oceanic crust.
2) They are peridotite slices tectonically derived from the Adriatic mantle which is situated quite near the surface in this part of the Alpine belt.

The recent discovery of metabasalts with MORB affinity along the Canavese zone makes the 1st interpretation more likely (Venturini 1994).

Studies of the complex structures along the Canavese line (Steck 1984, Heitzmann 1987, Schmid et al. 1987, 1989), dated by Zingg & Hunziker (1990) indicate that important vertical movements took place since the Oligocene uplift of most of the Alpine belt with respect to the Southern Alps. They went hand in hand with intense horizontal dextral displacements, probably resulting from a Late Oligocene dextral transpression between the Adriatic sub-plate and the European foreland (Marchant 1993).

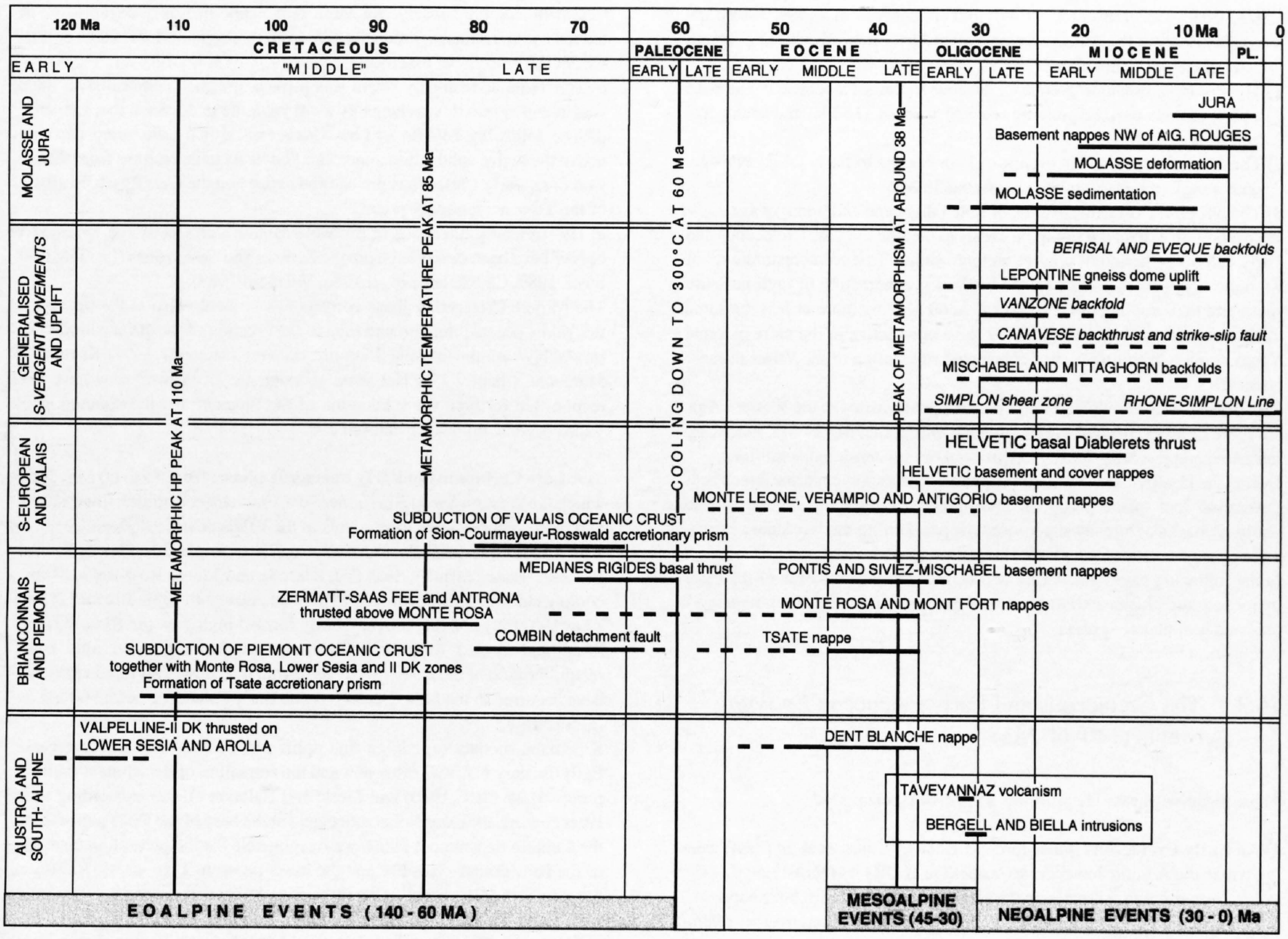

Figure 16-8
Chronology of some of the major Cretaceous and Tertiary Alpine events in the Western Swiss-Italian Alps.

The Ivrea zone:

The Ivrea zone s.s. represents a unique cross-section through the *lower (Adriatic) continental crust.* It is here that the Southern Alpine Moho comes closest to the present erosional surface. This lower crust is composed of high grade pre-Alpine gneisses containing large and smaller slices of mafic and ultramafic rocks (Schmid 1967, Bertolani 1968, Steck & Tièche 1976, Zingg et al. 1990). Paragneisses with granulite facies parageneses are common.
The mafic and ultramafic rocks are represented mostly by metagabbros and peridotites. Geochemical and petrological investigations indicate that they are deep-seated intrusions derived from the Adriatic asthenosphere (Garuti et al. 1980, Rivalenti et al.1984, Voshage et al. 1987, 1988).
The present position and the subvertical to overturned dips of the Ivrea rocks must be the result of Oligocene to Early Miocene ductile backfolding associated with shear zones around the Ivrea synform. "Brittle" back thrusting alone could never have caused the observed orientations and dips of the gneisses.
Alpine greenschist facies metamorphism developed only along the localised shear zones and along the Canavese line. It is probably of Eoalpine age.
SE of the Ivrea zone, basement rocks belonging to the *upper Adriatic continental crust* can be observed. They are mostly composed of phyllites, micaschists, gneisses and large granitoids (Schumacher et al., Chapter 15).

The Simme flysch nappe:

The Simme nappe consists of a thick complex flysch sequence of Middle Cretaceous age. It overrides the Dranses and lower nappes and probably forms the uppermost tectonic unit of the Préalpes, possessing also a most internal origin. It was only partly overthrusted by the Gets nappe during a Late Miocene event. In its middle part it includes a wildflysch with lenses of radiolarites and various limestones of Jurassic and Cretaceous age. The upper part contains the famous Mocausa conglomerate. Both the lenses in the wildflysch and the pebbles in the conglomerate have a South- or Austro-Alpine facies (Elter et al. 1966). Ophiolite-elements are rare or absent, but an ophiolitic source contributed to the fine grained material of the sandstones present in the flysch (Flück 1973). The rocks underwent only diagenetic alterations.
According to Argand (1909) and Elter et al. (1966) the original depositional basin of the Simme was situated in the Canavese zone (South-Alpine realm, Plate 16-1). It may also have been situated in a slightly more external position, where it was fed by the erosion of an eoalpine "pre-Simme" nappe of South-Alpine origin. This last solution is more in agreement with recent data on the Eoalpine metamorphism (Hunziker 1974, Zingg et al. 1976, Hunziker & Martinotti 1984, Cosca et al. in prep.), which implie that the Canavese basin did not exist any more as such in Middle Cretaceous times. The Canavese zone could be the "root" of this pre-Simme nappe, a way of reconciling the old Argand hypothesis with modern data.
The Simme nappe has been a major source for the clastic content of the Lower Freshwater Molasse, where large conglomerate fans are composed of pebbles derived from the upper Simme nappe (Trümpy & Bersier 1954).

16.3 Structural evolution

The Western Alpine arc has been created during the Cretaceous and Tertiary compression and transpression which caused the superposition of parts of the following seven main lithospheric units (from NW to SE):
1) The European continental crust and lithospheric mantle.
2) The Valais oceanic crust.
3) The Briançonnais continental crust (possibly formerly attached to the Iberic plate).
4) The Piemont oceanic crust.
5) The Austroalpine continental crust (probably without the Valpelline-II DK zones).
6) The Canavese thinned continental and possibly oceanic crust.
7) The Adriatic continental crust and lithospheric mantle (probably including the Valpelline-II DK zones).

The resulting stack has a dominant SE dip except in its internal part where backfolding and backthrusting caused important NW and N dips.
Following more or less the proposals by Dal Piaz et al. (1972), Trümpy

(1973, 1980), Debelmas et al. (1980) and Hunziker et al. (1989, 1992), the orogenic history of the Western Swiss-Italian Alps can be divided into 3 main periods of tectono-metamorphic activity (Figure 16-8).

1) The *Eoalpine* orogenic events, Cretaceous to Early Paleocene in age with a peak of metamorphic pressure reached at about 110 Ma, and a temperature peak at 85 Ma.
2) The *Mesoalpine* orogenic events, of Late Eocene to Early Oligocene age, with a peak of metamorphism at around 38 Ma.
3) The *Neoalpine* orogenic events, of Late Oligocene and younger age.

We propose to extend the Eoalpine events to include the Late Cretaceous and Early Paleocene period of relative tectonic calm ("Paleocene restoration" of Trümpy, 1980) characterised by the beginning exhumation of high-pressure rocks and their cooling down to 300°C at 60 Ma. At more or less the same time, compressional movements must have been active in the more external Valais domain, resulting in the SE oriented subduction of the Valais oceanic crust.

The Tertiary Mesoalpine and Neoalpine orogenic events in the Western Alps are more or less separated in time by Late Oligocene, 31–29 Ma, magmatic intrusions, representing locally extensional or transtensional conditions.

During the Eoalpine and Mesoalpine phases, syn-tectonic marine flysch sedimentation took place partly on undisturbed stratigraphic sequences and partly on stacks of already superposed nappes. During the Neoalpine events, molasse type sedimentation took place.

In the following pages an attempt will be made to give for each of the three major tectonic phases a short review of the successive structural, metamorphic and sedimentary events.

16.3.1 The Cretaceous and Early Paleocene *Eoalpine* events (140–60 Ma)

Three tentative phases are proposed for the Eoalpine period :

1) An **Early Cretaceous phase** (around 120 Ma, Cosca et al. in prep.), during which the Adriatic lower crust (Valpelline-II DK) was thrust ontop of the lower Sesia and future Dent Blanche (Arolla) units. This must have happened in an internal position, well before the closure of the Piemont oceanic realm. HP mylonite zones were formed at the contact between the two major nappes, remants of which can actually been found between the Valpelline zone and the Arolla series (Dal Piaz et al. 1972, Lardeaux et al. 1982 and Vuichard 1989).

This important Early Cretaceous event was probably synchronous to, or later than, the closure of the Canavese zone and the subduction of a Canavese oceanic crust. Another possibility is to imagine that the lower Adriatic crust of the Ivrea zone is not the direct equivalent of the Valpelline-IIDK units, and that the closure of the Canavese took place later.

During the Early Cretaceous, one could imagine the formation of a *pre-Simme nappe* which was expelled towards the NW and dismantled later, by submarine erosion, which resulted in the Middle Cretaceous Simme flysch deposits.

The metasedimentary sequences (Dolin, Cervino and Scalaro-Bonze) found within the Eclogitic Micaschists Complex and the Arolla series could have been included by folding and thrusting during or just after the same Early Cretaceous event. Anyway it must have happened before the Cretaceous subduction of the Gneiss Minuti and the Eclogitic Micaschist Complex. This Early Cretaceous stacking of Austroalpine nappes must have been limited to the Western Swiss-Italian Alps. More to the E, in Graubünden, Austroalpine sedimentation usually goes up to the Turonian and makes such an Early Cretaceous nappe formation impossible.

2) A **Middle Cretaceous phase**, between approximately 110 and 85 Ma characterised essentially by the closure of the Piemont domain, after and during a SE dipping subduction of the oceanic crust beneath the previously formed stack of Austroalpine and Adriatic nappes. This important tectonic event had the following direct consequences:

a) Rapid subduction to great depth (up to 80 km) of large oceanic crustal and mantle fragments (Zermatt–Saas Fee, Antrona, Lanzo) and associated continental crust pieces (Monte Rosa, Gneiss Minuti, lower II DK and Eclogitic Micaschists Complex). This resulted in HP eclogite facies mineral assemblages. Other continental fragments (Mont Fort and Valpelline-II DK) apparently underwent a slightly less pronounced HP metamorphism, as shown by their weaker blueschists facies. Finally, the presently outcropping parts of the Tsate and Arolla units were probably only subducted to no more than 20 km depth and display remnants of Middle Cretaceous greenschist facies mineral associations.

b) During this same period the Zermatt–Saas Fee and Antrona ophiolite zones were tectonically superposed, at depth, on the Monte Rosa continental basement. Simultaneously, the Mont Fort nappe probably began to be detached and translated towards the NW from its original Monte Rosa or internal Siviez–Mischabel basement.

c) The Tsate accretionary prism was formed and the Frilihorn cover nappe was included into this mélange by a not yet quite understood mechanism.

d) The following Middle to Late Cretaceous flysch units were deposited above the active subduction zone: The *Simme* flysch, resulting from the erosion of an Early Cretaceous pre-Simme nappe and the *Gets* flysch by erosion of the Tsate accretionary prism.

e) HP stretching lineations of probable Middle Cretaceous age, oriented W or NW have been described from the Zermatt and Sesia zones (Le Goff 1986, Steck 1989, Choukroune et al. 1986, Vuichard 1989).

The Middle Cretaceous phase corresponds probably also to the opening of the Valais oceanic domain and thus to the creation of the Briançonnais peninsula NW of the closing Piemont domain (Stampfli 1993, Stampfli & Marchant, Chapter 17). The same geodynamic mechanism may have been responsible for both the subduction of the Piemont and the opening of the Valais oceanic domains (Stampfli 1993).

3) A **Late Cretaceous to Early Paleocene phase**, from 85 to 60 Ma, during which the Western Swiss Alps underwent simultaneous uplift in their internal part, and compressional movements in the Valais oceanic domain.

Late Cretaceous to Early Paleocene uplift took place in the Sesia–Dent Blanche, Tsate, Zermatt–Saas Fee, Antrona and Monte Rosa units. Mineral cooling curves (Oberhänsli et al. 1985, Hunziker et al. 1989, Hurford & Hunziker 1989) suggest that the previously formed high pressure rocks were uplifted and cooled to greenschist facies temperature conditions before reequilibration of the isotherms by terrestrial heat flow. This rapid uplift must have occurred in the Late Cretaceous and Early Paleocene before 60 Ma ago (Figure 16-8).

Kinematic models explaining this uplift and cooling by Late Cretaceous-Early Tertiary NW–SE extension and the formation of detachment faults are proposed by Platt (1986) and Merle and Ballèvre (1992). According to the latter authors, the extensional movement at the base of the Tsate nappe (along the Combin detachment fault), was responsible for the present juxtaposition of the HP Zermatt–Saas Fee and the lower pressure Tsate rocks. A different mechanism for the rapid uplift of high-pressure rocks, during compression and continuing continental subduction, is proposed by Michard et al. (1993) and Escher & Beaumont (in press). It explains the uplift by flattening in depth of ductile rocks and a resulting upward nappe intrusion.

The timing of the thrust or normal fault activity at the base of the Préalpes Médianes Rigides (Gummfluh, Cosca et al. 1992) corresponds equally to this Late Cretaceous to Early Paleocene period. This, together with the SE direction of the thrusting, may well relate the basal Rigides movements directly to the large-scale uplift of the internal Alps. This would mean that the Couches Rouges sedimentation was partly syntectonic.

During these events, flysch sedimentation continued to be active NW of the Tsate accretionary prism. Thus the *Dranses Helminthoid*, the *Gurnigel-Schlieren* and the *Sub-Médiane* flyschs probably were deposited, on top of tectonically active zones.

At the end of the Eoalpine events, Late Cretaceous subduction of the Valais oceanic crust took place north of the passive central part of the Briançonnais domain. It mainly resulted in the formation of the *Sion-Courmayeur-Rosswald* accretionary prism, and was accompanied by HP/LT metamorphism starting around 80 Ma. This compressional movement may have resulted moreover in the initial formation of the external *Zone Houillère* and the *Monte Leone nappes*. Only few elements of the internal part of this accretionary complex escaped subduction, and ophiolitic remnants are scarse. Some are found in the Versoyen sequence in the Petit St-Bernard (Schürch 1987) and at Visp in Valais (Oberhänsli et al. 1985, Colombi 1989). Simultaneously, the *Niesen* flysch was probably deposited directly NW of the active accretionary prism, on top of a pile of early detached Lower Penninic nappes. The basal wedge of eroded Jurassic rocks found at the base of the present Niesen nappe could well belong to the top of one of these juvenile nappes. The sedimentation of the Niesen flysch continued into the Paleocene and Early Eocene.

16.3.2 The Eocene to Eearly Oligocene *Mesoalpine* events (45–30 Ma)

A lull in tectonic activity appears to have taken place during the Late Paleocene and the Early Eocene. The Mesoalpine events seem to be clearly separated, in time and in character, from the Eoalpine ones (Trümpy 1980).

In a general way, the Mesoalpine events caused the deformation of two hitherto undisturbed parts of the Alpine domain: The central part of the Briançonnais and the internal part of the European continental crusts. Tectonisation must have been caused mainly by continental subduction or underthrusting

oriented towards the S and SE, in direct geometric continuation of the preceding Piemont and Valais oceanic subductions. Deformation took place essentially in the upper crust, by pervasive ductile shear of the basement rocks and by the décollement of cover sequences. Two successive Mesoalpine phases are tentatively proposed: a Middle to Late Eocene and an Early Oligocene phase (Figure 16-8).

1) The **Middle to Late Eocene phase** resulted in the formation of the following ductile basement nappes: the *Briançonnais Monte Rosa, Mont Fort Siviez–Mischabel and Pontis nappes* and the *Lower Penninic (European) Monte Leone, Antigorio and Verampio units*. During this process, the *Préalpes Médianes, Brèche and Infra-Niesen cover nappes* were expelled towards the NW and escaped the intense deformation and metamorphism of the basement units. In contrast to the ductile fold nappe geometry of the basement units, these cover nappes display essentially the characteristics of brittle type thrust nappes (Escher et al. 1993, Epard & Escher 1996).
It is likely that at the same time the earlier formed Eoalpine nappe stack (Valpelline/Arolla) advanced further on top of the Briançonnais-derived units, forming thus the *Dent Blanche nappe*. This event took place around 40 Ma ago according to Cosca et al. (in prep.).
During these early Mesoalpine events, large amounts of Ultrahelvetic flysch continued to be deposited in front of the tectonically active zone, on a basement-cover unit situated somewhere between the Verampio and Mt Chetif nappes. It is possible that this flysch unit was partly enriched in foreign elements by a tectonic melange, during the underthrusting of the Helvetic units beneath the Lower Penninic ones as suggested by Jeanbourquin (1991, 1992).

2) During the **Early Oligocene phase** of the Mesoalpine events, after and partly during the deposition of the youngest Helvetic flysch sediments, the formation of the major *Helvetic nappes* began (Figure 16-8). The presence of spilitic material derived from the upper *Prealpine nappes* in some of the lowermost Oligocene flysch deposits indicate that these nappes had moved then into neighbourhood of the Helvetic domain.
Progressively from the SE to the NW the following basement units started to take shape: the *Mt Chetif, X-basement-Gotthard and Mont Blanc–Aar nappes*. Simultaneously, the corresponding cover nappes *(Sublage–Mont Gond–Diablerets–Ardon–Morcles)* were individualised. Tectonic inversion of previous normal faults likely played an important role during these early Helvetic events. At some stage during these events the Ultrahelvetic nappes probably were emplaced by gravity (diverticulation) on top of the early formed Helvetic units.
Finally, at the end of the Mesoalpine period, the internal part of the earlier formed Helvetic and Lower Penninic units was thrusted below the Middle Penninic nappes of Briançonnais origin. This was greatly facilitated by the extreme ductility of the Sion-Courmayeur and Rosswald sediments which acted as a real "Middle Penninic front".
According to Steck (1984) and Lacassin (1989), the described tectonic event was accompanied by an important dextral horizontal movement of at least 40 km. This ductile displacement took place along the *Simplon shear zone* which was contained inside the Sion-Courmayeur and Rosswald zones, separating the lower Monte Leone nappe from the upper Zone Houillère-Moncucco units. This means that the totality of the vertical and horizontal displacements were caused by a transpressive stress. It also means that the expulsion of the various Prealpine nappes followed an oblique path, with a strong deviation towards the E, as demonstrated by Sartori (1990) for the Préalpes Médianes Rigides nappe.
The ductile Simplon shear zone was active from around 35 to 30 Ma, and was later reactivated as a brittle shear zone, along the discrete Simplon–Rhône Line, as described in the following pages.

Prograde metamorphism took place during the Mesoalpine deformation in all the above described basement nappes, at temperatures above 300° C making a pervasive ductile strain almost inevitable (Voll 1976). Greenschist facies metamorphism affected parts of the external Helvetic nappes while amphibolite facies parageneses are present in the internal Helvetic and Penninic nappes. Heating of the deeper parts of the Mesoalpine nappe edifice by geothermal heat flow was responsible for this regional metamorphism. A peak of metamorphism was reached around 38 Ma (Hunziker et al. 1989, Hunziker 1992). Subsequent cooling, related to updoming and erosion, is recorded by the cooling curves of the Monte Rosa and Siviez-Mischabel nappes (Steck & Hunziker, in press). It obviously affected the entire nappe pile including the Zermatt-Saas Fee, Tsate and Dent Blanche nappes. This cooling and uplift may well correspond to the initial stage of the Late Oligocene formation of the Lepontine gneiss dome.
A strong stretching lineation parallel to the NW-SE transport direction of the nappes is present in most basement rocks (Heim 1921–22, Steck 1980, 1990, Malavielle et al. 1984, Lacassin 1987, Merle et al. 1989). Moreover a well developed SW oriented stretching lineation has been observed along the Simplon shear zone.

The Oligocene magmatic activity

Oligocene magmatic intrusions are widespread along the Periadriatic Line, separating the Canavese from the Ivrea zone (Figure 16-8). The most important intrusions are, from W to E, the Biella, the Bergell and the Adamello bodies, as well as a multitude of basalt to trachyandesite dikes. Their geochemistry indicates a mantle origin and a strong crustal contamination (Dal Piaz et al. 1977, Reusser 1987). Most of the Upper Oligocene intrusions took place inside a very short time interval beween 31 and 29 Ma (Dal Piaz et al. 1988), suggesting an extensional event at that time, probably related to the opening of the Algero-Provençal ocean.
Andesitic volcanism took place probably around 33 Ma (Hunziker et al. in prep.). Its feeder dikes are not known with certitude. Clasts of andesitic material are found in the Lower Oligocene Taveyannaz sandstone deposits on top of the stratigraphic sequences of the Helvetic Diablerets and Gellihorn nappes (Polino et al. 1990).

16.3.3 The Late Oligocene and younger *Neoalpine* events (30–0 Ma)

The Neoalpine orogenic events started around 30 Ma ago, at the end of the period of magmatic activity along the Periadriatic Line. They are characterised by intensive S and SE vergent backfolding and thrusting together with strong dextral strike-slip movements in the more internal part of the Western Alps. These large scale structures refolded and thus sealed the previously formed nappe piles. At the same time continued "forward folding" and thrusting took place in the more external zones. *A* generalised uplift of the entire Alpine belt , particularly of the Lepontine gneiss dome, and the deposition of continental molasse sediments along its front, took place during this same Neoalpine period.
Therefore it seems evident that the onset of large scale SE vergent movements combined with a continuing NW vergent ductile thrusting, must have initiated the present wedge shape of the Western Alps as seen on a vertical section (Plate 16-1). The interference between the backward and forward movements must also necessarily have created, possibly for the first time, a strong uplift of the Alpine wedge, and therefore a real mountain chain. with a high relief. This was accompanied by the deposition of Molasse type sediments in peripheral foredeep basins (Figure 16-8).
In order to better follow the highly complex Neoalpine events, a tentative division in 3 phases is proposed: a Late Oligocene, an Early to Middle Miocene, and finally a Late Miocene to present phase.

1) The Late Oligocene phase (30–25 Ma)

At the onset of the Late Oligocene at around 30 Ma, or even before a major event took place in the internal part of the Alpine belt: the originally shallow SE dipping axial surfaces and thrusts in the nappe stack became progressively steepened to attain finally subvertical to overturned dips. The reason for this may have been the addition of frontal imbricates resulting in the rotation of the older thrust sheets. Moreover the oversteepening of the units may have been caused by the resistance to uplift of the high-density Adriatic upper mantle, especially in its thicker internal part. The effects of the Late Oligocene verticalisation of the internal Alpine structures certainly triggered the development of large and small scale backfolds and backthrusts. The translation of ductile crustal material beeing blocked at depth to the SE, one major possible way to evacuate the material, was by upward movements to the SE, creating structures with NW dipping axial surfaces. It is only after the shaping of these backfolds which must equally have affected the Adriatic upper mantle and crust, that the latter acted as an "indenter" in the lower part of the European upper crust .
This fundamental inversion mechanism was probably the main cause of the final uplift of the Alps. The present position of the Lepontine dome structure, formed during the same Late Oligocene events, corroborates this idea. Its emplacement, where the Alpine belt is narrowest, and the fact that it represents the part of the belt which underwent the highest uplift, imply here that the backward movements too were probably the most pronounced.
The Late Oligocene blocking of the "normal" ductile flow by subduction of crustal material to the SE may have had another result: Important horizontal movements, mostly dextral, took place along the *Canavese Line* (Argand's Insubric phase), and along most of the simultaneously formed Boggioletto and Vanzone antiformal backfolds (Steck 1989, 1990, Steck & Hunziker 1994). Possibly the Mischabel and Mittaghorn backfolds (Plate 16-1) already started to take shape at approximately the same time, in association with continuing dextral movements along the Simplon Shear Zone.
In the NW peripheral Molasse basin, the deposition for the first time of

continental sediments correlates to the above described Late Oligocene generalised uplift, and therefore corroborates this interpretation. The Lower Freshwater Molasse contains in its upper part conglomerates made largely of pebbles derived from the erosion of older conglomerates of the Simme nappe. This indicates the vicinity of the latter nappe near the Alpine front at the end of the Oligocene.
It is most likely that at that time two major associations of Helvetic and Prealpine cover nappes were formed near the active front of the Western Swiss Alps, immediately to the SE of the Lower Freshwater Molasse basin:
1) An external composite unit formed by the superposition of, from bottom to top, *the Morcles, UH-Morcles, Médianes Plastiques, Gurnigel-Sarine, Dranses and Simme nappes.*
2) A more internal composite unit formed by the upward stacking of the *Diablerets, Mt. Gond, Sublage, UH, Infra-Niesen, Niesen, Sub-Médiane, Médianes Rigides, Brèche and Gets nappes.*

2) The Early to Middle Miocene phase (25–11 Ma)

During the Early Miocene, in the external part of the Alps, the above described composite nappe unit (2), was thrusted over the external one (1). This took place essentially along the *Diablerets basal thrust* (Crespo et al. 1995) and resulted in the separation between the Morcles and the Médianes Plastiques nappes along the ductile supra-Morcles Ultrahelvetic flysch (Plate 16-1). It also probably caused the overthrusting of the internal part of the Lower Freshwater Molasse by the Médianes Plastiques and its overlying upper Prealpine units. These movements were the principal cause for the deformation of the *Subalpine Molasse*. It seems likely that the directly following Burdigalian transgression of the Upper Marine Molasse was equally the result of the preceding tectonic events which may have caused a slightly increased subsidence of the Molasse basin.
In the internal Western Alps, during the Early Miocene, updoming and backfolding probably migrated slowly to the W, concomittent with the migration to the W of the "Adriatic intenter" as shown by Marchant (1993). At more or less the same time, the SW dipping structures on the Western side of the Lepontine dome were cut by erosion. Consequently, they could have acted as low angle extensional and/or gravity-induced normal faults. This resulted probably in the tectonic unroofing of the Lepontine dome, mainly along the ductile SW dipping Simplon Shear Zone.
During the Middle Miocene, the zone of active lithospheric subduction migrated further to the NW and generated the *Aiguilles Rouges and Infra-Rouges* basement nappes, probably by ductile internal deformation of the basement rocks. The wide ductile shear zone which thus created the inverted limb of the Infra-Rouges nappe passes upwards to a narrow shear zone or thrust. This major accident resulted in the superposition of the Gets unit on top of the Simme nappe. At the same time it brought into close tectonic contact the Médianes Rigides nappe with the Médianes Plastique nappe (Plate 16-1).
At the end of the Middle Miocene, the youngest S vergent *Evèque-Balmahorn* and *Berisal backfolds* were formed. They fold the 12 Ma Rb/Sr – biotite isochrone and are cut by the 11 Ma old Rhone-Simplon line (Steck & Hunziker 1994). It may well be that at the same time, in the more internal part of the Alps, the Vanzone and Boggioletto backfolds continued to be active and attained their presently tight geometry. A simultaneous activity of the dextral strike-slip Rhone–Simplon Line is probable (Soom 1990).

3) The Late Miocene to actual phase (11–0 Ma)

This last period in the history of the Western Alps has witnessed a decrease of the uplift rate throughout the mountain range and a further and probably final displacement towards the NW of the tectonic activity. The latter consisted mainly in a continued subduction of the European lithosphere underneath the frontal Prealpine nappes and the Molasse. It resulted in the following main events, all related directly to each other, from SE to NW:

1) The formation of an important anticlinal basement structure, somewhere under the frontal part of the Prealpes Médianes Plastiques. Due to a lack of precise seismic information, its position on the profile of Plate 16-1 is arbitrarily indicated. It appears to be associated with an important shear zone or thrust within the basement. This structure is visible on seismic sections, directly below the Aiguilles Rouges frontal fold, at a depth of approximately 20 km. It could be the main basement structure responsible for the Jura decollement and shortening.

2) The subalpine Molasse continued to be deformed, for instance by thrusts generated possibly by the above described anticlinal structure in the basement. The Molasse plateau, underwent also, though in a lesser degree, internal deformation resulting in large open folds, thrusts and strike-slip faults. This probably caused some NW–SE shortening, an increase in total thickness and thus a relative uplift (Laubscher 1974). As a direct consequence, the sedimentation in the Molasse basin stopped and was replaced by active erosion.

3) The Jura cover rocks were deformed following more or less the rules of thin skinned tectonics and using the Triassic evaporites as basal detachment horizon. Deformation started in the internal part, just N of the Molasse basin and migrated later by successive ramps and flats towards the NW. Probably during the Early Pliocene, the last deformation and translation took place by thrusting of the SW outer part of the Jura on top of the Bresse Graben. Displacement of the cover towards the NW in relation to the underlying basement increases from 10 km at the Bresse Graben to more than 30 km near the Molasse basin. The internal shortening attains thus approximatively 20 km. According to the "Fernschubhypothese" (Buxtorf 1907, Laubscher 1961, Jordan 1992), the origin of all these structures is probably to be found essentially in the frontal basement folds and thrusts situated below the Prealpine and Helvetic nappes (Plate 16-1). The cover of the Aiguilles Rouges massif having been proved to be autochthonous with respect to the massif, there remains theoretically the three following possibilities: (1) a basement ramp below the Aiguilles Rouges massif, (2) the Infra Rouges basement anticline, (3) the basement anticline situated below the external part of the Prealps. The first two structures were probably already formed during the Middle Miocene. Therefore it seems likely that the most external basement anticline (3), associated with a basement shear zone or thrust as described above, was responsible for the decollement of the Jura.
During all these events, in the more internal part of the Western Alps, oblique dextral strike slip movements took place along the discrete Rhône–Simplon Line. They represent probably a late manifestation of the pre-existing ductile Simplon shear zone, under retrograde conditions, associated with the uplift of the external massifs. The movements started 11 Ma ago and are probably still active. They may well represent one of the major potentially active seismic zones in the Western Alps.
The present day morphology of the Western Swiss Alps has been shaped to a large extent by the Pleistocene glaciers. Intense erosion intervened during and between glaciations. A large part of the Alpine range, especially the Molasse Basin, is covered by Pleistocene moraine deposits, gravels, sands and silts.

16.3.4 Conclusions

The **Cretaceous-Paleocene Eoalpine events** caused the deformation and partial disappearance by subduction below the overriding Adriatic lithosphere of the following units: the Carnavese continental and eventual oceanic crusts, the Austro-Alpine continental crust, the Piemont oceanic crust, and the Valais oceanic crust. Moreover the thinned parts of the continental crust, along the distal margins of the Briançonnais and European domains, were also involved in these tectonic events. This means that of the seven involved crustal domains only two remained more or less undeformed before the onset of the Mesoalpine orogenic events. This underlines the importance of the "early Alpine" events. It is in fact quite possible that important Cretaceous orogenic events took place in the internal Western Alps, without leaving a clear trace.
It remains puzzling, however, that no serious remnants of Cretaceous Molasse-type continental deposits are found. The abundance of Cretaceous flysch-type deposits indicates that much of the sedimentation during that period was submarine. This includes the Late Cretaceous–Paleocene phase of uplift of high grade rocks.

The effects of the later **Tertiary events** are of course much better preserved. It is therefore possible to get a relatively clear picture of how, and partly why, the Western Swiss-Italian Alps were formed during the Tertiary orogeny. The successive events followed several fundamental, though only partly well-known rules:

1) The absence of definite continental deposits, and the abundance of marine syn-tectonic flysch-type sediments suggests that during the *Mesoalpine* events, the main response to compressionnal stress was the underthrusting or subduction of continental crust and lithospheric mantle.

2) The Tertiary Mesoalpine continental subduction took place consistently with movements and shallow dips towards the SE, the dip and translation direction being most likely determined by the preceding orientation of the Cretaceous subduction of the Piemontais and Valaisan oceanic crusts.

3) The Mesoalpine events probably started in the SE with the formation of dominantly basement thrust-nappes of Austro- and South-Alpine origin. They are present in their final shape as the Dent Blanche nappe. This thick pile of overlying basement nappes formed a "traîneau écraseur", (Termier

1903) or tectonic lid (Laubscher 1988, Schmid et al. 1990) which created ductile conditions in the underlying rocks. It permitted the subsequent formation of basement fold-nappes in the lower and more external units. A "ductility front" probably limited this mechanism to the NW.

4) During the Mesoalpine and Neoalpine subduction of European and Briançonnais continental crust, deformation took place exclusively in its upper delaminated part. The lower, layered continental crust was probably subducted without important internal deformation. At least it appears very continuous, with only small variations in width.

5) Shortly before or during the generation of basement nappes, the corresponding cover-sequences were mostly detached along ductile basal horizons, if present, and migrated to the NW, escaping deformation and metamorphism at depth (Escher at al. 1993, Epard & Escher 1996). The so formed cover thrust-nappes display generally the characteristics of thin-skinned tectonics similar to those of the Folded Jura.

6) Tertiary deformation generally migrated from the internal SE part, progressively to the external NW part of the Western Swiss Alps. As proposed for the first time by Steck (1987), this was accompanied by the progressive ductilisation of the European upper crust and the simultaneous generation of successive basement nappes. At the same time the escaping cover nappes formed a superficial stack which continuously must have traveled in relative motion to the NW, always in front of the advancing earlier formed basement nappes, and above the new-formed ones. The frontal pile of cover nappes probably formed an extension to the NW of the Dent Blanche tectonic lid, permitting thus a continuing ductile deformation of the basement/cover interface below.

7) At the beginning of the Neoalpine events, the internal part of the SE dipping nappe pile was verticalised and even overturned. This created for the first time the Adriatic Indenter, and at the same time a brake to the "normal" to the SE and downward subduction of upper crustal material. Inevitably, new mechanisms for the escape of the compressed crust became active:
a) Large scale ductile backfolds with SE vergent axial surfaces which, in contrast to the NW vergent frontal structures caused the upward movement (to the SE) of crustal material.
b) Important dextral strike slip movements along generally ductile shear zones permitted sideways movements in response to the continuing compressive, and often transpressive stresses.

8) Neoalpine backfolding and associated uplift started in the internal SE part of the belt and migrated progressively to the external part, resulting finally in the generalised uplift and mountain building of the Alps. This activity probably was not continuous but episodic and took place over relatively short time intervals (Hurford et al. 1991). Logically, at the same time the syntectonic sedimentation changed from marine (flysch) to continental (Molasse).

9) During the NW migration of backfolding, the subduction and associated folding and thrusting along the front of the Alpine range continued to be active and also to migrate to the NW. Therefore during the Neoalpine events both NW and SE vergent folding took place simultaneously but never at the same place. As a direct result, at any location in the Western Swiss-Italian Alps backfolding is always younger than the NW vergent "forward-folding".

Acknowledgements

We thank very much Marcel Burri, Michael Cosca, Jean-Luc Epard, Marc Escher, Michel Jaboyedoff, Robin Marchant, Giorgio Martinotti, Gerard Stampfli and Guido Venturini for their generous help during the long elaboration of this paper. Daniel Bernoulli, Giorgio Dal Piaz and Pierre-Charles de Graciansky are also very much thanked for constructive critical reading which improved considerably the final quality of the manuscript.

Plate 16-1

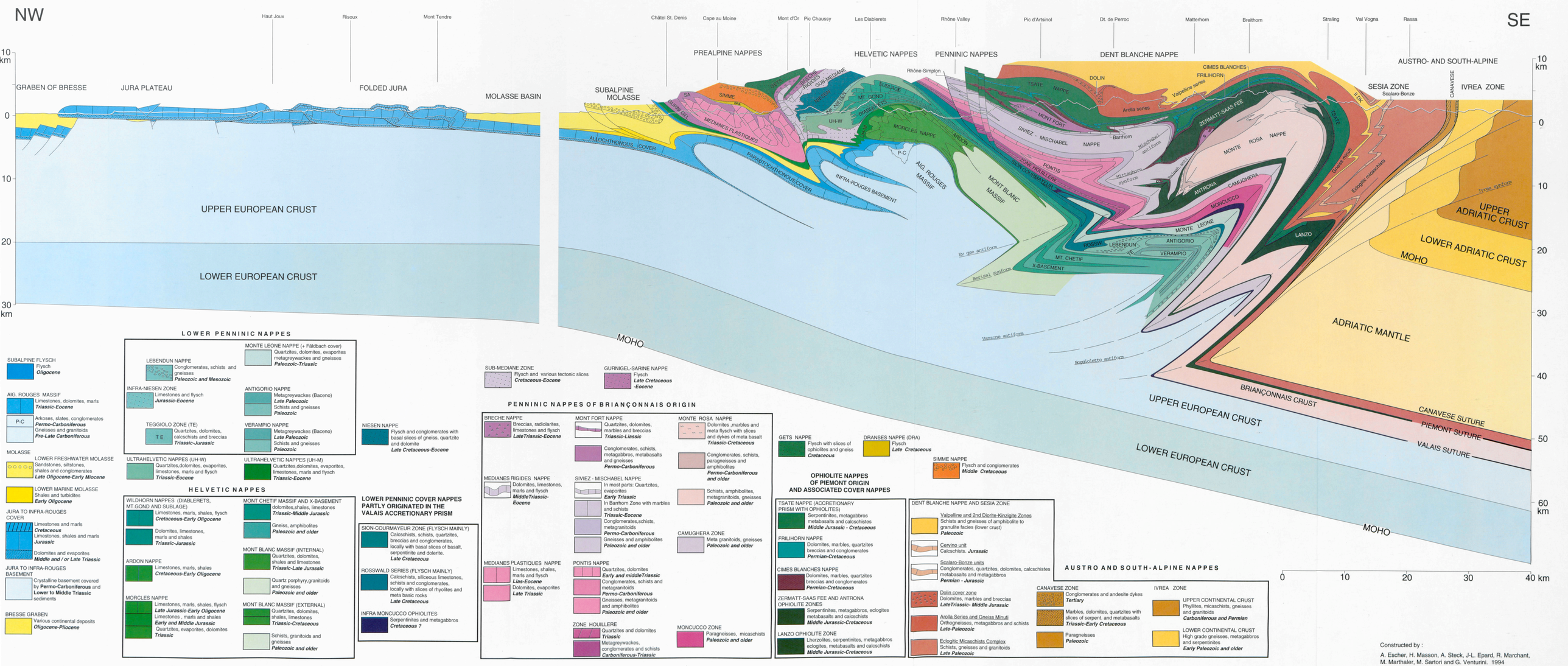

Constructed by :

A. Escher, H. Masson, A. Steck, J-L. Epard, R. Marchant, M. Marthaler, M. Sartori and G. Venturini. 1994

Section sciences de la terre BFSH-2 CH-1015 LAUSANNE

17 Geodynamic evolution of the Tethyan margins of the Western Alps

G. M. Stampfli & R. H. Marchant

Contents

17.1 General remarks

This paper is an update of the authors point of view on the geodynamic evolution of the alpine region, already presented and published elsewhere (Marthaler & Stampfli 1989; Stampfli & Marthaler 1990; Stampfli et al. 1991; Favre & Stampfli 1992; Marchant 1993; Marchant et al. 1993; Stampfli 1993). The connection between the Alpine domain and the Carpatho-Dinarid domains as well as the palinspastic position of units now pertaining to accretionary mélange have been reassessed.

This paper is based on a multidisciplinary approach to the interpretation of geological and geophysical data. Although centred around the Western Alps, the model is integrated in a larger scheme in order to clearly define the kinematic constraints in an area dominated by microplate movements. The present review is based on the structural and crustal structure of the Western Alps and lithospheric cross-sections presented in Chapter 24 by Marchant & Stampfli. These cross-sections are integrated into palinspastic models based on the geodynamic evolution of the Western Alpine Tethys margins.

The models presented here are based on a large data base accumulated through a century of field work aimed at elucidating the structural framework of the Alpine region. This framework, as presented in Chapter 16 by Escher et al. and Chapter 12 by Steck et al., is now widely accepted as the structural model for the Western Alps (see also Pfiffner et al. Chapter 13.1; Schmid et al. Chapters 14 and 22; Schumacher et al. Chapter 15). This structural framework of the Swiss Alps allows for reconstructions which are highly constrained in terms of the present day distributions of the different elements used in the palinspastic models. However we will see that the present day nappe pile represents the accretion of domains pertaining formerly to at least four lithospheric plates (Figure 17-1). This accretionary process was not done without some large- and small-scale "mélanges" and this paper will try to contribute to the re-ordering of the bits and pieces of lithosphere now scattered through this amazing Western Alps 3D puzzle. It is not possible in such a compilation to give the references for every bit of information; references of the original material should be found in the above mentioned papers.

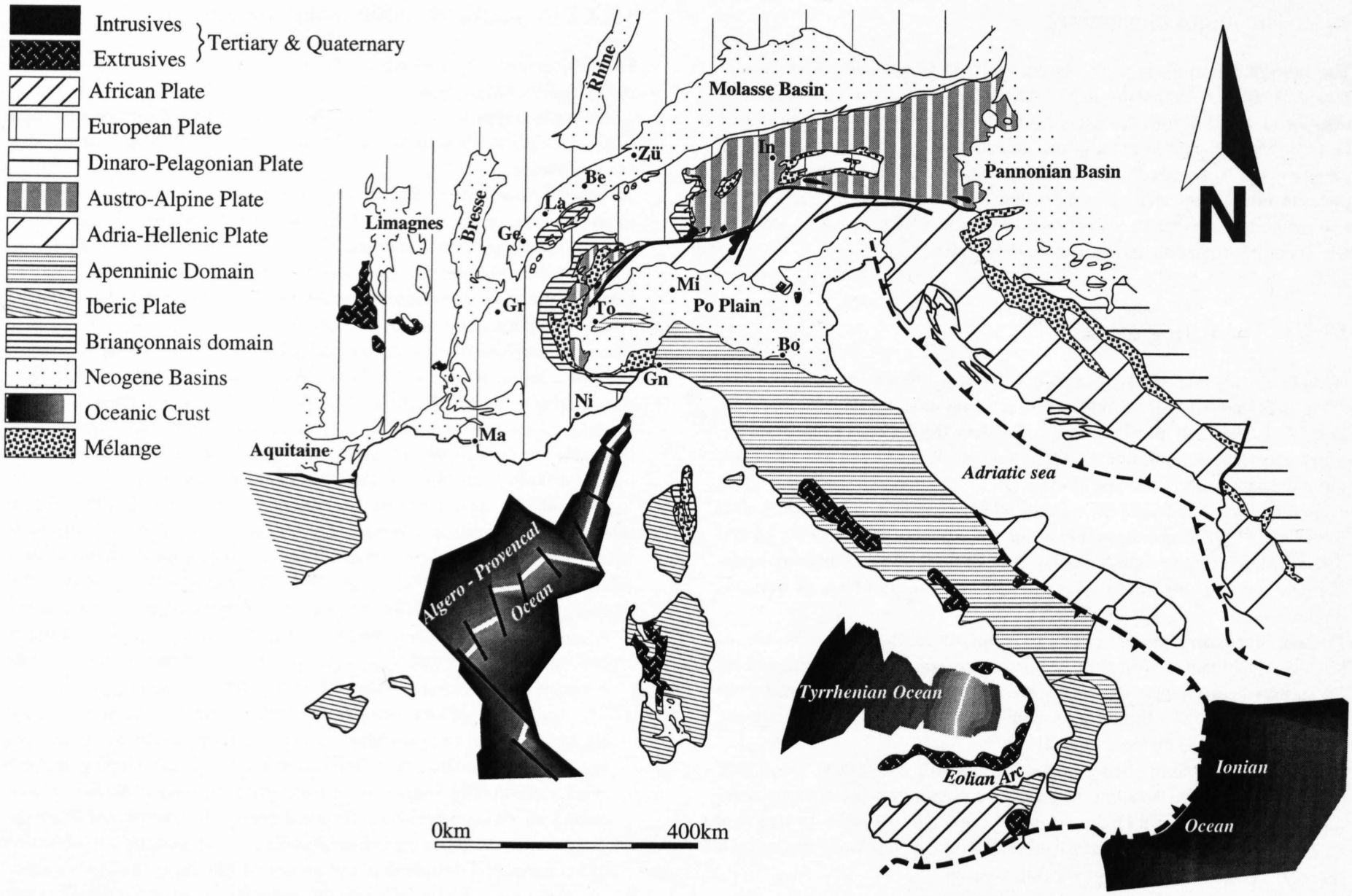

Figure 17-1
Present day distribution of the main geodynamic domains of the Alpine region. Exotic terrains in the Western Alps: the Briançonnais (narrow horizontal ruling) and part of the Austroalpine domain (grey with white stripes). Geographic landmarks: Be = Bern; Bo = Bologna; Ge = Genève; Gn = Genova; Gr = Grenoble; In = Innsbruck; La = Lausanne; Ma = Marseille; Mi = Milano; Ni = Nice; To = Torino; Zü = Zürich.

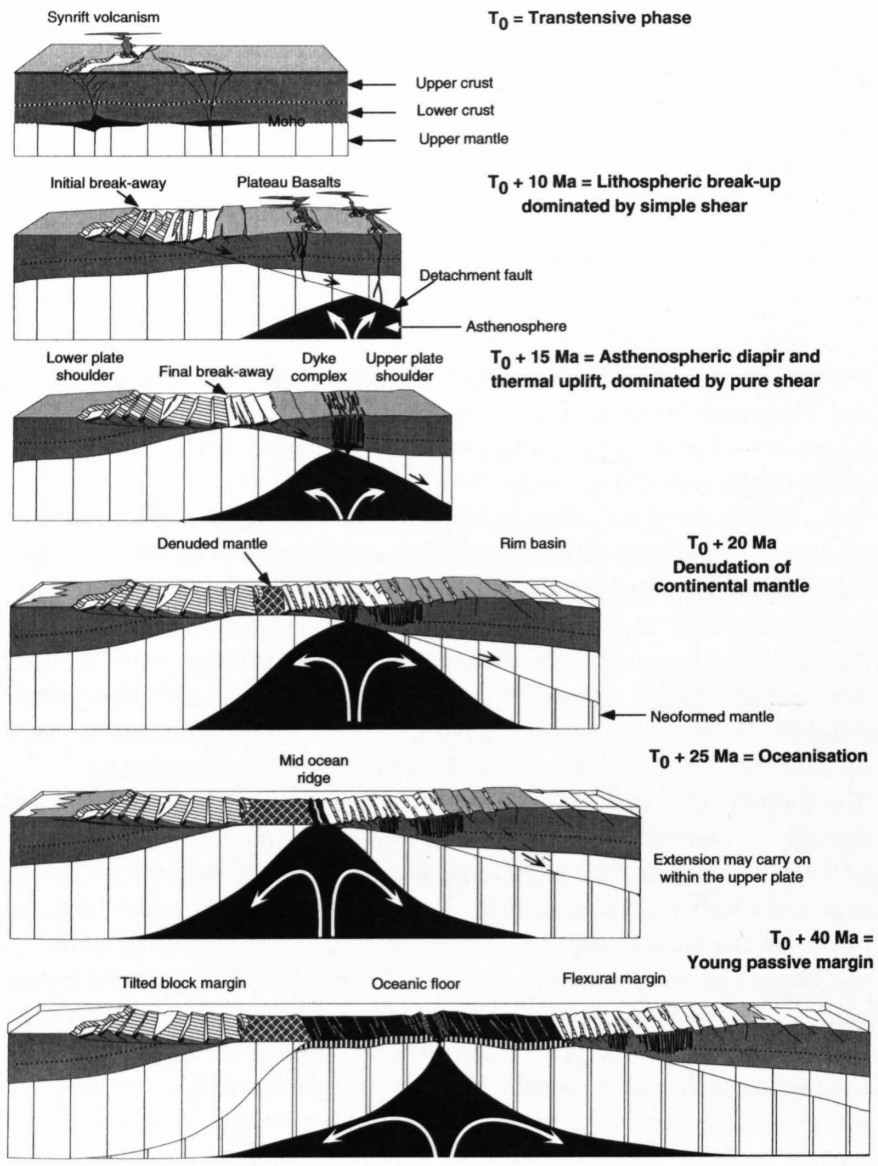

Figure 17-2
Geodynamic evolution of a Red-Sea type rift (modified after Voggenreiter et al. 1988 and Stampfli et al. 1991); see text for explanation.

17.2 The major constraints

The lithospheric cross-sections, as presented in Chapter 24 (Marchant & Stampfli), allow to define the size of the former elements of the continental margins involved in the Alpine collision. However other constraints should be taken into account in palinspastic models dealing with the evolution of passive margins. These concern the rifting concepts and the kinematics of the plates involved in the models. In the following sections we will discuss these two main elements before we proceed to present a palinspastic model into which our lithospheric cross-sections can be placed.

17.2.1 The rifting model

We have already published (Stampfli & Marthaler 1990; Stampfli et al. 1991; Favre & Stampfli 1992; Stampfli 1993) a rifting model based on actualistic data (Red Sea, Gulf of Suez) and older data (Morocco, central Atlantic, Alps), incorporating information from field work, refraction and reflection seismic. In the latter works we have shown the relation existing between the evolution of these different rift systems which eventually gave birth to slow spreading oceans. The comparison of the respective evolution of the central Atlantic and the Alpine Tethys shows a very similar pattern of thermal expansion and thermal subsidence. This model proposed the following scenario (Figure 17-2):

Transtensive rifting phase (phase 1): lasting from a few Ma to a few tens of Ma, evolving either into an aborted intracontinental rift/intracontinental basin, or into the formation of an new ocean. Locally the crustal extension can be large (10 to 20 %). Intrusion of mantle material will occur at depth and can be accompanied by local thermal uplift.

Simple-shear phase of rifting (phase 2): implying a complete shearing of the whole lithosphere usually weakened by the previous phase of transtensive rifting. The rift area will be the setting of important but local formation of fault-scarp breccias. This event will produce a decompression of the asthenosphere over the whole length of the future ocean.

One can grade slowly from phase 1 to phase 2, as was the case for the central Atlantic (Favre et al. 1991; Favre & Stampfli 1991), or one can start with phase 2, following a very short phase 1, as was the case for the Red Sea (Favre & Stampfli 1992).

Thermal expansion phase: this phase will be accompanied by important pure-shear, mainly at the level of the lower-crust and the base of the lithosphere; simple-shear will now be limited to the upper-crust. Sublithospheric erosion/assimilation of mantle material will also take place reducing the lithospheric thickness over the whole rift area. A general phase of uplift will follow the onset of asthenospheric diapirism. Within the rift this uplift is compensated by extension, outside the rift, the rift shoulders will attain a prominent relief (up to 3000 m in the Red Sea), generating a large amount of clastic material deposited within the rift area and also in surrounding rim-basins (Stampfli & Marthaler 1990). This phase will follow phase 2 by 5 to 10 Ma, and oceanisation of the rift area will start as soon as 20 Ma after initiation of phase 2 as in the case of the Red Sea (Stampfli et al. 1991).

Phase 1 is dominated by transtensional stress generated by plate interaction (Ziegler 1992a, 1992b), whereas during phase 2 the extension is guided by the rising asthenosphere diapir.

Sea floor spreading phase: this phase will induce thermal contraction of the former rift zone and thermal subsidence of the rift shoulders. The largest thermally induced subsidence of the former rift zone will occur during the first 20 Ma following the onset of sea floor spreading. As shown in Figure 17-2, post-oceanisation extension of the upper-plate can contribute to the subsidence. Then an early passive margin stage starts, marked by the flooding of the rift shoulders and generally accompanied by a phase of sediment starvation.

Rim-basin: during the phase of transtension (phase 1) the extensional processes can affect a large area and will create connected or isolated half-grabens. Emplacement of mafic material at depth can create local uplift, but will mainly contribute to accelerated subsidence of these areas sometimes already prior to phase 2. During phase 2 these half-grabens can be reworked and incorporated into the rift zone, or, if situated on the rift shoulder, they will be uplifted and eroded (Favre & Stampfli 1992). If located outside of the rift zone they will develop as rim-basins (Stampfli & Marthaler 1990). Their sedimentary sequence will record the process of shoulder erosion. After thermal subsidence of the shoulders they will become part of the new continental margin and after a relative phase of sediment starvation they will accommodate prograding sequences coming from the mainland. The rim-basins will trap most of the progradation which might never reach the rift area; in the absence of rim-basins the prograding margin is situated directly on the rift zone.

17.2.2 Asymmetric continental margin

The simple-shear phase of rifting at lithospheric-scale will generate asymmetric continental margins:

A lower-plate type with large-scale tilted-blocks and denuded upper-mantle at the continent to ocean transition. Extension there would stop with the onset of oceanisation.

An upper-plate type with a ramp-like or flexural geometry with limited tilted-blocks, trapp-like volcanism (not necessarily widespread) and a continent to ocean transition composed of basic intrusions as is the case for the Arabian side of the Red Sea (Bohannon 1986). As shown by this author, extensional processes can last some time after the onset of oceanisation and different generation of faults can develop.

The sedimentological environment and subsidence patterns will be different for both margins as shown for the central Atlantic conjugate margins (Morocco and the US coast; Favre & Stampfli 1992). However when dealing with continental margins involved in continental collision the discrimination between the two types is not so easy. Usually the rift part of the margin has disappeared during the collision. The rheological behaviour of the margin during the collision can still be used to characterise one type or the other. Putting all available information together (Figure 17-4, 17-5 & 17-6), we propose an asymmetry for the Alpine margins with a changing vergence somewhere in the eastern Swiss Alps (Manatschal 1995; Froitzheim & Manatschal 1996). The change of vergence explains some major features of the Alpine chain:

- A central and eastern Austroalpine upper-plate margin, mainly of upper-crust nature, could explain the large overthrusting of crustal material in the Austrian Alps, by simple obduction of this margin onto Europe.
- The Apulian plate had a lower-plate geometry which is much more resistant to strain than an upper-plate. During convergence the combined Austroalpine/Apulian margin becomes an active margin, developing an accretionary prism. The former lower-plate geometry of the Apulian margin creates an efficient back-stop for the accretionary process and the accretionary prism is rich in ophiolites (Tsaté type); the underplating of oceanic and continental lithosphere is also important. On the Austroalpine transect one can expect a far less efficient off-scrapping effect of this former upper-plate, more material will be subducted and the prism will be reduced.
- The Internal massifs (Monte Rosa, Gran Paradiso, Dora Maira and the Swiss lower Austroalpine elements: Dent Blanche and Sesia) can be seen as pieces of the toe of a lower-plate margin. MORB basaltic extrusions re-

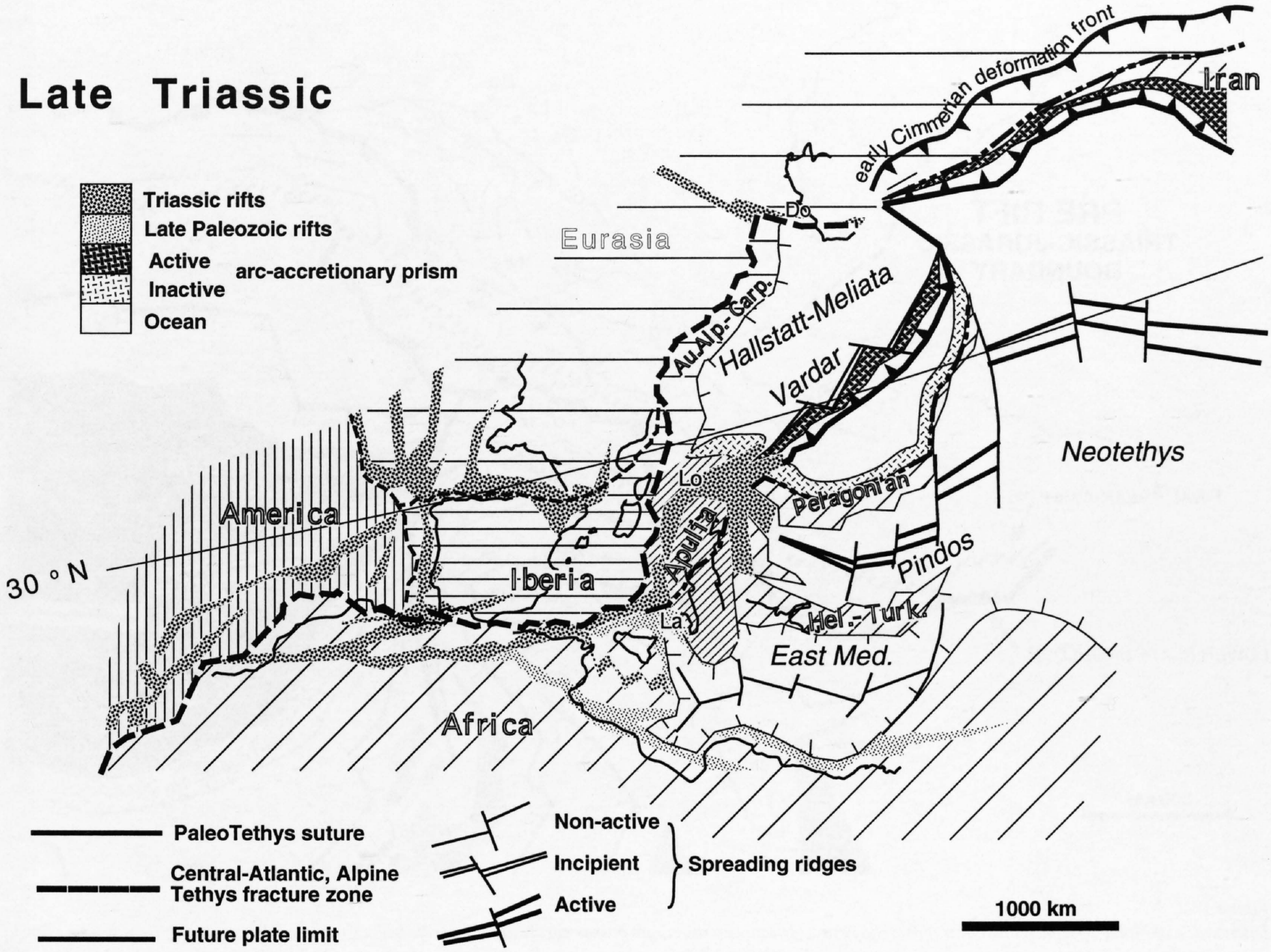

Figure 17-3
Late Triassic reconstruction of the Mesogean/Alpine regions. See text for discussion. Do = Dobrogea; La = Lagonegro-Sicanian basin; Lo = Lombardian rift.

cently described in the Sesia cover (Venturini et al. 1994; Venturini 1995) would fit that model. They are affected by Eoalpine HP-LT metamorphism, already starting in early Cretaceous (Sesia/Dent-Blanche domains; Cosca et al. 1994a, 1994b) and came back to a higher structural level without having been warmed up. They have been under-plated and thermally protected by subducting material. They may represent the transition zone between the upper (eastern Alps) and lower (Apulian) plate geometry. These elements have been incorporated in an active margin in early Cretaceous and formed a crustal-scale mélange involving ophiolites like the Zermatt-Saas unit. The Margna units of the eastern Swiss Alps are regarded as a similar piece of the toe of the lower Austroalpine margin (Trommsdorff et al. 1993; Froitzheim et al. 1994) involved in early Cretaceous subduction processes.

- The thick and dense European lower-plate will have no problem subducting under the Apulian plate. As shown by the present lithospheric scale cross-sections (see Figure 17-12a, 17-13a and 17-17a), up to 200km of continental lithosphere (denuded mantle, tilted-blocks, rift shoulder) have been subducted.
- The Apulian lower-plate margin was transformed into an upper-plate in terms of subduction geometry but it will eventually sink and develop as an indenter, creating a A-type subduction zone. This indenter will start an off-scrapping of the European plate to create the important back-folding of the Alpine chain (see Schmid et al., Chapter 22; Marchant & Stampfli, Chapter 24).

17.2.3 Rheological constraints and microplate size

When analysing a mountain belt mainly by means of cross-sections, one is easily lead to propose palinspastic models corresponding to in situ unfolding of structural units. Doing so for the Alps, most authors proposed a multi-ocean model with oceanic strips opening simultaneously and parallel to each other, separating micro-continents whose sizes are often of a few tens of kilometres.

The following considerations on plate-boundary rheological behaviour try to demonstrate the inadequacy of such a synchronous multi-ocean model:

a) When an oceanic spreading ridge is created, the surrounding lithosphere is mechanically far more resistant: all extensional (or compressional) strains will be accommodated by the ridge. It will thus be difficult to create another intracontinental extensional zone parallel and close to it. This is mainly due to isostatic disequilibrium between the mid-oceanic ridge (asthenospheric diapir) and the continent which induces a lateral stress directed towards the continent. These forces have been grouped under the label of "ridge push effect" (Allen & Allen 1990) which is certainly at its peak during early oceanisation. This will actually create enough lateral stress to deform mobile areas (like a rim-basin) within the continental plate as proposed for the Atlas system in mid-Jurassic time (Favre & Stampfli 1992), the Briançonnais domain at the same period (Septfontaine 1995) and the Provençal basin in Albo-Cenomanian times (Stampfli 1993).

b) The ridge corresponds at depth to a convective asthenospheric cell at least 200 to 300 km wide at its base. To create another spreading ridge is to create another cell which has to be at least 200 to 300 km away from an existing one in order not to become a single convective cell. Two parallel simultaneous spreading ridges would therefore define the isolation of a continental strip at least 200 to 300 km wide. In our present oceanic system the Seychelles-Mascarene plateau is effectively 300 km wide and 1500 km long; the Corso-Sardinian micro-continent is 200 to 300 km wide and 600 km long, but as a lithospheric plate it was certainly larger; the Rockall-Hatton bank (Ziegler 1988) in the northern Atlantic is also more than a thousand kilometres long and several hundred kilometres wide. In the Pacific ocean, the Chile rift system and the East Pacific rise, represent two parallel spreading ridges at present time, born from a triple junction. The two ridges were subsequently separated by at least 500 km of oceanic lithosphere.

These considerations give an idea of the constraints on the width of micro-

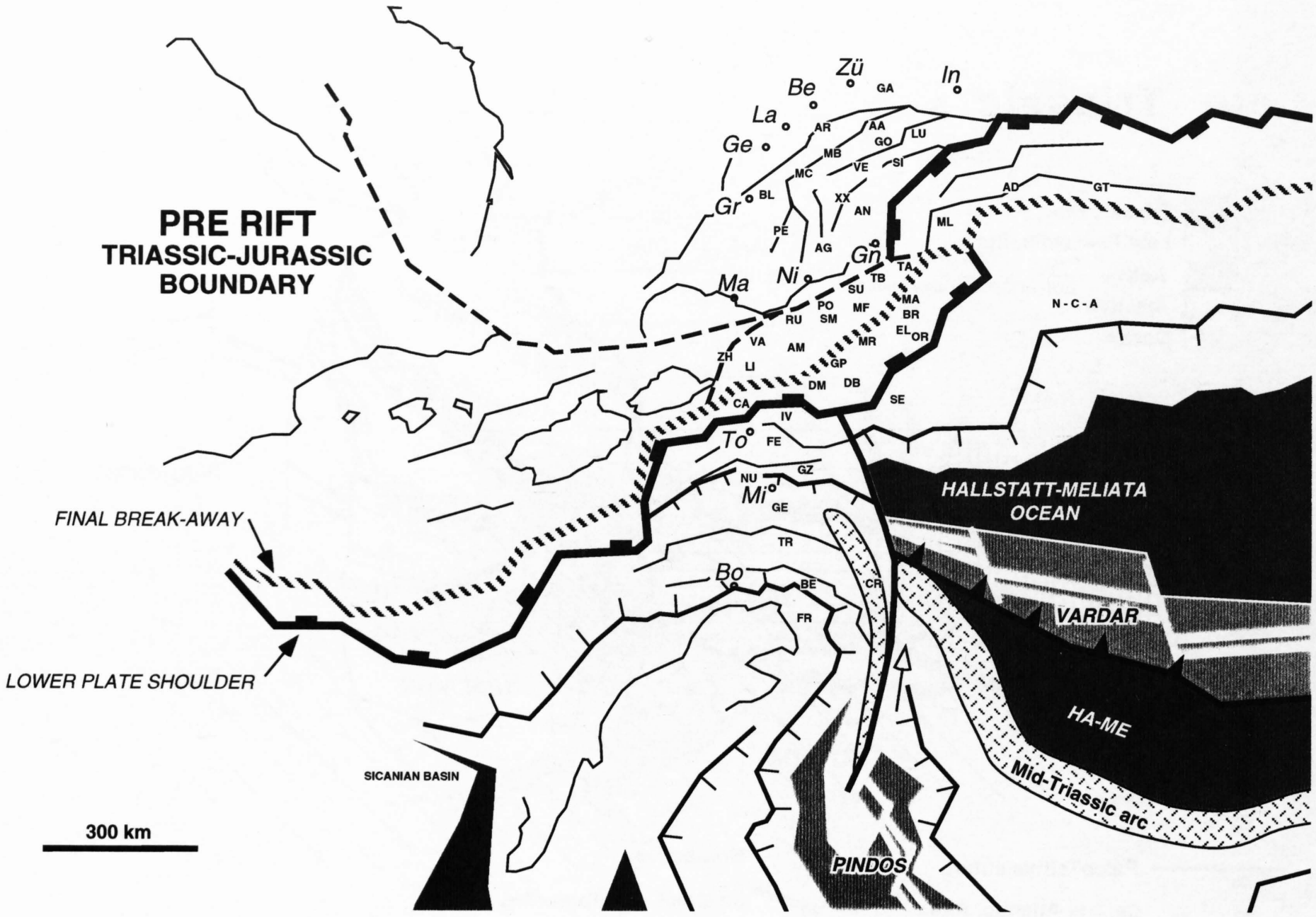

Figure 17-4
Distribution of Alpine basement and cover units. The flexural Briançonnais margin passes northward into a tilted-block margin, whilst on the other side of the future ocean the tilted-block Apulian margin passes northward into a flexural Austroalpine margin. Basements involved in the Alpine orogenesis are placed in their palinspastic location during early rifting (early Jurassic): AA = Aar; AD = Adula; AG = Argentera; AR = Aiguilles Rouges; AM = Ambin; AN = Antigorio; BE = Belluno; BL = Belledonne; BR = Bernina; CA = Canavese; DB = Dent-Blanche; DM = Dora Maira; EL = Ela; FE = Fenera; FR = Friuli; GA = Gastern; GE = Generoso; GP = Gran Paradiso; GO = Gotthard; GT = Tauern autochthonous; GZ = Gozzano; IV = Ivrea; LI = Liguran Briançonnais; LU = Lucomagno; MA = Margna; MB = Mont-Blanc; MC = Mont Chétif; MF = Mont-Fort; ML = Monte Leone; MR = Mont-Rose; NU = Monte Nudo; OR = Oertler; PE = Pelvoux; PO = Pontis; RU = Ruitor; SE = Sesia; SI = Simano; SM = Siviez-Mischabel; SU = Suretta; TA = Tasna; TB = Tambo; TR = Trento; VA = Vanoise; VE = Verampio; XX = buried basement nappe discovered on deep seismic profiles (Marchant et al. 1993a); ZH = Zone Houillère. We show a connection between the Generoso-Nudo rift and the opening of the Vardar back-arc ocean. The continental margin of the Hallstatt-Meliata ocean (HA-ME) represented by the Northern Calcareous Alps (N-C-A) would extend westward to the Sesia/Ivrea domains. Unlike Handy & Zingg (1991) we do not see a continuity between the Lombardian rifting and the Alpine Tethys rifting (see also Bertotti et al. 1993) a rift shoulder separates the two regions. The calc-alkaline volcanism affecting the Carnic Alps (CR) and adjoining regions in mid-Triassic (Marinelli et al. 1980) is seen as a result of the south-dipping subduction of the Meliata ocean. Geographic landmarks: Be = Bern; Bo = Bologna; Ge = Genève; Gn = Genova; Gr = Grenoble; In = Innsbruck; La = Lausanne; Ma = Marseille; Mi = Milano; Ni = Nice; To = Torino; Zü = Zürich.

continents and it is certain that the Internal massifs in the Alps as well as the Sesia or Margna blocks never had such dimensions. They have to be included in the complex accretionary wedge of the active Apulian margin as bits and pieces of the margins of a **unique Jurassic** Liguro-Piemont ocean (Stampfli 1994). Such a large-scale accretionary model was proposed by Polino et al. (1990). We also compared the Alps to a large accretionary prism (Stampfli & Marthaler 1990; Stampfli 1993), and in doing so we tried to separate different objects and stages of accretion:

- oceanic accretionary prism of the Piemont ocean,
- accretion of terrains (lower Austroalpine elements, Briançonnais) derived from the Austroalpine or Iberic plates,
- oceanic accretionary prism of the Valais ocean,
- accretion of the material of the former European continental margin (Helvetic domain s.l.).

Another example of plate boundaries adaptation to rheological constraints is offered by the Red Sea opening. It was demonstrated by Steckler & Bring (1986) that the Levant margin with its thinned crust attached to the old eastern Mediterranean oceanic lithosphere was "unbreakable". In response to that the Red Sea developed a transform system (Aqaba, Dead Sea) to accommodate the Arabic plate displacement towards the NE. The transform system parallels the Levant margin following a rheological boundary situated within the continent where the crust is the weakest (crust thicker than 30 km, 100 to 200 km inland – not at the toe of the margin nor within the ocean).

The proposed eastward extension of the Valais/Pyrenean transform system (Figure 17-6 & 17-7) submits to the same constraint and follows the Piemont margin a few hundreds of kilometres inland up to the point where it finally cuts through the margin. This point corresponds in our model to the change from upper- to lower-plate on the European margin, the lower-plate being far more resistant to strain than the upper-plate.

Although in our model the continental part of the Briançonnais peninsula is less than 200 km wide, it is, as a lithospheric plate (including its oceanic part), at least 400 to 600 km wide. This thin continental sliver, that detached from the European plate by early Cretaceous rifting, is similar in a way to the thin sliver of lower Austroalpine elements subducted under the southern margin at the same time. The largest lithospheric rheological contrast is situated somewhere within those former thinned continental margins.

Structural units can be grouped into relatively cylindristic patterns without producing nonsensical models, but in terms of paleogeography, lateral displacements of exotic terrains should be taken into account. In doing so, the cylindristic structural patterns will explode. Then, these elements have to be grouped together again and geodynamic markers like rift shoulders, synrift deposits or denuded mantle can be used.

Therefore the pre-rift sequences (basement included) cannot be readily used to say if a structural unit belonged to a margin or its conjugate opposite. So, there is nothing like a typical Austroalpine basement, a typical European Permian or a typical Briançonnais Triassic. Similar pre-rift sequences will be found on both sides of the rift. Jurassic geodynamic boundaries (rift break-away) are not necessarily Triassic paleogeographic limits, although locally they could coincide where the Jurassic break-away faults used older basement weaknesses which influenced the Triassic paleogeography.

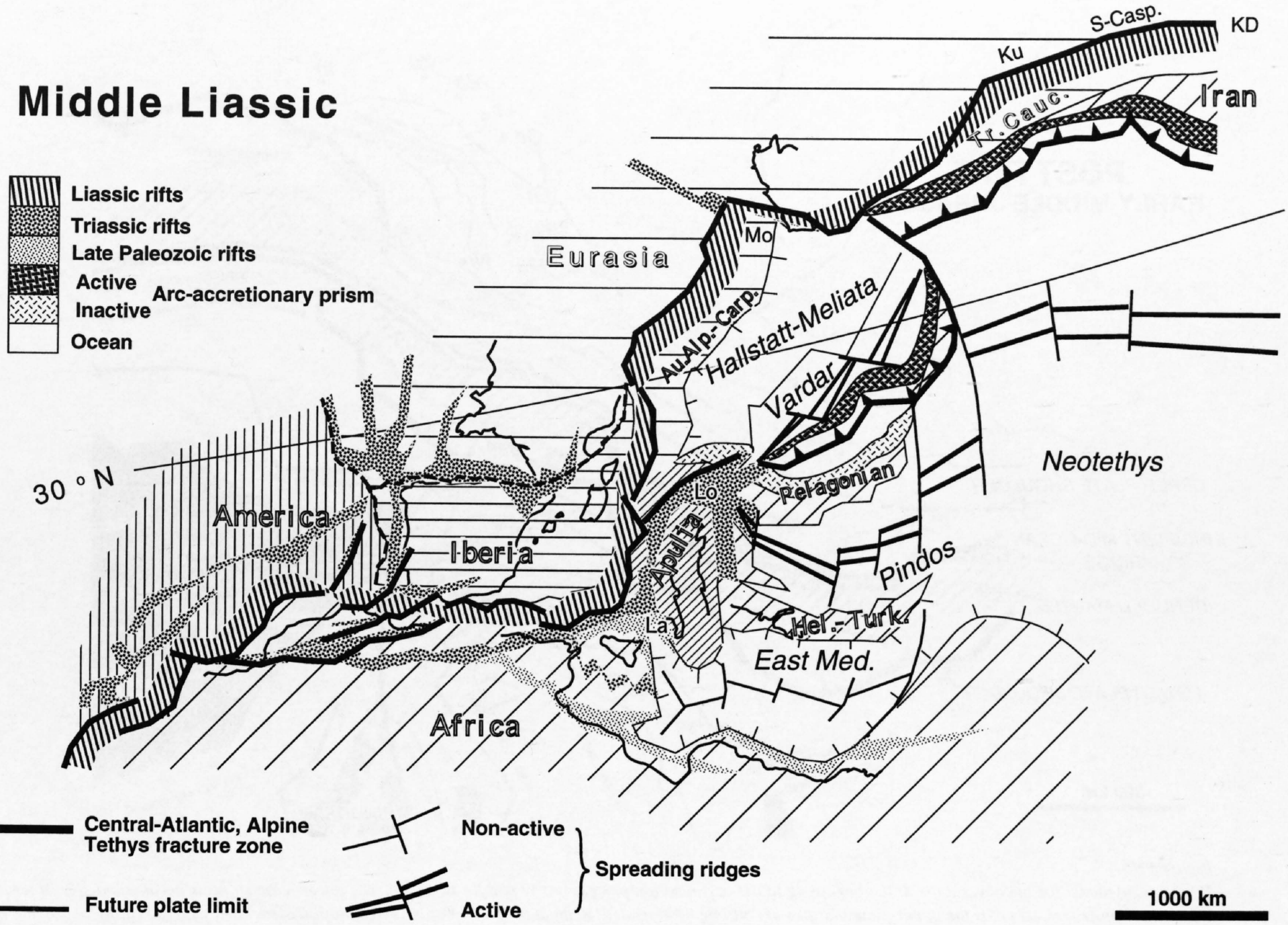

Figure 17-5
Middle Liassic reconstruction of the Mesogean/Alpine regions. See text for discussion. The Liassic rifts are shown with changing vergence of the simple shear plane. KD = Kopet Dagh basin, Ku = Kura depression; La = Lagonegro-Sicanian basin; Lo = Lombardian rift; Mo = Moesia; S-Casp. = South Caspian basin; Tr. Cauc = Trans-Caucasian massifs.

17.2.4 Plate kinematic constraints

Our reconstructions are mainly based on the latitudinal position of the Apulian plate as proposed by Scotese (1987), who gives a more northerly situation of that plate than the one proposed by Dercourt et al. (1985, 1993) or Fourcade & al. (1991) for the Jurassic. This position is in accordance with a plate model we developed (Figure 17-3) taking into account the likelihood of a late Paleozoic rifting and oceanisation of the eastern Mediterranean basin and a late closure of the Paleotethys (late Permian to Triassic) on a Greek and Turkish transect of the Tethyan realm (Stampfli et al. 1991; Stampfli 1996).
The name Apulia is used here when speaking of Mesozoic paleogeography, the name Adria is used for Tertiary paleogeography.
A review of paleomagnetic data regarding the Alpine and Mediterranean area suggests that this method cannot sort out paleopositions of small terrains having suffered small amounts of displacement. More data would be required to be able to discriminate between local and large-scale rotations (Guerricchio & Wasowski 1988) and to assess re-magnetisation problems. It is possible, however, to show that the Apulian plate suffered relatively little rotation in regard to Africa since late Permian (Channell 1992; Channell et al. 1990, 1992a, 1992b; Channell & Doglioni in press). On the other hand it was shown that the so-called Apulian autochthonous carbonate platform had been pushed by the Hellenic plate in Tertiary times and suffered a clockwise rotation (Tozzi et al. 1988). This leaves open the question of the Apulian plate being an African promontory. Also, the continuity between the active subduction zone under Greece and the outer Dinarides (Wortel & Spakman 1992; de Jonge et al. 1994) shows that there is a major oceanic separation between Apulia and Greece. In view of the age of the onset of thermal subsidence of the surrounding platform, this oceanic separation is certainly older than mid Triassic and is presently directly linked with the eastern Mediterranean basin.

Our plate kinematic model is based on the following main considerations:

a) Dercourt et al. (1985; 1993) consider the opening of the Ionian sea as an early Cretaceous event possibly linked with the splitting of Africa and opening of the south Atlantic. A preferred alternative model (Stampfli & Pillevuit 1993; Stampfli 1996) regards the Ionian sea as a southern extension of the Lagonegro/Sicanian basin (Figure 17-3, 17-5 & 17-7). The separation of Apulia and Africa would date then from the late Permian and no differential movement between the two plates would have happened after middle to late Triassic in accordance with the paleomagnetic data. Geophysical investigations done by Finetti (1985) on the Sicilian escarpment show a possible extension of the Permo-Triassic sequence over the oceanic crust of the Ionian sea; this author proposes a pre-middle Jurassic age for this oceanic lithosphere.
The Ionian Sea may represent a connection between the East Mediterranean ocean and the transform ocean north of Africa. It can be regarded as having evolved from late Paleozoic rifting associated to the opening of the East-Mediterranean ocean and its extensions westward (Tunisian Jeffara, Lagonegro, Sicily), marked by a continuous subsidence from at least late Permian. An attempt at opening a connection between southern Spain and the East-Mediterranean basin happened in late Triassic, early Jurassic and is affecting the southern Sicilian-Malta region (Antonelli et al. 1988). It is marked by widespread volcanism in the Iblean plateau during the whole Jurassic. Renewed volcanism in late Cretaceous could mark a new rifting phase affecting this area as a northern continuation of the Libyan Syrte basin and linked to the fracturation of Africa at that time. But these two phases of rifting were certainly not related to sea-floor spreading in the Ionian sea region since no major thermal uplift event is recorded.

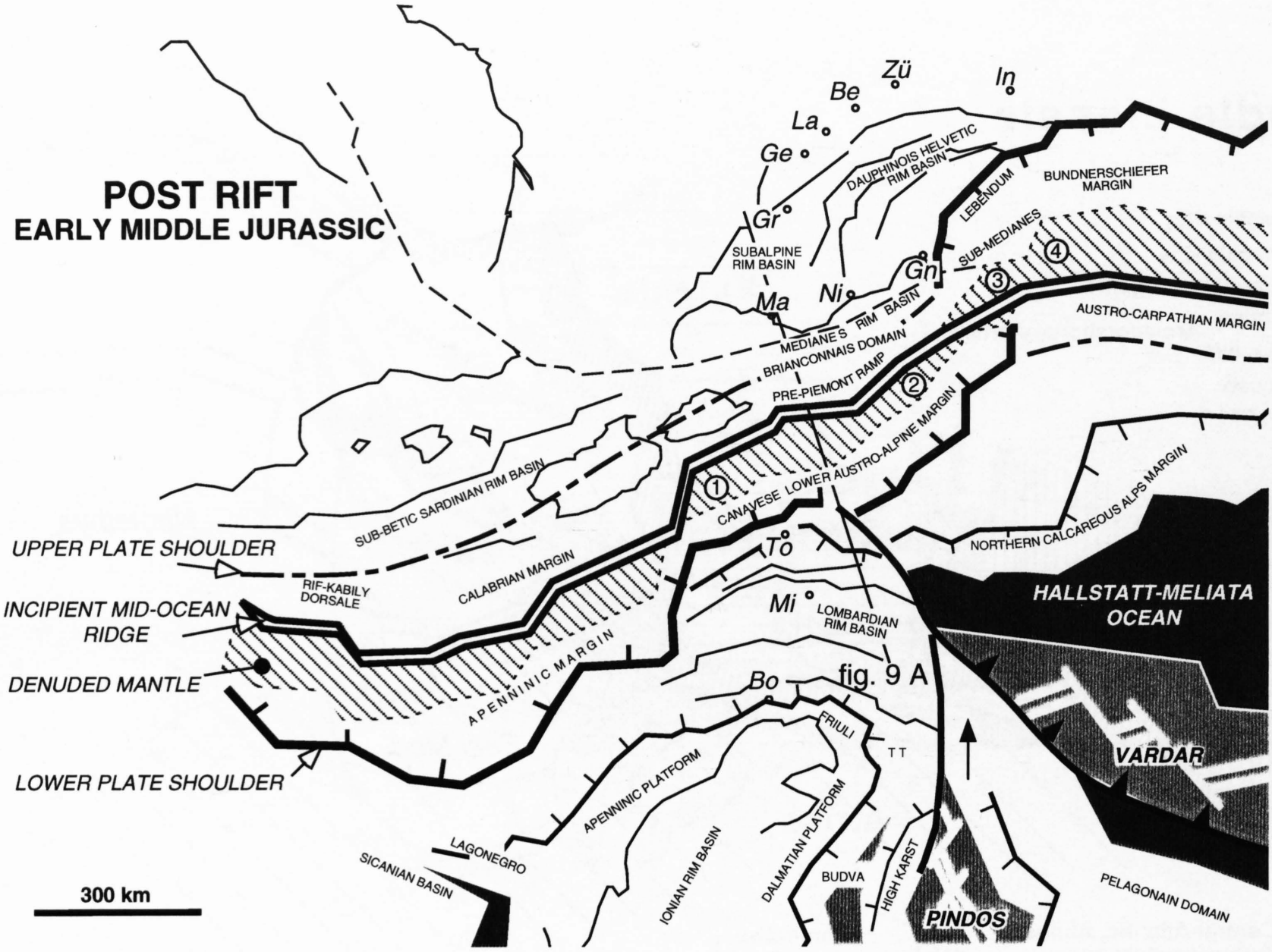

Figure 17-6
Palinspastic model for the cover units at the beginning of the oceanisation process (early middle Jurassic). The lower-plate margins became inactive in terms of extensional processes, whereas the upper-plate margins are still being extended. Remnants of upper-mantle denudation associated with the rifting phase and most likely attached to a lower-plate are found in: 1 = Lanzo; 2 = Malenco; 3 = Chiavenna; 4 = Geisspfad. The rift shoulder uplift is at its peak, generating a large quantity of sediments deposited in the rim-basins (Helvetic-Dauphinois, Subalpine; South Provence-Médianes, Lombardian). The Tolmin trough (TT) is connected westward to the Belluno graben and eastward either to the Bosnian trough or most likely to the Budva rift linked to the Pindos oceanic area of Greece. The Budva region is regarded as an aborted branch of this Pindos rifting. The Lagonegro and Sicanian (deep water Permian of Sicily, Catalano et al. 1988) basins represent a western prolongation of the East-Mediterranean oceanic basin initiated during Permian time. Most of the south Apenninic domain belongs to this Lagonegro-Sicanian basin and does not show any influences from the Alpine Tethys rifting.

b) The separation of the Iberic plate from North-America in late Jurassic implies a separation of the Iberic plate from Europe too (Figure 17-7). This separation is brought about by the Pyrenean pull-apart rift system that we extend eastward into the Valais or North Penninic suture zone. The rotation of Iberia in early Cretaceous (Moreau et al. 1992) as well as the closing of the remnant Meliata domain (see below) will induce the closure of the Liguro-Piemont ocean. This is marked by HP/LT metamorphism (Hunziker et al. 1992 and Chapter 20) of elements pertaining to the toe of the Austroalpine margin (Internal massifs) and of the accretionary prism s.str. (Tsaté nappe: Marthaler & Stampfli 1989; Stampfli & Marthaler 1990; Deville & al. 1992).

c) The Briançonnais domain (Figure 17-8) is attached to Corsica/Sardinia and therefore to the Iberic plate (Stampfli 1993). Its former position is thus more to the SE than usually proposed. The most internal south-Helvetic (Ultrahelvetic) domains, the Simplo-Ticinese nappes and the external Valais zone (lower Penninic, i. e.: zone Sub-Médiane and the Bündnerschiefer) are therefore considered as former elements of the northern Piemont oceanic margin. The Briançonnais domain is regarded as an exotic terrain whose eastward displacement induced a duplication of this Piemont margin in the present day Alpine orogen.

d) The exotic character of the upper Austroalpine terrain and the necessity to open an oceanic area between the internal part of the Carpathian domain and the Austroalpine domain is now widely accepted (Channell et al. 1990). This Meliata-Hallstatt ocean is now better known and its different parts have been studied and dated in some details (Kozur 1991; Haas et al. 1995). We consider the opening of this Meliaticum domain as a result of continuing subduction along the eastern part of the European margin in late Paleozoic times (Stampfli 1996). The northward subduction of a remnant Paleotethys may have induced the opening of a back-arc type ocean already in Permian time (Thöni & Jagoutz 1993). The spreading of this ocean lasted at least until middle to late Triassic (Kozur 1991); in the meantime, however, it started subducting southward and opened a new back-arc type ocean regarded here (Figure 17-4) as the Vardar (Bator back-arc basin of Kozur 1991; see also Kozur & Mock 1995).

e) The Austroalpine plate is also displaced westward (Frank 1987; Trümpy 1992; Froitzheim et al. 1994) in a tectonic escape movement related to the closure of the Vardar/Hallstatt-Meliata oceanic realms. This will induce trapping of Piemont oceanic crust or mantle between the Southern Alps and the Austroalpine as found between the Canavese zone and the Sesia nappe, as well as late Jurassic/early Cretaceous deformation within some part of the Austroalpine (Arolla/Valpelline thrusting: Venturini et al. 1994; Cosca et al. 1994a, 1994b; Venturini 1995).

f) The Alboran plate (Rif, internal Betic, Kabylies, Peloritan, Calabria microplates, Figure 17-6; Wildi 1983) forms the northern margin of the transform ocean north of Africa or the southern margin of the Iberic plate. This margin will be affected by subduction processes as from early Cretaceous (Puga et al. 1995). Resedimentation of the Dorsale Calcaire in the flysch basin starts in Cenomanian time, grading into major olistostrome deposits in Maastrichtian (Gübeli 1982; Thurow 1987). In Eocene/Oligocene times the Alboran (Iberic) plate locally collided with North-Africa. This collision graded into major terrain displacements during the late Tertiary opening of the Algero-Provençal and Tyrrhenian seas, liberating the Alboran blocks from their Iberic motherland. These displacements generated duplication of paleogeographic elements, creating pseudo-oceanic sutures. Our previous model considered a possible oceanic branch of the Piemont ocean going through the Betic area (Favre & Stampfli 1992). In view of the Alpine model developed here, we would now certainly favour a displacement toward the south of the

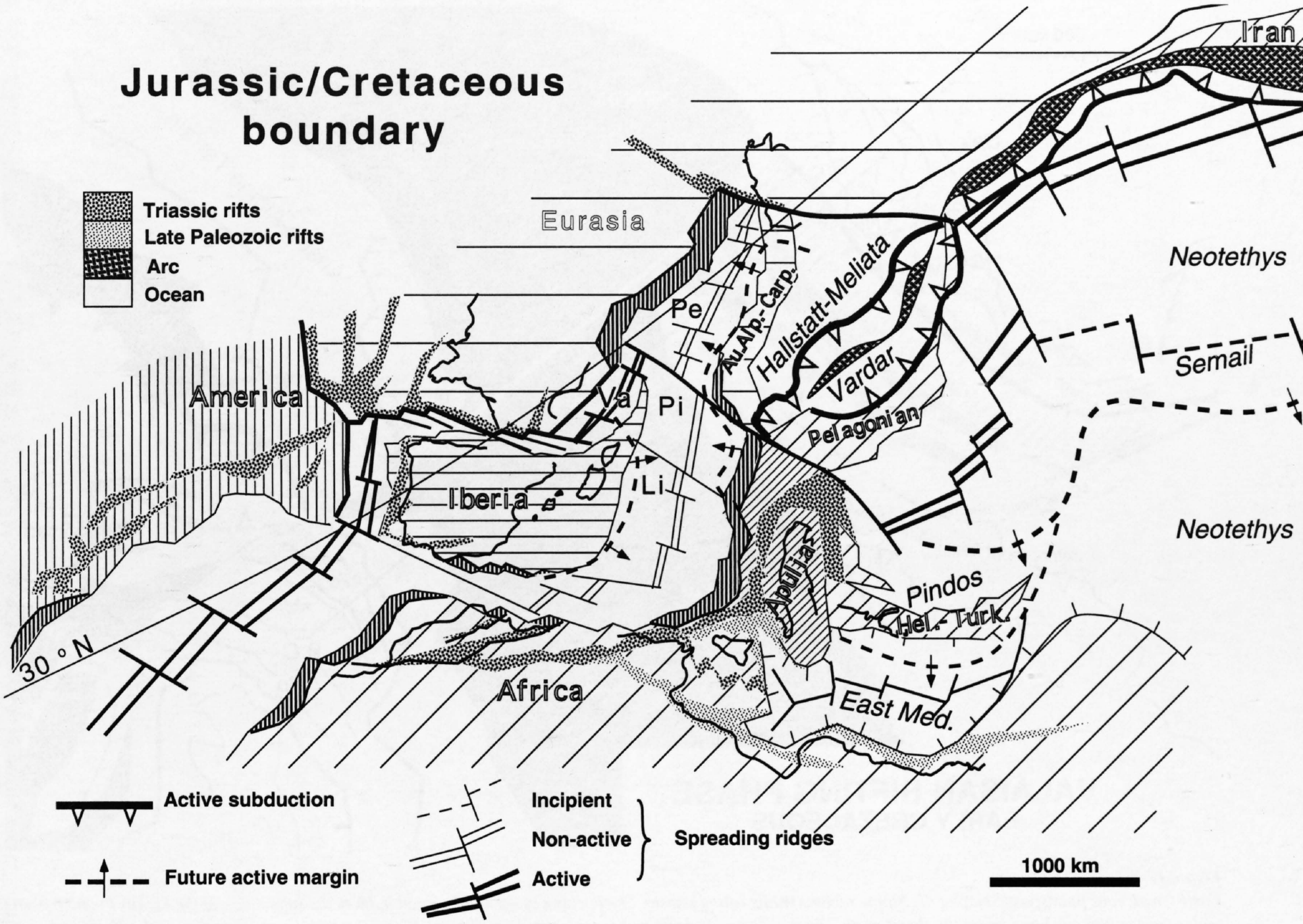

Figure 17-7
Jurassic/Cretaceous boundary reconstruction of the Mesogean/Alpine regions. See text for discussion. A major plate rearrangement induces the isolation of the Iberic plate and the opening of the northern Atlantic-Biscay-Valais (Va) rift system. A major transform fault links the Neotethys to this new rift system and induces the relative translation of the Austro-Alpine/Carpathian microplate. The Alpine Tethys (Li = Ligurian; Pi = Piemont; Pe = Penninic ocean) will soon stop spreading and subduction will start on both sides: under the Austro-Alpine/Carpathian plate and under the Iberic plate.

Internal Betic domains (together with the Rif) subsequently incorporated into the orogen as a terrain. The Iberic margin is seen as an active margin developing back-arc spreading (the Algero-Provençal basin) and the African margin as a passive margin.

g) The change of vergence of the Alpine Tethys subduction is still an intriguing problem. It is directly linked to the connection between the Alps and the Apennines. In that context the Braco ophiolitic ridge (Elter et al. 1966; Hoogenduijn Strating 1991) certainly plays an important role. It may represent the transform boundary between the Apenninic and Iberic plates, separating a northern Helminthoid flysch basin from a remnant Ligurian ocean to the south in Late Cretaceous time (Figure 17-10).

This complex situation of duplication of paleogeographic elements led to many paleogeographic interpretations, most of them done only on 2D cross-sections, not taking into account those large-scale lateral displacement of terrains. Most models propose several parallel small oceans, separating even smaller strips of continental crust. We have seen previously that these solutions are not feasible, mainly in regard to rheological constraints on plate boundaries.

17.3 Rifting stages

The Alpine Mediterranean area is affected by repeated phases of rifting, sometimes grading from one to the other, sometimes clearly separated in space and time. The following review will tend at clarifying this rather complex situation where the Alpine Tethys opening is viewed as a separate event, clearly related to a new cycle of rifting associated to the final break-up of Pangea in Jurassic times.

17.3.1 Paleozoic and Triassic rifting stages

Late Paleozoic transtensional basins accompanied by volcanism are quite widespread in the Alpine and south European domains. They start in late Carboniferous (like the zone Houillère from the Briançonnais: Cortesogno et al. 1992, 1993) and continue throughout the Permian. This polyphased rifting is usually regarded as post-collisional but, as it is quite often associated with calc-alkaline volcanism or plutonism (see for example the review of Giobbi Origoni, 1987, and references therein concerning the Southern Alps), we regard it as a type of Basin and Range situation in a still active SE European margin (Stampfli 1996).
In this context the Carnic/Julian northern part of the Apulian plate as well as the Dinaric/Pelagonian plate represent a complex domain due to the closure of the Paleotethys ocean. This closure was a continent/continent collision of Permian age for the South-Alpine domain (Carnic, Julian Alps), but eastward the Eurasian arc/accretionary prism remained active for a much longer period, developing the Hallstatt-Meliata ocean as a back-arc connected to a back-arc system extending further eastward along the Eurasian margin (Baud & Stampfli 1989).
The opening of the Meliata back-arc ocean could be correlated to the Ivrea zone denudation (Zingg et al. 1990) in the Southern Alps where Permian rifting and volcanism is well known (Winterer & Bosellini 1981); the Meliata rift extension in that region would have been of intracontinental type. At the eastern end of this rift, pillow basalts of MORB affinities are reported from the North Dobrogea area (Niculitel formation: Seghedi et al. 1990; Cioflica et al. 1980); they are interbedded in late Scythian (Spathian) limestone (Mirauta 1982). This spreading event probably originated in a back-arc setting following Permian, arc related, volcanic activity (Seghedi et al. 1992). In our reconstructions we consider Moesia to have been part of the Austro-Carpathian domain at that time and to be located west of its present

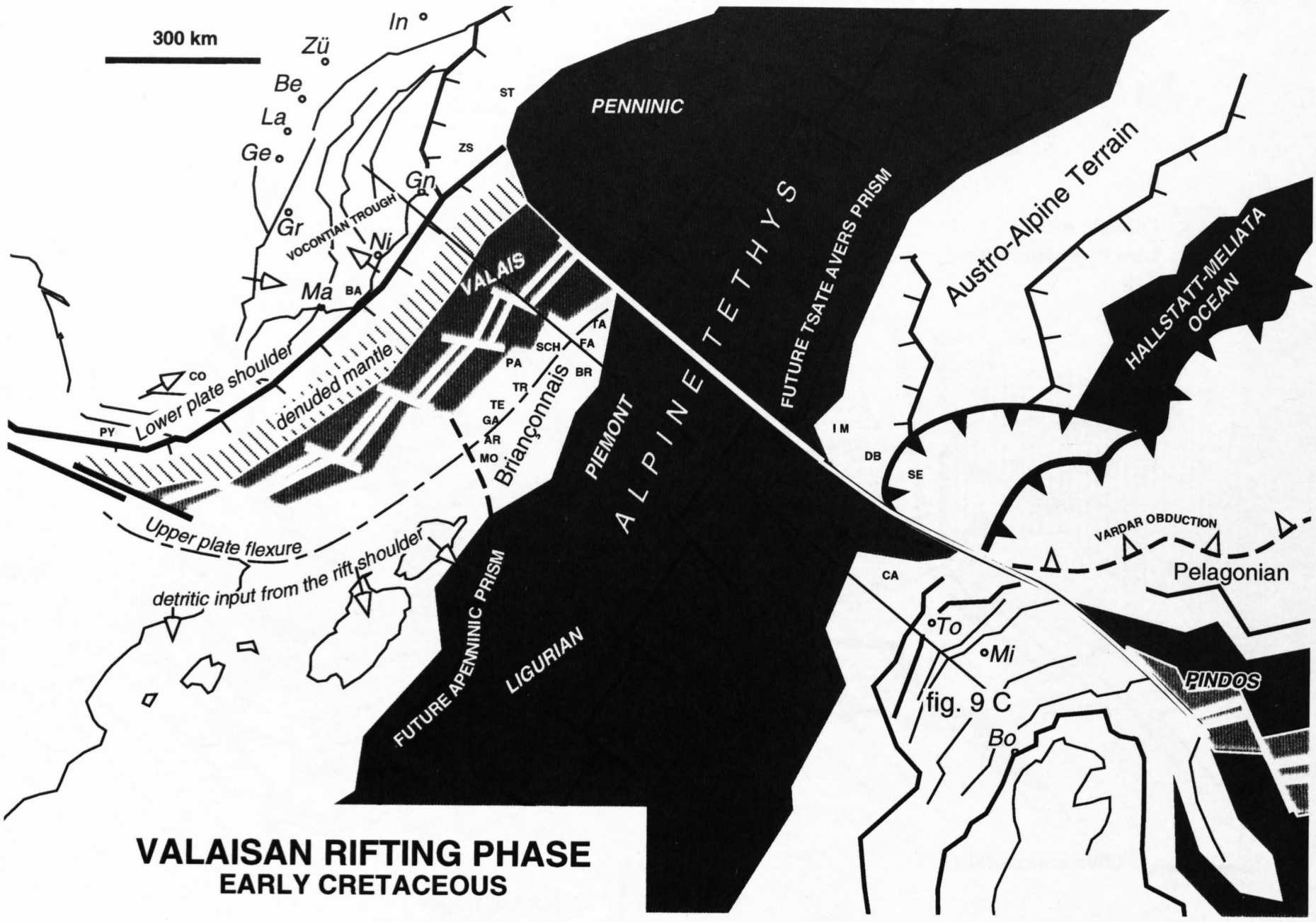

Figure 17-8
Early Cretaceous palinspastic map of the Alpine region (Valais rifting phase). The opening of the Valais ocean induces the subduction of the Liguro-Piemont ocean under the Apulian plate and under the Iberic plate. The Briançonnais domains becomes a peninsula of the Iberic plate. European remnants of the Piemont domain (ZS = Submédiane zone; ST = Simplo-Ticinese nappes) will get trapped north of the Valais spreading ridge. The Valais rift generates widespread breccia deposits starting in the late Jurassic: BA = Bandol; BR = Brèche nappe; CO = "brèche limite" from the Corbières; FA = Falknis; PA = Pierre-Avoi and related internal Valais units; PY = Pyrenean Kimmeridgian breccias; SCH = Schams; TA = Tasna; TE = Télégraphe; TR = Tarentaise. The shoulder uplift generates re-sedimentation starting in mid-Cretaceous in the following areas: AR = Argentière; GA = Galibier; MO = Morgon-Piolit. The southern margin is becoming an active margin accompanied by the subduction of some continental elements situated along the margin (IM = Internal Massifs) whereas other elements of the margin become part of the prism back-stop (CA = Canavese). The Austroalpine plate is being separated from the Apulian plate by the proto-Insubric line. Deformation along that line is quite important and marked by overthusting of some units (SE = Sesia; DB = Dent Blanche: Arolla/ Valpelline thrusting). Geographic landmarks: see abbreviations in Figure 17-1.

location. The North Dobrogean Triassic margin sequences are then part of the Meliata ocean northern margin (Figure 17-3). Through the opening of the Alpine Tethys, the Moesian block will shift eastward and actually deform this margin during a mid-Jurassic Cimmerian folding phase (Gradinaru 1988).

The drifting arc/accretionary prism detached from the SE European margin during the Permian finally collided with the Pelagonian part of the Gondwana (southern Paleotethyan) passive margin. These Cimmerian-type deformations are sealed by carbonate platforms, the oldest being of Late Permian age, the youngest of Liassic age (Stampfli et al. 1991) and are found in the Dinarides, the Hellenids, and in Turkey (Stampfli 1996).

The subduction to the south of the Hallstatt/Meliata ocean generated a widespread arc volcanism of mid to Late Triassic age found from northern Italy to Turkey (Pietra Verde type). The Vardar ocean opening can be located in the midst of this Triassic arc (or alternatively as an intra-Meliata opening) and the Lombardian rift could be the western end of this Late Triassic/Early Jurassic rift system (Bertotti et al. 1993) which extends southward under the northern Apennines (Figure 17-3 & 17-4). In the Larian (Lombardian) Alps the Ladinian platform deposits (with local volcanism) are followed by renewed clastic deposits of Carnian age which can be regarded as marking the beginning of this crustal extension (Gaetani et al. 1986). The obduction of the Vardar type ophiolites in the Hellenids and Dinarides occurred in Late Jurassic (Baumgartner 1985; Dercourt et al. 1985).

The Dinaric/Pelagonian plate is separated from the Apulian plate by the Pindos/Budva sub-oceanic realm (Gorican 1993) which may be linked to the Tolmin/Bosnian trough northward, extending up to the eastern Lombardian region (Belluno, see Figure 17-4). In view of what was said before on the separation of the Apulian and Hellenic plate already in Triassic times, it is possible that some of this oceanic domains were also linked to the East-Mediterranean ocean. Alternatively, and if the Vardar is rooted in a more internal structural position, the Pindos-Budva trough may have opened as a back-arc of the southward Meliata ocean subduction; the Vardar would then correspond to an intra-Meliata oceanisation.

The lines of weakness separating the future Apulian microplate of the Alpine domain s.l. can be regarded as inherited from terrain boundaries of the Variscan accretionary complex rejuvenated during the Permo-Triassic. Late Triassic ages obtained from the Southern Alps (Schmidt et al. 1987; Hunziker et al. 1992 and Chapter 20) witness this important transtensive event which will eventually develop into the opening of the central Atlantic/Alpine Tethys ocean and the final break-up of Pangea. The areas affected by transtension and emplacement of mafic material during the Permo-Triassic will become subsiding rim-basins of the Jurassic Alpine Tethys. The Jurassic rifting is actually cutting in between these zones of thinned and already cold lithosphere (Figure 17-5).

It has to be emphasised here that the thermal subsidence of large part of the future Alpine orogen started in Triassic time and this subsidence pattern was not affected by the Jurassic rifting. These different behaviours can be used to sort out paleogeographic units; they also indicate the importance of the Permo-Triassic lithospheric extensional phase. Other areas have recorded most of these extensional events as shown by subsidence curves done for example in the sub-Briançonnais domain (Borel 1995; Mosar et al. 1996).

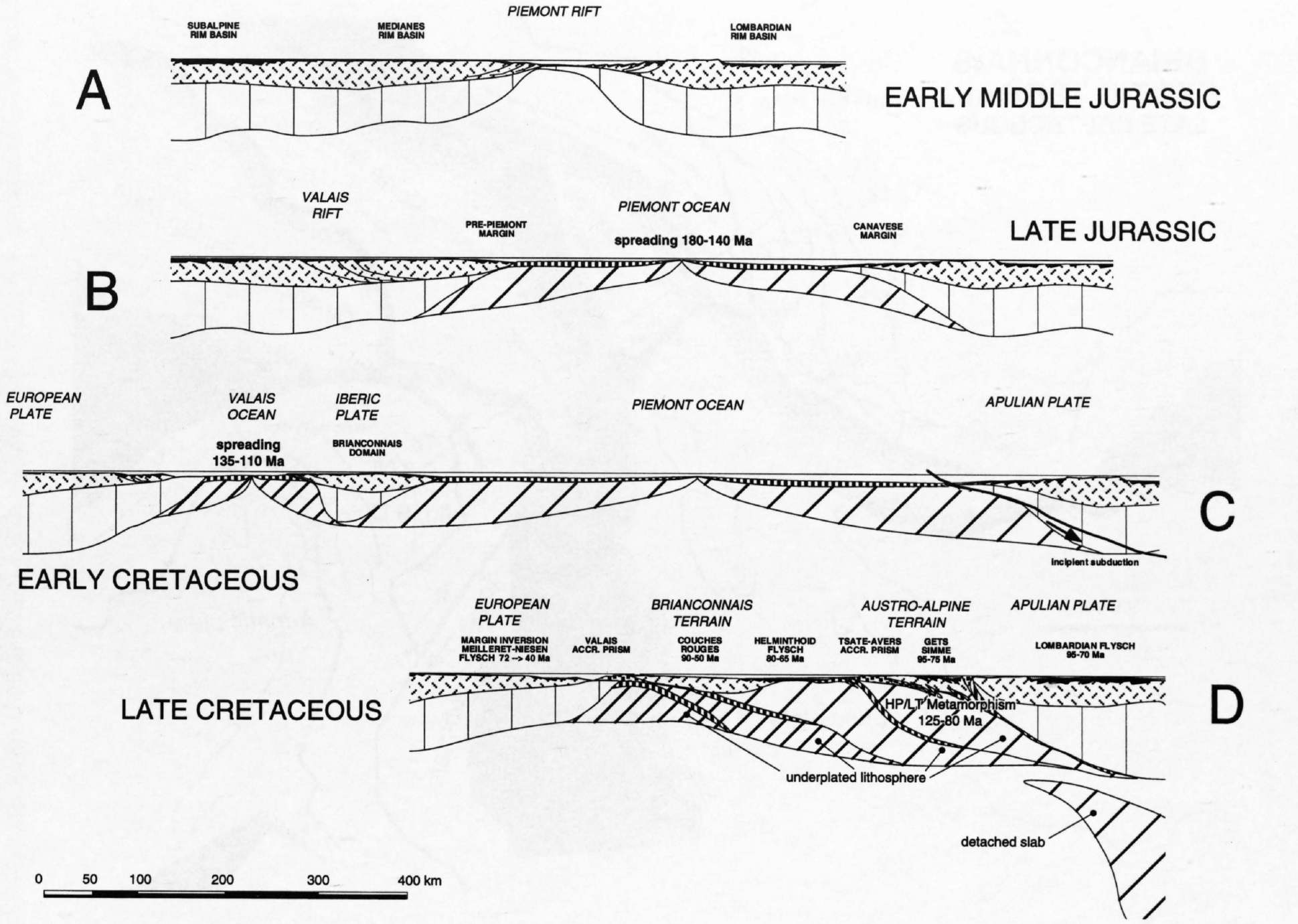

Figure 17-9
Middle Jurassic to Middle Eocene evolution of the Alpine continental margins (location of the cross-sections A, C & D are found in Figure 17-6, -8 & -10). Throughout this reconstruction the Briançonnais domain is kept fixed; it is drifting away from the Provençal part of the European margin in Late Jurassic and obducted into a more eastern portion of that margin in Tertiary times. This drifting is opening the Valais ocean s.str. and closing the Piemont ocean (see text). The subduction of the Piemont creates the Tsaté-Avers accretionary prism and is accompanied by HP/LT metamorphism. Large-scale crustal mélanges of elements pertaining to the most occidental parts of the Austroalpine plate (Sesia and the internal massifs) are found deeper in the prism.

17.3.2 Early Jurassic rifting in the Alps

The main geodynamic markers which can be recognised in the Alpine region and correlated to the different stages exposed above are given in the following (detailed analyses of these markers are to be found in Favre & Stampfli 1992, as well as in Schmid et al., Chapter 14, and Schumacher et al., Chapter 15):

The transtensive phase (phase 1): this phase affects a rather large area (300 to 500 km width) around the future rifting zone (Figure 17-4). In the Alpine regions as in the central Atlantic area, it is marked by instability of the Triassic deposits starting in Carnian times (Favre et al. 1991). In the Alps, it can be correlated to syn-sedimentary breccias found in Late Triassic deposits of the Briançonnais and Austro-Alpine domains. An older phase of rifting (Early to Middle Triassic) is affecting the Eastern Alps, the Southern Alps and the Dinaro-Carpathian regions. We link it to the opening of either the Vardar or Budva-Pindos rifts, in a back-arc setting. This rifting is influencing the Alpine region, generating major transcurrent fault systems, making a link with rifts situated in the Atlantic and the Pyrenees. These fault systems could have been reactivated during Cretaceous times for the opening of the Valais/Biscay rift system and for the proto-Insubric line separating the Austroalpine plate from the Apulian plate.

Rifting phase s.str. (phase 2): this phase is well known in most Alpine areas and corresponds to major sedimentological changes affecting the Early Jurassic carbonate platform, like increased subsidence and sedimentation of fault-scarp breccias. A typical example is the Brèche nappe, with kilometre thick mid-Liassic to early Dogger breccia deposits. Along the Briançonnais margin these Early to mid-Jurassic breccia deposits will characterise a future toe of the margin area that we call pre-Piemont ramp. These breccias were possibly deposited in a transfer zone within the Liguro-Piemont rift but not in a pull-apart system as often proposed (Steffen et al. 1990). It can be seen from the large-scale reconstruction that the Austroalpine part of the Alpine Tethys is not a transform ocean as proposed so far (e. g. Bernoulli & Lemoine 1980). The rotation pole was situated somewhere in the Black-Sea, and later on it moved north-westward but never defined a transform situation. Only the portion situated between Africa and Iberia was a transform ocean showing delayed thermal uplift (Favre et al. 1991; Favre & Stampfli 1992).

Thermal uplift phase: this phase is as conspicuous as the previous one, although not usually mentioned in the literature. The thermal uplift of the Alpine Tethys and Central Atlantic is nearly synchronous (Favre & Stampfli 1992) and characterises the Toarcian stage. It is often marked by a hiatus covering the whole Toarcian and part of the Domerian (Loreau et al. 1995) and cannot be related to an eustatic event as the Middle Toarcian generally corresponds to a high-stand. This hiatus therefore is erosional and created a large amount of fine clastics due to the dissolution of the pre-rift carbonate sequences on the raising shoulders, grading into coarser deposits as erosion reached basement. The fine clastics are represented by the Aalenian shales (the sedimentation resumes generally in the *Aalensis* zone which is late Toarcian). They are followed by Middle Jurassic deposits usually richer in quartz or even conglomerates. These clastic deposits are found on both sides of the shoulders, in the rift and the rim-basins. The time lag between the fault-scarp breccias of phase 2 and the coarse clastics related to the shoulder uplift, has been interpreted by some authors as two separate rifting events (Froitzheim & Eberli 1990). The onset of phase 2 breccias is not synchronous, starting in some areas during the Hettangian, in others during the Pliensbachian (Conti et al. 1994), whereas the onset of the fine clastics is synchronous all over the Alpine area and up to the central Atlantic. This is coherent with a 40 Ma long phase 1 and 2, first reactivating previous fractures and creating large-scale fault blocks generating non-synchronous breccias, followed by a widespread phase of thermal uplift generating synchronous fine clastics.

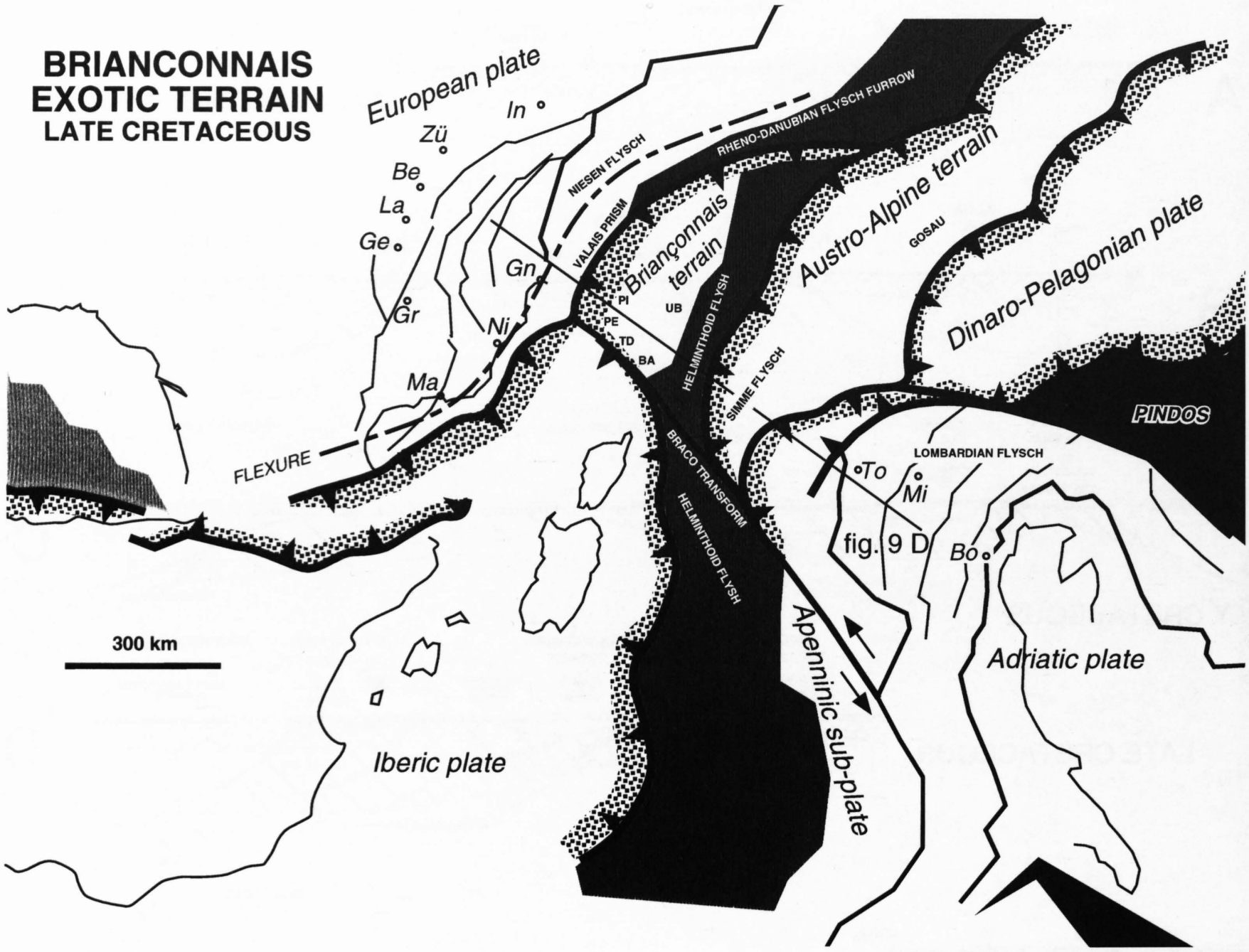

Figure 17-10
Late Cretaceous palinspastic map of the Alpine region: the Briançonnais as an exotic terrain. The Briançonnais domain is becoming an accreted terrain, severed from the Iberic plate along a transcurrent fault following the present day French and Italian sub-Briançonnais domain. These sub-Briançonnais units are characterised by re-sedimentation and flysch deposits starting in late Cretaceous and found in the following areas: BA = Baiardo; PE = Pelat; PI = Piolit; TD = Tende and also in Corsica: the Caporalino-S. Angelo flysch (Cascella et al. 1994). The Briançonnais and ultra-Briançonnais regions (UB) are also affected by numerous fractures and breccia deposits and even intra-plate type volcanism. Large-scale tectonic inversion takes place all along the European margin, starting already in late Turonian in the Pyrenees and becoming widespread in Maastrichtian time in the Pyrenees, Provence and the Alps (Niesen flysch). The Braco transform stands between a northern and a southern Helminthoid flysch basin. The Simme flysch basin evolves as a fore-arc basin and is replaced in late Cretaceous by the Schlieren flysch basin. Geographic landmarks: see abbreviations in Figure 17-1.

This phase of thermal uplift is also well recorded in terms of metamorphism and affects a large area around the Tethyan rift, with many low grade metamorphic ages centred around 180 Ma (late Toarcian: see Hunziker et al., Chapter 20).

Sea-floor spreading and thermal subsidence phase: for a slow spreading ridge, as was the case for the Alpine Tethys, 10 to 15 Ma might have been necessary to generate a large enough area of oceanic floor able to receive pelagic sediments. Therefore there will usually be a discrepancy between the age of the oldest recorded pelagic sediments and the beginning of oceanisation. In the Central Atlantic (Favre & Stampfli 1992), in Morocco (Favre & Stampfli 1992) and Fuerteventura (Hobson & Steiner 1994), the beginning of the oceanisation process (emplacement of transitional crust between the diverging plates) can be situated in the late Toarcian/early Aalenian (180 Ma), synchronous with the onset of thermal uplift.
In the Alpine area the oldest pelagic sediments found on oceanic basement are only Bathonian (165 Ma; De Wever et al. 1987). With a 0.5 cm/a spreading rate at the beginning of rifting, it would take 10 Ma to create 50 km of oceanic floor. That strip of a few tens of km of former oceanic floor (Aalenian to Bajocian) attached to the toe of the continental margin is unlikely to receive pelagic sediments only, the clastic input still being important (shoulder uplift phase). The next strip (Bathonian) might be far enough from the clastic sources and well enough into the phase of thermal subsidence to receive the first radiolaritic deposits. Radiolarian shales are also found on both sides of the oceanic realm resting on synrift sequences (pre-Piemont ramp, Canavese margin, lower Austroalpine ramp). They are mostly of Callovo-Oxfordian age and mark the general flooding of the clastic sources on the shoulders and the onset of the sediment starvation phase.
By the beginning of the Late Jurassic, between 150 and 300 km of oceanic crust had been formed accompanied by wide-spread and rapid subsidence of the rift shoulder. The Late Jurassic deposits correspond to the general drowning of the shoulders and the connection between the rim-basins (Helvetic and Préalpes Médianes, in the north; Lombardian in the south) and the Alpine Tethys.

Rim-basins: rim-basins are well developed in the Alpine area mainly due to Permo-Triassic rifting accompanied with the emplacement of mafic material at depth. Thermal subsidence of these areas started already sometime in the Triassic and continued throughout the Mesozoic; some of these basins accommodated up to 10 km of sediments (Subalpine basin). During the Early Jurassic rifting phase the rim-basins have shown some extensional activity linked to the reactivation of some Triassic faults; however the extensional factor stayed low ($b < 1.3$) (Wildi & Huggenberger 1993). They were affected mainly by the thermal expansion phase and the sublithospheric erosion and re-equilibration processes (Wildi et al. 1989). The rim-basin sequence recorded the erosion of the shoulder marked by resediments of Triassic and basement elements during the early and middle Jurassic. The areas affected by erosion and resedimentation can then be used as geodynamic markers for paleogeographic reconstructions (Stampfli 1993). The shoulder uplift and the ridge push effect generated some deformation of the rim-basins, mainly during the middle Jurassic. After that, the basins subsided together with the rift and shoulder areas and became part of the passive margin system.

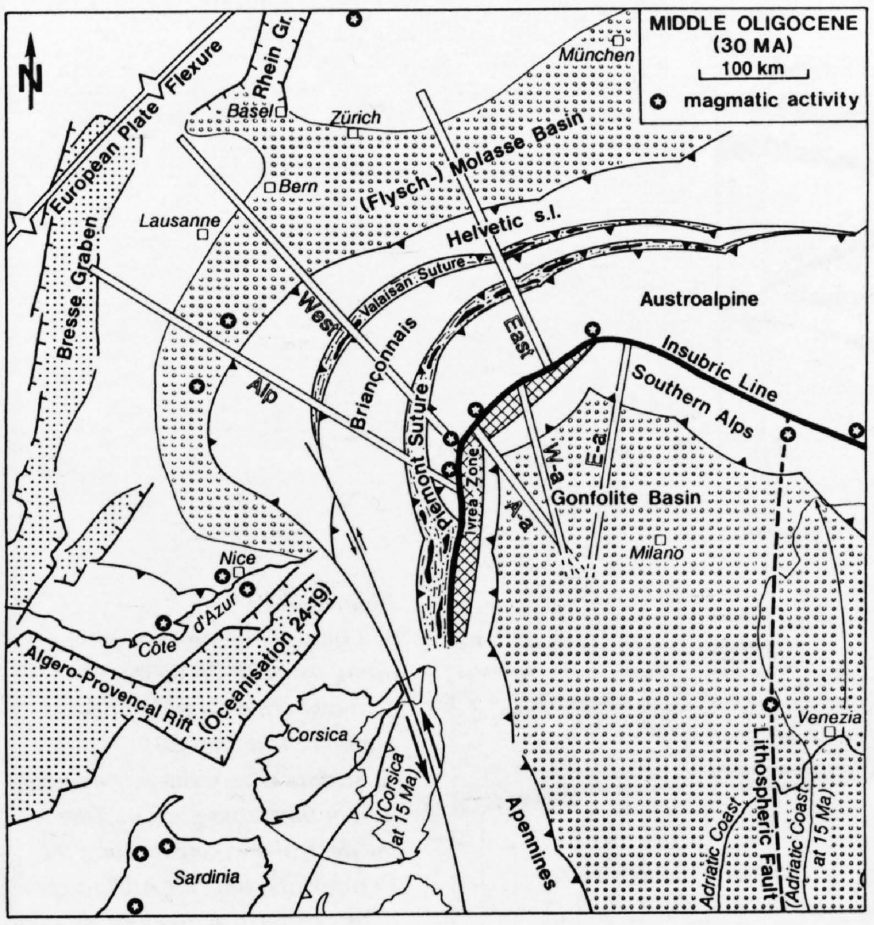

Figure 17-11
Palinspastic map at the Middle Oligocene. Alp, West & East = European, Briançonnais and Austroalpine segments of the ECORS-CROP, Western & Eastern traverses respectively; A-a, W-a & E-a = Adriatic segment of the ECORS-CROP, Western & Eastern traverses respectively corresponding to the cross-sections shown in Figure 17-17a, -12a and -13a.

Passive margin stage: the disappearance of the shoulder relief and the connection of large sedimentary areas (rim-basins) with the ocean generated a period of sediment starvation and deepening of the whole passive margin. This is represented in the entire Alpine region by the widespread pelagic to hemipelagic deposits of the late Jurassic. From early Cretaceous onward, sediment progradation began infilling the margin, starting from the hinterland (Jura, Massif Central, Friuli). However, the deepened rim-basin areas slowed down this progradation which never reached the former shoulder areas, or the rift. The shoulders were locally colonised by limited carbonate platforms which were able to keep up with subsidence (late Jurassic reef facies from the Préalpes Médianes Rigides: Heinz & Isenschmid 1988; Orbitolina limestone on the Canavese and Austroalpine shoulders, known from resediments in younger flysch deposits).
As early as early Cretaceous the southern margin was affected by tectonic inversion and became an active margin. The northern margin was affected at the same time by intracontinental rifting leading to the opening of the Valais ocean.

17.3.3 The mid-Cretaceous crisis and the Valais ocean

Geological arguments proving the existence of an intracontinental fracture zone north of the Briançonnais have been reviewed in Stampfli (1993). Part of that fracture zone has been described in detail in the Schams area (Schmid et al. 1990 and Chapter 14). The fracturation can be followed from the Grisons to the western part of the Briançonnais/sub-Briançonnais, then to Provence, the Pyrenees, the Parentis basin, and up to the Portuguese margin. These areas define the borders of the Iberian plate which became a free moving plate in the Late Jurassic (Moreau et al. 1992). From its eastern end, this fracture zone switched to a transform fault of the Piemont ocean (or the limit between denuded mantle and normal oceanic lithosphere) and joined a plate boundary in the form of the mid-oceanic ridge of the Piemont ocean. The latter was rapidly subducted at that time, the fracture system joining the subduction zone of the ocean beneath Apulia.
From much, sometimes contradicting data concerning the Iberian drift (Stampfli 1993), it can be determined that the opening of the Valais rift started in Late Jurassic times when Iberia detached itself from New-Foundland. The minimal opening would be 200 km following the data from Malod & Mauffret (1990) or 350 km using the data of Sibuet & Colette (1991). Discrepancies stem from the former situation of Iberia with regard to New Foundland. The data of Srivastava et al. (1990) and of Srivastava & Verhoef (1992) allow to narrow down these differences and their proposal was applied for our model.
The Valais rift was roughly parallel to the Central Atlantic rift between Iberia and New Foundland (Figure 17-7) and open at the same time. The oldest magnetic anomaly in that part of the Atlantic is M0 (118 Ma; Srivastava et al. 1990; Sibuet & Colette 1991) which is Hauterivian; however the oceanisation process is inevitably older than the first clear magnetic lineation (for the Central Atlantic the discrepancy is in the order of 10 to 15 Ma: Favre & Stampfli 1992). In the Valais ocean, the emplacement of oceanic floor could have started in the latest Jurassic or Early Cretaceous after a Late Jurassic transtensional phase. The major change of sedimentation in the Briançonnais domain is found at the top of the Calcaires Plaquetés (Python-Dupasquier 1990) and can be dated as Barremian (115 Ma). In the Pyrenean region, the thermal event linked to the emplacement of basic material started around 115 Ma and lasted until 80 Ma (Montigny et al. 1986). The Bay of Biscay opened during the rotation of Iberia, after the Valanginian (Moreau et al. 1992) and after the Atlantic opening between Iberia and America.
Thermal subsidence started in the Late Cretaceous for the Pyrenees and the Golf of Biscay region where the Cenomanian is largely transgressive on the former rift shoulders (Peybernès 1976; Peybernès & Souquet 1984; Simo 1986). It is expected that thermal subsidence started earlier in the Valais ocean; however, little is known of its rift shoulders. Both Valais margins actually disappeared into the lower Penninic suture zone and only resediments into the rim-basins can give some clues on their evolution:

a) The northern shoulder was situated somewhere offshore the French Côte d'Azur area and was subsequently affected by the Pyrenean orogenic event and the Algero-Provençal basin rifting (Séranne et al. 1995). Eastward this shoulder presently plunges under the Po plain and consists of the former Early Jurassic rift area of the most internal Ultrahelvetic areas or the highly metamorphic Simplon-Ticino nappes (Figure 17-8). In the Nice area, the lower Cretaceous sequence is very condensed and consists of glauconitic-phosphatic limestones forming a hardground resting on shallow water limestone of Purbeckian facies. The Albian is marked by the deposition of glauconitic sandstones followed by a marly Cenomanian and thick upper Cretaceous carbonate sequence. In the southern Provence a deepening of the sedimentation is noticed in the Aptian/Albian; sandstone deposition started in Cenomanian and stopped in the Campanian. If we admit that the pre-rift sequence consists of at least 1000 m of carbonates resting on basement, it would have taken considerable time to generate siliceous re-sediments derived from the shoulder erosion. Therefore the oceanisation/shoulder uplift must have started no later than Barremian to Aptian times. Deformation of the Provençal rim-basin (Albian normal fault, Cenomanian flexuring of the Durance region) can be related to the shoulder uplift and the ridge push effect. Albian metamorphism is also reported from wells drilled off-shore the Gulf of Lion (Gorini 1993).

b) The southern shoulder consisted of the most external sub-Briançonnais domain, the areas situated to the north-west of Corsica and Sardinia and the Spanish Pyrenees (Figure 17-8). Here too, major clastic input started in the Albian in Spain, Sardinia, Corsica and the sub-Briançonnais area (Stampfli 1993 and references therein). The mature Apto-Albian flysch of the Alboran plate (Gübeli 1982; Wildi 1983; Thurow 1987) should be related to this event too, suggesting that Alboran was still part of the Iberic plate at that time. The Préalpes Médianes lower Cretaceous sequence, certainly forming part of the shoulder area, is condensed (Python-Dupasquier 1990) but stayed in relatively deep water conditions throughout the Cretaceous. This region was formerly part of the Jurassic passive margin and was brought down to depth close to the CCD by thermal subsidence since late Middle Jurassic. The mid-Cretaceous thermal uplift was therefore insufficient to emerge it (Mosar et al. 1996). Westward, however, in the French sub-Briançonnais (Figure 17-8), important re-sediments are found in the Albian and early Cenomanian deposits (Kerckhove 1969; Kerckhove & Lereus 1987).

Following the eastward drift of Iberia and the subduction of the Liguro-Piemont ocean, an oceanic connection with the Atlantic system could have gone through the Valais/Pyrenean system. In that context it is interesting to note the similarity of facies between the Rheno-Danubian flysch and the Valais sequence from Albian to late Cretaceous (Stampfli 1993 and references therein). The continuity of deep water clastic facies in these two domains allows to assign them to the same position with regard to the European margin. The presence of contourites and strong and changing current directions along the basin (Hesse 1974) suggest a connection with the major oceanic domains. In the Ligurian domain such turbiditic deposits are absent, the Albo-Cenomanian formation being dominated by anoxic black-shale deposits. So the Valais trough, together with the Pyrenees and the Bay of Biscay, must be regarded as the connection between the Eastern Alpine Tethyan realm and the Atlantic (Figure 17-7).

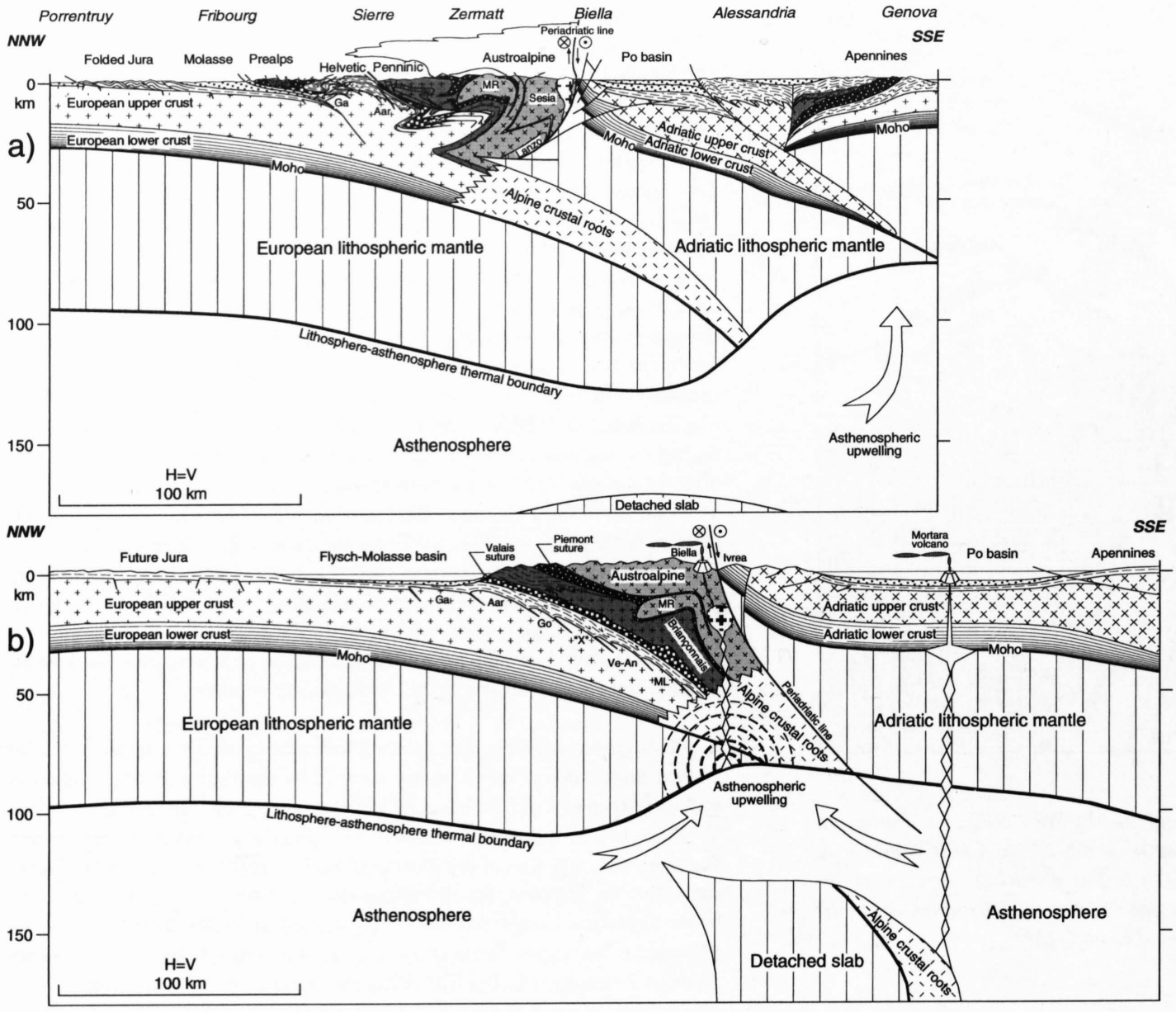

Figure 17-12
a) Lithospheric cross-section along the NRP 20 Western Traverse (from Marchant & Stampfli, Chapter 24).
b) Middle Oligocene reconstruction of this cross-section. Due to the dextral movement along the Periadriatic line, the Adriatic part of this reconstruction was situated about a 100 km east of the European part. Ga = Gastern massif; Go = Gotthard massif; ML = Monte Leone nappe; MR = Monte Rosa nappe; Ve-An = Verampio and Antigorio nappes; "X" = hypothetical nappe (Marchant et al. 1993).

17.4 Oceanic subduction stages

17.4.1 The Briançonnais exotic terrane and the lower Penninic

As shown in Figure 17-9, the Valais oceanic domain was subducted and the accretionary processes switched into the lower Penninic area at the close of the Cretaceous (Figure 17-10). Then the Briançonnais peninsula was severed from its Iberian motherland and incorporated as an exotic terrain into the accretionary complex of the active Apulian margin. This incorporation was not done before the end of the Couches Rouges deposits (Guillaume 1986) in mid-Eocene times. The absence of large-scale pre-Eocene deformation and flysch in the Briançonnais domain preclude any collision of this terrane with the Apulian margin before that time. Sedimentation in the Piemont ocean or pre-Piemont ramp lasted until Maastrichtian or early Paleocene times. It is characterised by the Helminthoid flysch sequence deposited from Albian to Maastrichtian (Caron 1972; Hoogenduijn Strating 1991). In former publications, we assumed a possible collision in mid-Cretaceous times, based on the assumption that the internal massifs were Briançonnais (Stampfli & Marthaler 1990; Stampfli 1993), but we now regard them as part of the southern margin and their metamorphism as essentially related to subduction processes.

During the rotation of Adria in the Tertiary, the escape of the Briançonnais terrane changed from NW to W and contributed largely to the formation of the French part of the Alpine arc (Marchant 1993; Marchant & Stampfli, Chapter 24). What was formerly a strike-slip intracontinental fault (Maury & Ricou 1983) separating the Briançonnais from Iberia turned into a major overthusting area (Platt et al. 1989), putting into contact internal elements of the Briançonnais terrane (Pre-Piemont to Piemont) with external autochthonous elements of the Iberian (Corsica) or European (Argentera massif) foreland (Figure 17-10).

In its frontal part, the Briançonnais terrane tended to override the lower Penninic accretionary prism. Few elements of the internal part of this accretionary complex escaped subduction and ophiolitic remnants are scarce: the MORB pillow basalts of Visp in Valais (Oberhänsli et al. 1985; Colombi 1989), the Versoyen sequence in the Petit Saint Bernard (Schürch 1987), for which work in progress (Cannic et al. 1994) shows the intraplate nature of this so-called ophiolitic sequence, regarded now as a remnant of rift-related or transform-type volcanism. Eastward the Bündnerschiefer margin (Steinmann et al. 1992; Hall et al. 1984) shows evidences of oceanic remnants possibly of both middle Jurassic (Piemont oceanic remnants) and middle Cretaceous (Valais ocean) age.

The closure of the combined Valais ocean and remnants of the Piemont ocean (northern Penninic ocean) were certainly not synchronous due to plate geometry and kinematics. The impingement of the prism onto the European margin was marked by inversion of the tilted-blocks of that margin and deposition of coarse clastics as found in the Niesen nappe (Figure 17-10) sequence and associated deposits (Ackerman 1986). We regard the relatively mature material of the Niesen conglomerate as possibly derived from inverted mid-Jurassic syn-rift deposits of Lebendun type (Spring et al. 1992). Such Maastrichtian inversion related deposits are also found in the Pyrenees (Simo 1986) and in Provence (Philip et al. 1987); they mark a general tendency towards the closure of the Valais/Pyrenean system. Inversion related deposits are however older in the Pyrenees and Provence, starting in Turonian time, and it should have been the same for the Valais domain. Therefore the St Christophe flysch (most likely Late Cretaceous age, Antoine 1971) could be considered a syn-orogenic deposit. Flysch deposits marking the final closure of the Valais domain, like the Meilleret flysch (Homewood 1974), are of Middle Eocene age, this intervall corresponding to the Pyrenean paroxysmal phase as well as the Ligurian phase in the Apennines. The closure of the Valais ocean was also accompanied by HP/LT metamorphism whose age is still debatable, but could have already started around 80 Ma and lasted until the Oligocene. The fact is that most of the southern active margin of the Valais ocean has been subducted; what is left of the Valais sequence is mostly represented by obducted elements of its northern margin. Only in the eastern Swiss Alps can one see the actual suture at deeper crustal levels between the Adula and Tambo nappes (see Schmid et al. Chapter 14). The HP/LT metamorphism related to the Valais ocean subduction in that region is placed at 55 to 50 Ma by Marquer et al. (1994), but this age may not date the onset of subduction.

While the Valais ocean was being closed, the Briançonnais was the setting of the Couches Rouges deposition (Guillaume 1986). The southward onlap of that sequence shows a displacement of a flexure separating the Couches Rouges basin from the Helminthoid flysch to the south. The flysch deposit finally impinged upon the Couches Rouges basin since the Middle Eocene ("flysch à lentilles"). Flexing of the Briançonnais is well documented in its French part where it is accompanied by important extensional faulting (Chaulieu 1992).

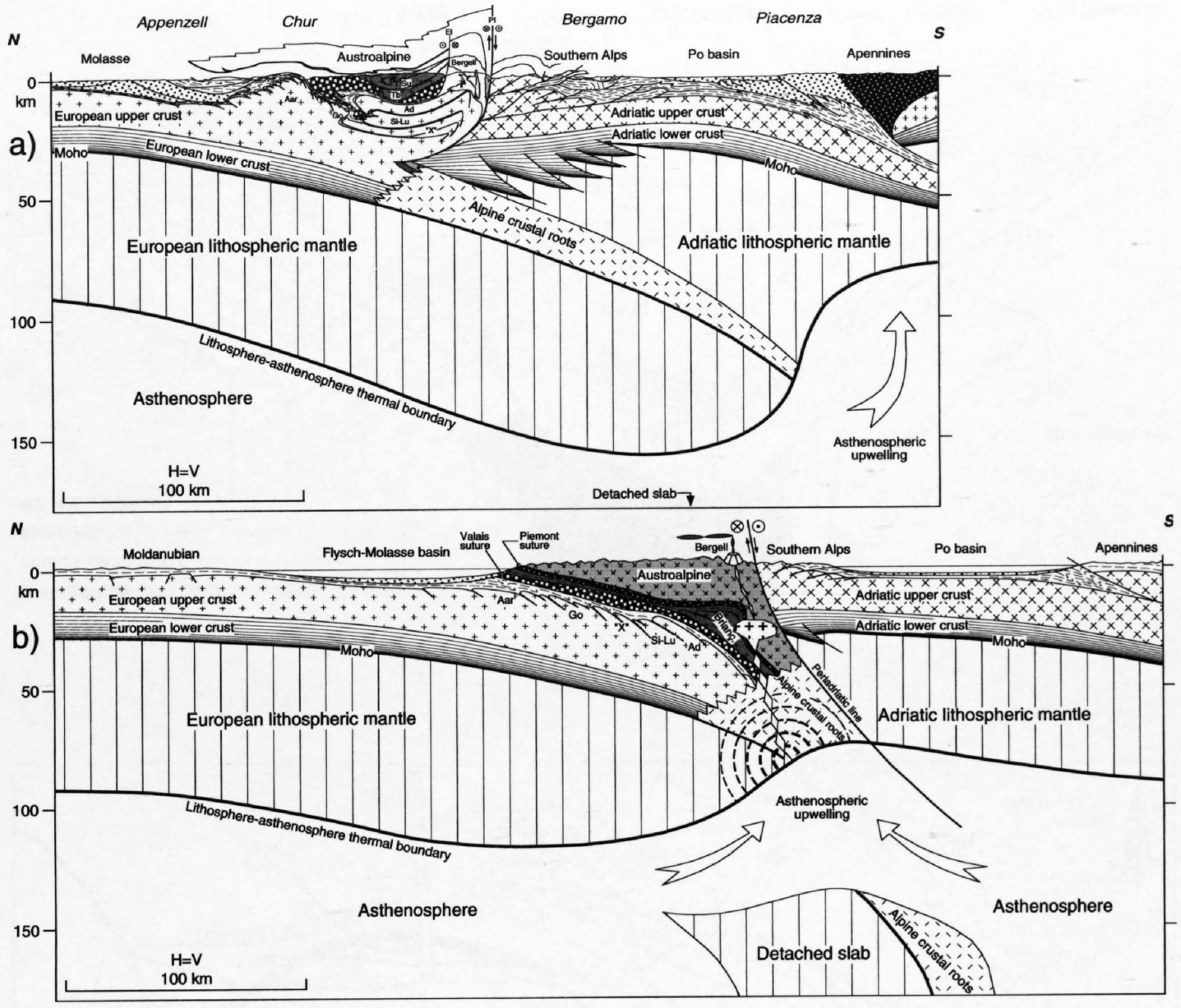

Figure 17-13
a) Lithospheric cross-section along the NRP 20 Eastern Traverse (from Marchant & Stampfli, Chapter 24).
b) Middle Oligocene reconstruction of this cross-section. Due to the dextral movement along the Periadriatic line, the Adriatic part of this reconstruction was situated about a 100 km east of the European part. Ad = Adula nappe; EL = Engadine line; Go = Gotthard massif; Lu = Lucomagno nappe; Pl = Periadriatic line; Si = Simano nappe; Su = Suretta nappe; Tb = Tambo nappe; "X" = hypothetical nappe (Marchant et al. 1993).

17.4.2 The subduction stages and exhumation of HP/LT elements

Since the Jurassic, the Briançonnais terrane has moved about 300 km eastwards relative to Europe (Stampfli 1993) and the Austroalpine terrain about a 150 to 200 km westwards relative to Adria (Trümpy 1992 and references therein). These considerable strike-slip movements were mainly transpressional or locally transtensional (Merle & Ballèvre 1992; Froitzheim et al. 1994), and were probably the main cause for the exhumation of the high-pressure eclogites related to the Piemont subduction zone. Rather than invoking mechanisms such as "corner flow" (Cowan & Silling 1978), we believe that considerable strike-slip movements are likely to rapidly exhume deep seated slabs of rocks in ductile conditions. In that context, the whole Western Alps represent a former transcontinental left lateral strike slip fault at lithospheric scale (the strike-slip intracontinental fault of Maury & Ricou 1983) separating the Briançonnais from Iberia (Corsica). Thus the Western Alps offer a lithospheric cross section of the Penninic/Southern Alps upper plate over-thrusted on the European lower plate. Between the two plates one can observe underplated elements presenting increasing HP/LT metamorphism toward the south (from the Monte Rosa to the Dora Maira massifs) and finally the southernmost outcrop is represented by mantle rocks of the Lanzo massif.
Along the Piemont subduction zone, the units which suffered high pressure metamorphism during the Early Cretaceous were exhumed in a large-scale flower structure, affecting not only the accretionary prism but also the units below (the southern Briançonnais margin) and above (the Austroalpine terrane). An interesting feature along the proto-Insubric line is the different configuration of the Adriatic plate. On its western part, which was a lower-plate margin, the uplifted upper-mantle was eroded already in the Late Cretaceous, as suggested by the presence of chromite in the Varesotto flysch (Bernoulli & Winkler 1990). We thus already had an Adriatic Moho bent towards the surface (Stampfli & Marthaler 1990), similar to the present situation on the deep seismic profiles which cross the Ivrea mantle body (Marchant 1993; Marchant & Stampfli, Chapter 24). This fact is further corroborated by cooling ages (Hunziker et al. 1992) which reveal that the Ivrea zone was already partly uplifted since 180 Ma. Whereas along its eastern part (corresponding to the southern side of the intra-continental proto-Insubric line), the Adriatic Moho was situated at a normal depth around 30 km. This is also confirmed by cooling ages (Hunziker et al. 1992) measured in the Southern Alps: no significant uplift affected this area since 230 Ma. So already before the Tertiary, the structure and the rheological properties of the future Adriatic indenter were very different along the Eastern Traverse compared to the other traverses situated further to the west, along the Ivrea mantle body.
These lateral variations of the depth of the Moho may correspond to differences in the geodynamic evolution of these areas. The Ivrea zone corresponds to denuded lithosphere of a Permian rift regarded here as a western continuation of the Hallstatt-Meliata ocean. During the Jurassic it became part of the Piemont rift shoulder area, separating this new oceanic realm from the aborted Lombardian rift to the east (Bertotti et al. 1993). During the Cretaceous the Ivrea/Canavese area became the back-stop of the Adriatic active margin and was certainly further uplifted, forming a lower crust structural high. The Eastern Alps indenter, on the other hand, corresponds to an area which was affected by the Lombardian late Triassic-early Jurassic rifting phase. During the Jurassic and the Cretaceous this area had subsided and represented a structural low. In the Late Cretaceous and Tertiary, the rifted Lombardian crust was imbricated to form a thick pile of crustal ramps representing now the Eastern Alps indenter.

17.5 Continental collision stages

This stage can be subdivided into three main phases, the first one corresponding to the Mesoalpine crustal subduction, followed by slab-detachment. The next and last two phases (Neoalpine) can be directly related to oceanisation events in the Western Mediterranean Sea, which induced significant rotations (Vanossi et al. 1994) and translations, and perhaps also the fracturation of the Adriatic plate. Therefore we have called the first of these two events the Algero-Provençal phase (from 32 to 15 Ma) and the second the Tyrrhenian phase (from 15 to 0 Ma), corresponding respectively to the opening and spreading of these two small oceans. In the Apennines these two phases correspond to the Ligurian and the Tuscan phases.

17.5.1 The Mesoalpine phase

This Eocene to early Oligocene phase, which followed the Palaeocene relative lull (or "Palaeocene restoration"; Trümpy 1980), is initiated by a NW thrusting of the Adriatic plate over the European plate s.l., producing NW vergent folds and thrusts. When the European margin became too thick for subduction, slab detachment of the Valais ocean, together with part of the Alpine Crustal root, occurred (Marchant & Stampfli, Chapter 24). Tomographic images of the Western Alps reveal a slab of high velocity (i. e. cold) material in the upper mantle situated between 200 and 400 km below the Po plain

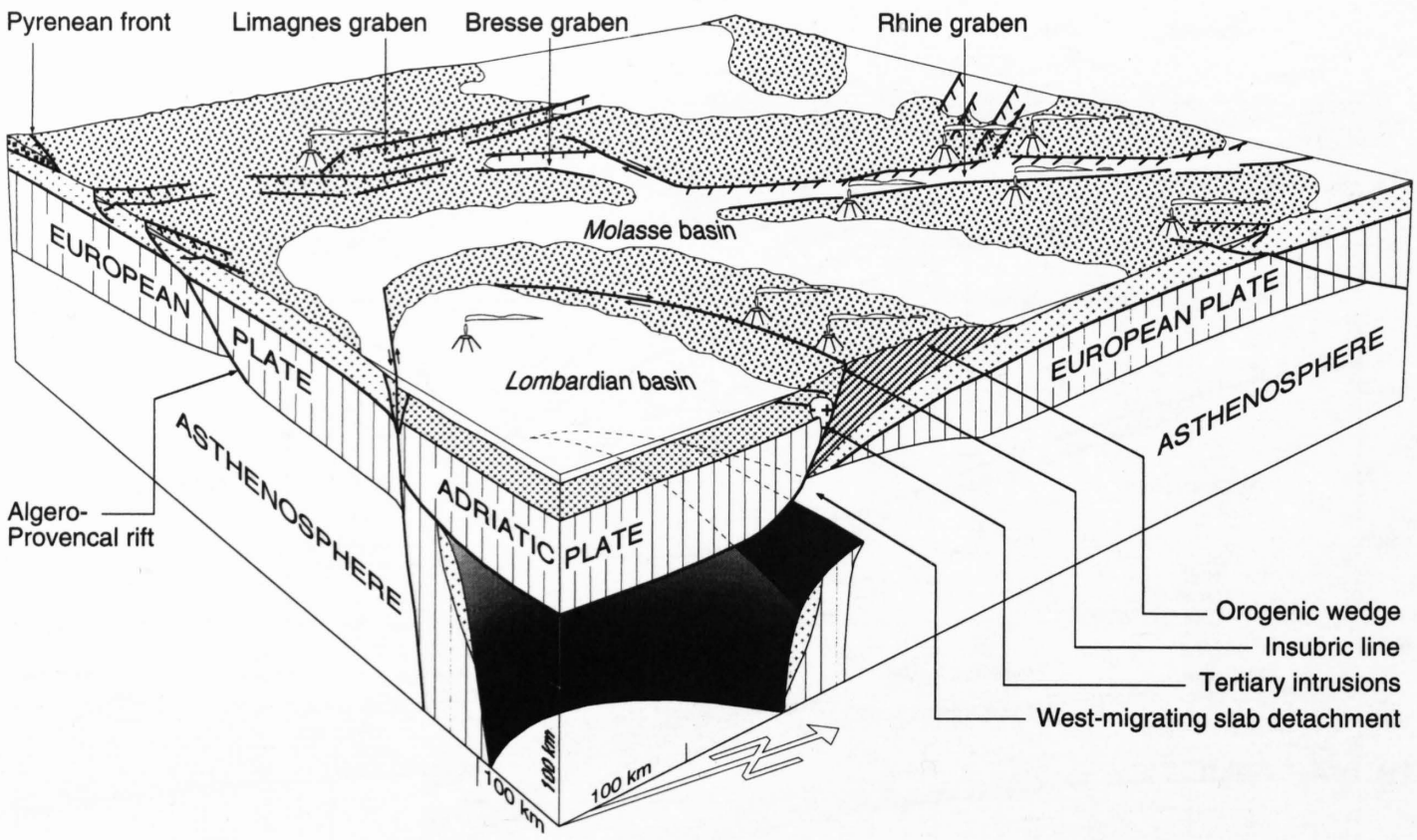

Figure 17-14
3D block-diagram of the Western Alps and the European foreland at Oligocene times. The Eocene slab-detachment migrated from east to west.

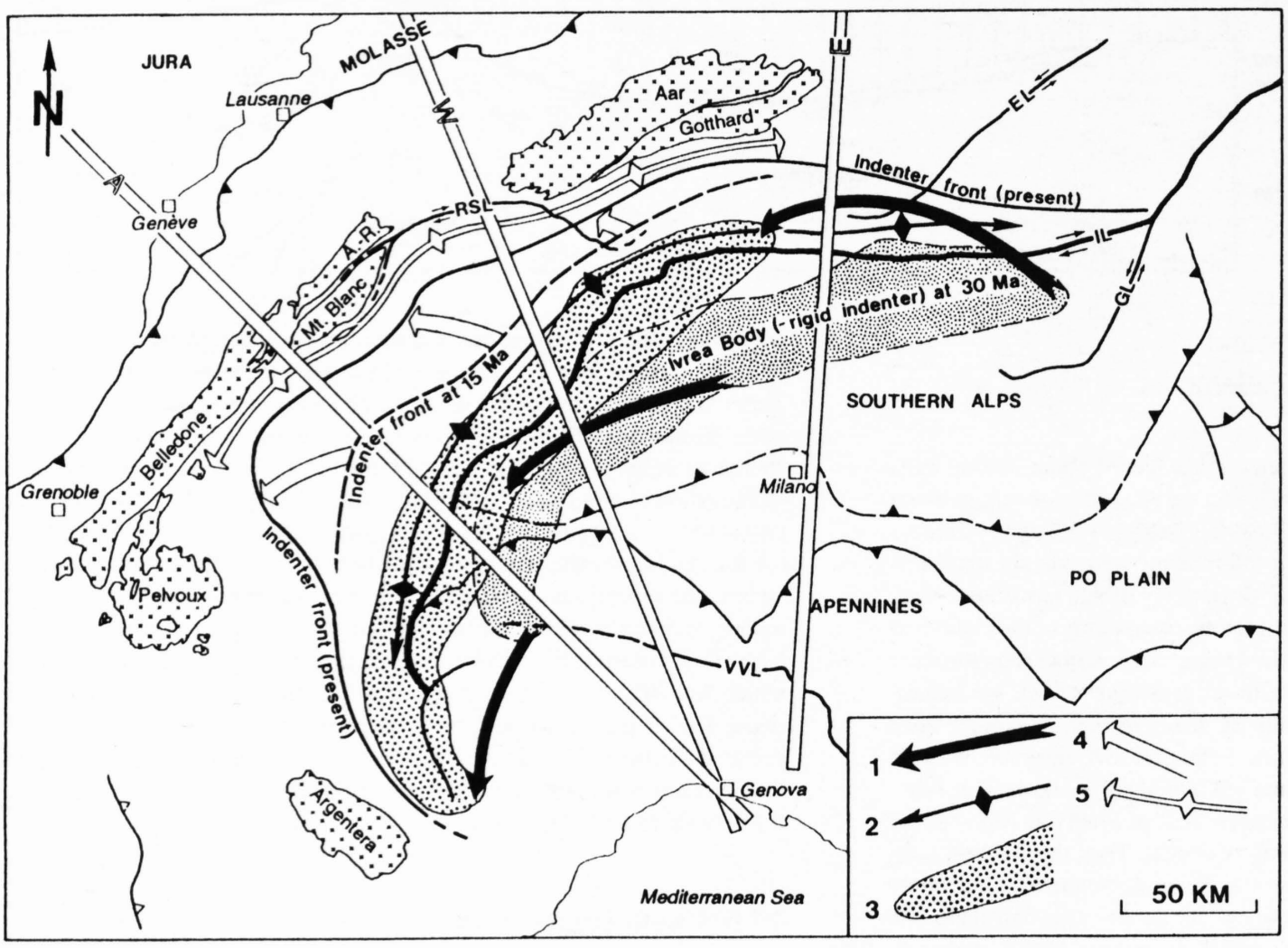

Figure 17-15
Tectonic sketch-map showing the motions of the Adriatic rigid indenter from 30 Ma to present.
1 = movement of the rigid indenter (mainly the Ivrea mantle body) from 30 to 15 Ma;
2 = area affected by backfolding from 30 to 15 Ma;
3 = present position of the Ivrea gravity anomaly defined by the 40 mgl isoline;
4 = movement of the rigid indenter (mainly the "mantle slice") from 15 to 0 Ma;
5 = area affected by backfolding from 15 to 0 Ma;
A = ECORS-CROP Alp traverse;
A-R = Aiguilles Rouges massif;
E = Eastern traverse; EL = Engadine line; GL = Giudicarie line;
IL = Insubric line; RSL = Rhone-Simplon line; VVL = Villalvernia-Varzi-Levanto line; W = Western Traverse.

(Spakman et al. 1993; see also Marchant & Stampfli, Chapter 24, Figure 24-8). This near-vertical, south-dipping slab is presently detached from the European continental lithosphere (Wortel & Spakman 1992) and most probably corresponds to the subducted Tethyan ocean(s) (de Jonge et al. 1994). This raises the question of when the detachment occurred. According to Wortel & Spakman (1992), slab-detachment induces a sudden change of the state of stress at the plate boundary as the effect of slab-pull is sharply decreased, thus causing a process of rebound type.

For the Valais ocean slab-detachment most probably occurred at mid-Eocene times as can be deduced from the pressure/time curve of the Tambo nappe (Marquer et al. 1994, Figure 5) which shows a sudden and very sharp pressure decrease around 35 Ma. This timing is further corroborated by the evolution of the European fore-bulge (Stampfli & Marchant 1995). From the end of the Cretaceous to Early Eocene, the European plate was progressively flexed by subduction and by overriding of the prograding orogen, causing an uplift of the fore-bulge well above sea-level and thus significant erosion of the European platform (see Figure 3c of Burkhard 1988) accompanied by flysch deposits since Maastrichtian (Niesen flysch). During Lutetian times (46–40 according to the time-scale of Odin 1994) this fore-bulge abruptly subsided (Allen et al. 1991, Figure 4) and the resulting transgression can be explained by a deflexuration of the European plate, most likely in relation to slab-detachment (Wortel & Spakman 1992). As this process migrates laterally (Wortel & Spakman 1992), it is most likely that in the Western Alps, slab-detachment migrated from east to west (Figure 17-14), as shown by the Eocene transgression in the Helvetic domain, which occurred earlier in eastern than in western Switzerland (Herb 1988). On the upper plate, i.e. the Briançonnais terrain, the mid Eocene is marked by a short period of flysch sedimentation deposited after progressively deeper pelagic sedimentation (Guillaume 1986). No sediments younger than mid Eocene are known in this basin, thus a significant uplift of the upper plate can be related to slab-detachment. This process probably triggered the onset of large-scale backfolding in the internal Alps (around 35 Ma according to Steck & Hunziker 1994): numerical models of orogens (eg. Beaumont et al. 1994a, 1994b; Beaumont & Quinlan 1994) show that backfolding starts once part of the crust is not allowed to subduct. Slab-detachment also generated asthenospheric upwelling through the gap and led to a peak of Tertiary regional metamorphism at around 38 Ma (Steck & Hunziker 1994). Magmatism followed in an intra-orogenic position close to the Periadriatic line with ages clustering around 30 to 32 Ma: the calc-alkaline volcanic clasts found in the Helvetic flysch (Ruffini et al. 1993), the dikes in the internal part of the orogen (Sesia, Canavese) and Bergell type

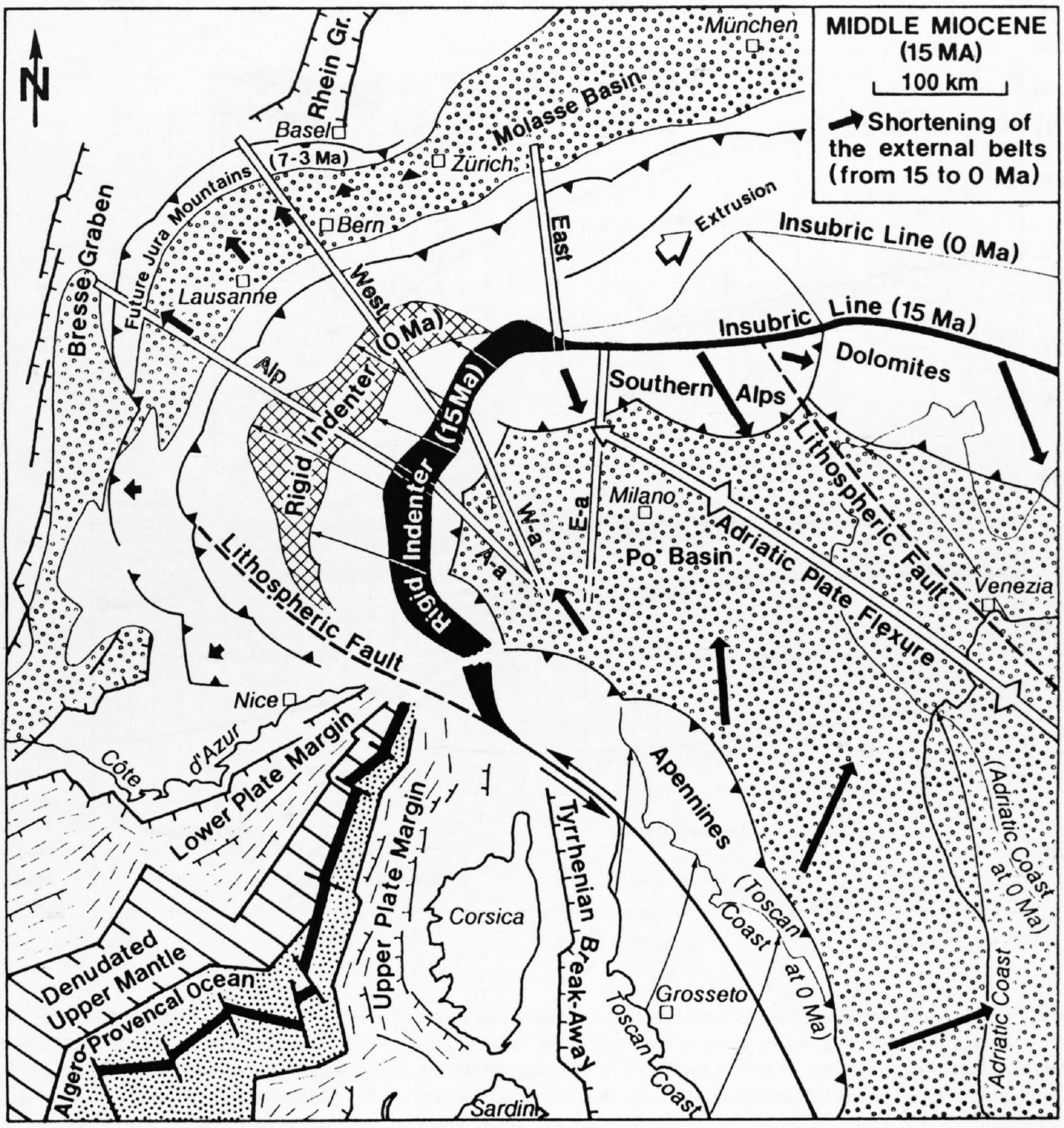

Figure 17-16
Palinspastic map at the Middle Miocene showing the main movements occurring from 15 to 0 Ma. Same abbreviations as Figure 17-11.

plutonism (von Blanckenburg & Davies 1995). It is interesting to note that these last authors (Davies & von Blanckenburg 1995; von Blanckenburg & Davies 1995), on the basis of a totally different approach to ours, come to the same conclusions that slab-detachment of the Valais ocean must have occurred in mid-Eocene times.

We have illustrated the continental collision with reconstructions during the Middle Oligocene (32–30 Ma). This period is characterised by intense magmatic activity (Figure 17-11), part of which is directly linked to the Algero-Provençal rift (Provence and Sardinia); another part occurs along the Insubric line which can be related to slab-detachment and some calc-alkaline volcanism takes place in the Po basin, such as the Mortara volcano (R. Ruffuni, pers. comm.), which can be considered as arc magmatism.

Figure 17-12b depicts this Middle Oligocene situation along the Western Traverse. The depth of most units can be roughly constrained by cooling ages (Hunziker et al. 1992). At this time, no significant backfolding has affected the units which show dominant north-vergent folds and thrusts. Mass-balancing on a lithospheric-scale implies that quite an important amount of the Briançonnais and Austroalpine terranes (together with relicts of the Valais and Piemont oceans) must be found at depth (Marchant & Stampfli in prep.). Most of this material was subsequently subducted to even greater depths (the Alpine Crustal root, Figure 17-12a) together with the European lithosphere. It is also most probable that some slabs of upper-mantle got incorporated in this continental accretionary prism, such as the Lanzo peridotitic unit, which we interpret as originating from the western Austroalpine lower-plate margin (see Figure 17-6).

But for the Adriatic plate, the Middle Oligocene situation along the Eastern Traverse (Figure 17-13) is rather similar, although the size of the Briançonnais terrane is getting smaller. Here again cooling ages help to determine the approximate depth of several units such as the Adula and the Briançonnais nappes (Hunziker et al. 1992; Marquer et al. 1994). About 100 km (50 to 150 km depending on estimates from various authors) of dextral strike slip took place along the Insubric line during the Late Oligocene and the Early Miocene. Therefore the segment of Adriatic lithosphere which indented the European segment of the Eastern Traverse must be presently found further to the west and would more or less correspond to the Adriatic segment of the Central Traverse. This is most important as there is a great difference in the lithospheric structure of these two segments of the Adriatic plate. The structure of the Central traverse indenter is similar to the Western Traverse indenter (both traverses are situated on the Ivrea mantle body), and both indenters are composed mainly of upper mantle, rheologically a very rigid material. On the contrary the Adriatic segment of the Eastern Traverse shows a much weaker indenter, made of mainly lower-crustal material.

The map of Figure 17-15 shows the trajectory followed by this rigid indenter, i. e. the Ivrea mantle body, since the Middle Oligocene (30 Ma). The trajectory followed by the Ivrea mantle body coincides perfectly with the presence of the intense backfolding which occurred just north of the Insubric line, suggesting that the intense backfolding is due to the indentation of this rigid body. East of the Middle Oligocene position of the Ivrea mantle body, the intensity of this backfolding decreases sharply together with the decrease of the rigidity of the Adriatic indenter. To the west, the movement of the rigid indenter can be followed along the Lepontine dome: fast uplift starts in the Bergell area around 32–30 Ma and then migrates westwards, reaching the Simplon area around 20 Ma (Steck & Hunziker 1994).This indentation induces "lateral extrusion" and block rotation along the Engadine line (Ratschbacher et al. 1991a, 1991b; Schmid & Froitzheim 1993). Once the rigid wedge had indented the European segment of the Eastern Traverse and moved further to the west, a more ductile portion of the Adriatic plate, made of mainly lower-crust, creeped into the gap created by the rigid indenter.

17.5.3 The Tyrrhenian phase (15 to 0 Ma)

A slowing down of extensional activity in the Western Mediterranean occurred between the end of the Algero-Provençal oceanisation around 19 Ma (Burrus 1984; Burrus et al. 1985) and the beginning of extension in the Tyrrhenian Sea around 12 Ma (Blundell et al. 1992). A similar decrease of deformation activity seems also to have occurred in the Western Alps, where cooling ages (Steck & Hunziker 1994) and structural data (Figure 17-15; eg.

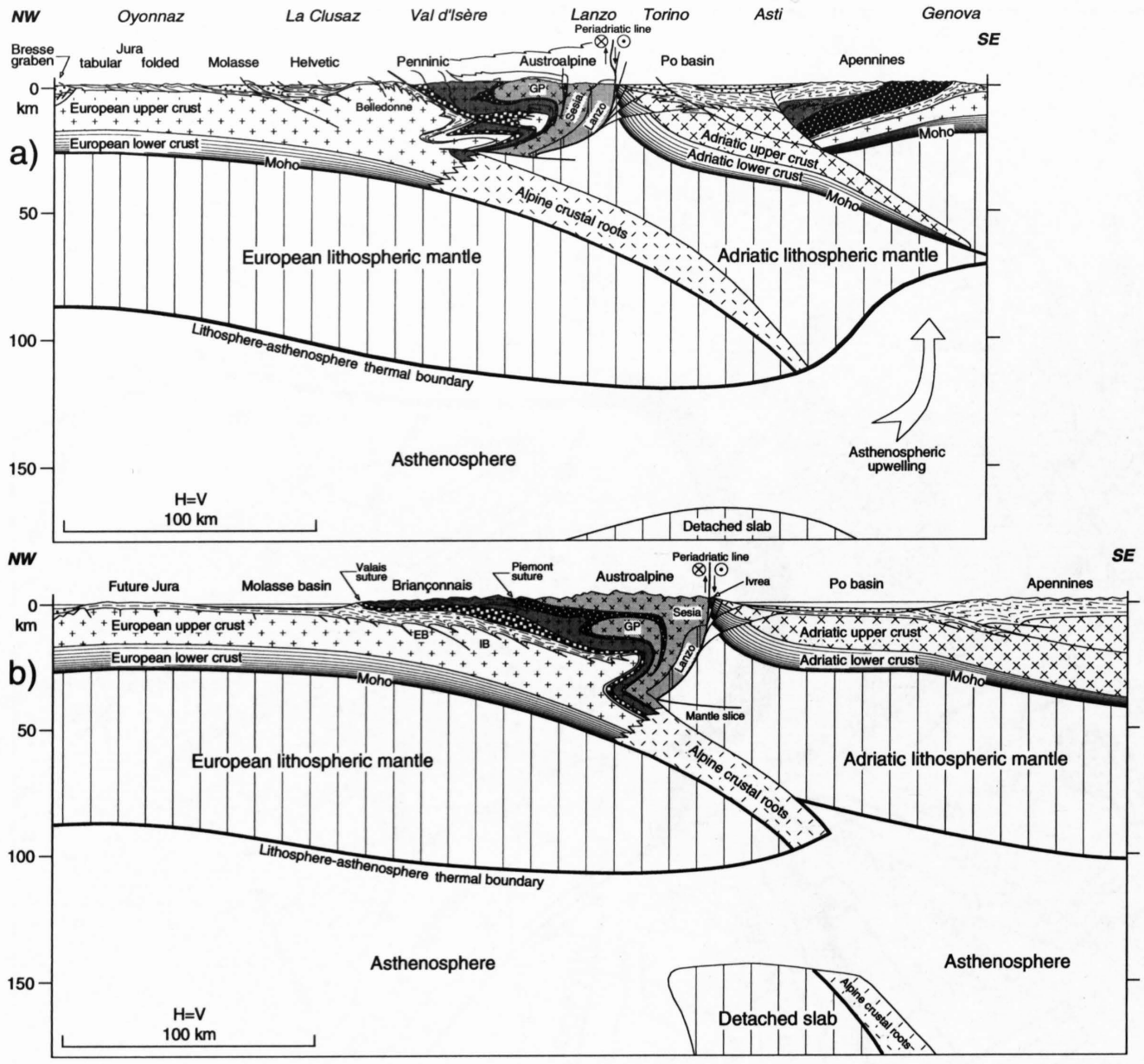

Figure 17-17
a) Lithospheric cross-section along the Ecors-Crop Alp traverse (from Marchant & Stampfli, Chapter 24).
b) Middle Miocene reconstruction of this cross-section. EB = External Belledonne massif; GP = Gran Paradiso massif; IB = Internal Belledonne massif.

Steck 1990) clearly demonstrate two distinct backfolding phases. The generation of backfolds, affecting mainly the area just north of the Insubric line, had an intensity peak between 25 and 18 Ma (Steck & Hunziker 1994) and, as mentioned above, it can be directly related to the indentation of the rigid Ivrea mantle body, an indentation itself related to the rotation and translation of the Adriatic plate due to the opening of the Algero-Provençal ocean.

The latest generation of backfolds mainly affects the southern side of the external crystalline massifs and this phase probably started around 12 Ma, as can be deduced from cooling ages (Steck & Hunziker 1994). Here again there is coincidence in ages with extension events in the Western Mediterranean Sea: the opening of the Tyrrhenian ocean from 12 Ma to present (Blundell et al. 1992). We have illustrated this phase with the map of Figure 17-16: this map is a reconstruction of the Middle Miocene situation (15 Ma) but it also features major deformations, such as the shortening of the external belts, which occurred from 15 Ma up to now.

The triangular opening of the Tyrrhenian rift provoked once again an anticlockwise rotation of the Adriatic plate (Vanossi et al. 1994) and also a northern translation which probably took place along the subcrustal discontinuities (called lithospheric faults on Figure 17-16) shown by the lithospheric studies of Guyoton (1991) and Babuska & Plomerova (1990). Part of the displacement of the Adriatic plate was absorbed by the Apennines, which show a subduction of a few tens of kilometres of the Adriatic crust below the Apennines (see for example: Giese & Buness 1992; Giese et al. 1992). Another part of this displacement was absorbed in the Dolomites and the eastern part of the Southern Alps where Laubscher (1988) estimates the shortening for this period (the Milan phase) to be 80 km. According to Schönborn (1992), the amount of shortening in the eastern Southern Alps increases considerably towards the east. This is also corroborated by the fact that in the western part of the Southern Alps, there seems, on the contrary, to have been no shortening at all as witnessed by the undeformed Burdigalian to Quaternary sequences found in the western Po plain (eastern end of the ECORS-CROP Alp deep seismic profile: Roure et al. 1990b; Marchant & Stampfli, Chapter 24). Here again one can assume that the displacement of the Adriatic plate was transmitted at depth through the rigid indenter, and in particular through what we have called the "mantle slice" on our seismic interpretations (see Marchant & Stampfli, Chapter 24). We have illustrated the situation prior to this second indentation phase along the ECORS-CROP Alp deep seismic profile (Figure 17-17). This second indentation phase mainly affected regions further to the NW than the first phase, inducing backfolding at depth along the internal side of the external crystalline massifs, basement thrusts at the front of these massifs and further to the NW the folding of the Jura Mountains. Probably both the internal backfolding and the external thrusting of the external crystalline massifs are responsible for the faster uplift of the Helvetic domain compared to the Penninic domain (Steck & Hunziker 1994) which occurred during the last 10 Ma.

On map view (Figure 17-16) a very good correlation appears between the intensity of this second indentation phase and the amount of the shortening of the Jura belt (amount taken from Burkhard 1990, Figure 7; see also Wildi & Huggenberger 1993). Furthermore there is also good correlation with the intensity of the backfolding of the external crystalline massifs which peters out on both ends of the rigid indenter. For instance, along the Eastern Traverse where the rigid indenter is not present, only little backfolding affected the external crystalline massifs as most of the movement of the Adriatic plate was absorbed by the Southern Alps. A change in rheology of the indenter could also explain the formation of the Giudicarie sinistral fault system, which was contemporaneous (Laubscher 1988) to this second indentation phase. West of the Giudicarie line, the compression was transmitted at depth through the rigid indenter, causing rather intense backfolding. Whereas east of this fault, where the Adriatic indenter shows a much weaker rheology (as a former upper-plate margin), the compression was expressed mainly through an overthrusting of the Adriatic crust, shifting the Insubric line 70 km further to the north (Laubscher 1988) and causing very little backfolding north of this line; the backfolding being replaced by SE-backthrusting of the Adriatic upper crust.

17.6 Discussion: orogenic processes and rifting

We have seen that two major phases of rifting accompanying the paroxysmal orogenic phase contributed to the complexity of the Alpine chain:

- The opening of the Algero-Provençal basin (Figure 17-11) inducing a general break-up of the Iberic plate and the drifting of the Corso-Sardinian plate and Alboran microplates in Late Oligocene/Early Miocene.
- The opening of the Thyrrenian sea since the Late Miocene (Figure 17-16) affecting the south-eastern part of the Corso-Sardinian plate and generating the drifting of the Pelorito-Calabrian microplate.

These rifts gave birth to small oceanic domains which are usually regarded as back-arc or marginal oceanic basins following the subduction of remnants of the Liguro-Piemont ocean (Malinverno & Ryan 1986). Large parts of the latter, however, had been subducted already in Late Cretaceous-Paleogene

times. During the Tertiary, the subducting ocean was most likely a remnant of the ocean situated between Africa and the Iberic plate and a possible connecting branch toward the Ionian Sea. Thus we are not sure whether we are dealing with a typical situation of back-arc sea-floor spreading. It could also be that the subduction envisaged for such a back-arc type rifting was the subduction to the south of the Valais ocean. The closure of this (sub)oceanic domain between Corsica-Sardinia and southern France started in Late Cretaceous as shown by Philip et al. (1987) and ended in Late Eocene times (Tempier 1987). But as mentioned by the latter author, flexuring of the Provence is not important and no large foreland basin developed in front of the south-Provence orogenic belt, suggesting the Valais-Biscay basin did not close completely. Further closure could therefore have happened in Oligocene times, grading into back-arc type rifting in Late Oligocene.

Another factor to consider would be rifting as a consequence of flexuring of the lithosphere following large-scale overthrusting of plate borders. Good examples of this type of rifting are found on the European plate, like the Rhine, Bresse and Limagnes grabens (Figure 17-14). These have usually been interpreted as a response of the European plate to transtensional stress generated by the Alpine collision (Bergerat 1987; Le Pichon et al. 1988). However transtensional displacements in these rifts are not very important and the rifts tend to disappear going away from a major flexure area parallel to the Alpine chain. Paleogeographic maps (eg. Ziegler 1990; Dercourt et al. 1993) show that the flexure had already been present in Paleogene, thus predating the rifting. The uplift of the flexure (elastic rebound), though not very large (few hundred meters), could favour asthenospheric decompression at depth and emplacement of mafic material at crustal level using transtensional faults. This in turn could generate rifting in the upper-crust accompanied by relatively large shoulder uplift (1 to 2 km) on top of mafic pillows. The opening of the Algero-Provençal rift could be linked to a similar process affecting the Iberic plate which is being subducted under the European plate in the Pyrenees and under the Apulian plate on its NE border. Plate flexuring most certainly played a role in the Tertiary rifting processes, as well as the thermal reequilibration of the lithosphere and upper mantle during the continent-continent collision. Syn-collisional rifting is certainly a normal response to this re-equilibration process, accompanying changing stress regimes and plate motion. Its expression at the surface is quite different depending upon which area of the orogen it affects; inside the orogen it appears as unroofing or delamination of the thickened crust and is accompanied by magmatism (Periadriatic magmatism), possibly grading into partial assimilation of lithospheric material giving birth to features like the Pannonian basin. Outside the orogen it generates Rhine graben type rifts on the lower (subducted) plate or back-arc type of rifts on the upper-plate (Algero-Provençal/Tyrrhenian oceanic basins).

Concerning these basins, we are presently in a situation similar to the Late Cretaceous opening of the Valais/Biscay oceanic connection when subduction started around the Adriatic plate. Eventually this connection disappeared producing the Pyrenees and the Alps. Similarly the Algero-Provençal and Tyrrhenian oceans will disappear if Africa becomes closer to Europe. This future orogen will then present a multi-staged collision quite similar to the Alpine system in its western part and to many other orogens.

17.7 Conclusions

Our deep seismic interpretations, based on a variety of different and often independent data (geophysical and geological), reveal striking similarities from one line to the other but also many changing features along strike. These differences highlight the non-cylindricity of the Western Alps when considered at a lithospheric-scale. Most of these differences can be explained in the geodynamic evolution of this mountain belt, in particular when the palinspastic reconstructions are based on actualistic geodynamic models (i. e. giving a proper geometry and size to continental margins) and when careful positioning of the various microplates and terranes involved in the Alpine orogeny is applied. In particular, we have shown that an intimate relationship exists between the Jurassic morphology of the Adriatic margin and the present geometry of the Adriatic indenter. Another intimate relationship has been highlighted between the indentation phase and the rotation of the Adriatic plate, a relationship already pointed out by Vialon et al. (1989).

Furthermore our palinspastic reconstructions outline the importance of lateral movements during the Alpine orogenic cycle, a fact also emphasised by other authors such as Ricou & Siddans (1986), Le Pichon (1988) or Trümpy (1988, 1992) The importance of these transform movements is such that it makes 2D mass-balancing along a single Alpine cross-section nearly irrelevant, a problem often cited by Laubscher (1988, 1990a, 1990b). For a global understanding of the evolution of the Western Alps, 3D mass-balancing at a lithospheric-scale is essential.

We are aware of the limitations of our interpretations and models, and hope that more deep seismic lines will be shot in the Alps in the near future, particularly in the Eastern Alps or through the Argentera massif, in order to obtain a more refined understanding of this mountain belt.

Acknowledgements

We have largely benefited from discussions with our colleagues from Lausanne, mainly on subjects concerning the structural geology of the Western Alps, and we want to thank them here and all the generations of field geologists who made available sums of information on this beautiful and still puzzling mountain belt. This contribution has much benefited from the reviews by E. Kissling, R. Meissner, A. Pfiffner and an anonymous reviewer.